Master's thesis

2021

Karoline Hanssen

NTNU
Norwegian University of
Science and Technology
Faculty of Natural Sciences
Department of Chemistry

Karoline Hanssen

Synthetic Studies Toward Dysoxylactam A

June 2021

NTNU
Norwegian University of
Science and Technology

NTNU
Norwegian University of
Science and Technology

NTNU

Norwegian University of
Science and Technology

Synthetic Studies Toward Dysoxylactam A

Karoline Hanssen

Master of Science, Chemistry
Submission date: June 2021
Supervisor: Eirik Johansson Solum

Norwegian University of Science and Technology
Department of Chemistry

Acknowledgment

This master thesis titled *Synthetic Studies Toward Dysoxylactam A* was conducted at the Department of Chemistry at the Norwegian University of Science and Technology (NTNU) in Trondheim between August 2020 and June 2021 as a part of my Master of Science, Chemistry degree.

First I would like to thank my supervisor, Associate Professor Eirik Johansson Solum, for providing an interesting and challenging master project. Through this project you have given me valuable guidance and encouraging words. In addition, you have shared your great knowledge about organic and medicinal chemistry through many good conversions. I would also like to thank Roger Aarvik for quick deliveries of chemicals and solvents and Dr. Susana Villa Gonzales for the MS-analysis and for the educational discussion of the results.

I would also like to thank my fellow students at the D2-211 laboratory for the countless hours we shared and for always being able to discuss both the successful and the not so successful reactions. I want to especially thank Sarah Førsund, Vanja Thorbjørnsen Stavland and Anna Røsvik for being my study mates and close friends for the past five years.

I want to thank my parents Vibeke Victoria Nordnes and Arve Dag Hanssen for teaching me the importance of hard work and to never to give up, it has never been more important than for this year. I would also like to thank my sister Veronika Hanssen and my best friends Ingrid Hallquist and Emma Sofie Bakke Karlsson for being so interested in my project and for always being great listeners. Finally, I want to thank my boyfriend, Martin Skoglund Sørum, for the being the perfect support throughout this year, for always encouraging me in my work and for just making life easy.

Karoline Hanssen
Trondheim, June 2021

Sammendrag

Naturproduktet dysoxylactam A (**1**) ble isolert fra barken av *Dysoxylum* Hongkongense i 2019 og ble funnet til å være en potent inhibitor av P-gp i kreftceller. Målet for dette master prosjektet var å utvikle en ny tilnærming til total syntesen av dysoxylactam A (**1**) og gjøre fremgang i de syntetiske stegene. Planen for total syntesen av dysoxylactam A og syntesen av fragment **10**, **67** and **72** er beskrevet in **Skjema i**. Syntesen er basert på de tre kommersielt tilgjengelige kirale utgangsstoffene (*R*)-Roche ester **24**, primær alkohol **65** og *N*-Cbz-beskyttet *L*-Valine **31,** i tillegg til cycloheptene **68**.

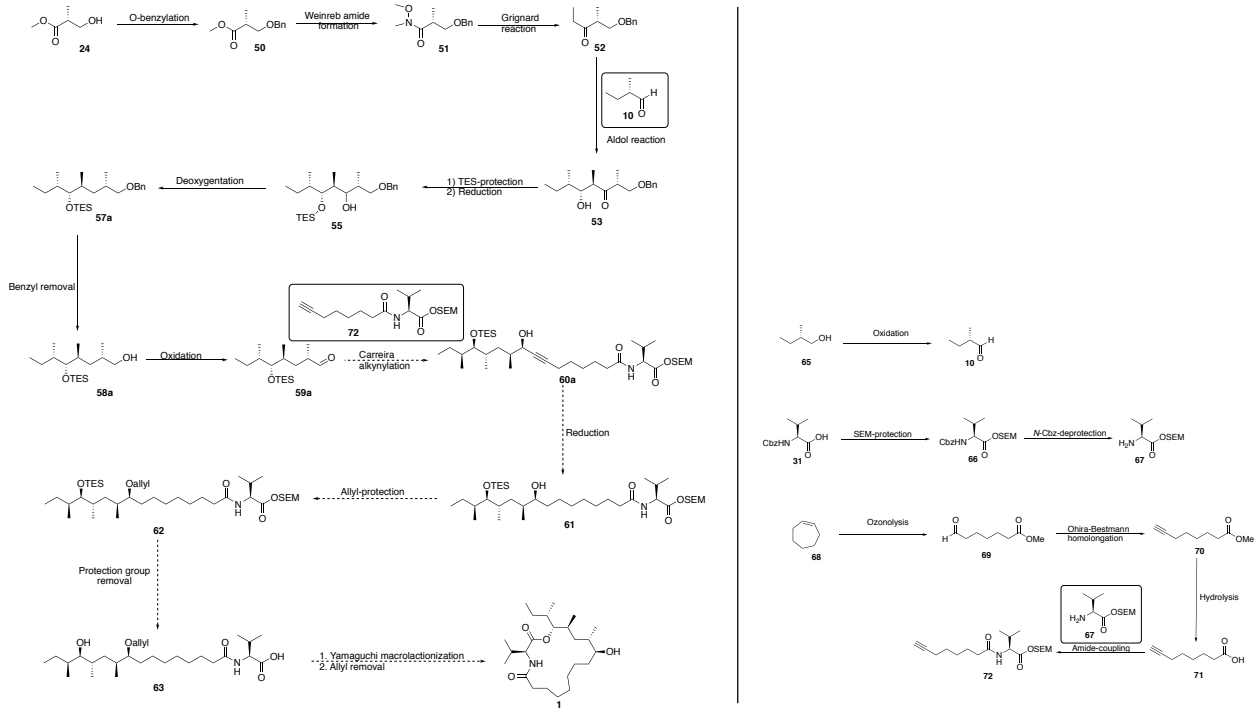

Scheme i Den syntetisk tilnærmingen til Dysoxylactam A (**1**), som viser de oppnådde reaksjonene og de gjenværende reaksjonene med stiplete piler. Til høyre vises syntesen av fragment **10**, **67** og **72**.

Den tre-trinns syntesen av ketone **52** fra **24** var vellykket og **52** ble koblet til aldehyde **10** gjennom en *anti*-selektiv Paterson aldol reaksjon som ga aldol addukt **53**. Den første planen for deoksygenere av keton funksjonaliteten var gjennom dannelse av det korresponderende dithiane og fjerning av svovel med Raney-Nickel. Denne tilnærmingen var ikke vellykket og ketonet ble istedenfor redusert til sekundær alkohol **55,** etterfulgt av en Barton McCombie deoksygenering. Barton McCombie deoksygeneringen ga det ønskede produktet **57a** i tillegg til dens regioismer **57b** (isomer ratio 0.40). I en to-trinns sekvens med fjerning av benzyl gruppen og okidasjon ble aldehyde **59a** og **59b** dannet. Den viktige Carreria alkynyleringen ble testet med isomer **59b**, men reaksjonen var ikke vellykket. Nye reaksjonsbestingelser må oppsøkes før alkynyleringen med det verdifulle aldehyde **59a** blir testet.

Abstract

The natural product dysoxylactam A was isolated from the bark of *Dysoxylum Hongkongense* in 2019 and was found to be a potent *in vitro* inhibitor of P-gp in cancer cells. The aim of this master thesis was to find a new synthetic approach for the total synthesis of dysoxylactam A (**1**) and to make progress in the synthetic plan. The plan for the total synthesis of dysoxylactam A (**1**) and the synthesis of the fragment **10**, **67** and **72** is shown in **Scheme i**. The synthesis was based on three commercially available chiral starting materials, the (*R*)-Roche ester **24**, the primary alcohol **65** and the *N*-Cbz-protected *L*-Valine **31,** in addition to cycloheptene **68**.

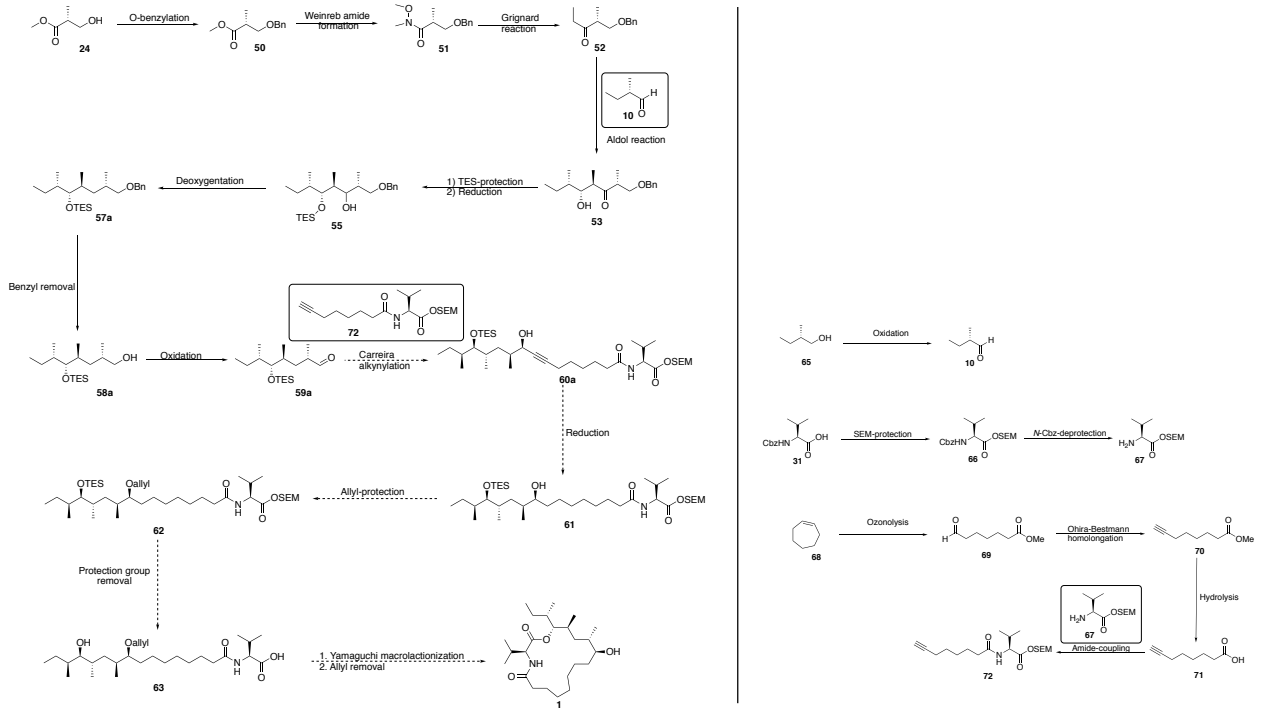

Scheme i The synthetic approach to Dysoxylactam A (**1**), showing the reactions obtained in this project and the remaining reaction with a dotted arrow. the synthesis of the fragment **10**, **67** and **72**

The ketone **52** was synthesized successfully in three steps from **24** and coupled to aldehyde **10** through the *anti*-selective Paterson aldol reaction to generate aldol adduct **53**. The initial approach for the key deoxygenation of the ketone moiety was through formation of the corresponding dithiane accompanied by Raney-Nickel desulfurization. This approach was not successful and the ketone was reduced to the corresponding secondary alcohol **55** followed by Barton-McCombie deoxygenation. The Barton-McCombie deoxygenated gave desired product **57a** and the its regioisomer **57b** (isomer ratio 0.40). In a two-step sequence of benzyl removal and oxidation, the aldehyde **59a** and **59b** was obtained. With the isomer **59b** the Carreira alkynylation was attempted but not successful and modification of the reaction conditions are required before the alkynylation of valuable **59a**.

Abbreviations

ABC	ATP-binding casette
ABNO	9-Azabicyclo [3.3.1] nonane *N*-Oxyl
AcO	Acetate
Ac_2O	Acetic anhydride
ADR	Adrenamycin resistance
AIBN	Azobisisobutyronitrile
Ar	Aromatic
ASAP	Atmospheric solid analysis probe
ATP	Adenosine triphosphate
BIAB	(Diacetoxyiodo)benzene
BMIM	1-Butyl-3-methylimidazolium
BINOL	1,1'-Bi-2-naphtol
Bn	Benzyl
Boc	*tert*-Butoxycarbonyl
Bpy	2,2′-Bipyridine
Bu	Butyl
Bz	Benzoyl
Cb	*N*,*N*-Diisopropylcarbamoyl
Cbz	Benzyloxycarbonyl
CoA	Coenzyme A
COSY	Correlation Spectroscopy
Cy	Cyclohexane
CYP450	Cytochromes P450
d	Doublet
DABAL-Me_3	Bis(trimethylaluminum)-1,4-diazabicyclo [2.2.2]octane
DCC	1,3-Dicyclohexylcarbodiimide
DIBAL-H	Diisobutylaluminium hydride
DIPEA	*N*,*N*-Diisopropylethylamine
DMP	Dess-Martin periodinane
DMAP	4-Dimethylaminopyridine
DMF	Dimethylformamide
EDC	1-Ethyl-3-(3-dimethylaminopropyl) carbodiimide
EDCI	1-Ethyl-3-(3-dimethylaminopropy) carbodiimide hydrochloride
ES	Electrospray ionization
Et	Ethyl
EtOCb	*O*-Ethyl-*N*,*N*-Diisopropylcarbamate
FAS	Fatty acid synthase
GC	Gas chromatography
h	Hour
HATU	1-[Bis(dimethylamino)methylene]-1*H*-1,2,3-triazolo[4,5-b]pyridinium 3-oxid hexafluorophosphate
HMBC	Heteronuclear Multiple-Bond Correlation
HMPA	Hexamethylphosphoramide
HOAt	7-Aza-1-hydroxybenzotriazole
HOBt	1-Hydroxybenzotriazole
hpt	Heptet
Hz	Hertz
i	*iso*
IC_{50}	Half maximal inhibitory concentration

Ipc	Isopinocampheyl
IR	Infrared
LA	Lewis acid
LAH	Lithium aluminium hydride
m	Multiplet
MDR	Multidrug resistance
Me	Methyl
MS	Mass spectrometry
Ms	Methanesulfony
n	*normal*
NaHMDS	Sodium bis(trimethylsilyl)amide
NME	*N*-methylephedrine
NMR	Nuclear magnetic resonance
P-gp	P-glycoprotein
Ph	Phenyl
Pin	Bis(pinacolato)diboron
Piv	Pivaloyl, 2,2-dimethylacetyl
ppm	Part per million
PPTS	Pyridinium p-toluensulfonate
Pr	Propyl
qnt	Quintet
QSAR	Quantitative structure-activity relationship
RCM	Ring-closing metathesis
RF	Fold reversal
rt	Room temperature
s	Singlet
s	*sec*
SAM	*S*-adenosylmethionine
SEM	2-(Trimethylsilyl)ethoxymethyl
sxt	sextet
t	Triplet
t	*tert*
TBDMS	*tert*-Butyldimethylsilyl
TBDPS	*tert*-Butyldiphenylsilyl
TBS	*tert*-Butyldimethylsilyl
TCBC	2,4,6-Trichlorobenzoyl chloride
TCDI	Thiocarbonyl diimidazole
TEMPO	(2,2,6,6-Tetramethylpiperidin-1-yl)oxyl
TES	Triethyl silyl
TFA	Trifluoroacetic acid
TfO	Triflate or trifluoromethanesulfonate
THF	Tetrahydrofurane
TIPS	Triisopropylsilyl
TLC	Thin layer chromatography
TMEDA	*N*, *N*,*N*′,*N*′-Tetramethylethylendiamine
TMS	Trimethyl silyl
TOF	Time of flight
TTMS	Tris(trimethylsilyl)silane
UV	Ultraviolet

Compound Library

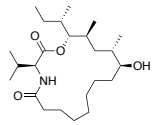
1

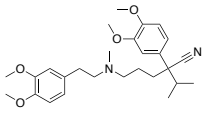
2

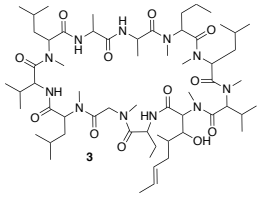
3


4

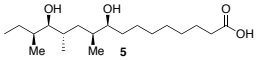
5

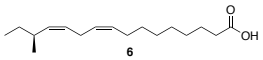
6


7


8


9


10

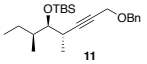
11

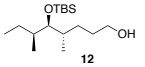
12

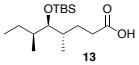
13


14

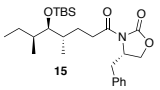
15

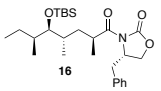
16

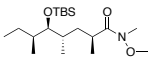
17

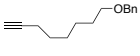
18

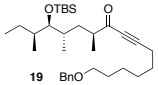
19

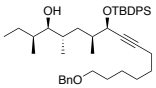
20


21

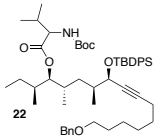
22

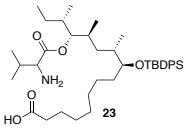
23

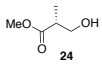
24

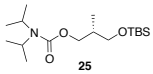
25

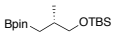
26

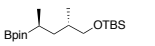
27

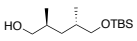
28

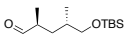
29

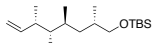
30


31

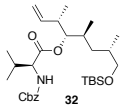
32

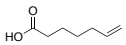
33

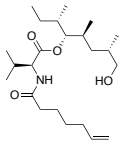
34

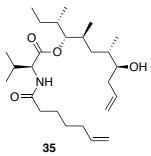
35


36


37

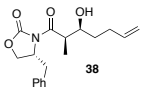
38

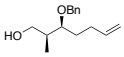
39

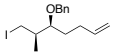
40

41

42

43

44

45

46

47

48

49

50

51

52

53

54

55

56a

56b

57a

57b

58a

58b

59a

59b

60a

60b

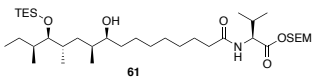

61

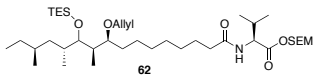

62

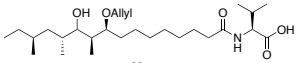

63

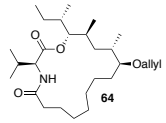

64

65

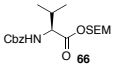

66

67

68

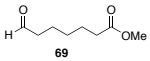

69

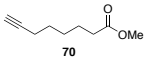

70

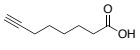

71

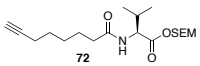

72

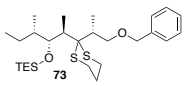

73

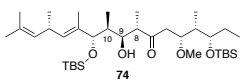

74

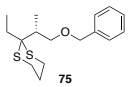

75

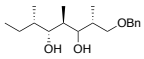

76

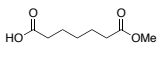

77

List of Content

1 Introduction

For treatment of cancer, multidrug resistance is one of the major challenges, an effective strategy to reverse the mechanism of resistance is by developing P-glycoprotein inhibitors.(1) Despite extensive efforts, until this date no p-glycoprotein inhibitors are approved for clinical use.(2) In 2019, dysoxylactam A (**1**) was isolated from the bark of the *Dysoxylum hongkongense*. As cycloliopeptides have a wide range of biological activities, the newly isolated natural product was tested for its *in vitro* potency as a P-glycoprotein inhibitor to reverse multi-resistance of chemotherapeutic agents. The initial testing revealed that sensitivity was restored for chemotherapeutic agents that are substrates for P-glycoprotein. The potency of dysoxylactam A (**1**) has made it the lead compound to combat multidrug resistance.(3)

The fascinating structure and the high potency has made the novel compound an interests for both medicinal and synthetic chemists. One year after the isolation three total synthesis of dysoxylactam A (**1**) was reported and will be reviewed in here.(4-6) However, the aim of the project is to set up a new synthetic approach to dysoxylactam (**1**) and will be focusing on the synthetic steps toward the new total synthesis of dysoxylactam A (**1**).

2 P-Glycoprotein Mediated MDR in Cancer Cells

The major obstacle to an effective cancer treatment is anticancer drug resistance and is consequently the main cause of mortality in cancer patients.(1) When chemotherapeutics are administered to a cancer patient, often an initial effect is observed. However, the cancer cells can acquire resistance to an anticancer agent, by a variety of mechanisms. When a cancer cell becomes resistance to a wide-range of mechanistically and structurally diverse anticancer drugs, it is called multidrug resistance (MDR). One of these mechanisms of resistance are expressed by efflux pumps.(7, 8)

Efflux pumps are a part of the adenosine triphosphate (ATP)-binding cassette (ABC) superfamily. These are integral membrane protein that hydrolyses ATP to change conformation, enabling active transport of substrates across their concentration gradient.(9) 48 members of these energy-dependent transporters are found in humans, which export lipids, peptides, sterols, ions and toxins out of the cell.(9) Among these transporters, there are three MDR-related proteins: P-gp, (multidrug resistance protein 1, MDR1 or ABCB1), MDR-associated protein 1 (MRP1 or ABCC1) and breast cancer resistance protein (BCRP or ABCG2).(10-13)

The P-gp is expressed in normal healthy tissues in the brain, liver and kidney, where it is an important part of the cell detoxification process.(14, 15) However, cancer cells can express multiple of these efflux pumps and by overexpression it gives an enhanced expulsion of a variety of structurally different drugs. As a result, the anticancer drugs are not accumulated intracellularly over a sufficient period of time to exhibit its effect, thereby reducing the response of the chemotherapeutics.(8)

2.1 Brief History of P - gp Inhibitors

Since the first MDR transporter P-gp was discovered over 40 years ago, it has been widely studied and characterized, and these proteins are acknowledged as a possible target of MDR.(10) As a result, a strategy to overcome MDR can be to co-administer the anticancer drug with an agent that can inhibit or reverse the efflux of P-gp. Today, several small molecule drugs have been investigated and found to be modulators or inhibitors of P-gp.(16) These molecules have been classified under four categories depending on their binding site: competitive inhibition by direct interaction with the P-gp drug-binding site, non-competitive binding by allosteric inhibition, non-competitive inhibition by inhibiting the binding of ATP or by interacting with the membrane lipid layer to disturb the membrane. As well as inhibiting the efflux pump, the expression can be down-regulated by inhibition of a variety of signalling pathways by a modulator.(2)

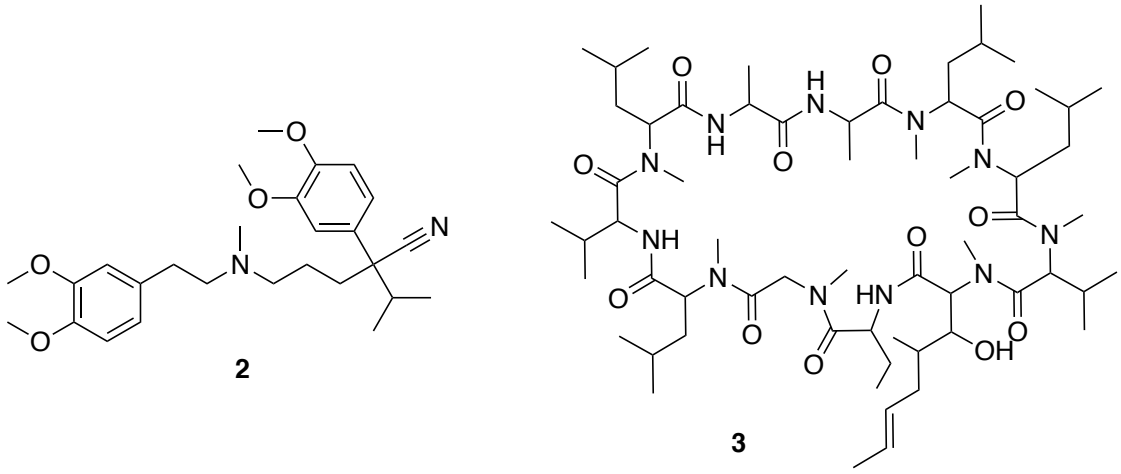

Figure 2-1 Structure of verapamil (**2**) and cyclosporin A (**3**). (17)

The first generation P-gp inhibitors include, competitive inhibitors such as verapamil (**2**) and cyclosporine A (**3**) (see **Figure 2-1**). These compounds showed high cytotoxicity and low affinity for P-gp, therefore their clinical use was limited.(17) The second generation was developed focusing on structurally modifying the first generation to improve the adverse effect

and to increase the affinity for P-gp.(16) Valspodar, a cyclosporine D analogue, showed promising results in initial trials with higher affinities.(18) However, it had unexpected pharmacokinetic interactions and low selectivity, where it also inhibited other ABC efflux pump as well as cytochrome P450 enzymes. By a phase III clinical trial, it was concluded that valspodar did not improve the outcome of the treatment.(19)

The third generation of P-gp inhibitors was developed by employing quantitative structure-activity relationship (QSAR) and combinatorial chemistry. This strategy use the knowledge of previous known P-gp inhibitors to generate novel compounds with improved efficacies and biological activity.(16) The acridone caroxamide, anthranilamide and diflurocyclopropyl quiniline derivatives elacridar, tariquidar and zosuquidar, respectively, showed increased affinities from P-gp. However, the QSAR could not predict how they would interact with unresolved structures of ABC transports and CYP450. Despite promising initial results, phase II and III trials for both tariquidar and zosuquidar were suspended early due to toxic side effects and low effects.(16, 20-23)

Subsequently, the fourth generation of P-gp inhibitors were generated by looking to nature, where natural products like flavonoids and their derivatives have been investigated, in addition to peptidomimetic and dual ligands. (2, 24-26) The four generations of small molecules are structurally divers, but a common factor is that the P-gp inhibitors are lipophilic.(16)

Despite decades of investigating several hundreds of molecules to this date no P-glycoprotein inhibitors are approved for clinical use and the challenge of P-gp mediated MDR is still not overcome.(2) A Few of these molecules have reached clinical trials, where they have failed due to lack of potency and high toxicity. The hope is that a new and potent *in vitro* P-gp inhibitors can be evaluated further and potentially are found to have high efficacy and low toxicity *in vivo*. (2, 16)

3 Dysoxylactam A (1)

3.1 Isolation, Chemical Structure and Biosynthesis of Dysoxylactam A (1)

Dysoxylum is a large genus of plants from the mahogany family (meliaceae), which are distributed from Australia to South East Asia. The wood of these trees are used in furniture trade, in addition to being investigated for their chemical and medicinal properties.(27) The bark and the leaves of the South Chinese plant, *Dysoxylum hongkongense*, have a long history of being used as a traditional medicine to treat malaria. However, the chemistry of the plant was not studied until 1998, where four novel dammarane triterpenoids and four known steroids were isolated from the leaves of the plant.(28) Since then, Yue et al. isolated from the leaves and twigs, a meroditerpenoid and four ascorbylated diterpenoids, as well as publishing the total synthesis of the latter.(29) Moreover, in 2019 they continued their search for biologically important and structurally interesting compounds from *Dysoxylum hongkongense* and their newest discovery was dysoxylactam A (**1**), shown in **Figure 3-1**, isolated from the bark of the plant.(3)

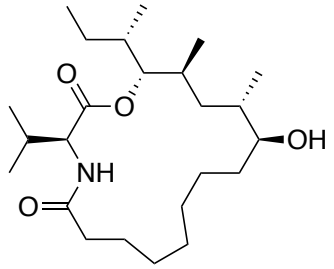

1

Figure 3-1 Structure of Dysoxylactam A (**1**).(3)

After the isolation, the structure of dysoxylactam A (**1**) was elucidated by a combination of the spectroscopic techniques, nuclear magnetic resonance (NMR) and mass spectrometry (MS). The IR spectrum showed absorptions at 3365, 3311, 1732, 1649 cm^{-1}, which suggest that the molecule includes hydroxyl, amino and two carbonyl groups. The relative configuration of the six stereogenic centers were established by extensive NMR studies, and X-ray crystallography of acylated dysoxylactam A (*p*-bromobenzoate derivative) confirmed the relative conformation as well as determined the absolute configuration.(3)

Dysoxylactam A (**1**) is classified as a cycloliopeptide, which is a rare and structurally divers class of natural products.(3) Cyclolipeptides are lactone or lactam rings constructed of a lipid tall coupled to a short peptide chain. This class of compounds are structurally divers due to

many combinations of lengths and functionality of the fatty acid in addition to the amino acid variation, configuration and coupling.(30) **1** consists of a 17-membred cyclic core that contains only one *L*-amino acid (*L*-valine), which is linked to the acid moiety of the lipid by an amide bond, as well as an ester bond between the acid moiety of the amino acid and a hydroxyl-group on the fatty acid.(3).

A biosynthetic pathway of dysoxylactam A (**1**) was proposed by Yue et al. It was suggested that the novel fatty acid dysoxylic acid (**5**) is the lipid tall of **1**, coupled to *L*-valine (**4**) through esterification and peptide formation, see **Scheme 3-1**. The highly branched dysoxylic acid (**5**) originate from 14-methylhexadeca-9,12-dienoic acid (**6**). It is suggested that **5** is generated by cascade of methylation, where the methyl groups are introduced by the alkylation agent *S*-adenosylmethionine (SAM). The electrophilic intermediate is quenched by hydroxylation, the synthesis of **5** for **6** is depicted in **Scheme 3-2**.(3)

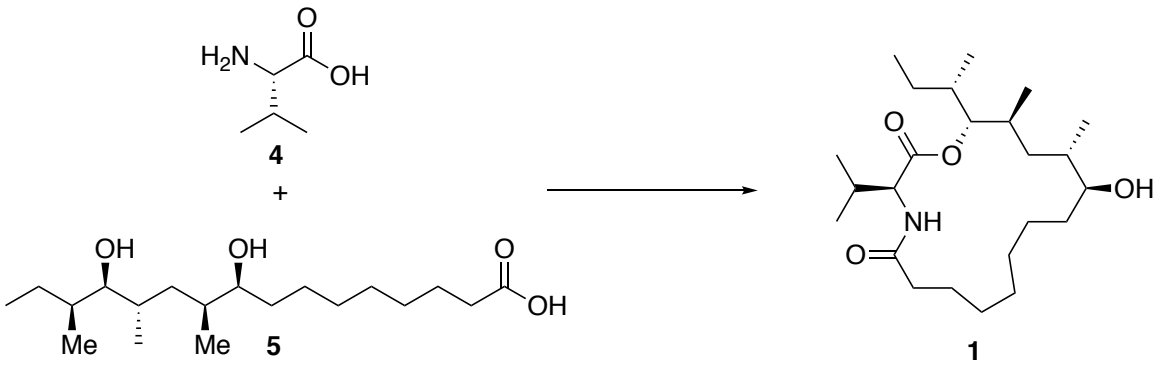

Scheme 3-1 Proposed biosynthesis of dysoxylactam A (**1**).(3)

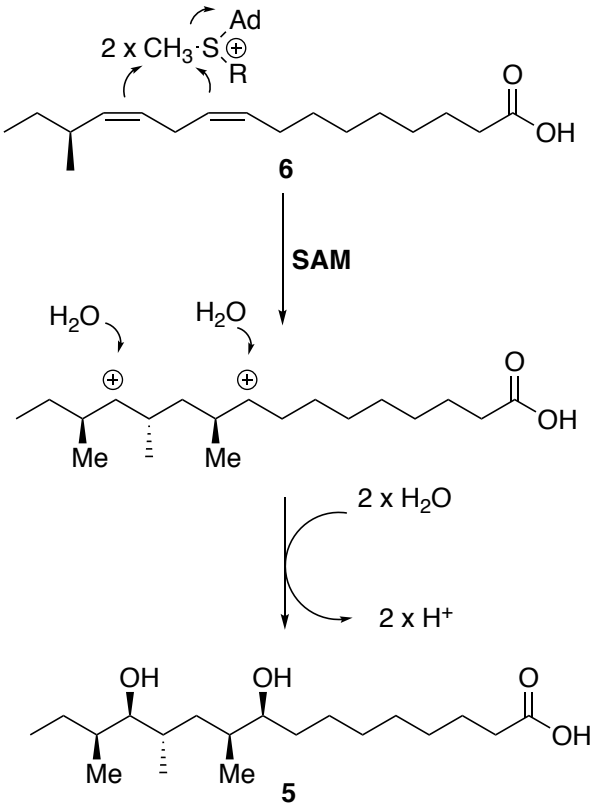

Scheme 3-2 The possible biosynthesis of dyoxylic acid (**5**) from 14-methyl hexadeca-9, 12-dienoic acid (**6**) by a cascade of methylation and hydroxylation reactions.(3)

Fatty acid are polyketides, biosynthetically derived from the acetate pathway. They are acetate metabolites, and their biosynthesis are aided by enzyme fatty acid synthase (FAS). The biosynthesis of linear fatty acids starts with condensation of one acetyl-CoA with one malonyl-CoA, to generate the poly β-keto ester. The poly β-keto ester is then reduced to the corresponding β-hydroxyl, which is dehydrated and reduced. To elongate the chain several condensation reactions occur with malonyl-CoA, where two carbon units are added each time, until the desired length is obtained. Coenzyme A is then hydrolyzed to form the saturated fatty acid. The general fatty acid synthesis is shown in **Scheme 3-3**.(31) However, for the branched **6**, the starting unit is not acetyl-CoA but 2-methylbutyryl-CoA derived from isoleucine and six units of malonate-CoA is added to form **6**.(3)

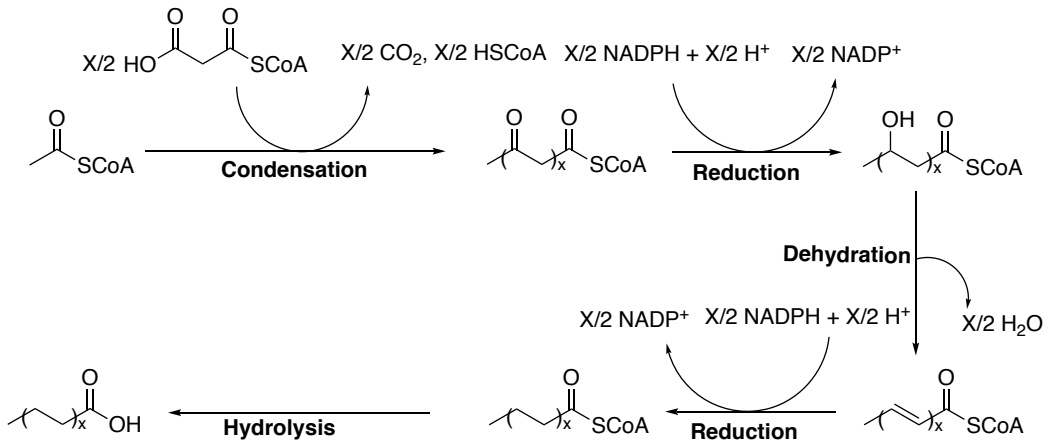

Scheme 3-3 Biosynthesis of fatty acids from acetyl-CoA condensation with malonyl-CoA reduction, dehydration, reduction and hydrolysis to obtain the desired fatty acid.(31)

3.2 Biological Activity of Dysoxylactam A (1)

After the isolation of dysoxylactam A (**1**) in 2019, the potency of dysoxylactam A (**1**) as a P-gp inhibitor was evaluated by Yue et at. The study was conducted with the tumour cells K262, MCF7 and KB and their analogue multidrug-resistant strain K562/ADR, MCF7/ADR and KBV200, which overexpress P-gp. Dysoxylactam A (**1**) was tested in combination with the chemotherapeutic agents adriamycin, vincristine or paclitaxel, that are known P-gp substrates. A positive control of the study was performed with the first generation P-gp inhibitor verapamil (**2**).(3)

The half maximal inhibitory concentration (IC_{50}) values and the fold reversal (RF) values of the study on the resistant cancer cells, are shown in **Table 3-1**. As a potency parameter the RF-value provides information about how the sensitivity is restored by using a P-gp inhibitor in combination of the anticancer drug compared to its individual performance. By looking at these values it shows that the resistance of the chemotherapeutic agent is reversed in the MDR cancer cells, for both dysoxylactam A (**1**) and verapamil (**2**). The RF-value for dysoxylactam A (**1**) ranges from 28.4 to 1039.7 at a noncytotoxic concentration of 10 μM, while the RF-values for verapamil (**2**) ranges from 15.1 to 143.8 at the same concentration. Furthermore, the use of P-gp inhibitors displayed no increased sensitivity with the non-resistant cancer cells. In addition to reversing the resistance, the RF-values of dysoxylactam A (**1**) are always higher than those of verapamil (**2**), which reveals that dysoxylactam A (**1**) is a more potent P-gp inhibitor.(3)

Table 3-1: IC_{50}-values and the RF-value of the three chemotherapeutic agent individually or in combination with dysoxylactam A (**1**) and verapamil (**2**) for the three resistant tumour cells K562/ADR, MCF7/ADR and KBV200. The RF-value was calculated by dividing the IC_{50} value of the chemotherapeutic agent individually by the chemotherapeutic agent with either dysoxylactam A (**1**) or verapamil (**2**) as P-gp inhibitor.(3)

Drug	MCF7/ADR		K562/ADR		KBV200	
	IC_{50} [nM]	**RF-value**	**IC_{50}** [nM]	**RF-value**	**IC_{50}** [nM]	**RF-value**
Adriamycin	12295.0 ± 2043.5	-	4836.0 ± 591.1	-	1800.5 ± 1611.2	-
Adriamycin + 1	388.2 ± 8.6	31.7	57.9 ± 9.5	83.5	22.9 ± 7.7	78.5
Adriamycin + 2	598.3 ± 41.5	20.5	303.3 ± 4.1	15.9	71.7 ± 19.6	25.1
Vincristine	7820.5 ± 1068.4	-	648.0 ± 52.8	-	188.9 ± 39.5	-
Vincristine + 1	20.5 ± 9.5	381.4	0.6 ± 0.1	1039.7	1.1 ± 0.4	174.3
Vincristine + 2	58.5 ± 1.4	133.8	5.7 ± 1.4	113.6	1.3 ± 0.2	143.8
Paclitaxel	1656.0 ± 244.7	-	953.7 ± 9.2	-	102.3 ± 1.6	-
Paclitaxel + 1	58.3 ± 32.1	28.4	2.1 ±1.4	469.7	1.6 ± 0.1	63.1
Paclitaxel + 2	90.0 ± 13.9	18.4	63.0 ± 9.6	15.1	2.5 ± 0.4	40.2

To further determine the inhibitory function and potency of dysoxylactam A (**1**), a Rho -123 assay was used to determine if Rho-123 accumulated in the MCF7/ADR cell in the presence of dysoxylactam A (**1**) and verapamil (**2**). The results proved that dysoxylactam A (**1**) increased the accumulation of Rho-123 inside the cell, in addition to reducing the efflux of adriamycin. In the multidrug resistant cancer cells evaluated, the P-gp expression was not altered in the presence of dysoxylactam A (**1**). By taking the results of the study together, it shows that dysoxylactam A (**1**) are able to revers multidrug resistance by inhibiting P-gp efflux. Dysoxylactam A (**1**) has therefor proven to be a strong candidate to reverse P-gp-mediated MDR, and as no P-gp inhibitors are currently approved. Further research of dysoxylactam A (**1**) is urgently needed to determine the *in vivo* efficacy, drug-drug interactions, pharmacokinetics and pharmacodynamics as well as the potential toxic properties of dysoxylactam A (**1**).(3)

4 Synthesis of Dysoxylactam A (1)

4.1 Review of Previously Reported Synthesis of Dysoxylactam A (1)

The interesting chemical structure and the highly promising bioactivity of dysoxylactam A (**1**) has so far lead to the development of three total synthesis of the novel compound. The first synthesis of **1** was published in January 2020, almost one year after the isolation of the natural product. The total synthesis by S. Raghavan and S.S. Chandankar is shown in **Scheme 4-1**. The first step of the synthesis was a Merck-Carreira propargylation of acetaldehyde **7**. The propargylic alcohol product was mesylated before the it was coupled to aldehyde **10**, using the Marshall's propargylation protocol and the resulting alcohol was TBS-protected to give **11**. Alkyne **11** was completely hydrogenated, while simultaneously removing the benzyl ether to give primary alcohol **12**. Alcohol **12** was oxidized to the corresponding carboxylic acid **13**, to which the chiral auxiliary **14** was introduced by mixed-anhydride activation. The chiral auxiliary gave a distereoselective methylation of **15** to give **16**. After hydrolysis of the imide, the Weinreb amide **17** was generated, to enable formation of propargylic ketone **19** in a reaction with the lithium acetylide of alkyne **18**. Stereoselective reduction of the ketone **19** with the Noyori catalyst gave the propargylic alcohol which was protected as its TBDPS ether, followed by a selective deprotection of the TBS ether using PPTS to afford alcohol **20**. *N*-Boc-L-valine **21** was coupled to **20** by a DCC-activated esterification which resulted in an inseparable epimeric mixture of **22**. Alkyne **22** was reduced, while also cleaving the benzyl ether to free the alcohol before it was oxidized to the corresponding acid **23**. The *N*-Boc-protection group was cleaved followed by the key intramolecular amide coupling with HATU to finally generate a separable mixture of the two epimers. Only the epimer with the correct configuration was TBDPS-deprotected to afforded macrocyclic **1**. The total synthesis of dysoxylactam A (**1**) was achieved in 16 step with the overall yield of 22.2%.(6)

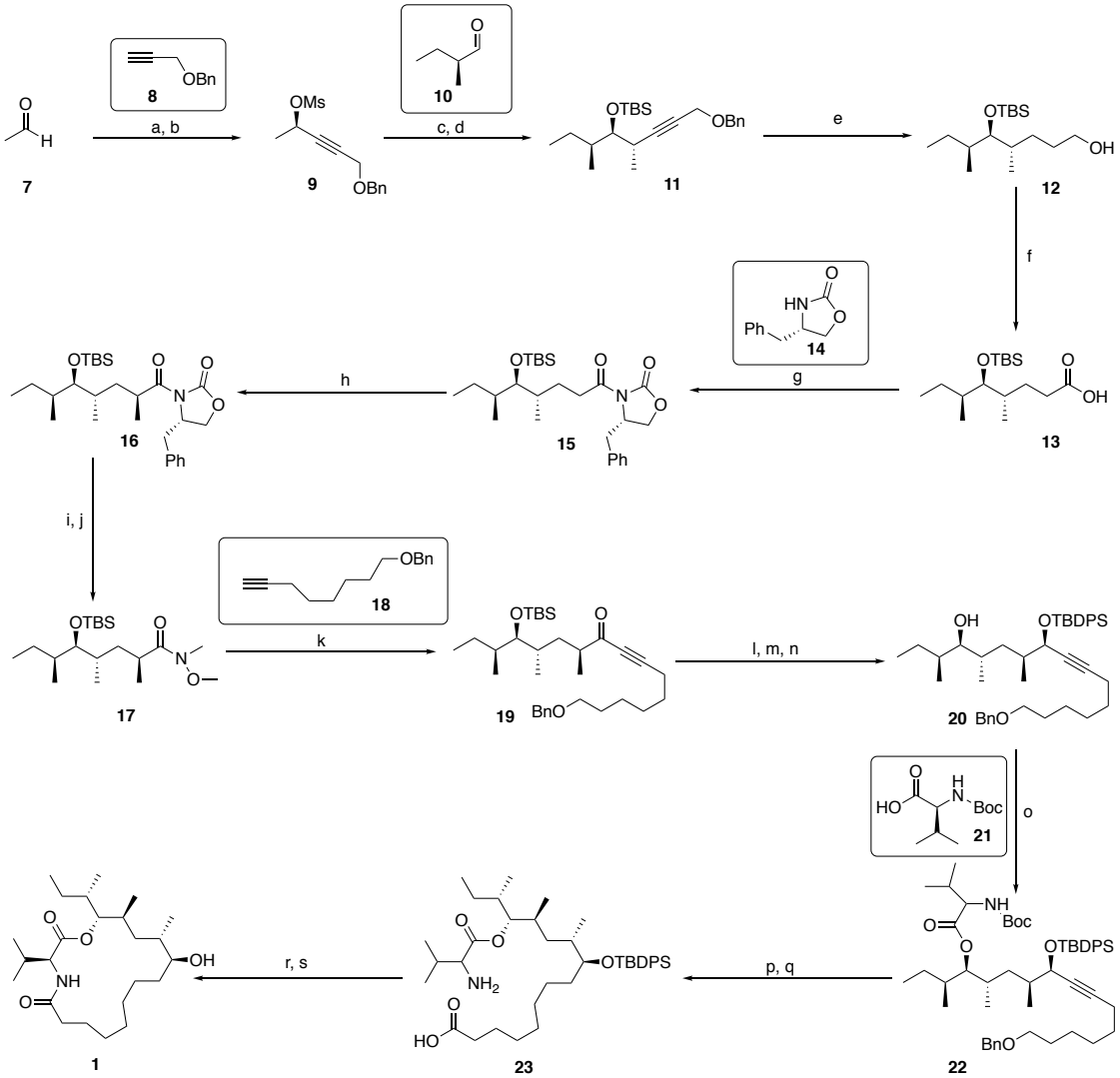

Scheme 4-1 a) $Zn(OTf)_2$ (1.2 eq.), Et_3N (1.2 eq.), **8** (1.2 eq.), (+)-N-methylephedrine (1.1 eq.), toluene, 0℃- 15 ℃, 18 h, 96% ee, 90%. b) Et_3N (2.5 eq.), MsCl (1.2 eq.), CH_2Cl_2, 0 ℃, 1 h, 97%. c) **10**, $Pd(Ph_3)_2Cl_2$ (0.05 eq.), Et_2Zn (3.0 eq.), THF, 0 ℃, 2 h, 86%, 92:8 ds, d) 2,6-Lutidine (2.5 eq.), TBSOTf (1.1 eq.), CH_2Cl_2, −40 ℃, 30 min, 98% e) 10% Pd-C (10%Wt/Wt), EtOAc, rt, 12 h, 98% f) TEMPO (0.20 eq.), BIAB (2.0 eq.),CH_3CN:H_2O (2:1), 0 ℃ - rt, 2 h, 97% g) Et_3N (3.0eq.), Piv-Cl (1.1 eq.), LiCl (1.0 eq.), **14**, −10℃, 1 h, 93%, h) NaHMDS (1.2 eq.), MeI (2.0 eq.), −78 ℃, 2.5 h, 87% i) H_2O_2 (3.0 eq.), LiOH (3.0 eq.), THF, 0 ℃ - rt, 2 h, 96% j) MeN(OMe)H·HCl (1.1 eq.), *i*Pr_2NEt (5.0 eq.), EDC·HCl (1.1 eq.), HOBt (1.0 eq.), 0 ℃, to rt, 3 h, 95% k) **18** (2.0 eq.), *n*-BuLi (2.0 eq.), THF, −78℃- 0℃, 1.5 h, 91% l) Noyori cat. (0.01 eq., EtOAc, H_2O (1:1), HCOONa (10.0 eq.), BMIM-PF_6 (0.02 eq.), 18 h, 92%, >95:<5 ds m) Imidazole (2.2 eq.), TBDPS-Cl (1.05 eq.), CH_2Cl_2, 0 ℃- rt, 1 h, 98% n) PPTS (0.025 eq.), MeOH, 50 ℃, 12 h, 85% o) DCC (2.0 eq.), DMAP (1.0 eq.), **21** (2.0 eq.), rt, 6 h, 97% p) 10% Pd-C (10%Wt/Wt), EtOAc, rt, 6 h, 98% q) TEMPO (0.2 eq.), BIAB (2.0 eq.),CH_3CN:H_2O (2:1), 0 ℃ - rt, 2 h, 98% r) TFA:CH_2Cl_2 (2.5:7.5), 0 ℃ - rt, 2 h, DIPEA (2.5 eq.), HATU (1.2 eq.), 0 ℃ - rt, 3h, 92% overall yield s) HF/pyridine (2.0 eq.)), 0 ℃ - rt, 1 h, 95.(6)

The second synthesis of **1** was published by Ye et al. one month later, in February of 2020. This synthesis is shown in **Scheme 4-2**. The starting point for the synthesis was the commercially available (*R*)-Roche ester **24**, which was transformed in a three step procedure to the TBS-protected carbamate **25**.(32) Carbamate **25** was converted to the primary pinacol boronic ester **26**, followed by the Aggarwal homolongation which provided the secondary boronic ester **27** in high stereochemical outcome. The Matteson homolongation procedure was utilized to afford alcohol **28**, which was then oxidized to aldehyde **29**. *Syn*-homoallylic alcohol **30** was obtained through the Brown crotylation of aldehyde **29** and cis-2-butene. *N*-Cbz-L-valine **31** was TCBC-activated to enable the Yamaguchi esterification of **30** to afford **32**, epimerization was not observed by NMR analysis. The alkene was hydrogenated, under the same condition the benzyl ether and TBS ether was cleaved. Amide **34** was provided by the amide coupling with acid **33**, mediated by HATU. To install the second alkene, a Krische allylation was conducted directly from the primary alcohol **34**. The alcohol **35** was TMS-protected and the crucial cyclization was performed by a ruthenium-catalyzed ring-closing metathesis (RCM), the macrocyclic alkene was hydrogenated accompanied by the TMS-removal to give **1**. The totals synthesis of dysoxylactam A (**1**) was attained by 15 steps as the longest linear sequence with an overall yield of 8.8%. (4)

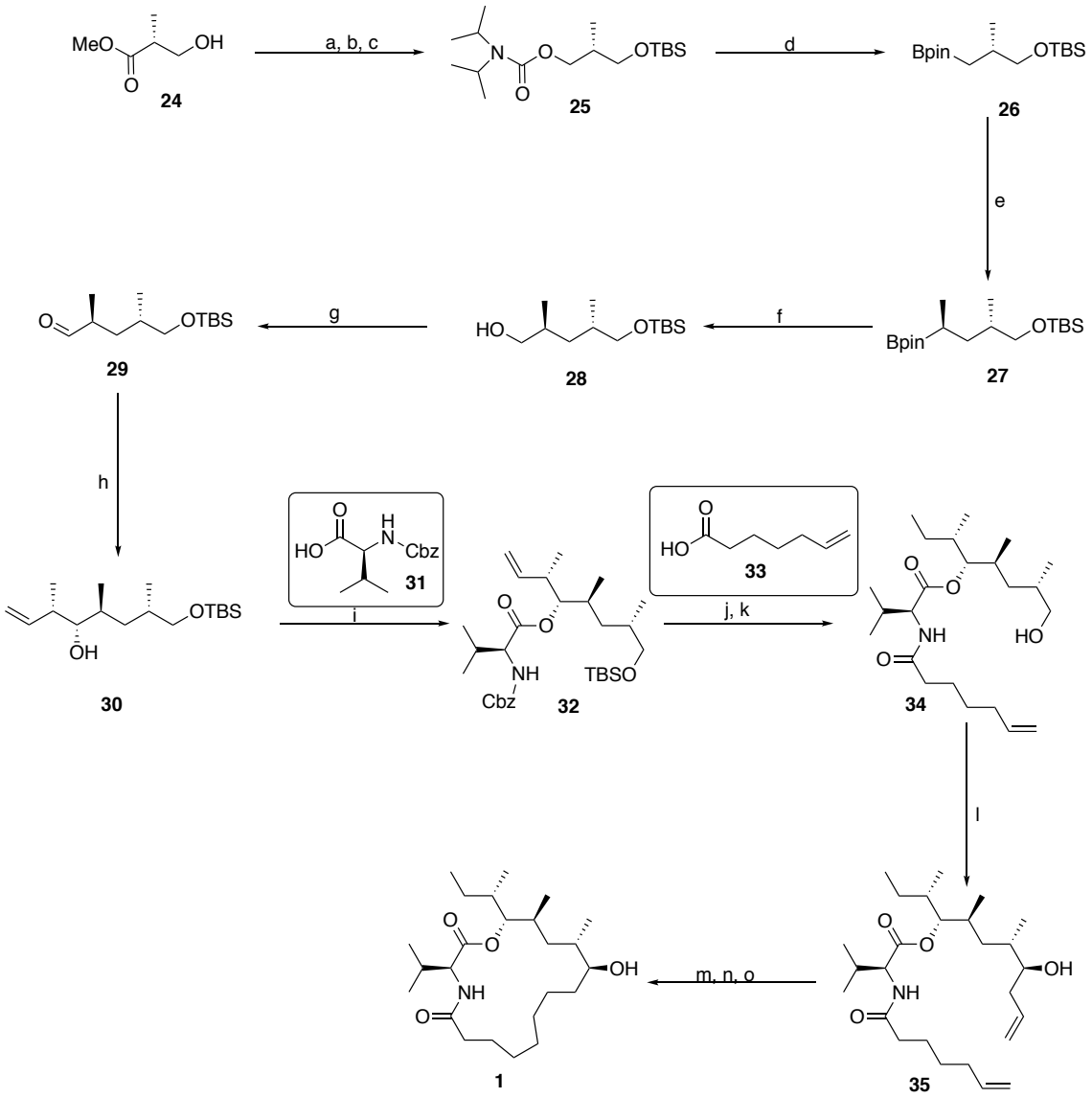

Scheme 4-2 a) TBSCl (1.4 eq.), imidazole (2.4 eq.), DMAP (0.12 eq.), CH_2Cl_2, rt, 2 h b) DIBAL-H (2.2 eq.), THF, −78 ℃, 2 h, 30 min c) Cb-Cl (1.5 eq.), Et_3N (1.5 eq.), CH_2Cl_2, 40 ℃, 48 h (32) d) *s*-BuLi (2.0 eq.), TMEDA (2.2 eq.), HBpin (3.0 eq.), Et_2O, −78 ℃, to 40 ℃, 13 h, 83% e) EtOCb (3.0 eq.), *s*-BuLi (3.0 eq.), (+)-sparteine (4.0 eq.), Et_2O, −78 ℃, to 50 ℃,18 h, >20;1 dr, 91% f) iodochloromethane (20.0 eq.), *n*-BuLi (5.0 eq.), THF, $NaOH/H_2O_2$, 12 h, 90% g) $NaHCO_3$ (3.0 eq.), TCCA (1.2 eq.), TEMPO (0.1 eq.), 0 ℃, 2 min, 99% h) *n*-BuLi (2.0 eq.), *t*-BuOK (2.0 eq.), *cis*-butene (5.0 eq.), (+)-$(Ipc)_2$BOMe (3.0 eq.), $BF_3{\cdot}Et_2O$ (4.0 eq.), THF, −78 ℃- 60 ℃, 12 h, >20:1 dr, 87% i) TCBC (3.0 eq.), Et_3N (4.0 eq.), DMAP (5.0 eq.), **31** (2.0 eq.), toluene, 0 ℃, 12 h, 91%, j) $PdCl_2$ (0.4 eq.), H_2, MeOH, rt, 4 h, k) **33**, DIPEA (10.0 eq.), HOAt (2.0 eq.), HATU (4.0 eq.), DCM/DMF (20:1), 10 h, rt, 58% for two steps l) cat [Ir] (0.4 eq.), 4-CN-3-NO_2BzOH (1.0 eq.), allyl acetate (10.0 eq.), Cs_2CO_3 (1.2 eq.), H_2O, THF, 100 ℃, 72 h, 71%, dr >20:1 m) TMSOTf (10.0 eq.), Et_3N (20.0 eq.), 5 h, rt, 92% n) Grubbs-II (0.1 eq.), CH_2Cl_2, 40 ℃, 24 h, 70% o) $PdCl_2$ (0.5 eq.), H_2, MeOH, 4 h, rt, 99%.(4)

The third synthesis of **1** was published in July of 2020 by B. Yu and D. P. Reddy. (see **Scheme 4-3**) First, the aldol adduct **38** was obtained by an Evans *syn*-aldol reaction, of **36** and **37** which established two stereogenic centers successfully. The chiral auxiliary was removed under Soai's reductive conditions to give a 1,3-diol, that was directly protected as its benzaldehyde acetal. The acetal was regioselectively cleaved at the less hindered oxygen, leaving **39** as a primary

alcohol, which was converted to the corresponding iodoalkane **40**. In an alkylation reaction of **40** with the chiral lithium enolate of **41**, the *anti*-methyl **42** was afforded. The chiral auxiliary was hydrolyzed to the carboxylic acid, which was reduced to the corresponding primary alcohol. The primary alcohol was oxidized to aldehyde **43** under Dess-Martin periodinane conditions. The aldehyde **43** was reacted in another Evans *syn*-aldol reaction with **36**, to give the aldol adduct **44**. The chiral auxiliary was removed reductively to give the 1,3-diol, where the primary alcohol was regioselectively tosylated to give **45**. The chain was homolongated by treatment with methyllithium in the presence of CuI to give the key polyketide fragment **46**. *N*-Boc-*L*-Valine **21** was EDCI-activated to enable esterification, the ester **47** was given as an inseparable mixture of the two epimers. The *N*-Boc protection group was removed to prepare for the HATU-mediated amide coupling with acid **48** to give diene **49**, still as an inseparable epimeric mixture. **1** and its epimer was accessed by a ruthenium-mediated RCM followed by hydrogenation of the macrocyclic alkene accompanied by benzyl ether removal. The total synthesis was accomplished with 17 step as the longest linear sequence with an overall yield of 9.5%.(33)

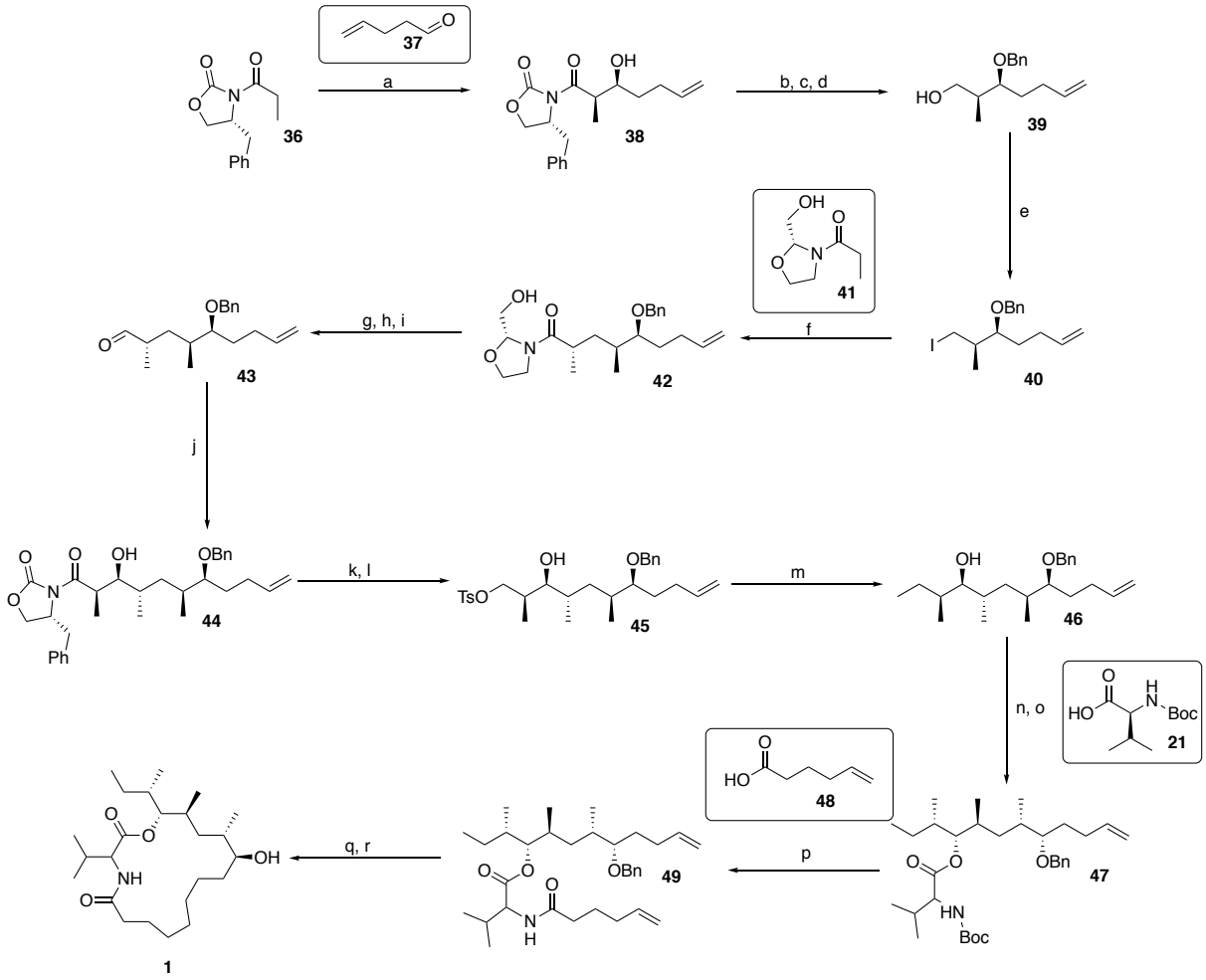

Scheme 4-3 a) **37** (1.1 eq.), n-Bu_2BOTf (1.1 eq.), DIPEA (1.1 eq.), CH_2Cl_2, −78 ℃ - rt, 6 h, 89% b) $LiBH_4$ (685 eq.), Et_2O, MeOH, 0 ℃ - rt, 1 h c) $PhCH(OMe)_2$ (2.0 eq.), CS (0.1 eq.), CH_2Cl_2, rt , 2 h, 84% over 2 steps, d) DIBAL-H (2.0 eq.), CH_2Cl_2, −20 ℃, 1 h, 93% e) I_2 (2.2 eq.), imidazole (2.0 eq.), Ph_3P (2.0 eq.), THF, 0 ℃ - rt, 1 h f) **41**(1.3 eq.), LDA (2.9 eq.), HMPA (2.7 eq.), THF, −78 ℃ - rt, 6 h, >98: ds, 82% g) 1N HCl, 70℃, 6 h h) LAH (3.1 eq.), THF, 0 ℃ - rt, 2 h, 95% yield over 2 steps i) DMP (1.5 eq.), CH_2Cl_2, 0 ℃ - rt, 2 h j) **36** (1.1 eq.), n-Bu_2BOTf (1.1 eq.), DIPEA (1.1 eq.), CH_2Cl_2, −78 ℃ - rt, 6 h, >20:1 dr, 78% k) $LiBH_4$ (685 eq.), Et_2O, MeOH, 0 ℃ - rt, 2h, 87% l) TsCl (1.1 eq.), Bu_2SnO (0.2 eq.), Et_3N (2.0 eq.), DMAP (cat.) CH_2Cl_2, 0 ℃ - rt, 6 h, 89% m) MeLi (10.0 eq.), CuI (5.0 eq.), Et_2O, −20 ℃, 2 h, 86% n) **21** (2.0 eq.), EDCl (2.0 eq.), DMAP (5.0 eq.), CH_2Cl_2, rt, 6 h o) TFA, CH_2Cl_2, rt, 1 h p) **48** (1.9 eq.), HATU (1.9 eq.), DIPEA (4.8 eq.), CH_2Cl_2, 0 ℃ - rt, 6 h, 72% yield over 2 steps q) Grubbs-II (0.2 eq.), CH_2Cl_2, 50 ℃, 16 h r) H_2, Pd-C, THF, rt, 6 h, 72% yield over 2 steps.(33)

4.2 The New Synthetic Approach to Dysoxylactam A (1)

The aim of this project is to investigate a new synthetic approach to dysoxylactam A (**1**). As a highly functionalized 17-membred macrocyclic lipid, the complex structure of **1** in combination with its six stereogenic centers involves the incorporation of stereoselective reactions as well as the search commercially available chiral starting materials. As a complex bioactive molecule the total synthesis of **1** will expand over multiple steps. The functional groups generated in one step might not be compatible with the reaction conditions of the next step and protective groups

are essential for the success of the synthesis. The protection groups temporarily block other reactive sites in the molecule to avoid undesired side reactions, and they should be stable under the reaction conditions. As a part of the synthetic plan the installation and removal of protections groups must be included. The addition and removal of a protection group must be selective to allow for orthogonal protection strategies.

The synthetic plan for the synthesis of dysoxylactam A (**1**), is provided as a retrosynthetic analysis and the retrosynthetic disconnections are outlined in **Scheme 4-4, Scheme 4-5**, **Scheme 4-6** The crucial ring closing is envisioned to be by a Yamaguchi macrolactonization of **63**. The synthesis of propargylic alcohol **60a** take advantage of the stereoselective Carreira alkynylation that enable C-C coupling of the two key fragments **59a** and **72** and the formation of a new stereogenic center.

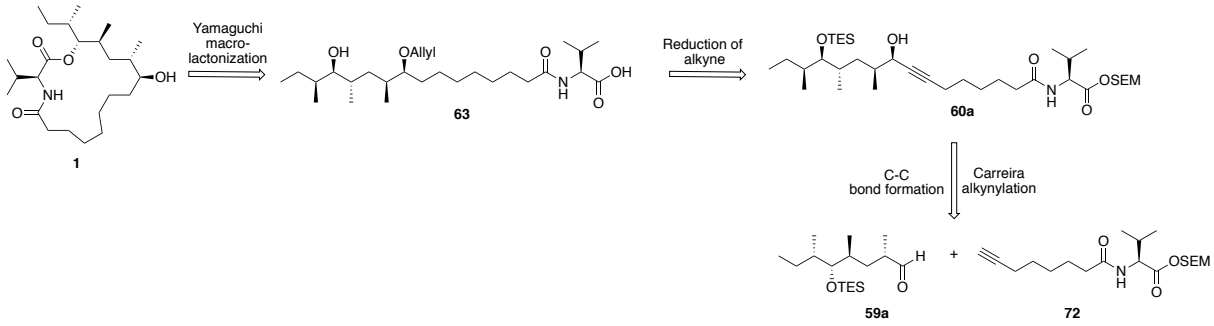

Scheme 4-4 Retrosynthetic disconnections of **1.**

Aldehyde **59a**, can then be obtained by oxidation of the corresponding primary alcohol **58a**, generated by deoxygenation of the aldol adduct **53**. The Paterson aldol reaction of ketone **52** and aldehyde **10** is anti-and facial-selective and two new stereogenic centers can be introduced. The aldol reaction utilizes two chiral starting materials and the branch of the polyketide fragment can be installed in one reaction. Ketone **52** can be prepared through a Grignard reaction of the Weinreb amide **51** and an *O*-benzylation of the commercially available **24**. The chiral aldehyde **10** is derived from oxidation of the commercially available primary alcohol **65**.

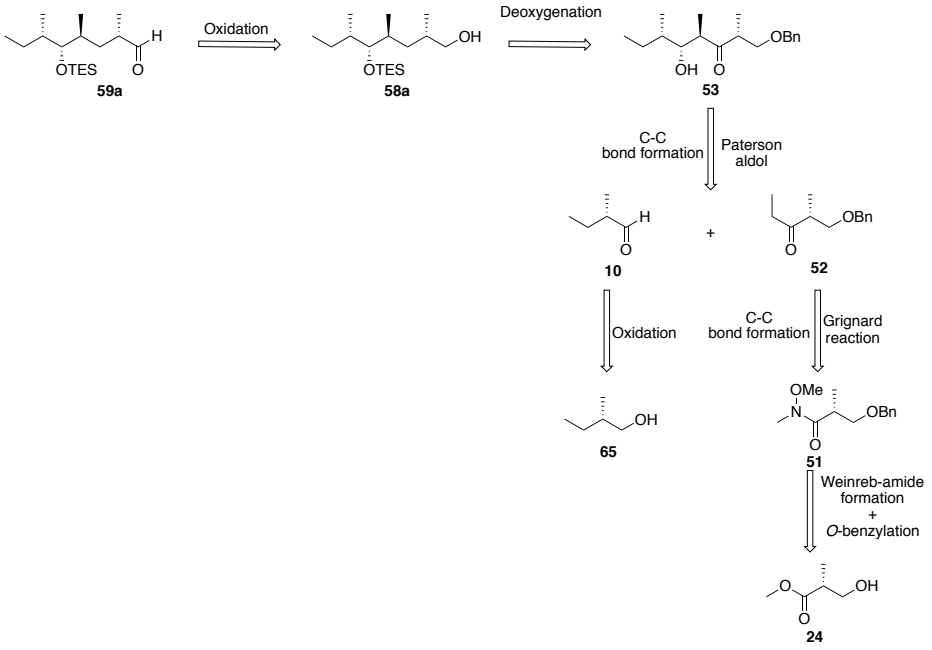

Scheme 4-5 Retrosynthetic disconnections of **1.**

The other major fragment **72** can be prepared through an amide coupling of **71** and **67**. The acid **71** can be obtained by hydrolysis of the Ohira-Bestmann product **70**. The Ohira-Bestmann reaction is a homolongation of aldehyde **69**, which can be obtained through ozonolysis of commercially available cycloheptene **68**.

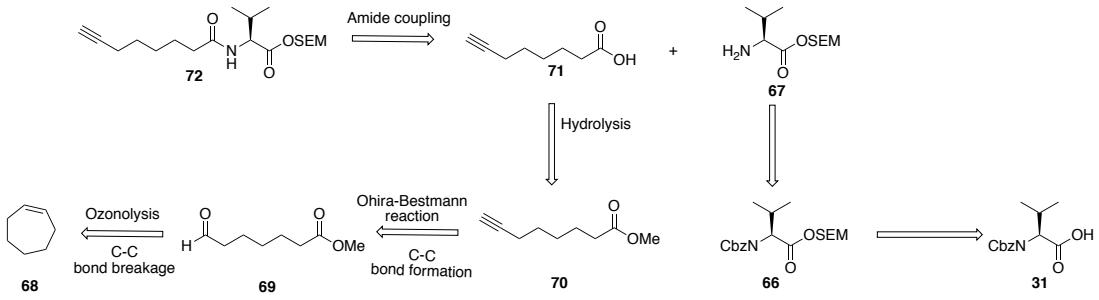

Scheme 4-6 Retrosynthetic disconnections of **1.**

The stereochemical issues of **1** is tackled by the use of three commercially available chiral starting materials, the (*R*)-Roche ester **24**, the primary alcohol **65** and the *N*-Cbz-protected *L*-Valine **31**. The other chiral centres in **1** can be introduced by the Ian Patterson aldol reaction and the Carreira alkynylation. In addition, free alcohols are protected as either its benzyl ether, silyl ether or allyl ether at different stages in the synthesis to allow for orthogonal protection.

5 Mechanisms

5.1 *O*-Benzylation of Alcohols

Benzyl ethers can be synthesized from alcohols through an acid catalysed reaction with benzyl 2,2,2-trichloroacetimidate. Benzyl 2,2,2-trichloroacetimidate is an electrophilic transfer agent that can be prepared by reacting the benzyl alcohols with trichloroacetonitrile.(34). The mechanism of the triflic acid catalysed reaction of alcohol **24** with benzyl 2,2,2-trichloroacetimidate is shown in ***Scheme 5-1***.(35)

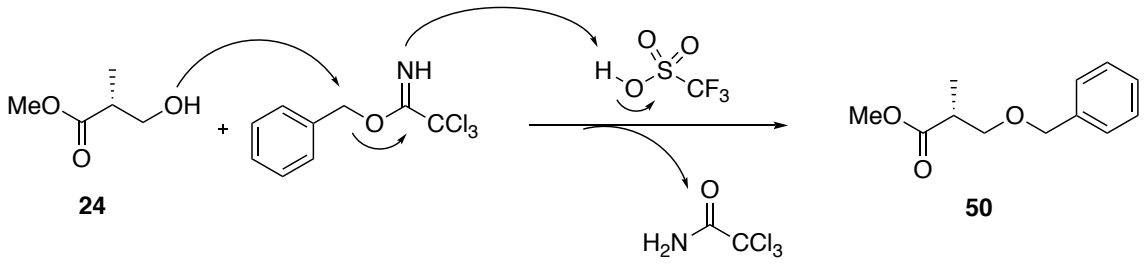

Scheme 5-1 The mechanism of the triflic acid catalysed reaction of alcohol **24** with benzyl 2,2,2-trichloroacetimidate to form benzyl ether **50**.(35)

5.2 The Grignard Reaction

The Grignard reaction is named after Victor Grignard, who was awarded the Nobel prize in 1912 for the discovery of organomagnesium halides.(36) The Grignard reaction is an important tool for formation of new carbon carbon bonds and are widely used in organic synthesis.(37) The reaction is based upon the Grignard reagent, which is a strong base and a highly reactive carbon nucleophile.(38) It is classified as an organometallic reagent because it is prepared by reacting an alkyl or aryl halide magnesium metal.(39) It is mainly used in the reaction with carbonyl compounds to generate various alcohols, but also with other electrophiles like CO_2, nitriles and imines to obtain carboxylic acids, ketones and amines, respectively.(38)

In Grignard reactions with aldehydes and ketones, one equivalent of the Grignard reagent can be added to form the secondary and tertiary alcohol, respectively. However, carbonyl compounds with a potential leaving group are able to add two equivalents of the Grignard reagent. For esters, after the first addition of the Grignard reagent the tetrahedral intermediate is formed and the alkoxide is eliminated to form the ketone. The ketone cannot be isolated, due to the direct addition of a second equivalent of the reagent to give a tertiary alcohol.(38) For synthesis of ketones from esters, the ester can be converted to the corresponding Weinreb amide, to avoid the over-addition of the Grignard reagent.(40) The transformation of ester **50**

can be carried out by activating the *N,O*-dimethylhydroxylamine by the non-nucleophilic isopropyl magnesium chloride. The deprotonated amine is activated for a nucleophilic attack of the ester, in the tetrahedral adduct the alkoxide will be eliminated to afford amide **51**. The mechanism for the formation of the Weinreb amide **51** is depicted in **Scheme 5-2**.(41)

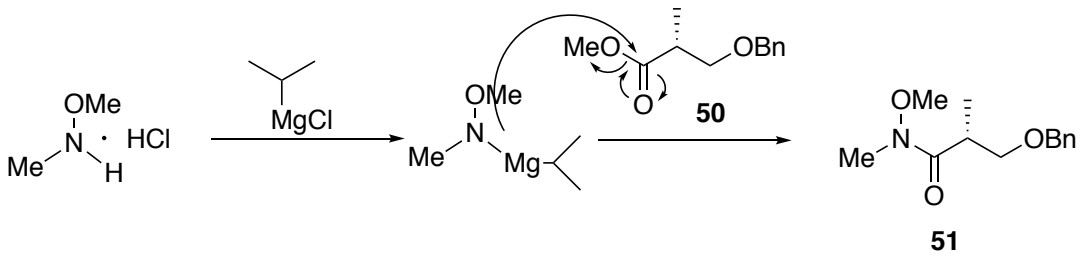

Scheme 5-2 The mechanism for addition of the activated *N,O*-dimethylhydroxylamine to the ester **50** to form the Weinreb amide **51**.(41)

With Weinreb amide **51** in place, it can be reacted with a nucleophilic Grignard reagent like ethyl magnesium bromide, shown in **Scheme 5-3**. The Weinreb amide **51** provide a chelate transition state which allow for only one equivalent of ethyl magnesium bromide being added, whereas the ester **50** would make it possible for the addition of two equivalents and a tertiary alcohol would be formed. The chelate formed during the reaction is destabilized by an acidic work-up to give the desired ketone **52**.(40)

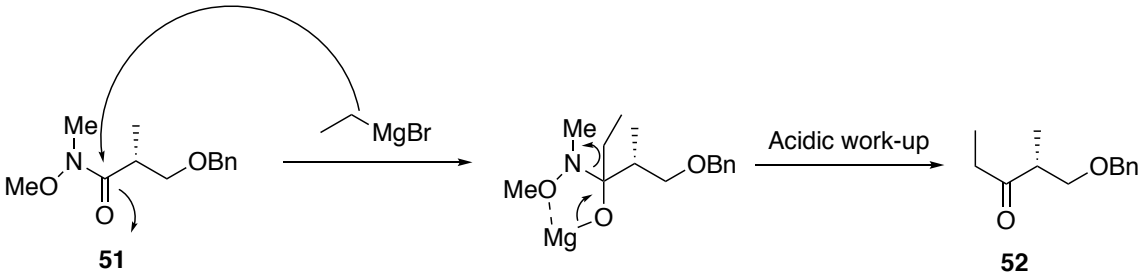

Scheme 5-3 The mechanism for the Grignard reaction of Weinreb amide **51** with EtMgBr to form ketone **52**.(40)

5.3 The Aldol Reaction

The aldol reaction is another powerful carbon carbon coupling reaction. From a retrosynthetic perspective it is a 1,3-disconnection, that allows for regio- and stereochemical control and is widely used in synthesis of complex molecules. The basis of the reaction is the formation of the enolate, where the carbon has a nucleophilic character that can attack an electrophilic aldehyde generating the aldol adduct. The reaction conditions have a significant effect on the structure and the stereochemistry of the product. Different variations of solvents, temperatures,

bases and the use of other reagents must be carefully considered to direct the aldol addition to achieve the specific regio- and stereochemical outcome.(38)

The first step of the aldol reaction mechanism is the deprotonation of the α-hydrogen of the carbonyl group. Asymmetric starting materials like ketone **52** have two possible α-hydrogens that can generate two different enolates, see **Scheme 5-4**. The thermodynamic enolate will go through the deprotonation that will lead to the most stable enolate, whereas the kinetic product is the enolate that is formed faster. To enable a regioselective reaction, using low temperatures and aprotic solvents will favour the kinetically controlled deprotonation.(38)

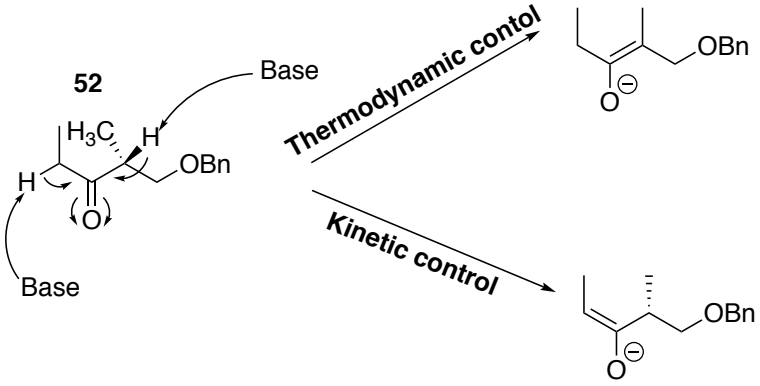

Scheme 5-4 The thermodynamic and dynamic deprotonation of ketone **52**.(38)

Similar to substituted alkenes, the enolate can have either *Z*-or *E*-conformation. The conformation of the enolate decide the stereochemical relationship between the hydroxyl and the methyl group in the aldol adduct. The *Z*-and *E*-conformation give the *syn*-and *anti*-isomers, respectively. The formation of either *Z*-or *E*-conformation can be directed by using dialkyl boron reagents to form boron enolates. Boron enolates give enhanced stereoselectivity with its compact structure in cyclic transition state due a short O-B bond. By preparing the boron enolate with the bulky dicyclohexyl borane chloride and a small tertiary amine the formation of the *E*-conformation is favoured. In contrast, boron enolates prepared from *n*-butyl boron triflate with a bulky amine favours the formation of the *Z*-conformation. The boron *E*-enolate can therefore be prepared by using dicyclohexyl borane chloride and triethyl amine in a reaction with the ketone at low temperature. After the formation of the boron *E*-enolate, the electrophilic aldehyde can be added, and the mechanism of the addition is based upon the six membered cyclic transition state, shown in **Scheme 5-5**.(42, 43)

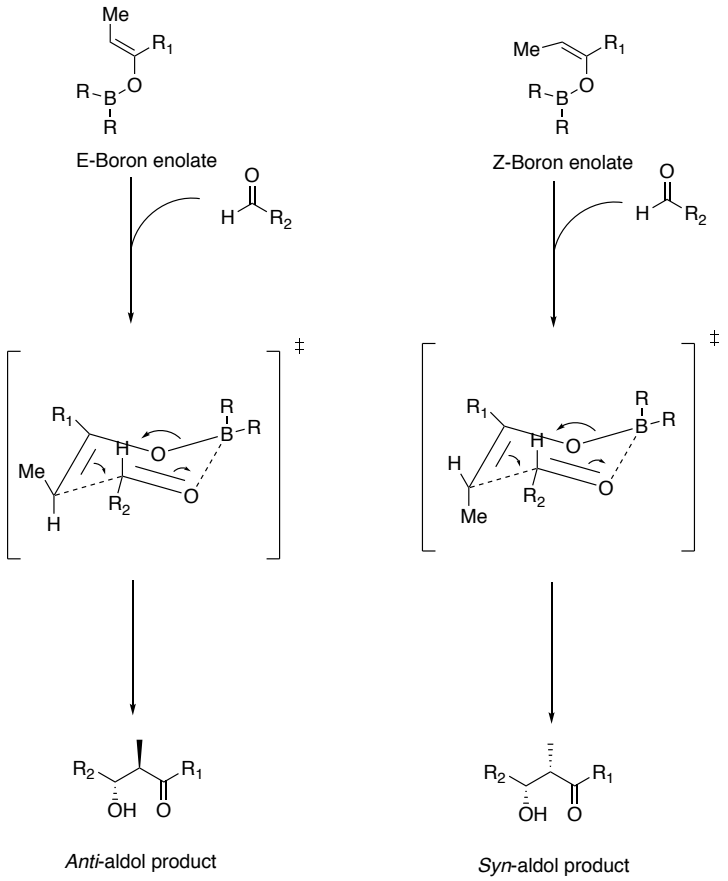

Scheme 5-5 The cyclic transition state for *E*- and *Z*-boron enolate for the formation of *anti*-and *syn*-aldol adduct, respectivly.

Facial selectivity is also an important factor to consider in the aldol reaction. Ketones with inherent chirality of a α-or β-substituent can direct the facial selectivity, otherwise temporary chiral auxiliaries can be installed.(44) Therefore, two transition states are possible for the addition of the *E*-boron enolate of ketone **52** to aldehyde **10**, the two transition states are shown in **Scheme 5-6**. The favored adduct is the one where an additional stabilizing hydrogen bond can be formed in the transition state. In the case of ketone **52**, the stereogenic center of the α-substituent allow for this hydrogen bond only in the transition state to the left and the (2*R*, 4*R*, 5*R*, 6*S*)-aldol adduct **53** is favored over the (2*R*, 4*S*, 5*S*, 6*S*)-aldol adduct **53***.The overall aldol reaction mechanism is given in **Scheme 5-7**.(45)

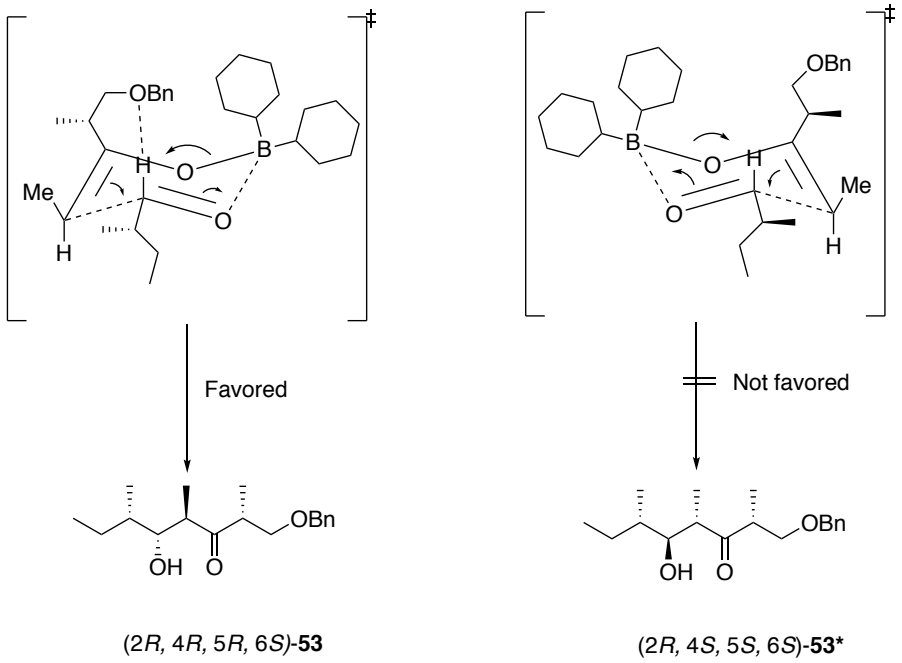

Scheme 5-6 Facial selectivity by the formation of hydrogen bond in the 6-membered transistion state. (45)

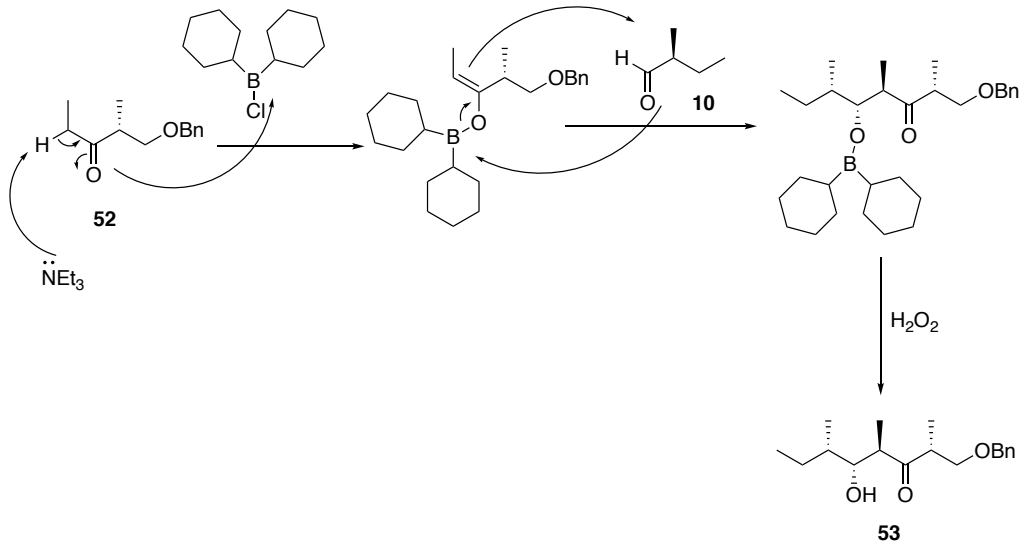

Scheme 5-7 The overall aldol reaction mechanism.

5.4 Silyl Ether Protection Group for Alcohols

Frequently, trisubstituted silyl ether are used as protective groups of alcohols, their reactivity and also their robustness can easily be modified by changing the substituents on the silicone atom. When deciding upon a silyl ether both steric and electronic effects must be considered, electron withdrawing substituents will decrease susceptibility of acid hydrolysis, but increase sensitivity toward base catalyzed hydrolysis.(46) A quantitative relationship between the different silyl ethers have been developed, to see how the steric factors of the substituents play a role by a nucleophilic attack on the silicon atom which will lead to the hydrolysis of the

protection group in acidic or basic environment. The stability of the typical silyl ether under acidic condition: TMS (1) < TES (64) < TBS (20 000) < TIPS (700 000) < TBDPS (5 000 000).(47) The stability of the typical silyl ether under basic condition: TMS (1) < TES (10–100) < TBS ~ TBDPS (20 000) < TIPS (100 000).(48) For the structure of TMS-, TES-, TBS-, TIPS, TBDPS-silyl ethers, see **Figure 5-1**.

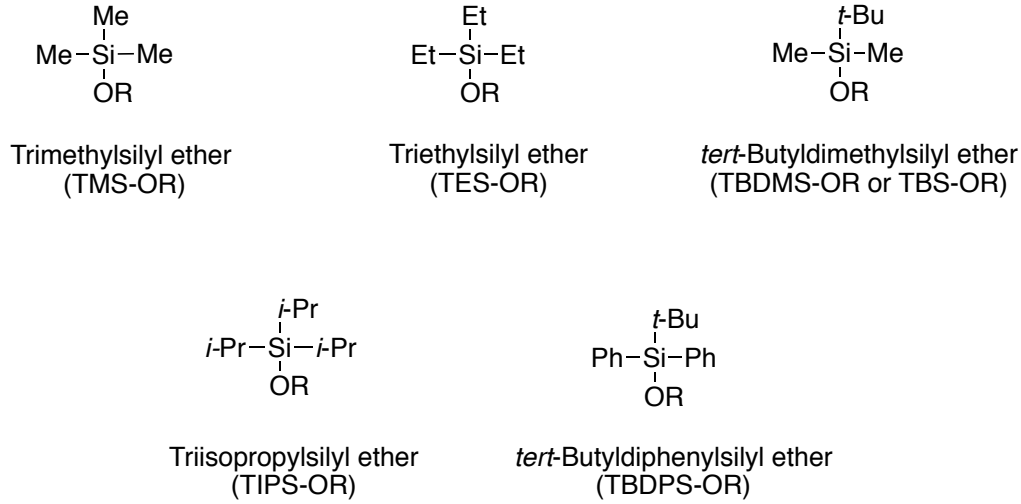

Figure 5-1 The structure of TMS-, TES-, TBS-, TIPS, TBDPS-silyl ethers. (46)

For the formation of silyl ethers from alcohols, the alcohol is treated with a base and can then react with the trisubstituted silyl chloride or triflate. Triflates are good leaving groups and milder bases, like 2,6-lutidine can be used in the reaction. The mechanism for the formation TES-protected alcohol **53** is shown in **Scheme 5-8**. The alcohol **53** displaces the triflate, and 2,6-lutidine will deprotonate the positive intermediate and the TES ether **54** is formed.(38, 46)

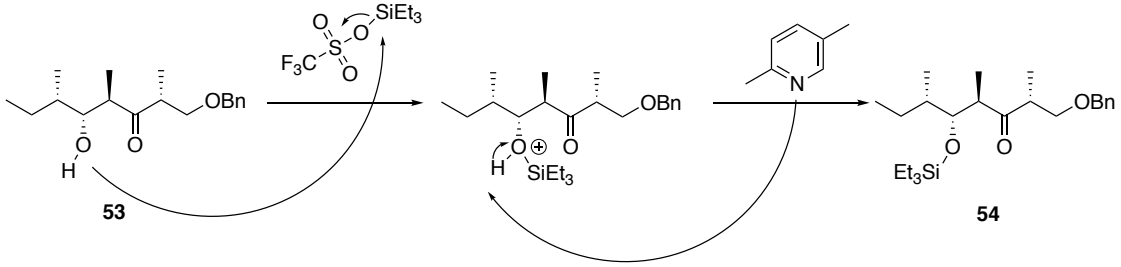

Scheme 5-8 The mechanism for the formation of TES-protected aldol product **53** to form TES ether **54**.(38, 46)

5.5 Removal of Ketone Through Dithiane Formation and Raney-Nickel

1,3-Dithianes can be prepared by treating ketones or aldehydes with 1,3-propanedithiol in the presence of an Brönsted or Lewis acid (LA). The 1,3-dithianes from aldehydes are also a classic acyl anion equivalent.(49) These compounds are stable under a wide range of nucleophiles, bases and hydride reduction agents and are also useful protection groups. However, they are rapidly desulfurized by the Raney- Nickel hydrogenation catalyst, which induce hydrogenolysis of the C-S bonds.(38, 46) In a two-step sequence, the ketone moiety can be converted to a

methylene group, by thioacetylation of the ketone followed by desulfurization of the 1,3-dithiane. The mechanism of the thioacetylation of ketone **54**, followed by treatment of Raney-Ni and H_2 resulting in hydrogenolysis of both the dithiane and the benzyl group is shown in **Scheme 5-9**.(50) (51)

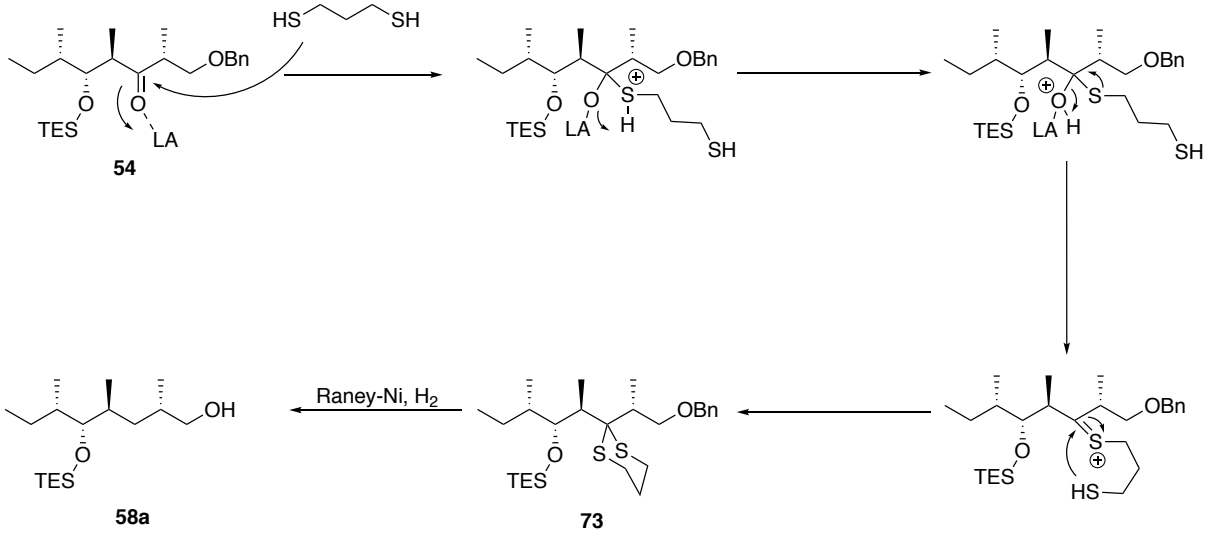

Scheme 5-9 The mechanism of the thioacetylation of **54** for the formation of 1,3-dithiane **73**, following the treatment of Raney Ni and H_2 resulting in hydrogenolysis of both the dithiane and the benzyl group to give primary alcohol **58a**.(50) (51)

5.6 Reduction of Ketones

Routinely, reductions of carbonyl compounds are performed by hydride transfer agents, like sodium borohydride ($NaBH_4$) or lithium aluminium hydride (LAH). $NaBH_4$ reduce aldehydes and ketones rapidly to the corresponding primary and secondary alcohols respectively. However, it is considered a mild reducing agent due to its slow reactivity toward other carbonyl compounds and it is therefore possible to use aqueous or alcoholic solvents. LAH is a more powerful reducing agent and will quickly donate hydrides to a variety of carbonyl compounds, including aldehydes and ketones. LAH is strongly basic and aprotic solvents are using in the reaction.(38) Both $NaBH_4$ and LAH have four hydrides that can be transferred during the reaction, the alkoxyboranes are solvolyzed during the reaction to give the product and the aluminium alkoxide are hydrolysed in the aqueous work up.(52)The mechanisms for reduction by $NaBH_4$ and LAH are similar to each other and the mechanism for the reduction of ketone **54** by LAH is shown in **Scheme 5-10**.(38)

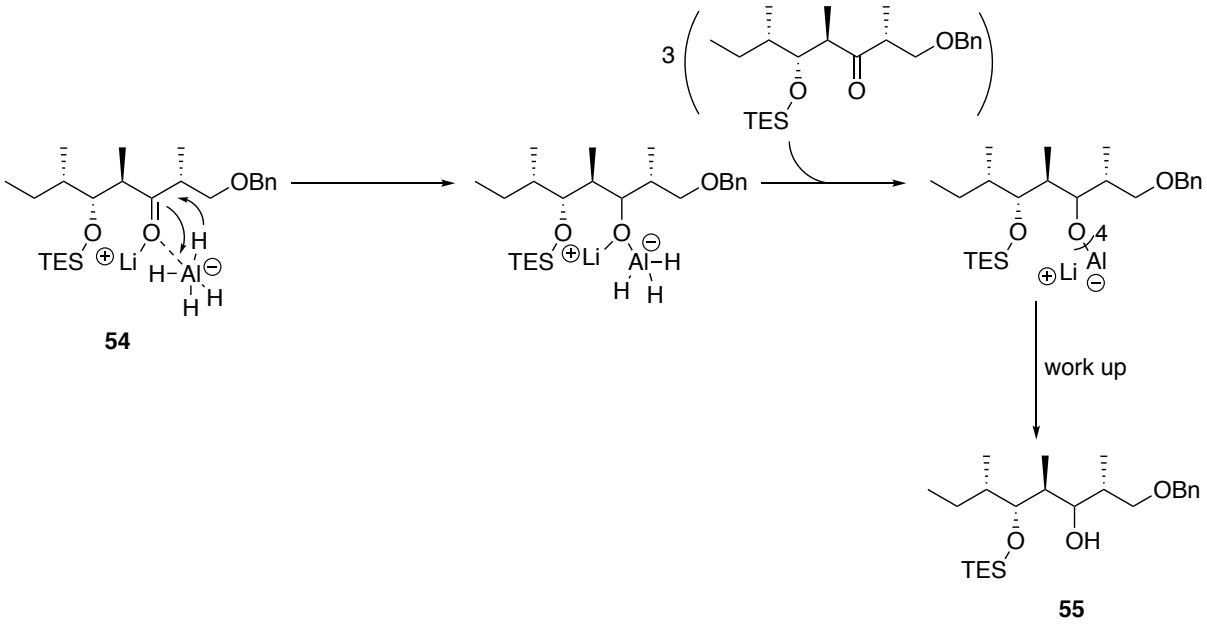

Scheme 5-10 The mechanism for the reduction of ketone **54** to secondary alcohol **55** by LAH.(38)

5.7 Barton-McCombie Deoxygenation

In 1975 D. Barton and S. McCombie reported a method for deoxygenation of secondary alcohols, to replace the hydroxyl group with a hydrogen atom. The deoxygenation involves a two-step sequence, where the alcohol is first transformed to the thiocarbonate derivative. The second step is the removal of the thiocarbonyl group through a free-radical reaction where the thiocarbonyl group is eventually replaced by a hydrogen atom.(53) Different thiocarbonyls will undergo this type of reaction, and the preparation of these compounds can be achieved with reagents like thiocarbonylimidazole (TCDI) or carbon disulfide in combination with iodomethane.(54, 55)

For the mechanism for the *S*-methyl carbonodithioate **56a** formation with NaHMDS, CS_2 and MeI is shown in **Scheme 5-11**. The alcohol **55** is deprotonated by the strong base, making the alkoxide reactive towards a nucleophilic attack on carbon disulfide. The negative charge is transferred and the negative intermediate can attack the electrophilic iodomethane creating the *S*-methyl carbonodithioate **56a**.(53)

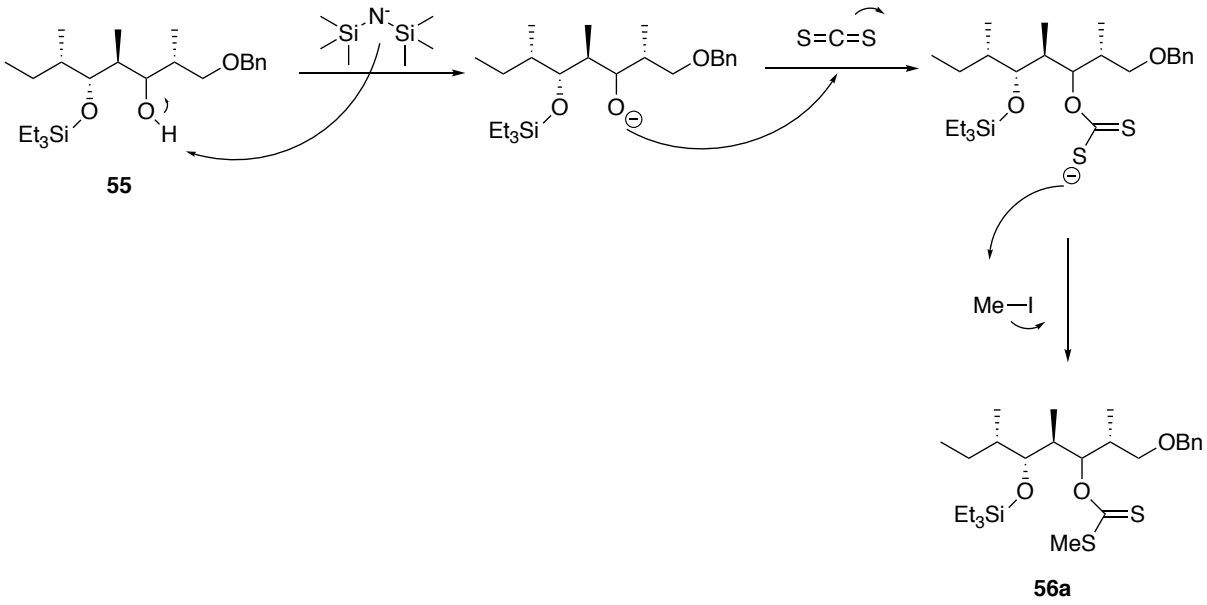

Scheme 5-11 The mechanism of the first step of the Barton-McCombie deoxygenation, where the secondary alcohol **55** is transformed into the *S*-methyl carbonodithioate **56a**.(53)

In the second step of the deoxygenation, requires a radical initiator, commonly used is AIBN or triethyl borane, and a hydrogen carrier, tris(trimethylsilyl)silane or tributyltin hydride. For the radical mechanism of the deoxygenation with Et_3B and Bu_3SnH is shown in ***Scheme 5-12***. Et_3B is autooxidised by O_2 at room temperature which forms the radical specie that transfers a radical to Bu_3SnH.(56) The tributyltin radical will add to the carbon-sulfur double bond generating an radical adduct. A homolytic cleavage of the C-O bond is induced, the fragmentation is driven by the formation of the carbonyl from the thiocarbonyl. The carbon radical abstracts a hydrogen of another equivalent of tributyltin hydride, which forms a tributyltin radical that propagate the reaction and give the completed deoxygenation product **57a**.(53, 57)

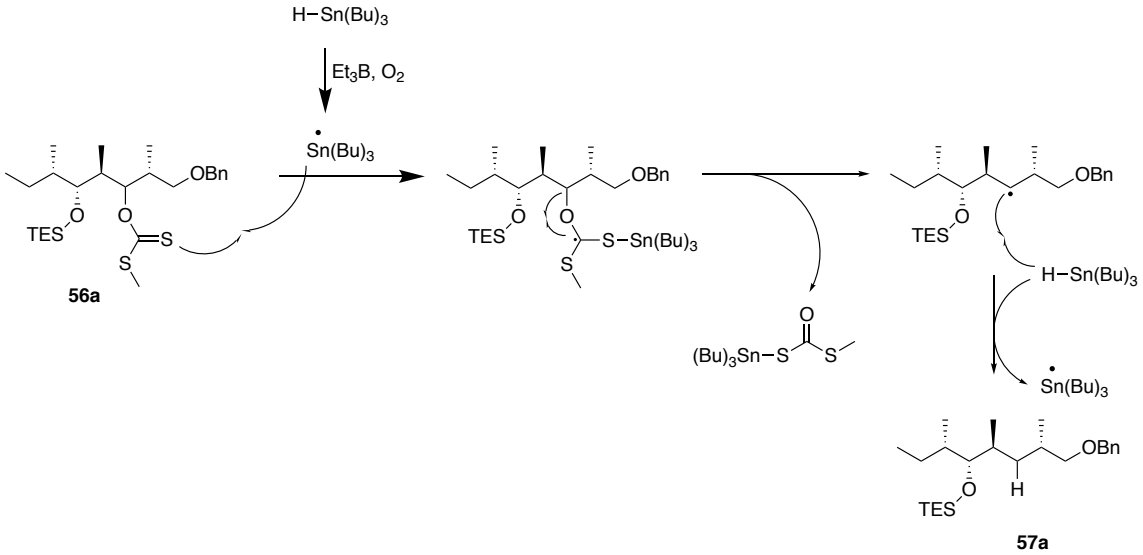

Scheme 5-12 The second step of the Barton-McCombie deoxygenation of the S-methyl carbonodithioate **56a** to form **57a**, involving a radical mechanism with Et_3B-O_2 initator and Bu_3SnH as the hydrogen donor.(53, 56, 57)

5.8 Removal of Benzyl Group

Hydrogenolysis catalysed by palladium on activated charcoal is commonly used to convert benzyl ethers to the corresponding alcohol and toluene. (58) Despite that the reaction is widely used the mechanism of the benzyl removal is not definitively established.(38) However, several mechanisms have been proposed, where it is the first step include an oxidative addition of the either benzyl ether or H_2 to Pd^0 resulting in a Pd^{II} complex. For the proposed mechanisms where the benzyl ether is first added the dispute is whether the mechanism goes through σ-bond metathesis or coordination to H_2 followed by deprotonation. While the proposed mechanism that goes through H_2 addition first debate whether the mechanism goes through a deprotonation giving the an anionic Pd-complex or if it goes through an insertion of the benzyl ether accompanied by β-alkoxy elimination and β-hydride elimination. All the proposed mechanisms are cyclic and the end step is a reductive elimination to regenerate Pd^0, resulting in the liberation of the alcohol and toluene. For the mechanism of the removal the benzyl group in **57a** to form the primary alcohol **58a** is shown in **Scheme 5-13**.(38, 59)

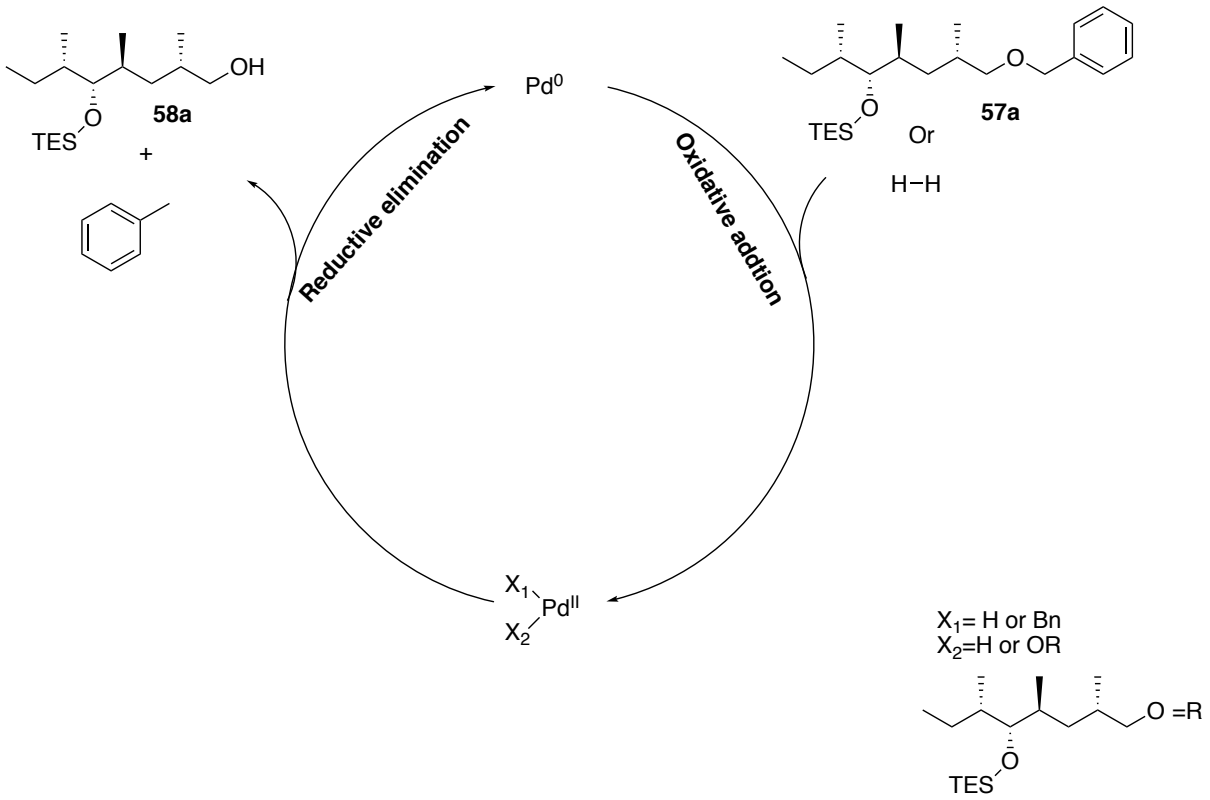

Scheme 5-13 The proposed mechanism for the benzyl removal of **57a**, including oxidative addition to Pd^0 to obtain the Pd^{II} complex. The primary alcohol **58a** and toluene is obtained by a reductive elimination to restore Pd^0.(38, 59)

5.9 Hoover-Stahl Oxidation of Primary Alcohols

Oxidation of aliphatic alcohols is one of the most important and challenging methods of oxidation, due to their extensive use, low reactivity compared to allylic and benzylic alcohols and because they are prone to over-oxidation to the corresponding carboxylic acid. In 2011 J. Hoover and S. Stahl reported a new catalytic system that gives selective oxidation for allylic, benzylic and aliphatic primary alcohols to aldehydes. The reaction is a copper(I)-catalysed aerobic oxidation, where commonly tetrakis(acetonitrile)copper(I) with triflate as the counter ion is used as a source of copper(I). In the reaction copper(I) becomes 2,2'-bipyridyl ligated, indicated by a change in color of the reaction mixture to dark brown. The system also uses TEMPO as the nitroxyl radical, *N*-methyl imidazole in combination with a polar aprotic solvent like acetonitrile. The catalytic cycle in **Scheme 5-14**, include both the oxidation of the catalyst by O_2 and the oxidation of the primary alcohol **58a** to aldehyde **59a**.(60)

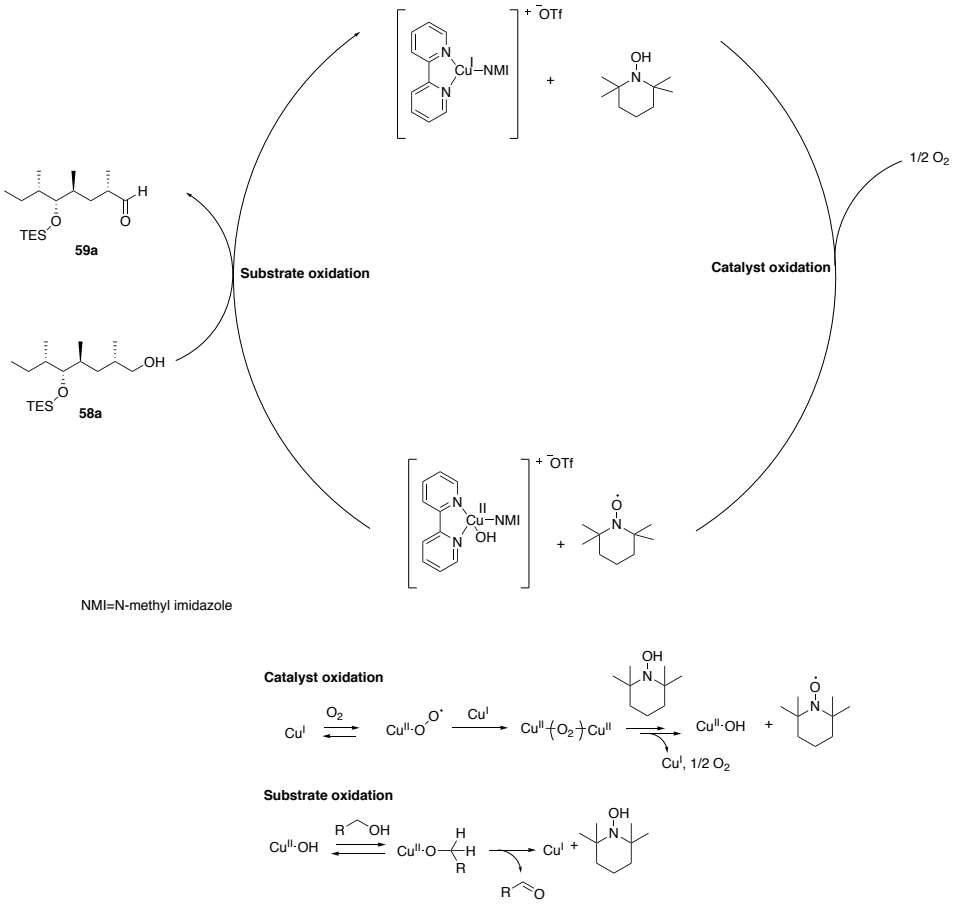

Scheme 5-14 The catalytic cycle of the oxidation of the catalyst by O_2, followed by the oxidation of primary alcohol **58a** to the aldehyde **59a**.(61)

The catalytic system is chemoselective and compatible with a broad range of functional groups and gives negligible over-oxidation. Furthermore, the reaction is selective for oxidation of primary alcohols, due to the sterically hindered nitroxyl radical TEMPO, and secondary alcohols can be present without the need for protection groups.(60) Complementary, in the Steves-Stahl oxidation, by changing to a less hindered nitroxyl radicals like ABNO, also secondary alcohols can be oxidized.(62)

With activated or reactive allylic, benzylic primary alcohols the reaction time is generally shorter than for aliphatic structures. Usually reactions show full consumption after 2-3 hours, while days and even elevated temperatures can be required for aliphatic structures. The study of the mechanism shows that for aliphatic structures, the turnover-limiting step of the catalytic reaction is the cleavage of the C-H bond through a bimolecular reaction between TEMPO and a Cu^{II}-alkoxide intermediate. However, for activated alcohols the C-H bond is weaker which gives a more rapid cleavage and the turnover-limiting step in these reaction is the oxidation of copper(I) by O_2.(62)

5.10 The Carreira Alkynylation

In 2000 E. M. Carreira et al. reported a novel process for the formation of new asymmetric C-C bonds by nucleophilic addition of terminal alkynes to aldehydes without using strong pyrophoric bases. The reaction depends upon the *in situ* formation of a reactive zinc acetylide complex from terminal alkynes, by using the mild Lewis acid zinc triflate in combination with tertiary amines.(63)

The addition of zinc acetylide to the aldehydes result in the formation of chiral propargylic secondary alcohols. The mechanism for the formation of propargylic alcohol **60a** by the alkynylation of alkyne **72** with aldehyde **59a** is shown in **Scheme 5-15**. A new stereogenic center is formed in the reaction, and the addition is made facial selective, by the addition of a chiral ligand to the reaction. Often the chiral ligand *N*-methylephedrine is used, because it is inexpensive and both enantiomers, (1*R*, 2*S*)- (−)- or (1*S*, 2*R*)- (+)-*N*-methylephedrine (NME) are available.(63, 64)

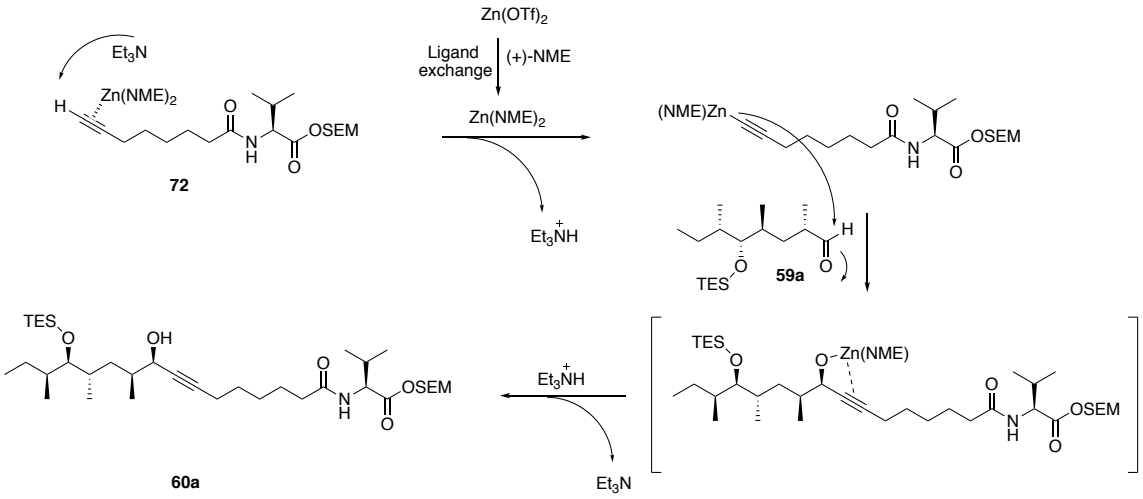

Scheme 5-15 The mechanism for the Carreira alkynylation, using $Zn(OTf)_2$, the chiral ligand (+)-NME and triethyl amine for the *in situ* formation of the zinc acetylide of alkyne **72**. The zinc acetylide is then added to the aldehyde **59a** to form propargylic alcohol **60a**.(63, 65)

5.11 Protection of Carboxylic Acids

To avoid undesired side reaction carboxylic acids can be protected as its SEM esters.(46) To enable the esterification of carboxylic acid **31** with 2-(trimethylsilyl)ethanol, the carboxylic acid can be activated by dialkylcarbodiimides in the presence of catalytic amounts of DMAP.(66) A postulated mechanism for the esterification is depicted in **Scheme 5-16**. The

activating agent EDC is attacked by the deprotonated carboxylic acid, followed by the formation of the acyl pyridinium ion. The acyl pyridinium ion is then activated for the attack of 2-(trimethylsilyl)ethanol to from the SEM ester **67**.(38, 67)

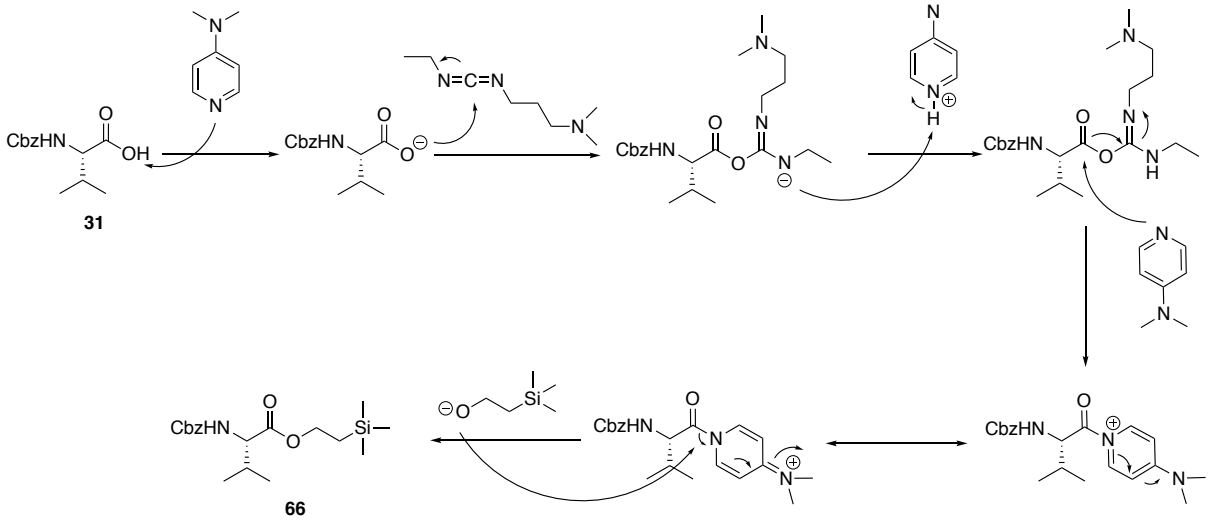

Scheme 5-16 The postulated mechanism of carboxylic acids **31** activation of introduction of the SEM protection group to **66**.(67, 68)

5.12 Deprotection of Benzyl Carbamate Amines

Amines are susceptible to oxidation, deprotonation by organometallic reagents and can act as a nucleophile, due their reactivity amines are commonly protected in synthesis. Amines can be concealed as benzyl carbamates, installed by acylation using benzyl chloroformate. The removal of the benzyl carbamate can be conducted by a Pd-C catalyzed hydrogenolysis. The Bn-O bond of the benzyl carbamate is under these conditions cleaved similar to the benzyl removal described in section 5.8, resulting in the carbamic acid and toluene.(38, 59) The carbamic acid is then spontaneously decarboxylated, releasing CO_2 gas and restoring the amine. The removal of the benzyl carbamate in **66** to generate amine **67** is shown in **Scheme 5-17**.(69)

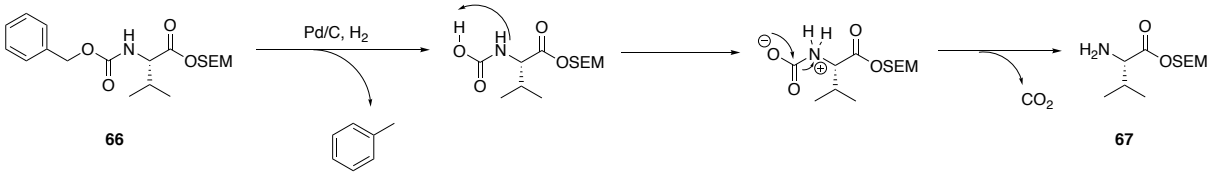

Scheme 5-17 Hydrogenolysis of **66** catalyzed by Pd-C, followed by spontaneous decarboxylation to form amine **67**.(38, 59, 69)

5.13 Ozonolysis

Ozonolysis is a reaction where ozone goes through a 1,3-dipole cycloaddition to alkenes. This results in the cleavage of the carbon carbon double bond in a selective method at the low

temperature of −78 ℃ resulting in different carbonyl products depending on the conditions during the work up.(70) The first intermediate product of the reaction is a five membered 1,2,3-trioxolane (initial ozonide or malozonide). These are unstable and decomposes rapidly, which breaks a C-C bond and one of the weak O-O bond.(71) The intermediate is another 1,3-dipole zwitter ion that prefers cycloaddition to the carbonyl function to generate the more stable isomer 1,2,4-trioxolane (ozonide). These ozonides are more stable than the initial ozonides, however they may decompose explosively and must be handled with care.(71, 72) The 1,2,4-trioxolane is therefore *in situ* subjected to either a reductive (dimethyl sulfide) or oxidative (hydrogen peroxide) work up, to give the aldehyde/ketone or carboxylic acid respectively.(73) However, when alcohols are used as a solvent in the reaction, the 1,3-dipol can instead of forming the 1,2,4-trioxolane be entrapped as a α-hydroperoxy ether.(74)

The mechanism for the ozonolysis of **58** is shown in **Scheme 5-18**. After the cycloaddition of ozone to **58**, the initial ozonide decompose to generate the intermediate free aldehyde and the zwitter ion which is subsequently attacked by methoxide to form the α-hydroperoxide methyl ether. This intermediate is further reacted with acetic anhydride and triethyl amine to form the desired methyl ester aldehyde **69**. (71, 73)

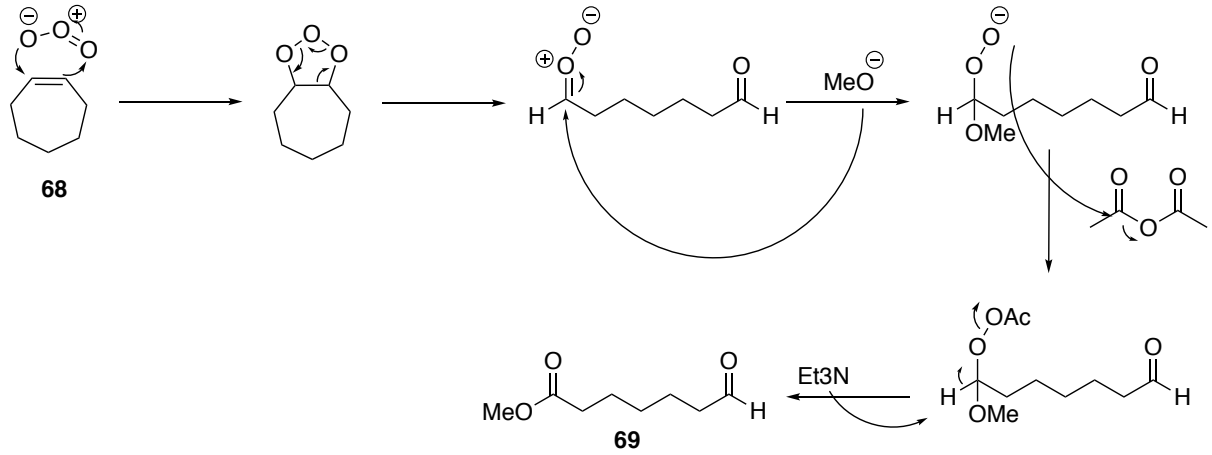

Scheme 5-18 The mechanism of the ozonolysis of **68**, in the presence of methanol to generate the α-hydroperoxide methyl ether, which further is reacted with acetic anhydride and triethylamine to generate the methyl ester aldehyde **69**. (71, 73)

5.14 Alkyne Synthesis by Ohira-Bestmann Homolongation

The Wittig reaction is a well-established reaction for generation of alkenes from aldehydes or ketones by using a phosphine reagent. In the work by Horner, Wadsworth and Emmons a modified Wittig reagent is describe for the synthesis of alkenes, where phosphonate is used to improve the reaction conditions. Related to this modification, the Seyferth-Gilbert reagent, a diazophosphonate transfer reagent can be used in the synthesis of alkynes. These reagents are depicted in **Figure 5-2**.(75, 76)

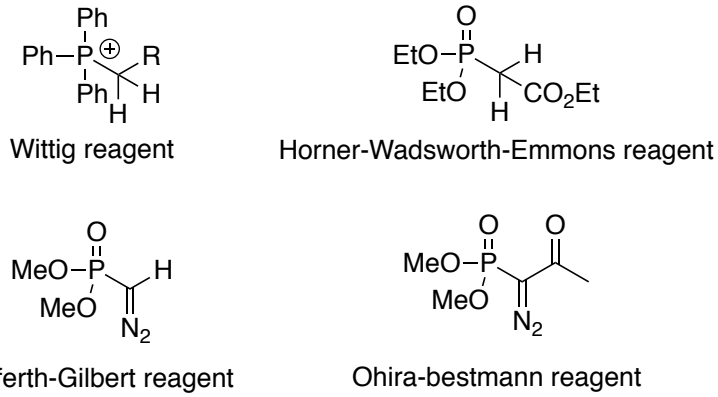

Figure 5-2 The Wittig reagent, the Horner-Wadsworth-Emmons reagent, the Seyferth-Gilbert reagent and the Ohira-Bestmann reagent.(75-78)

In this homolongation reaction, alkynes with one additional carbon atom can be generated from aldehydes or aryl ketones. The reaction uses a strong base to deprotonate the dimethyl diazomethylphosphonate reagent that subsequently reacts with aldehydes or aryl ketones at low temperatures (−78 °C). However, there are several challenges with this reaction, the reagent is not commercially available and must be synthesized in multiple steps, also the reaction requires low temperatures, inert atmosphere and the use of a strong base like *t*-butyl oxide or *n*-butyllithium. For base-sensitive substrates low yields are observed due to undesired side reaction, where enolizable aldehydes can self-condensate in an aldol reaction. (75)

For these reasons, the structure of the reagent was modified by Ohira and further examined by Bestmann to generate the Ohira-Bestmann reagent, dimethyl diazo-2-oxopropylphosphonate. This reagent is commercially available or can be synthesized in a one-pot procedure and accommodates for the use of ambient temperatures and a milder base like potassium carbonate. (77-79)

For the mechanism of the Ohira-Bestmann homolongation of aldehyde **69** to form alkyne **70**, see **Scheme 5-19**. Similar to the Horner-Wadsworth-Emmons modification for alkene

synthesis, the base generates a negatively charged carbanion which can attack the electrophilic aldehyde **69**. Through a cyclic transition state, the water soluble phosphate anion is eliminated which leaves the (diazo)alkene. In contrast to a simple alkene formation, the diazo alkene will react further and the removal of nitrogen gas generates the unsaturated carbene intermediate that undergoes a spontaneous 1,2-migration to give alkyne **70**.(75)

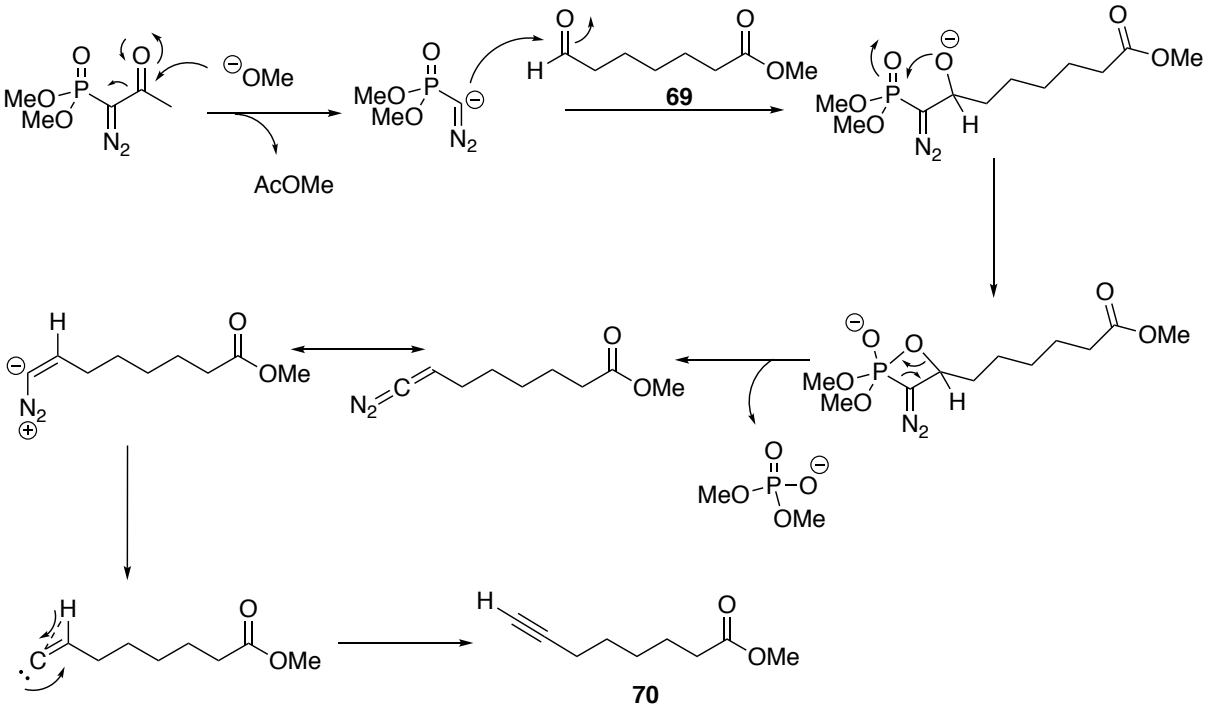

Scheme 5-19 The mechanism of the homolongationation of aldehyde **69**, by a base-promoted reaction with the Ohira-Bestmann reagent to give alkyne **70**.(75)

5.15 Ester Hydrolysis

The mechanism of the base catalyzed ester hydrolysis of **70** is given in **Scheme 5-20**.(80)

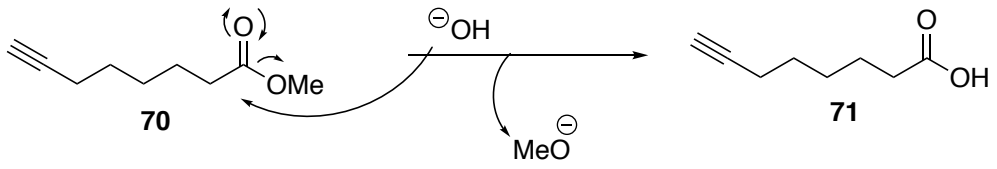

Scheme 5-20 The mechanism of the base catalysed ester hydrolysis of **70**.(80)

5.16 Amide Coupling

To enable amide coupling, coupling agents are commonly used to catalyze the reaction. HATU is a coupling agent that reacts with the deprotonated carboxylic acid to form an activated ester, the activated form can them react further with the amine.(67) The mechanism of the HATU-mediated amide coupling for acid **71** and amine **67** is shown in **Scheme 5-21**.

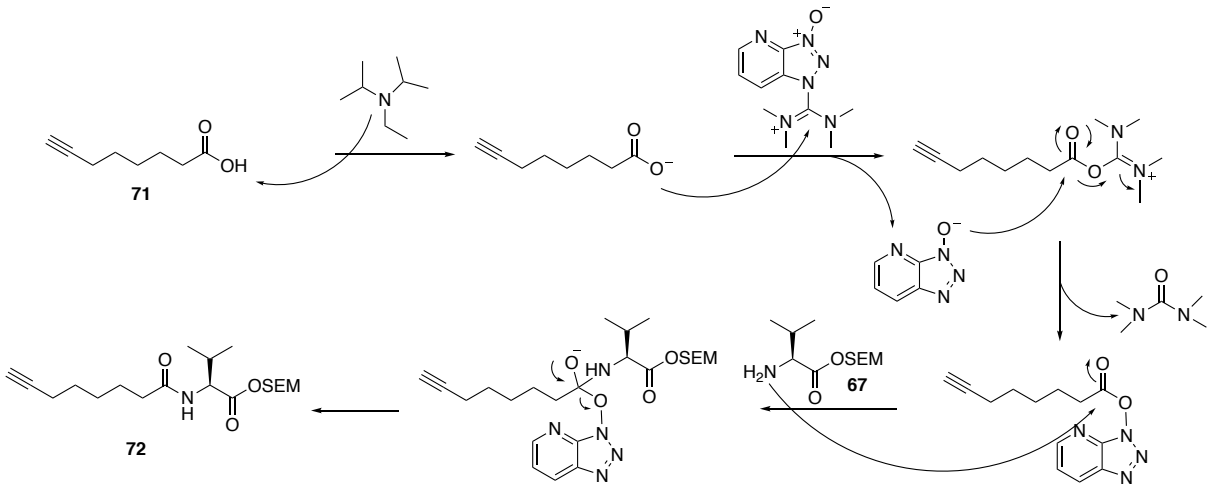

Scheme 5-21 The mechanism of amide coupling of **71** and **67** with HATU as the coupling agent and DIPEA as the base to form amide **72**.(67)

6 Results and Discussion

6.1 The O-Benzylation of Primary Alcohol 24

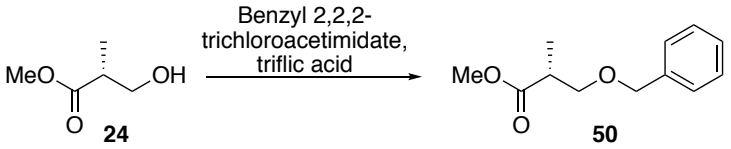

Scheme 6-1 Acid catalyzed *O*-benzylation of **24** to give benzyl ether **50**.

The *O*-benzylation of the commercially available **24**, is reported in the literature by Paterson et al..(45, 81) The procedure from 2011, describe the *O*-benzylation of (*R*)-**24** with benzyl 2,2,2-trichloroacetimidate (1.1 eq.) and triflic acid (0.3 eq.) in THF, which afford the product in 95% yield.(45) This method was first attempted, however precipitation of byproduct trichloroacetamide in hexane was not possible, leaving an inconvenient amount of the yellow viscous oil, resulting in the low yield of 9.4%. In 1994, a *O*-benzylation of (*S*)-**24** was reported, the procedure used benzyl 2,2,2-trichloroacetimidate (1.1 eq.) and triflic acid (0.4 eq.) carried out in a binary solvent system of CH_2Cl_2: cyclohexane (1:2), and gave the product in 81% yield.(81) Due to the low yields attained with the first method, the binary solvent system was tested as an alternative. This system allowed for precipitation of trichloroacetamide and increased the yields of the reaction significantly to 63.4-68.8%.

Table 6-1
Reaction conditions for the *O*-benzylation of **24** to from benzyl ether **50**.

Starting material (s.m)	Reagents	Solvent	Reaction conditions	Yield/Comment	Ref.
24 4.90 g 41.5 mmol	Benzyl 2,2,2-trichloroacetimidate (1.1 eq.) Triflic acid (0.3 eq.)	THF	18 h, 0 ℃ to rt	**50** 0.8155 g 3.92 mmol 9.4%	(45)
24 2.00 g 16.9 mmol	Benzyl 2,2,2-trichloroacetimidate (1.1 eq.) Triflic acid (0.4 eq.)	CH_2Cl_2: cyclohexane (1:2)	28 h, rt	**50** 2.237 g 10.74 mmol 63.4%	(81)
24 2.00 g 16.9 mmol	Benzyl 2,2,2-trichloroacetimidate (1.1 eq.) Triflic acid (0.4 eq.)	CH_2Cl_2: cyclohexane (1:2)	48 h, rt	**50** 2.425 g 11.64 mmol 68.8%	(81)

6.2 The Formation of Weinreb Amide 51

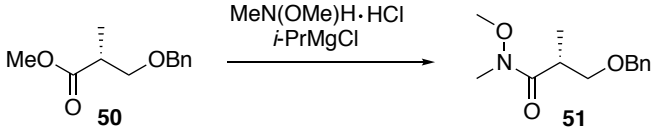

Scheme 6-2 The reaction for the formation of Weinreb amide **51** from methyl ester **50**.

Following the procedure described by Paterson et. al, the *N*-methoxy-*N*-methylamide **51** was prepared from the methyl ester **50**, afforded **51** in yields ranging from 66.5-82.6%.(45)

Table 6-2

Reaction conditions and yields for the formation of Weinreb amide **51** from methyl ester **50**.

Starting material (s.m)	Reagents	Solvent	Reaction conditions	Yield/comment	Ref.
50 2.20 g 10.56 mmol	MeN(OMe)H·HCl (1.6 eq.) *i*-PrMgCl (3.0 eq)	THF	4 h, −15 ℃	**51** 1.66 g 7.03 mmol 66.5%	(45)
50 2.08 g 9.98 mmol	MeN(OMe)H·HCl (1.6 eq.) *i*-PrMgCl (3.0 eq)	THF	5 h, −15 ℃	**51** 1.96 g 8.24 mmol 83.8%	(45)

6.3 The Grignard Reaction of Weinreb Amide 51

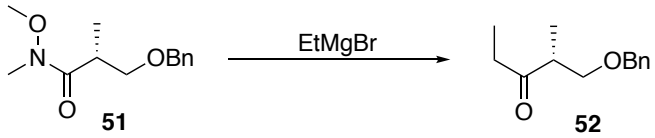

Scheme 6-3 The grignard reaction with Weinreb amide **51** to from ketone **52**.

The ketone **52** was prepared from the Weinreb amide **51** in a Grignard reaction with EtMgBr, following the procedure described by Paterson et. al, but increasing the EtMgBr equivalents to 2.2, the ketone **52** was afforded in yields ranging from 89.6 to 95.5%.(45)

Table 6-3

Reaction conditions and yields for the formation of ketone **52** to from Weinreb amide **51**.

Starting material (s.m)	Reagents	Solvent	Reaction conditions	Yield/comment	Ref
51 1.95 g 8.22 mmol	EtMgBr (2.2 eq.)	THF	4.5 h, 0 ℃	**52** 1.52 g 7.36 mmol 89.6%	(45)
51 1.57 6.61 mmol	EtMgBr (2.2 eq.)	THF	4.5 h, 0 ℃	**52** 1.30 g 6.31 mmol 95.5%	(45)

6.4 The Aldol Reaction of Ketone 52 and Aldehyde 10

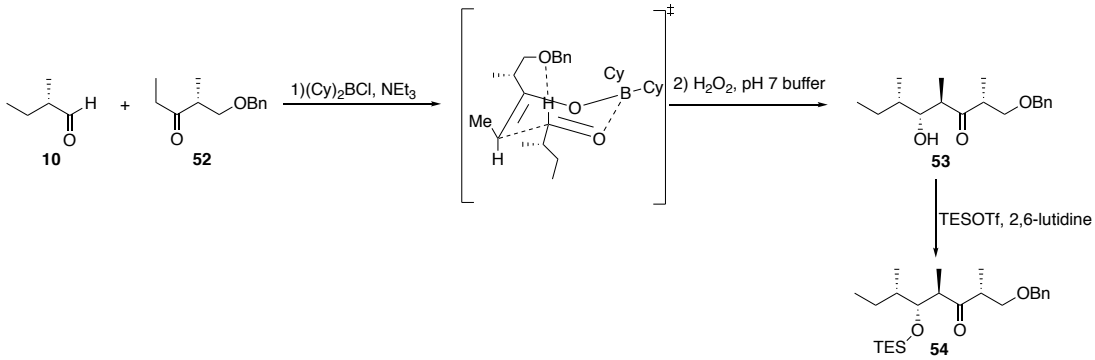

Scheme 6-4 The aldol reaction of aldehyde **10** and ketone **52** and the TES-protection of the aldol adduct **53**.

The aldol adduct **53** was prepared by the method described by Paterson et al. in this procedure the ketone **52** was reacted with acetaldehyde, resulting in the *anti*-product as a single diastereomer in 99% yield.(45) In the procedure 8.0 eq. of the acetaldehyde was added to the reaction, from **Table 6.4** slightly higher yields were observed by increasing the equivalents of aldehyde **10** from 3.5 to 5.1. By otherwise using the same reagents and by following the same procedure, the *anti*-product was expected in this reaction. In the ^{1}H-NMR spectrum of **53** the H-5 and H-1 protons were overlapping resulting in a multiplet and the coupling constants could not be calculated. The optic rotation of **53** was measured to $[\alpha]_D^{20} = -7.6\,^{\circ}$ (c 1.0, $CHCl_3$).

However, by protecting the C-5 hydroxyl group as its TES ether **54**, the H-5 and H-1 protons were separated. The triethyl ether **54** was prepared in high yield of 92.9%, by following a method by Evans et al.(82) The ^{1}H-NMR signal of the H-5 was given as a dd with the coupling constants of J=8.5 Hz and J=1.9 Hz. By comparing the coupling constants with coupling constants of structurally related compounds **74** ($J_{H\text{-}8,H\text{-}9}$=9.8, $J_{H\text{-}9,H\text{-}10}$=1.4 Hz) and the coupling constant of the corresponding H-13 proton in the structure of **1** (dd, J=8.8, 2.9 Hz), reveals the anti-conformation of **53**.(3, 83) There was no visible trace of other diastereomers.

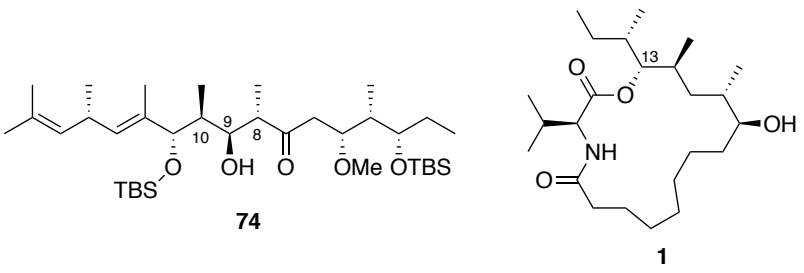

Figure 6-1 Structure of intermediate product **74** in the synthesis of Gephyronic Acid and the structure of dysoxylactam A (**1**).(3, 83)

Table 6-4

Reaction conditions and yields for the aldol reaction of ketone **52** and aldehyde **10** to form aldol adduct **53**.

Starting material (s.m)	Reagents	Solvent	Reaction conditions	Yield/Comment	Ref
52 1.50 g 7.27 mmol	1) $(Cy)_2BCl$ (1.5eq.) NEt_3 (1.6 eq.) **10** (3.5 eq.) 2) H_2O_2, pH 7 buffer	Et_2O	1) 0 ℃-−78 ℃-−19 ℃, over night 2) 1.5 h	**53** 1.74 g 6.00 mmol 82.0%	(45)
52 1.28 g 6.22 mmol	1) $(Cy)_2BCl$ (1.5 eq.) NEt_3 (1.6 eq.) **10** (5.1 eq.) 2) H_2O_2, pH 7 buffer	Et_2O	1) 0 ℃-−78 ℃-−19℃, over night 2) 1.5 h, 0 ℃	**53** 1.66 g 5.69 mmol 91.5%	(45)

At a later point in the synthesis alcohol 54 attempted to be protected as its TBS ether in a reaction with TBS-Cl and imidazole, however the reaction did not proceed and the starting material was regenerated.(84)

Table 6-5

Reaction conditions and yields for formation of TES-protected **54** and the attempted TBS protection of **53**.

Starting material (s.m)	Reagents	Solvent	Reaction conditions	Yield/comment	Ref.
53 1.32 g 4.51 mmol	2,6-lutidine (1.2 eq.) TESOTf (1.1 eq.)	CH_2Cl_2	1 h, 0 ℃	**54** 1.70 g 4.19 mmol 92.9%	(82)
53	Imidazole (2.8 eq.) TBSCl	CH_2Cl_2	2 days, rt	No conversion of s.m	(84)

6.5 The Deoxygenation of ketone 54

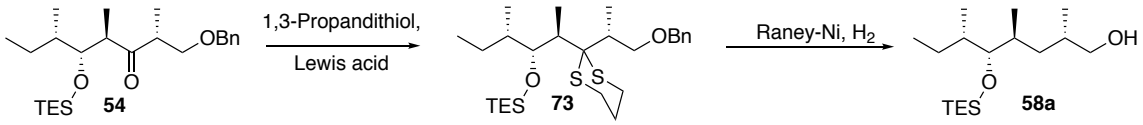

Scheme 6-5 The initial plan for the deoxygenation of the ketone functionality in **54**, first by thioacetalization to form dithiane **73** followed by Raney-Nickel desulfurization to give primary alcohol **58a**.

The initial plan for the removal of the ketone in **54** was through the two-step sequence shown in **Scheme 6-5**. Involving the formation of dithiane **73**, followed by a Raney-Nickel desulfurization to afford the saturated alkane **58a**. The Raney-Nickel reagent could also remove the benzyl group, allowing for two modifications in two steps.(51) The dithiane **73** could be synthesized through a Lewis acid catalyzed thioacetalization of ketone **54** with 1,3-propandithiol. The thioacetylation attempts are summarized in **Table 6-6**.

First, the thioacetalization of **54** was attempted by using I_2 as the Lewis acid.(85) After 2 hours of reaction time the starting material was no longer present of the TLC plate, however several new spots were observed. After flash chromatography, the different compounds arising from degradation of the starting material could not be identified by NMR. The distinguishable peaks of the TES-group could be identified in the first collected fractions (as the main signal) and was not observed in the other fractions. This indicates that the point of degradation started with the TES-deprotection. The mild Lewis acid iodine is also recognized as a reagent for both silyl ether protection and deprotection of alcohols.(86) Using a 1% I_2 in MeOH at room temperature results in the cleavage of TBS ethers. However, sterically more hindered TIPS ethers required 1-1.5 days for complete desilylation.(87) Under these conditions, the active agent of the silyl ether cleavage is not known with certainty. Although, it is connected to the polarization of the ether oxygen by iodine and trace amounts of hydrogen iodide generated from the dissolution of iodine in methanol.(87-89)

Due to the decomposing of **54** under I_2 conditions, the thioacetalization of was attempted with $BF_3{\cdot}Et_2O$, a source of the Lewis acid BF_3. After 1 hour, full consumption of the starting material and several new spots were observed, which indicated that the reaction conditions also lead to decomposing of the starting material. The main degradation product **75**, was identified by NMR and confirmed by MS (TOF MS ES^+ *m/z* $[M+H]^+$ calc. for $C_{16}H_{25}OS_2$ 297.1347, ion observed 297.1350). The NMR analysis of **75** is given in section 0. For the deprotection of silyl ethers fluoride reagents are often used, due to fluoride ions high affinity for silicone. The cleavage is

attributed to the formation the Si-F bond that is 30 kcal/mol greater than the strength of the Si-O bond.(46) $BF_3 \cdot Et_2O$ can act as a deprotection agent, where it coordinates to the silyl ether moiety inducing the cleavage of the protection group by formation of the silyl ether fluoride.(90, 91) In addition, the $BF_3 \cdot Et_2O$ is believed to form an adduct with the ketone **53** resulting in a retro-aldol reaction giving the ketone **52**. The resulting ketone **52** can again coordinate with the $BF_3 \cdot Et_2O$ and in the presence of 1,3-propanedithiol gives the dithiane **75**.(92) To further investigate this mechanism, a reaction of the unprotected aldol product **53** was exposed to the same reaction conditions. This reaction also led to the formation of the same degradation product **75**. The proposed reaction mechanism of the degradation is shown in **Scheme 6-6**.

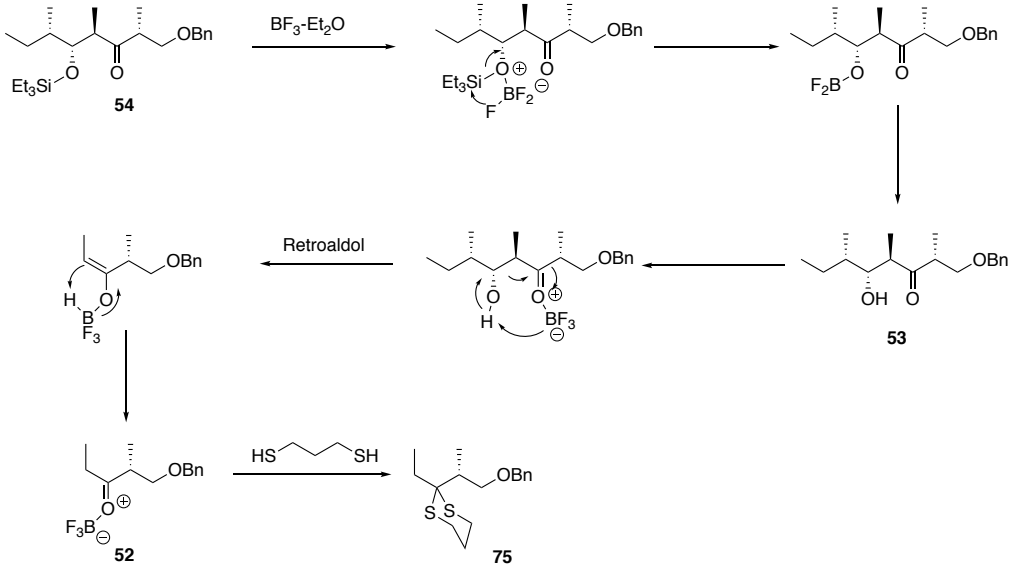

Scheme 6-6 The proposed mechanism for the degradation of **54** in the presence of BF_3- Et_2O and 1,3-propandithiol, giving the retroaldol dithiane **75**. (90-92)

$TiCl_4$ have a strong affinity for oxygenated compounds and is a useful catalyst for thioacetalization reactions.(93) J. Cossy et al. also reported degradation of their TBS-protected aldehyde substrate when BF_3-Et_2O was used in the dithiane formation. The problem was resolved by changing the Lewis acid to $TiCl_4$.(94) Deprotection of TBS ethers with $TiCl_4$-Lewis base complexes have been reported, however these reagents are more reactive than $TiCl_4$ alone.(95) Since a solution of $TiCl_4$ was available in the laboratory and $TiCl_4$ was tested in the thioacetalization reaction of **54**.(94) The first reaction showed no conversion of the starting material after 6 hours, and the starting material was regenerated. Reactions with $TiCl_4$, 1,3-propandithiol and ketones are expected to have longer reactions times than more reactive aldehydes and the second reaction attempt was left for 24 hours.(93) The reaction then showed

full consumption of the starting material and the reaction was quenched. However, the desired product that was not formed and several unidentified degradation products were observed, and once more the characteristic TES-group shifts was not found in NMR.

A last attempt of the thioacetalization was conducted with the milder Lewis acid $LiClO_4$, that is compatible for acid-labile carbonyl compounds, that also decomposed by in the presence of BF_3-Et_2O. Both protected and non-protected alcohols were used in the reaction and therefore both the aldol product **53** and the TES-protected **54** was used as starting materials.(96) After 4 days, the two reactions showed low conversion of the starting material and the desired product was not observed in NMR.

Table 6-6

The summary of reaction conditions and outcome of the thioacetalization attempts of **54** and **53**

Starting material (s.m)	Reagents	Solvent	Reaction conditions	Comment	Ref.
54	I_2 (0.1 eq.) 1,3-propandithiol (1.2 eq.)	CH_2Cl_2	2 h, rt	Degradation of s.m to nonidentified products	(85)
54	BF_3-EtO_2 (8.0 eq.) 1,3-propandithiol (1.1 eq.)	CH_2Cl_2	2 h,−10 ℃	Degradation of s.m and formation dithiane **75**	(97)
53	BF_3-EtO_2 (8.0 eq.) 1,3-propandithiol (1.1 eq.)	CH_2Cl_2	1 h, −10 ℃	Degradation of s.m and formation dithiane **75**	(97)
54	$TiCl_4$(0.13) 1,3-propandithiol (1.3 eq.)	CH_2Cl_2	6 h, −10 ℃ to rt	No conversion of s.m	(93)
54	$TiCl_4$ (0.26 eq.) 1,3-propandithiol (1.3 eq.)	CH_2Cl_2	25.5 h, −10 ℃ to rt	Degradation of s.m to nonidentified products	(93)
54	$LiClO_4$ (2.0 eq.) 1,3-propandithiol (2.0eq.)	Et_2O	4 days, rt	Low conversion of s.m, desired product was not formed	(96)
53	$LiClO_4$ (2.0 eq.) 1,3-propandithiol (2.0 eq.)	Et_2O	4 days, rt	Low conversion of s.m, desired product was not formed product was not formed	(96)

An entirely new approach was tested parallel to the thioacetalization, the plan was to reduce the ketone **54** to the corresponding secondary alcohol **55** followed by the two step Barton-McCombie deoxygenation, see **Scheme 6-7**.

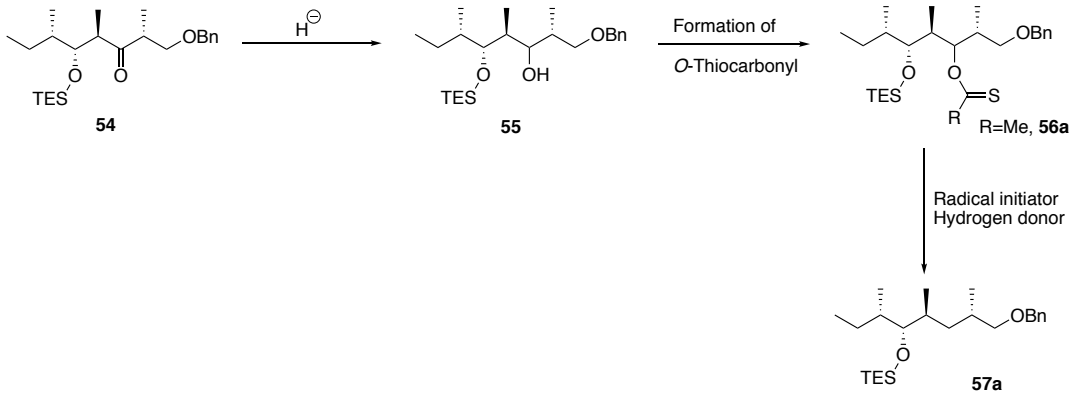

Scheme 6-7 The alternative approach for the deoxygenation of **54**, by reduction of the ketone **54** to secondary alcohol **55** followed by the two-step Barton McCombie deoxygenation to generate **57a**.

The reduction of ketone **54** was first attempted with DIBAL-H, a strong but bulky reducing agent.(98)The reaction was left for 21.5 hours, and there was no conversion of the starting material. The reaction was quenched by addition of 4 M HCl, after the work up an additional spot was observed on the TLC plate (7% EtOAc: hexane, R_f=0.058). The starting material was generated in 61.6% and the additional spot was identified as the aldol product **53** and was formed in 37.1% yield. The aldol product **53** was formed during the acidic work up as a result of a TES-deprotection in acidic environment.(46)

Another reducing agent, $NaBH_4$ both in MeOH and EtOH was tested for the reduction of ketone **54**. Both reactions showed conversion of the starting material to the desired alcohol **55**. However, the conversion was very slow, and the more powerful reductant LAH was tested to achieve shorter reaction times. The reaction with LAH provided a rapid reduction of the ketone **54** to the secondary alcohol **55**, in 70.7- 72.7% yield (20% EtOAc: hexane, R_f=0.65). An additional spot was observed in the reaction (20% EtOAc: hexane, R_f=0.14). The byproduct of the reaction is believed to be the diol **76**, formed as a result of a TES-deprotection (17.2-21.9% yield). A reductive cleavage of silyl ethers are observed in similar 1,3-systems , when the ketone is in close the proximity to the silyl ether and the coordination of LAH can result in a hydride delivery to the silicone atom.(99) Without direction by a neighboring group, deprotection by LAH is usually not observed, and silyl ethers further away in the chain stay intact.(100, 101) In synthesis this can be useful for selective silyl ether cleavage, however this side reaction should

be avoided and the reactions conditions for the reduction should be optimized further to increase the yield of the desired product **55.**(102)

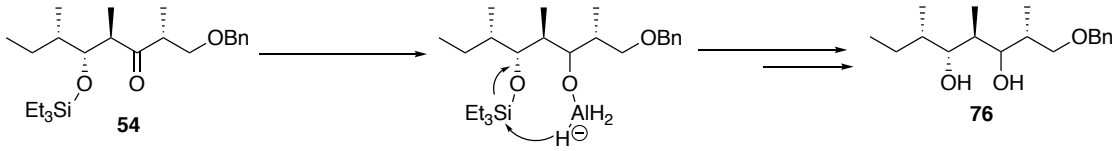

Scheme 6-8 The mechanism for the reductive cleavage of the TES-group, given diol **76** as the possible byproduct.(99)

Table 6-7

The summary of the reaction conditions for the reduction of ketone **54** to secondary alcohol **55**.

Starting material (s.m)	Reagent	Solvent	Reaction conditions	Comment/Yield	Ref.
54 106 mg 0.261 mmol	DIBAL-H (2.0 eq.)	CH_2Cl_2	21.5 h, −78 ℃ to rt	No conversion of s.m.* **54** 65.6 mg 0.161 mmol 61.6% **53** 28.3 mg 0.0968 mmol 37.1%	(98)
54	$NaBH_4$ (2.0 eq.)	MeOH	23 h	Slow conversion of s.m, product **55** observed	(103)
54	$NaBH_4$ (2.0 eq.)	EtOH	21 h	Slow conversion of s.m, product **55** observed	(103)
54 55.4 mg 0.136 mmol	LAH (2.5 eq.)	THF	50 min, −78 ℃	**55** 39.3 mg 0.0962 mmol 70.6% yield **Diol 76** 6.9 mg 0.0234 mmol 17.2% yield	(104)
54 1.10 g 2.69 mmol	LAH (2.5 eq.)	THF	55 min, −78℃	**55** 800 mg 1.96 mmol 72.7% yield **Diol 76** 174 mg 0.591 mmol 21.9% yield	(104)

*Acidic work up, 4M HCl

With the alcohol **55** in place the first step of Barton-McCombie, the *O*-thiocarbonyl introduction was tested with TCDI as the electrophilic agent in toluene (See **Table 6-8**). After 4.5 h with reflux, there was no conversion of the starting material and the starting material was generated. Alcohol **55** is highly branched, and sterically hindered alcohols report long reaction times.(105) A second reaction was attempted with TCDI in 1,2-dichloroethane. After 27 hours and no conversion of the starting material, DMAP was added to catalyse the reaction.(106) In addition, more TCDI was added to the reaction mixture to increase the reagent concentration.(105) After two more days of reaction time, several spots were observed including the starting material. The starting material was regenerated in low yield and several unidentified degradation products were observed however not the desired product.

It was believed that a smaller reagent could be added to alcohol **55**, and to form the *S*-methyl carbothioate **56a** the reaction conditions were changed. At −78℃ the strong base NaHMDS was added and was left for 30 min to from the alkoxide, before CS_2 was added. The reaction was again left for 30 min before the addition of iodomethane, 30 min later the reaction was quenched.(55) The TLC of the reaction showed two spots of similar R_f-values, R_f=0.41 and R_f=0.46 (TLC 3% EtOAc: pentane), that was inseparable by flash chromatography (1% EtOAc: pentane). By studying ^{1}H-NMR it was at this point believed that the two compounds were stereoisomers, arising from the non-selective reduction with LAH. As a part of the second step of the Barton-McCombie deoxygenation the stereogenic center would be removed and the inseparable mixture was used in the next step. The formation of the *S*-methyl carbothioate **56** was confirmed by MS **(**TOF MS ES$^+$ *m/z* $[M+Na]^+$ calc. for $C_{26}H_{46}O_3SiS_2Na$ 521.2555, ion observed 521.2550.) The mixture of the two isomers were obtained in yields ranging from 80.1-91.7%.

Table 6-8

The reaction conditions for the attempted for the formation of imidazole-carbothioate of **55** and the reaction conditions and the yield for the formation of the *S*-methyl carbothioate **56a** and **56b**.

Starting material (s.m)	Reagent	Solvent	Reaction conditions	Comment/Yield	Ref.
55	TCDI (2.0 eq.)	Toluene	4.5 hours, reflux	No conversion of s.m	
55	TCDI (3.0 eq) DMAP (0.2 eq., after 27 h)	1,2-Dichloroethane	3 days, reflux	Low conversion of s.m, degradation of s.m	(106)
55 51.8 mg 0.127 mmol	1) NaHMDS (10 eq.) 2) CS_2 (20 eq.) 3) MeI (30 eq.)	THF	1) 30 min 2) 30 min, 3) 30 min Total reaction time 1.5 h, −78 ℃	Mixture **56a** and **56b** 51.2 mg 0.103 mmol 80.1%	(55)
55 700 mg 1.71 mmol	1) NaHMDS (10 eq.) 2) CS_2 (20 eq.) 3) MeI (30 eq.)	THF	1) 30 min 2) 30 min, 3) 30 min Total reaction time 2h, −78 ℃	Mixture **56a** and **56b** 784 mg 1.57 mmol 91.7% yield	(55)

The second step of the Barton-McCombie reaction was first attempted with the thermal radical initiator AIBN and TTMS as the hydrogen donor (**Table 6.9**). After 6 hours under reflux the reaction was quenched. Flash chromatography of the reaction gave a mixture of the **57** and the **56**, confirmed by MS (TOF MS ES^+ $[M+Na]^+$= 415.3005 and $[M+ Na]^+$=521.2537). The reaction did not give full conversion of the starting material, and the next reaction was left for 26 hours. After flash chromatography the starting material was no longer present in the mixture, however the product and another byproducts were inseparable by flash chromatography chromatography (1% EtOAc: pentane).

In an attempt to reduce the reaction time and formation of byproducts, Et_3B another radical initiator that does not require high temperatures and the more reactive hydrogen donor, Bu_3SnH was used. After 22 hours, TLC showed full conversion of the starting material but the two different compounds where still present in the mixture. The compounds were of low polarity and were inseparable flash chromatography (1% EtOAc:pentane). However, by optimizing the eluent to 20% CH_2Cl_2: pentane, the two compounds were finally separated. By studying both compounds by 2D-NMR techniques it was possible to determine that the two compounds were in fact regioisomer **57a** and **57b**. The possible origin for the formation of the two isomers are traced back to the first step of the Barton McCombie deoxygenation, see the proposed mechanism in **Scheme 6-9**. The formation of the alkoxide generated an intramolecular

nucleophile, which made it possible for a silyl ether migration from one hydroxyl group to the other. This resulted in two possible sites for the addition of CS_2, giving the two regioisomers **57a** and **57b** after the removal of the *S*-methyl carbothioate.(46) **57a** was afforded in 23.3% and **57b** in 58.2% yield. (20% CH_2Cl_2: pentane, R_f= 0.22 (**57a**) and R_f= 0.39 (**57b**)). The ratio of the between the isomers were calculated to be 0.40, where the desired isomer **57a** was given in the lowest yield.

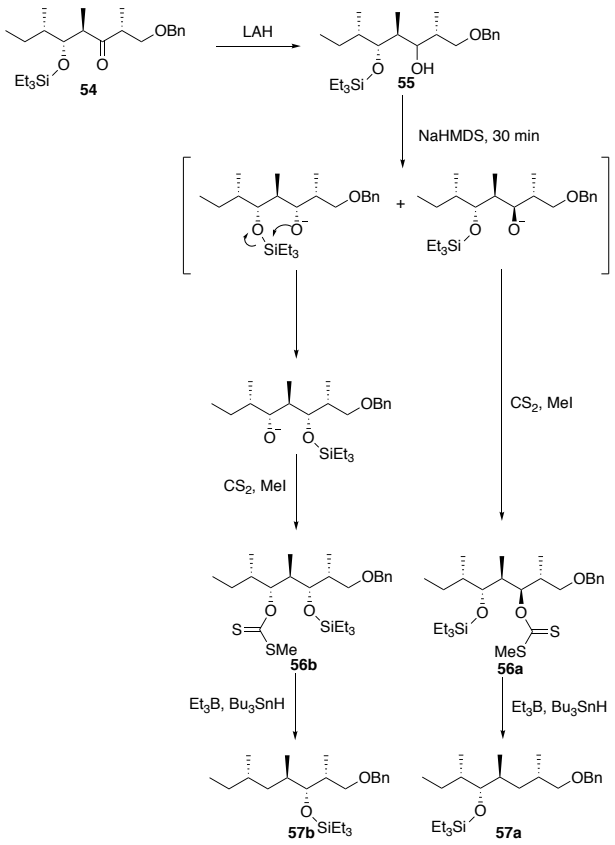

Scheme 6-9 The possible mechanism for the origin of the formation of the two isomers **57a** and **57b**.

Table 6-9
The reactions conditions and yields for the formation of **57a** and **57b** from the mixture of **56a** and **56b**

Starting material (s.m)	Reagents	Solvent	Reaction conditions	Yield/ Comment	Ref.
Mixture **56a** and **56b**	AIBN (0.4 eq.) TTMS (1.2 eq.)	Toluene	Reflux, 6h	Not full conversion of s.m, product and s.m mixture	
Mixture of two isomers **56a** and **56b**	AIBN (0.4 eq.) TTMS (3.4 eq.)	Toluene	Reflux, 26 h	Full conversion of s.m, nonpure mixture of the two isomers	
Mixture of two isomers **56a** and **56b**	Et_3B (1.2 eq) Bu_3SnH (9.6 eq.)	Toluene	22 h, rt	Full conversion of s.m, mixture **57a** and **57b**	(83)
Mixture of two isomers **56a** and **56b** 579 mg 1.16 mmol	Et_3B (1.7 eq.) Bu_3SnH (9.8 eq.)	Toluene	49 h, rt	**57a** 106 mg 0.2704 mmol 23.3% **57b** 265 mg 0.676 mmol 58.2% Isomer Ratio=0.40	(83)

6.6 Removal of Benzyl Group in 57a and 57b

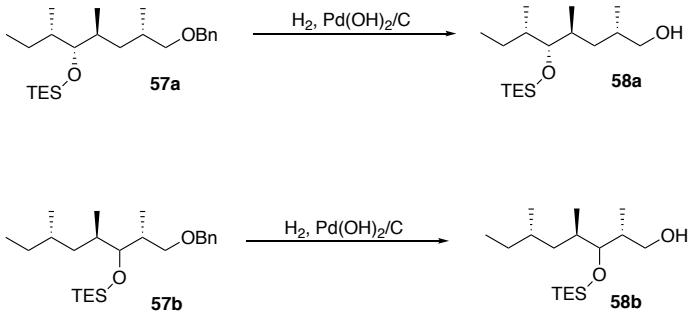

Scheme 6-10 The removal of the benzyl group in **57a** and **57b** to form primary alcohol **58a** and **58b**, respectively.

The removal of the benzyl group was first tested on the mixture of the two isomers **57a** and **57b** with Pd-C carried out in either MeOH or EtOAc, these reactions did not give any significant conversion of the starting material.(107, 108) After the two isomers **57a** and **57b** were separated the benzyl removal was tested with $Pd(OH)_2$ in THF. The isomer **57b** was used in the test reaction, due to the similar chemical properties and functional groups a successful reaction for **57b** could transfer to a successful reaction for the desired isomer **57a**.(45) The reaction with $Pd(OH)_2$ showed a full conversion of the starting material after 1 hour and product was filtered on celite. The alcohol **58b** was afforded in 89.8-94.6% yield. The reaction was then performed on the desired isomer **57a** and the alcohol **58a** was afforded in 78.7% yield.

Table 6-10

The reaction conditions and yields for the removal of the benzyl group in **57a** and **57b** to form primary alcohol **58a** and **58b**, respectively.

Starting material (s.m)	Reagents	Solvent	Reaction conditions	Yield/ Comment	Ref.
Mixture of isomers **57a** and **57b**	10% Pd-C H_2	MeOH	48 h, rt	No conversion of s.m	(107)
Mixture of isomers **57a** and **57b**	10% Pd-C H_2	EtOAc	24 h, rt	No conversion of s.m	(108)
57b 44.2 mg 0.113 mmol	$Pd(OH)_2$ H_2	THF	1 h, rt	**58b** 32.2 g 0.106 mmol 94.6%	(45)
57b 164 mg 0.417 mmol	$Pd(OH)_2$ H_2	THF	1.5 h, rt	**58b** 113 mg 0.374 mmol 89.8%	(45)
57a 101 mg 0.256 mmol	$Pd(OH)_2$ H_2	THF	2 h, rt	**58a** 60.6 g 0.200 mmol 78.7% yield	(45)

6.7 Hoover-Stahl Oxidation of Primary Alcohol 58a and 58b

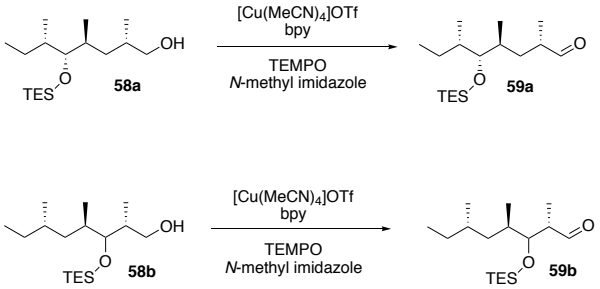

Scheme 6-11 The Hoover-Stahl oxidation of **58a** and **58b** to form aldehyde **59a** and **59b**, respectively.

The Hoover-Stahl oxidation of the primary alcohol was also tested with isomer **58b**, to identify and later avoid potential degradation of the isomer **58a**. Due to low amount of the starting material, to be able to measure out the reagents in the correct ratio, 0.2 equivalents of $[Cu(MeCN)_4]OTf$, bpy and TEMPO and 0.4 equivalents of *N*-methyl imidazole were used.(60) The same work up as described for the preparation of aldehyde **10** was used, the aldehyde **59b** was given in 57.1% yield, however the acidic work up also resulted in small amounts of a TES-deprotection aldehyde (15% EtOAc: hexane, Rf= 0.27, the characteristic TES shifts was not present in ^{1}H-NMR and O-H stretch in IR). The oxidation of **58b** was then tested without the acidic work up and the aldehyde **59b** was afforded in 85.7% yield. The oxidation of **58a** was performed by using the same procedure and the aldehyde **59a** was obtained in 81.0% yield.

Table 6-11

Reaction conditions and yields for the Hoover-Stahl oxidation of primary alcohol **58a** and **58b** to aldehyde **59a** and **59b**, respectively.

Starting material (s.m)	Reagents	Solvent	Reaction conditions	Yield/ Comment	Ref.
58b 29.1 mg 0.0962 mmol	$[Cu(MeCN)_4]OTf$ (0.2 eq.) Bpy (0.2 eq.) TEMPO (0.2) *N*-methyl imidazole (0.4 eq.) O_2-balloon	CH_3CN	48 h, rt	**59b** 16.5 mg 0.0549 mmol 57.1%* TES-deprotected aldehyde 0.0042 g	(60)
58b 133 mg 0.439 mmol	$[Cu(MeCN)_4]OTf$ (0.2 eq.) Bpy (0.2 eq.) TEMPO (0.2) *N*-methyl imidazole (0.4 eq.) O_2-balloon	CH_3CN	48 h, rt	**59b** 113 mg 0.376 mmol 85.7%	(60)
58a 59.5 mg 0.197 mmol	$[Cu(MeCN)_4]OTf$ (0.2 eq.) Bpy (0.2 eq.) TEMPO (0.2) *N*-methyl imidazole (0.4 eq.) O_2-balloon	CH_3CN	47 h, rt	**59a** 47.9 g 0.159 mmol 81.0%.	(60)

*Acidic work up, 1 M HCl

6.8 The Carreira Alkynylation Attempt with Aldehyde 59b and Alkyne 72

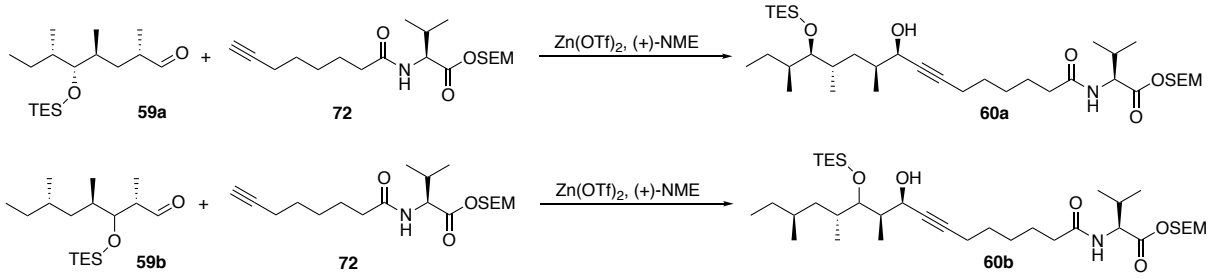

Scheme 6-12 The reaction for the Carreira alkynylation of aldehyde **59a** and **59b** with alkyne **72** to generate **60a** and **60b**, respectively.

The Carreira alkynylation was attempted with aldehyde **59b** and alkyne **72,** first a reaction was tested at room temperature, after 4 days and no conversion the reaction was quenched and the starting materials were generated. A new reaction was attempted at elevated temperatures, with more equivalents of the reagents and dried $Zn(OTf)_2$, as the reaction proceeded new spots appeared on the TLC-plate, but the starting materials were still present. The reaction was quenched after 4 days, purified by flash chromatography, but the desired product was not observed. However, racemization of the aldehyde **59b** was indicated by ^{1}H-NMR (400 MHz, $CDCl_3$) where two aldehyde shifts at 9.79 (d, J=2.5 Hz) and at 9.73 (d, J=1.1) were observed. A common by-reaction of the Carreira alkynylation is self-condensation of the aldehyde due to enolate formation in the presence of Et_3N and Lewis acid $Zn(OTf)_2$, which also allow for racemization of α-substituents.(109) Due to the failed Carreira alkynylation under the described reaction conditions with aldehyde **59b**, new reaction conditions must be found before the reaction is attempted with the valuable aldehyde **59a**.

Table 6-12

Reaction conditions for the Carreira alkynylation attempt with aldehyde **59b** and alkyne **72**.

Starting material (s.m)	Reagents	Solvent	Reaction conditions	Yield/ Comment	Ref.
59b	$Zn(OTf)_2$ (1.1 eq.) (+)-NME (1.2 eq.) Et_3N (1.2 eq.) **72** (1.2 eq.)	Toluene	4 days, rt	No conversion of the s.m	(64)
59b	$Zn(OTf)_2$ (2.1 eq.) (+)-NME (2.1 eq.) Et_3N (2.2 eq.) **72** (2.0 eq.)	Toluene	4h, rt – 60 ℃	Low conversion of the s.m and racemization of **59b**, no product observed	(110)

6.9 The Hoover-Stahl Oxidation of Primary Alcohol 65

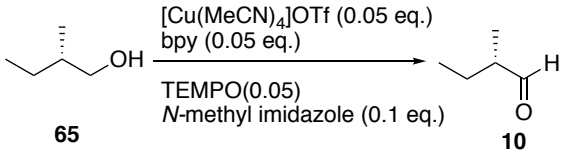

Scheme 6-13 The Hoover-Stahl oxidation of primary alcohol **65** to aldehyde **10**

The Hoover-Stahl oxidation gave the optically active aldehyde **65** in yields ranging from 47.3-54.0%. The reaction time was significantly increased by using a O_2- balloon instead of leaving the reaction open to air. The aldehyde **10** is volatile and the pentane used in the extraction was removed by distillation. However, the solvent was still present and the yield of the reaction was calculated from the aldehyde **10** to pentane ratio by ^{1}H-NMR. The product was successfully used in the aldol reaction without the need for further purification.

Table 6-13

Reaction conditions and yields for the Hoover-Stahl oxidation of primary alcohol **65** to aldehyde **10**.

Starting material (s.m)	Reagents	Solvent	Reaction conditions	Yield/ Comment	Ref.
65 4.75 g 53.9 mmol	$[Cu(MeCN)_4]OTf$ (0.05 eq.) Bpy (0.05 eq.) TEMPO (0.05) *N*-methyl imidazole (0.1 eq.)	CH_3CN	96 h, rt, air	**10** 2.20 g 25.5 mmol 47.3%	(60)
65 5.23 g 59.4 mmol	$[Cu(MeCN)_4]OTf$ (0.05 eq.) Bpy (0.05 eq.) TEMPO (0.05) *N*-methyl imidazole (0.1 eq.)	CH_3CN	24 h, rt, O_2-atmosphere	**10** 2.76 g 32.01 mmol 54.0%	(60)

6.10 Preparation of Amine 67

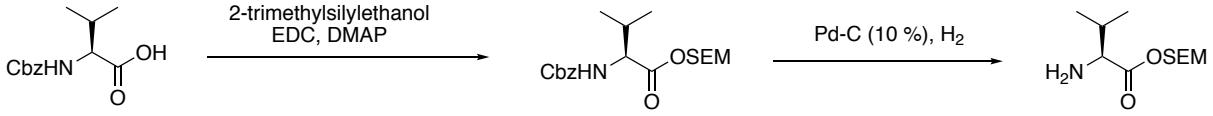

31 **66** **67**

Scheme 6-14 The reaction for the *N*-Cbz protected carboxylic acid **31** as its SEM ester **66** and the removal of the benzyl carbamate to form amine **67**.

The protection of the carboxylic acid in **31** as its SEM ester was performed by following the procedure described by Gellman et al. (111) The reaction was monitored by both TLC and ^{1}H-NMR, when left overnight full conversion of the starting was observed and there was no visible byproduct on the TLC plate, the SEM ester **66** was obtained in yield ranging from 42.5-43.9%.

Table 6-14

Reaction conditions and yield for *N*-Cbz protected carboxylic acid **31** as its SEM ester **66**.

Starting material (s.m)	Reagents	Solvent	Reaction conditions	Yield/ Comment	Ref.
31 1.10 g 4.39 mmol	2-trimethylsilyl ethanol (1.3 eq.) EDC (1.3 eq.) DMAP (0.01 eq.)	CH_2Cl_2	17.5 h, rt	**66** 674 mg 1.92 mmol 43.6%	(111)
31 2.11 g 8.39 mmol	2-trimethylsilyl ethanol (1.3 eq.) EDC (1.3 eq.) DMAP (0.01 eq.)	CH_2Cl_2	20 h, rt	**66** 1.30 g 3.69 mmol 43.9%	(111)
31 1.31 g 5.21 mmol	2-trimethylsilyl ethanol (1.3 eq.) EDC (1.3 eq.) DMAP (0.01 eq.)	CH_2Cl_2	19 h, rt	**66** 780 mg 2.22 mmol 42.5%	(111)

After the protection of the carboxylic acid moiety, the benzyl carbamate in **66** was removed to form amine **67**. First the removal was conducted with 10% Pd-C with 4.4% formic acid in MeOH as the hydrogen donor.(111) After 4 h the reaction showed full consumption of the starting material and it was filtered on celite. In the spectrum of the product, formic acid was present, which was attempted to be removed be addition of toluene to form an azeotropic mixture. The product was not purified further.(111) To avoid the removal of formic acid an alternative approach with H_2 as the hydrogen source was tested, these reaction was stirred at rt for 2-3 h and filtered on celite.(107) The products was then purified by flash chromatography and amine **67** was afforded in yields ranging from 60.6-72.5%.

Table 6-15

Reaction conditions and yields for the removal of the benzyl carbamate protection group in **66** to from amine **67**.

Starting material (s.m)	Reagents	Solvent	Reaction conditions	Yield/ Comment	Ref.
66 430 mg 1.22 mmol	10% Pd-C	4.4% formic acid in MeOH	4 h, rt	**67** 298 mg 1.37 mmol 112%*	(111)
66 505 mg 1.44 mmol	10% Pd-C H_2	MeOH	3 h, rt	**67** 189 mg 0.870 mmol 60.6%	(107)
66 764 mg 2.17 mmol	10% Pd-C H_2	MeOH	2.5 h, rt	**67** 298 mg 1.37 mmol 63.1%	(107)
66 780 mg 2.22 mmol	10% Pd-C H_2	MeOH	2 h, rt	**67** 350 mg 1.61 mmol 72.5%	(107)

*Trace of formic acid in ^{1}H-NMR spectrum, not purified by flash chromatography

6.11 Ozonolysis of Cycloheptene 58

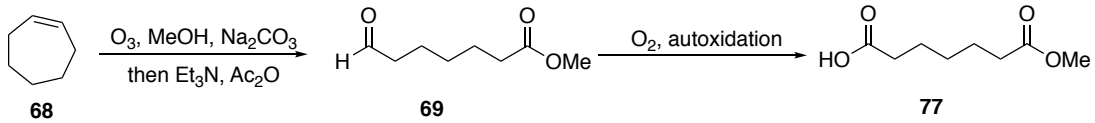

Scheme 6-15 The ozonolysis of cycloheptene **68** to form methyl ester aldehyde **69**, and autoxidation during storage.

The methyl ester aldehyde **69** was prepared in 79.2% yield by ozonolysis of the commercially available **68**, following the procedure described by Carreira et al.(112) By comparing the NMR-spectrum of a newly flashed sample of **69**, a sample that has been stored for 3 months −19 ℃ and a sample stored for 3 months at room temperature. The sample left at room temperature showed that the aldehyde (CHO, ^{1}H-NMR shift at 9.75 ppm) had been completely oxidized to the carboxylic acid **77** (COOH, ^{1}H-NMR shift 10.03 ppm) however the sample stored at −19 ℃ for the same amount of time had only partly been oxidized. It is possible that the aldehyde **69** can be autoxidation by atmospheric O_2, and it is therefore essential to not store the aldehyde over a significant period of time to avoid the oxidation to the carboxylic acid **77**. The NMR analysis of **77** is given in section 8.12 and the ^{1}H-NMR of the samples are given in appendix R, X and Y. (113)

Table 6-16

Reaction conditions and yield for the ozonolysis of cycloheptene **68** to methyl ester aldehyde **69**.

Starting material (s.m)	Reagents	Solvent	Reaction conditions	Yield/ Comment	Ref.
68 1.57 g 16.3 mmol	1) $NaHCO_3$ (0.3 eq.) O_3 2) Et_3N (1.5 eq.) Ac_2O (2.9 eq.)	CH_2Cl_2: MeOH	1) 25min, −78℃ 2) 2 h, 0 ℃	**69** 2.05 g 12.9 mmol 79.2%	(112)

6.12 The Ohira-Bestmann Homolongation of Aldehyde 69

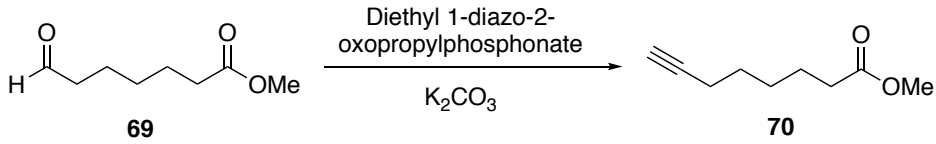

69 **70**

Scheme 6-16 The Ohira-Bestmann homolongation of aldehyde **69** to generate alkyne **70**.

For the conversion of aldehyde **69** to the terminal alkyne **70**, the modified Ohira-Bestmann reagent diethyl 1-diazo-2-oxopropylphosphonate was used in combination with K_2CO_3 in MeOH. The aldehyde was slowly added to the solution at 0 °C, warmed to room temperature and stirred overnight. After 24 h, the reaction showed full conversion of the starting material, the alkyne **70** was achieved in yields ranging from 35.5-38.7%. The synthesis of **70** from **69** through the Ohira-Bestmann reaction is reported in literature in the yield of 41%.(114) However, the related 2-methyl-oct-7-ynonic acid methyl ester, achieved significantly higher yields of 78%.(115) It is possible that the oxidation of the aldehyde to the corresponding carboxylic acid during the short storage time or in reaction itself can contribute to low reaction yields.

Table 6-17
Reaction conditions and yields for the Ohira-Bestmann homolongation of aldehyde **69** to alkyne **70**.

Starting material (s.m)	Reagents	Solvent	Reaction conditions	Yield/ Comment	Ref.
69 478 mg 3.02 mmol	diethyl 1-diazo-2-oxopropylphosphonate (1.3 eq.) K_2CO_3 (2.0 eq.)	MeOH	24 h, 0 °C to rt	**70** 166 mg 1.07 mmol 35.5%	(114, 115)
69 613 mg 3.88 mmol	diethyl 1-diazo-2-oxopropylphosphonate (1.1 eq.) K_2CO_3 (2.6 eq.)	MeOH	24 h, 0 °C to rt	**70** 0.232 g 1.50 mmol 38.7%	(114, 115)

6.13 The Hydrolysis of Methyl ester 70

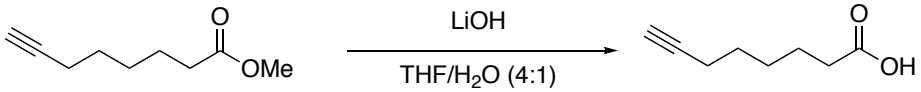

70 **71**

Scheme 6-17 The base catalysed ester hydrolysis of **70** to form the carboxylic acid **71**.

A facile hydrolysis of methyl ester **70** mediated by LiOH in aqueous THF, afforded the carboxylic acid **71** in high yields, without further purification necessary, see **Table 6-18**.

Table 6-18

Reaction conditions and yield for the hydrolysis of ester **70** to **71**.

Starting material	Reagents	Solvent	Reaction conditions	Yield/ Comment	Ref.
70 106 mg 0.671 mmol	LiOH (3.0 eq.)	4:1 THF-water	24 h, 0 ℃ to rt	**71** 92.9 mg 0.663 mmol 98.7%	(115)
70 257 mg 1.62 mmol	LiOH (3.0 eq.)	4:1 THF-water	20.5 h, 0 ℃ to rt	**71** 241 mg 1.72 mmol 105.7%*	(115)

*Trace of solvent in product ^{1}H-NMR spectrum

6.14 Amide coupling of 70/71 and Amine 67

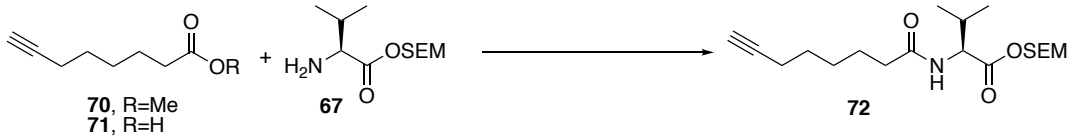

70, R=Me
71, R=H
67
72

Scheme 6-18 The amide coupling of amine **72** with either ester **70** or the carboxylic acid **71** to form amide **72**.

The amide coupling was first attempted by activating the carboxylic acid **71** with isobutyl chloroformate giving a mixed anhydride intermediate. After 24 hours the reaction was quenched, several unidentified products were formed in the reaction however the desired product was not observed. To avoid hydrolyzing the ester **70** to the carboxylic acid **71** prior to the amide coupling an alternative approach was tested. The reaction used the air-stable DABAL-Me_3, that can activate the amine by formation of an aluminium amide.(116-118) The reagent was shown to not be compatible with the SEM protected **72**, and the reagent is viewed as to aggressive for peptide synthesis due to its reactivity toward both esters and carboxylic acids.(117) The byproduct of the reaction was not identified, however NMR-analysis suggested

that the C-O bond of the ester **70** was cleaved mediated by the Lewis acidity of DABAL-Me_3.(119)

Another coupling agent used for activation the carboxylic acid **71** was tested. The reaction was conducted with HATU and Huing's base (DIPEA).(120) The first reaction was left for 3 h and was flashed several times to optimize the eluent ratio and gave the amide **72** in 53.3 % yield. The second reaction attempt was left for four hours and was only flashed once and reaction gave the desired amide **72** in 91.9% yield.

Table 6-19

Reaction conditions and yields for the amide coupling of amine **66** with carboxylic acid **71** and the reaction conditions for other amide coupling attempts.

Starting material (s.m)	Reagents	Solvent	Reaction conditions	Yield/ Comment	Ref.
71	*N*-methylmorpholine (1.0 eq.) Isobutyl chloroformate (1.1 eq.) **72** (2.0 eq.)	CH_2Cl_2	24 h, 0 °C to rt	Desired product not observed	(121)
70	DABAL-Me_3 (1.5 eq.) **72** (1.4 eq.)	CH_2Cl_2	24 h, reflux	Desired product not observed	(118)
71 43.7 mg 0.312 mmol	DIPEA (31.5 eq.) HATU (3.2 eq.) **72** (1.3 eq.)	DMF	3 h, 0 °C to rt	**72** 56.6 mg 0.167 mmol 53.3%	(120)
71 193 mg 1.37 mmol	DIPEA (31.5 eq.) HATU (3.2 eq.) **72** (1.4 eq.)	DMF	4 h, 0 °C to rt	**72** 430 mg 1.27 mmol 91.9%	(120)

7 Conclusion and Further Work

The synthetic steps conducted in this project is summarized in **Scheme 7-1** and **Scheme 7-2**. By following the procedures by Paterson. et al the important ketone **52** was synthesized successfully and was through the *anti*-selective Paterson aldol reaction coupled to aldehyde **10** to generate the aldol adduct **53** in high yields as the single diastereomer. The hydroxyl group was protected as its TES ether **54** before the deoxygenation was attempted.(45, 81) The TES ether as a hydroxyl protection group was chosen for this project, because it allowed for orthogonal protection strategy and it is small than other more robust silyl ethers, which accommodates for modifications at the ketone position without given too much steric hindrance. However, observed through the project the TES-protection group have been involved in many of the challenges that was faced, because it was cleaved under many of the reaction conditions. A more robust protection group can be installed, the TBS-protection of **53** was attempted with TBSCl and imidazole, but the reaction did not preceed. However other silyl ether protections can be tested with trialkylsilyl triflat which is a better leaving group and with another base system.(46)

The initial plan for the deoxygenation of ketone **54** was through the formation of dithiane **73** accompanied by Raney-Nickel desulfurization. Extensive efforts were made in the attempted to generate the desired dithiane **73**. However, the ketone **54** was sensitive to the reaction conditions, where the TES-protection group was readily cleaved under the Lewis acid catalyzed thioacetylation, which allowed for further degradation of the starting material.

As an alternative approach the ketone **54** was reduced to the secondary alcohol **55** followed by the two-step Barton McCombie deoxygenation. The approach lead to the desired deoxygenation product **57a**, however the regioisomer **57b** was also generated (isomer ratio=0.40). The formation of the isomer was traced back to a silyl ether migration during the *S*-methyl carbothioate formation. The reaction had a 30 min waiting period between the addition of the base and the addition of CS_2, this allowed for the formation of intramolecular nucleophile and the silyl ether migration. In a method described by Laschat et al., where a molecule with a similar 1,3-system was the starting material (compound **74** in **Figure 6-1**) the reaction was carried out with absolute CS_2 as the solvent.(83) The electrophile was therefore present in the reaction mixture before the base was added. By following this procedure, the silyl ether migration might be reduced or avoided. A stereoselective reduction of the ketone **54** to form

the *anti*-alcohol might also reduce the proximity of the generated alkoxide to the silyl ether. In addition, this type of reduction might to reduce the formation diol **76** that was formed by reductive cleavage of the TES-protection group. Alternatively, a new reaction pathway for the deoxygenation can be tested. In this project the Wolff-Krishner reduction was considered, which uses hydrazine for the reduction of carbonyl compounds.(38) However, the Barton-McCombie deoxygenation was tested first, but the Wolff-Krishner reductions is a possible pathway for further work on this project.

With the deoxygenated product **57a** and **57b** in hand, to prepare for the Carreira alkynylation the benzyl group was removed under $Pd(OH)_2/H_2$, followed by the Hoover-Stahl oxidation of the primary alcohol to give **59a** and **59b**, respectively. The key coupling reaction of the major fragments by Carreira alkynylation was only attempted with the aldehyde **59b** and alkyne **72**. The reaction was conducted with 2 equivalents of the reagents, at elevated temperature and where the $Zn(OTf)_2$ was dried prior to the reaction. The desired product was not formed and racemization of the aldehyde **59b** was observed. New reaction conditions are required before attempting the alkynylation with the valuable aldehyde **59a**. Generally, the alkynes utilized in the Carreira alkynylation are of short chains and a new reaction can be attempted with the alkyne **70**, which can be amide coupled to amine **67** at a later point.(122) The Carreira alkynylation can also be attempted with catalytic amounts of the reagents at elevated temperatures with a slow addition of the aldehyde.(123) However, there are several different alkynylation approaches for the coupling of aldehydes and alkynes. Three other alkynylation methods that have received attention is described by the groups of Trost, Wolf and Shibasaki. In the alkynylation method by Trost et al. a proline-derived bimetallic catalyst in combination with 3 eq. of Me_3Zn is utilized to afford the propargylic alcohol.(124) The group of Wolf describe a bisoxazolidine-catalyzed alkynylation that are compatible for both linear and branched alkynes, where the propargylic alcohol is obtained in high yields and enantioselctivty.(125) The alkynylation by Shibasaki et al. is promoted by catalytic In(II)/BINOL complex system, which allow mild reaction conditions for the formation of propargylic alcohols from a variety of substrates.(126)

The alkyne **72** used in the attempted Carreira alkynlation, was prepared by the amide coupling of amine **67** prepared in two steps from *N*-Cbz-L-Valine (**31**) and the carboxylic acid **71** derived from cycloheptene (**68**). Cycloheptene **68** was the starting material for the ozonolysis which lead to the methyl ester aldehyde **69**. **69** was used in the Ohira-Bestmann homolongation, where

the alkyne moiety was introduced. The reaction provided alkyne **70** in low yields, possibly attributed to a rapid autoxidation of the aldehyde **69** to the corresponding carboxylic acid **77**. The aldehyde **69** should not be stored over a significant period of time and should be kept under N_2-atmosphere in the freezer.

The aim of the project was to find an alternative approach and obtain the synthetic steps toward a dysoxylactam A, the projected reached the Carreira alkynylation, which was attempted but was not successful in obtaining the desired product. Further work on this project will focus on optimizing the deoxygenation of the aldol adduct with the alternative procedures discussed above and to establish the Carreira alkynylation. When the Carreira alkynylation is established the alkyne **60a** can be reduced to **61** and the propargylic alcohol protected as it allyl ether **62**. To prepare for the Yamaguchi macrolactonization the TES ether and the SEM ester in **62** can be removed simultaneously to liberate the hydroxyl group and the carboxylic acid in **63**, respectively. In the total synthesis of **1** described by S. Raghavan and S.S. Chandankar and by B. Yu and D. P. Reddy they reported epimerization of N-Boc-Valine the esterification mediated by DDC- and EDCl-activation, respectively. Where the epimerization could be identified by 4 shifts above 150 ppm in ^{13}C-NMR.(5, 6) However, the esterification of N-Cbz-L-valine mediated with the Yamaguchi reagent in the total synthesis by Ye et al , epimerization was not visible by NMR analysis.(4) This is included as a note and something to look for with the key macrolactonization.

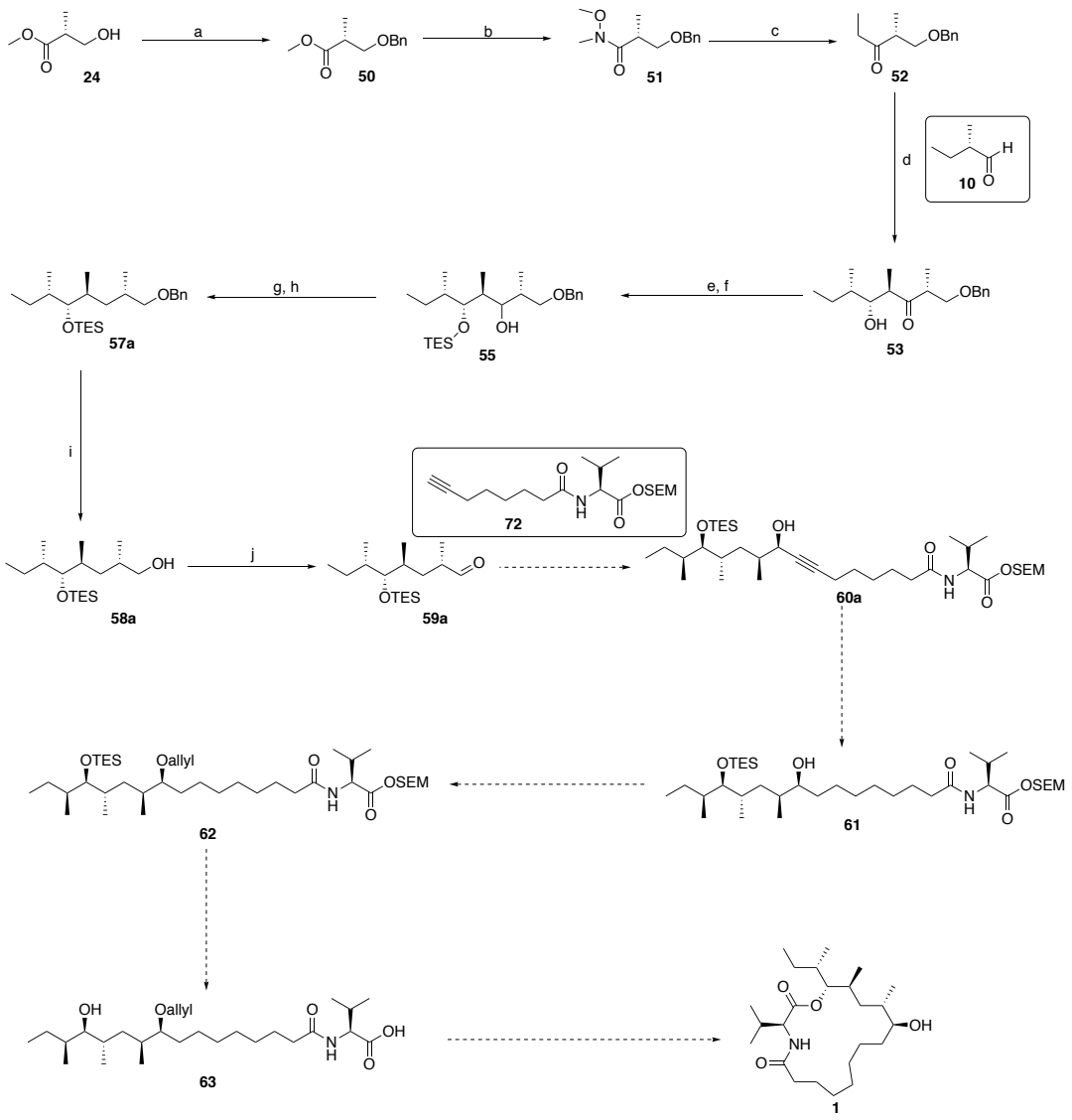

Scheme 7-1 Benzyl 2,2,2-trichloroacetimidate (1.1 eq.), triflic acid (0.4 eq.), CH_2Cl_2: cyclohexane(1:2), rt, 48 h, 68.8%, b) MeN(OMe)H·HCl (1.6 eq.) *i*-PrMgCl (3.0 eq), −15 ℃, 5 h, 83.8% c) EtMgBr (2.2 eq.), THF, 0 ℃, 4.5 h, 95.5% d) i)$(Cy)_2BCl$ (1.5 eq.), NEt_3 (1.6 eq.), **10** (5.1 eq.), 0 ℃-−78℃-−19℃, overnight ii) H_2O_2, pH 7 buffer, 0 ℃, 1.5 h, 91.5% e) 2,6-lutidine (1.2 eq.), TESOTf (1.1 eq.), 0 ℃, 1 h, 92.9% f) LAH (2.5 eq.), THF, −78℃, 55 min, 72.7% g) NaHMDS (10 eq.), CS_2 (20 eq.), MeI (30 eq.), 2 h, −78℃, 91.7% over all yield of the two isomers h) Et_3B (1.7 eq.), Bu_3SnH (9.8 eq.), toluene, rt, 49 h, 23.3% yield of **57a** and 58.2% yield of **57b** i) $Pd(OH)_2/H_2$, THF, rt, 2 h, 78.7% j) $[Cu(MeCN)_4]OTf$ (0.2 eq.), Bpy (0.2 eq.), TEMPO (0.2), *N*-methyl imidazole (0.4 eq.), O_2-atmosphere, rt, 47 h, 81.0%.

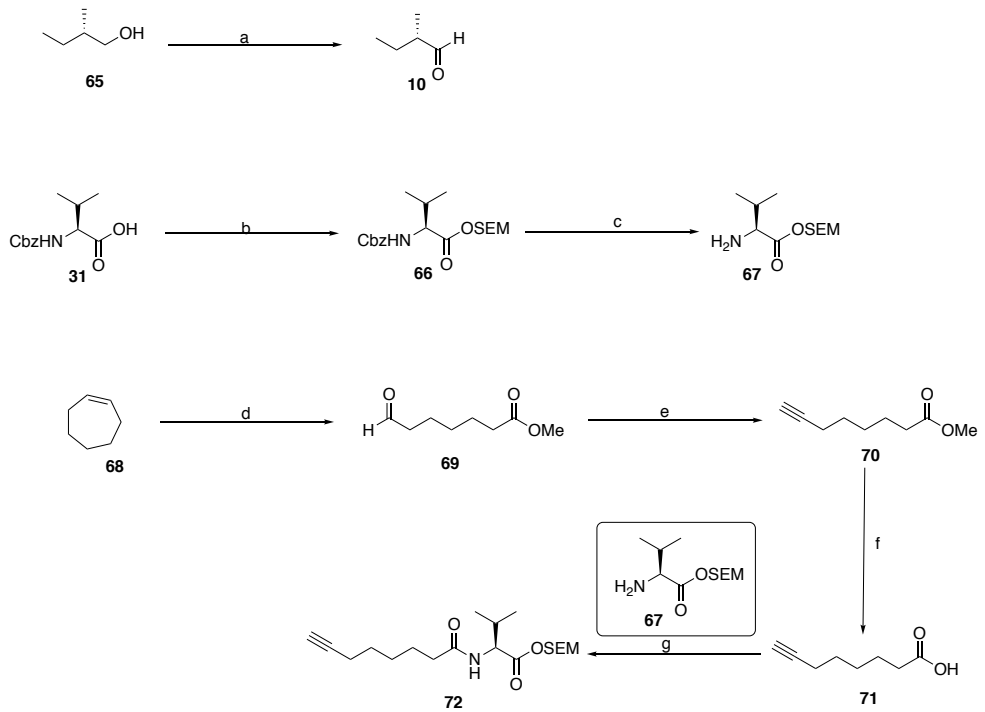

Scheme 7-2 a) [Cu(MeCN)$_4$]OTf (0.05 eq.), Bpy (0.05 eq.), TEMPO (0.05), *N*-methyl imidazole (0.1 eq.), O_2-atmosphere, CH_3CN, 24 h, 54.0% b) 2-trimethylsilyl ethanol (1.3 eq.), EDC (1.3 eq.), DMAP (0.01 eq.), CH_2Cl_2, rt, 20 h, 43.9% c) 10% Pd-C, H_2, MeOH, rt, 2 h, 72.5% d) i) $NaHCO_3$ (0.3 eq.), O_3, CH_2Cl_2 : MeOH, −78°C, 25 min ii) Et_3N (1.5 eq.), Ac_2O (2.9 eq.), 0°C, 2 h, 79.2% e) diethyl 1-diazo-2-oxopropylphosphonate (1.1 eq.), K_2CO_3 (2.6 eq.), MeOH, 0 °C - rt, 24 h, 38.7% f) LiOH (3.0 eq.), 4:1 THF-water, 0 °C-rt, 24 h, 98.7% g) DIPEA (31.5 eq.), HATU (3.2 eq.), **67** (1.4 eq.), 0 °C - rt, 4 h, 91.9%.

8 Spectroscopic Analysis and Characterization

8.1 General Information of the Spectroscopic Method

This section will present the compounds that are not previously reported in the literature. The novel compounds have been characterized based upon their ^{1}H- and ^{13}C-shifts, and the ^{1}H-^{13}C were assigned by HSQC. The connectivity of the structure was then elucidated by the 2D-NMR techniques COSY and HMBC.

The NMR spectra are recorded by either Bruker 600 MHz Avance III HD equipped with a 5-mm cryogenic CP-TCI z-gradient probe and SampleCase or 400 MHz Avance III HD equipped with a 5-mm SmartProbe z-gradient probe and SampleCase, and will be specified for each compound. All spectra are processed, analyzed and prepared by the software Bruker Topspin 3.6.0.

The chemical shifts for each compound will be presented in a table. Each position corresponds to a numbered carbon atom in the compound structure, unless otherwise is noted. The ^{1}H-shift will be appointed along with the integral (int.), the multiplicity (multi.) and the coupling constant (J) given in Hertz (Hz) for each peak. Splitting patterns for a ^{1}H-signal are indicated as singlet (s), doublet (d), triplet (t), quintet (qnt), sextet (sxt), heptet (hpt) or multiplet (m). Both ^{1}H- and ^{13}C-shifts are given in parts per million (ppm).

8.2 (*2R,4R,5R,6S*)-1-(benzyloxy)-5-hydroxy-2,4,6-trimethyloctan-3-one (53)

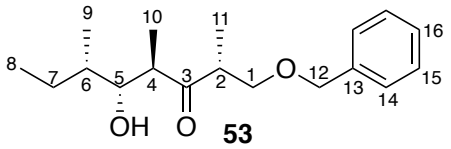

53

Figure 8-1 Numbering of carbon atoms in compound **53** for NMR assignment.

Table 8-1

Assigned NMR-shifts for compound **53**, shown in **Figure 8-1** (600 MHz, $CDCl_3$). NMR-spectra are given in appendix D.

Position	^{1}H [ppm] (int., multi., J[Hz])	^{13}C [ppm]	COSY	HMBC
13	-	137.9	-	12, 12’
15	7.35-7.27 (5H, m)	128.4		
14		127.5		
16		127.6		
12	4.51 (1H, d, J=12.2)	73.8	-	1, 1’, ArH
12’	4.46 (1H, d, J=11.9)			
1		72.1	1’, 2	2, 11,12
	3.74-3.67 (2H, m)			
5		75.4	OH, 4, 6	OH, 4, 6, 7, 9, 10
1’	3.43 (1H, dd, J= 9.0, J= 4.9)	72.1	1, 2	2, 11, 12
2	3.13-3.06 (1H, m)	45.6	1, 1’,11	1, 1’, 4, 11
4	2.89-2.83 (1H, m)	49.5	5, 10	OH, 5, 10
OH	2.46 (1H, m)	-	5	-
6		36.3	5, 7’, 7, 9	OH, 4, 5, 7, 7’, 8, 9
	1.50-1.40 (2H, m)			
7		26.9	6, 8	5, 6, 8, 9
7’	1.34-1.25 (1H, m)	26.9	6, 7, 8	5, 6, 8, 9
11	1.06 (3H, d, J=3.2)	13.8	2	1, 1’, 2
10	1.04 (3H, d, J=3.2)	13.3	4	4, 5
8	0.91 (3H, t, J=7.2)	11.9	7, 7’	6, 7, 7’
9	0.86 (3H, d, J=6.7)	12.3	6	5, 6, 7, 7’
3	-	218.0	-	1, 1’, 2, 4, 5, 10, 11

8.3 (2*R*,4*R*,5*R*,6*S*)-1-(benzyloxy)-2,4,6-trimethyl-5-((triethylsilyl)oxy)octan-3-one (54)

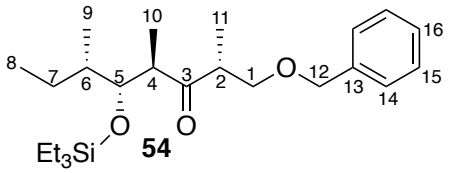

Figure 8-2 Numbering of carbon atoms in compound **54** for NMR assignment.

Table 8-2

Assigned NMR-shifts for compound **54**, shown in **Figure 8-2**. (600 MHz, $CDCl_3$). NMR-spectra are given in appendix E.

Position	^{1}H [ppm] (int., multi., J[Hz])	^{13}C [ppm]	COSY	HMBC
13	-	138.3	-	12, 12’
15	7.36-7.26 (5H, m)	128.3		
14		127.5		
16		127.5		
12	4.52 (1H, d, J=12.0)	73.2	-	1, 1’, ArH
12’	4.47 (1H, d, J=12.1)			
5	3.92 (1H, dd, J=8.5, J=1.9)	77.2	4, 6	4, 6, 7, 7’, 9, 10
1	3.67 (1H, dd, J=9.0, J=6.7)	72.1	2	2, 11, 12, 12’
1’	3.51 (1H, dd, J=9.1, J=5.5)	72.1	1’, 2	2, 11, 12, 12’
2	2.98-2.86 (2H, m)	47.1	1, 11	1, 11
4		49.6	5, 10	5, 10
6	1.42 (2H, m)	38.1	7, 7’	4, 5, 7, 7’ 9
7		26.8	6	5, 6, 8, 9
7’	1.19 (1H, dqnt, J=7.2, J=2.9)	26.8	6	5, 6, 8, 9
11	1.08 (3H, d, J=7.0)	13.0	2	1, 2
8		12.4	7, 7’	7, 7’
10	0.93 (15H, t, J=7.9)	13.5	4	4
$Si(CH_2\mathbf{CH_3})_3$		7.1	$Si(\mathbf{CH_2}CH_3)_3$	$Si(\mathbf{CH_2}CH_3)_3$
9	0.85 (3H, d, J=6.8)	13.1	6	5,6,7
$Si(\mathbf{CH_2}CH_3)_3$	0.56 (6H, q, J=7.8)	5.4	$Si(CH_2\mathbf{CH_3})_3$	$Si(CH_2\mathbf{CH_3})_3$
3	-	214.7	-	1, 2, 4, 5, 10, 11

8.4 (2*R*,4*S*,5*R*,6*S*)-1-(benzyloxy)-2,4,6-trimethyl-5-((triethylsilyl)oxy)octan-3-ol (55)

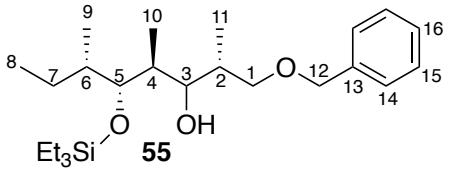

Figure 8-3 Numbering of carbon atoms in compound **55** for NMR assignment.

Table 8-3

Assigned NMR-shifts for compound **55**, shown in **Figure 8-3** (400 MHz, $CDCl_3$). NMR-spectra are given in appendix F.

Position	^{1}H [ppm] (int., multi., J[Hz])	^{13}C [ppm]	COSY	HMBC
13	-	138.8	-	12, 12’
15	7.37-7.26 (5H, m)	128.3		
14		127.6		
16		127.4		
12	4.55 (1H, d, J=11.9)	73.3	-	1, 1’, ArH
12’	4.51 (1H, d, J=12.0)			
3	3.81-3.70 (1H, m)	73.5	4	1, 1’, 10, 11
1		74.6	1’, 2	2, 3, 11, 12
	3.64-3.57 (2H, m)			
5		81.4	4, 6	3, 4, 6, 7, 7’, 9, 10
1’	3.45 (1H, dd, J=8.8, J=6.0)	74.6	1, 2	2, 3, 11, 12
2	2.00-1.87 (1H, m)	35.2	1, 1’, 3, 11	1, 1’, 3, 4, 11
4	1.82-1.71 (1H, m)	39.5	3, 5, 10	3, 5, 10
6		40.2	5, 7’	3, 5, 7, 7’, 8, 9
	1.54-1.39 (2H, m)			
7		26.7	6, 8	5, 6,
7’	1.31-1.11 (1H, m)	26.7	6, 8	5, 6
$Si(CH_2\mathbf{CH_3})_3$	0.98 (9H, t, J=7.8)	7.0	$Si(\mathbf{CH_2}CH_3)_3$	$Si(\mathbf{CH_2}CH_3)_3$
8	0.94-0.87(9H, m)	12.3	7, 7’	6, 7, 7’
9		14.2	6	5, 6, 7, 7’
11		9.3	2	1, 1’, 2, 3
10	0.79 (3H, d, J=6.9)	15.4	4	3, 4, 5
$Si(\mathbf{CH_2}CH_3)_3$	0.66 (6H, q, J=7.8)	5.2	$Si(CH_2\mathbf{CH_3})_3$	$Si(CH_2\mathbf{CH_3})_3$

8.5 (((3*S*,4*R*,5*S*,7*S*)-8-(benzyloxy)-3,5,7-trimethyloctan-4-yl)oxy)triethylsilane (57a)

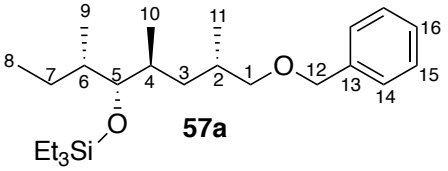

Figure 8-4 Numbering of carbon atoms in compound **57a** for NMR assignment.

Table 8-4

Assigned NMR-shifts for compound **57a**, shown in **Figure 8-4** (600 MHz, $CDCl_3$). NMR-spectra are given in appendix H.

Position	^{1}H [ppm] (int., multi., J[Hz])	^{13}C [ppm]	COSY	HMBC
13	-	138.9	-	12
15	7.36-7.27 (5H, m)	128.3		
14		127.5		
16		127.4		
12	4.51(2H, s)	73.0	-	1, 1', ArH
1		77.0	1', 2	2, 3, 11, 12
	3.32-3.29 (2H, m)			
5		80.8	4, 6	4, 6, 7, 7'
1'	3.25(1H, dd, J=9.0, 6.9)	77.0	1, 2	2, 3, 11, 12
2	1.87-1.80 (1H, m)	31.0	1, 1'	1, 1', 3, 6,
4	1.70-1.62 (1H, m)	34.4	3, 3' 5, 10	3, 3' 5, 10
6	1.50-1.44 (1H, m)	37.7	5, 7, 7', 9	5, 7, 7', 9
7	1.40-1.33 (1H, m)	27.6	6, 7', 8	5, 6, 8
3	1.27-1.21 (1H, m)	36.3	2, 4, 3'	1, 1', 2, 4, 5, 10, 11
3'		36.3	2, 4, 3	1, 1', 2, 4, 5, 10, 11
	1.20-1.13 (2H, m)			
7'		27.6	6, 7, 8	5, 6, 8
$Si(CH_2\mathbf{CH_3})_3$	0.97 (9H, t, J=7.9)	7.2	$Si(\mathbf{CH_2}CH_3)_3$	$Si(\mathbf{CH_2}CH_3)_3$
8		12.1	7, 7'	6, 7, 7'
	0.90-0.86 (6H, m)			
11		16.4	2	1, 1', 2, 3, 3', 4
9	0.84 (3H, d, J=3.2)	14.0	6	5, 6, 7, 7'
10	0.83(3H, d, J=3.3)	16.3	4	2, 3, 3', 4, 5
$Si(\mathbf{CH_2}CH_3)_3$	0.60 (6H, q, J=7.9)	5.7	$Si(CH_2\mathbf{CH_3})_3$	$Si(CH_2\mathbf{CH_3})_3$

8.6 (((2*R*,4*R*,6*S*)-1-(benzyloxy)-2,4,6-trimethyloctan-3-yl)oxy)triethylsilane (57b)

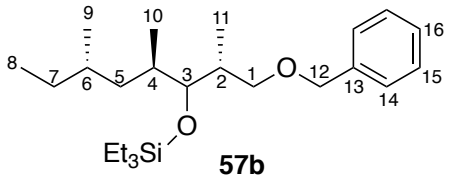

57b

Figure 8-5 Numbering of carbon atoms in compound **57b** for NMR assignment.

Table 8-5

Assigned NMR-shifts for compound X, shown in **Figure 8-5** (600 MHz, $CDCl_3$). NMR-spectra are given in appendix J.

Position	^{1}H [ppm] (int., multi., J[Hz])	^{13}C [ppm]	COSY	HMBC
13	7.35-7.26 (5H, m)	138.75	-	12, 12’
15		128.3		
14		127.6		
16		127.4		
12	4.52 (1H, d, J=12.0)	72.9	-	1, 1’, ArH
12’	4.46 (1H, d, J=12)			
1	3.55 (1H, dd, J=6.1, J=2.8)	74.3	2	2, 3, 11
1’	3.38 (1H, dd, J=8.9, J=7.2)			
3	3.24 (1H, dd, 8.9, J=6.7)	77.1	2, 4	1, 1’, 2, 4, 5, 5’, 10,11
2	1.98 (1H, dsxt, J=6.7, J=2.6)	35.9	1, 1’, 3, 11	1, 1’, 3, 4, 11
4	1.64 (1H, m)	35.2	3, 5, 5’, 10	2, 3, 5, 5’, 6, 9
6	1.37(1H, m)	31.8	5, 5’, 7, 7’, 9	4, 5, 5’ 7, 7’, 8, 9
7	1.31-1.23 (1H, m)	31.0	6, 7’, 8	6, 8, 9
7’	1.22-1.14(2H, m)	31.0	6, 7, 8	6, 8, 9
5		40.0	4, 6	3, 4, 6, 7, 7’, 9, 10
5’	1.05 (1H, m)	40.0	4, 6	3, 4, 6, 7, 7’, 9, 10
$Si(CH_2\mathbf{CH_3})_3$	0.95 (9H, t, J=8.0)	7.1	$Si(\mathbf{CH_2}CH_3)_3$	$Si(\mathbf{CH_2}CH_3)_3$
8	0.90 (6H, m)	11.6	7, 7’	6, 7, 7’
11		11.6	2	1, 1’, 2, 3, 4
10	0.82 (3H, d, J=6.8)	15.8	4	3, 4, 5, 5’
9	0.79 (3H, d, J=6.6)	18.6	6	5, 5’, 6, 7, 7’,
$Si(\mathbf{CH_2}CH_3)_3$	0.58 (6H, dq, J=7.7, J=1.8)	5.6	$Si(CH_2\mathbf{CH_3})_3$	$Si(CH_2\mathbf{CH_3})_3$

8.7 (2*S*,4*S*,5*R*,6*S*)-2,4,6-trimethyl-5-((triethylsilyl)oxy)octan-1-ol (58a)

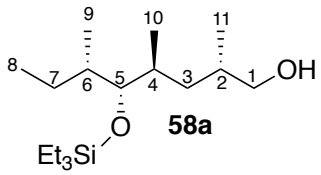

58a

Figure 8-6 Numbering of carbon atoms in compound **58a** for NMR assignment.

Table 8-6

Assigned NMR-shifts for compound **58a**, shown in **Figure 8-6** (600 MHz, $CDCl_3$). NMR-spectra are given in appendix K.

Position	^{1}H [ppm] (int., multi., J[Hz])	^{13}C [ppm]	COSY	HMBC
1	3.48 (1H, m)	69.6	OH, 2	OH, 2, 3, 3', 11
1'	3.43 (1H, m)			
5	3.31 (1H, dd, J=5.5, J=3.9)	80.9	4, 6	3, 3', 4, 6, 7, 7 ', 9, 10
2		33.4	1, 1', 3, 3', 11	1, 1', 3, 3' 4, 11
	1.68 (2H, m)			2, 3, 3', 5, 10
4		34.2	3, 3', 5, 10	
6	1.48 (1H, m)	37.8	5, 7, 7', 10	4, 5, 7, 7', 8, 9
7	1.37 (1H, m)	27.5	6, 7', 8	5, 6, 8, 9
OH	1.29 (1H, t, J= 5.3)	-	1, 1'	-
3	1.24 (1H, m)	35.8	2, 3', 4	1, 1',2, 4, 5, 10, 11
7'	1.20-1.15 (1H, m)	27.5	6, 7, 8	5, 6, 8, 9
3'	1.12 (1H, m)	35.8	2, 3, 4	1, 1',2, 4, 5, 10, 11
$Si(CH_2\mathbf{CH_3})_3$	0.96 (9H, t, J=8.0)	7.2	$Si(\mathbf{CH_2}CH_3)_3$	$Si(\mathbf{CH_2}CH_3)_3$
8		12.1	7, 7'	6, 7, 7'
	0.90-0.86 (6H, m)			
11		15.8	2	1, 1', 2, 3, 3'
10		16.4	4	3, 3', 4, 5
	0.84 (6H, d, J=6.9)			
9		14.1	6	5, 6, 7, 7'
$Si(\mathbf{CH_2}CH_3)_3$	0.61 (6H, q, J=8.0)	5.7	$Si(CH_2\mathbf{CH_3})_3$	$Si(CH_2\mathbf{CH_3})_3$

8.8 (2*R*,4*R*,6*S*)-2,4,6-trimethyl-3-((triethylsilyl)oxy)octan-1-ol (58b)

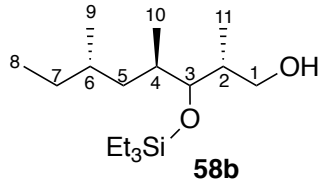

58b

Figure 8-7 Numbering of carbon atoms in compound **58b** for NMR assignment.

Table 8-7

Assigned NMR-shifts for compound **58b**, shown in **Figure 8-7** (600 MHz, $CDCl_3$). NMR-spectra are given in appendix L.

Position	^{1}H [ppm] (int., multi., J[Hz])	^{13}C [ppm]	COSY	HMBC
1	3.61-3.56 (2H, m)	66.9	OH, 2	2, 3, 4, 11
3		78.0	2, 4	1, 1'2, 4, 5, 5', 10, 11
1'	3.48 (1H, m)	66.9	OH, 2	2, 3, 4, 11
2	1.87(1H, dsxt, J=7.0, J=2.9)	38.6	1, 3, 11	1, 1', 3, 4, 11
OH	1.70 (2H, m)	-	1, 1 '	-
4		34.6	3, 5, 5', 10	2, 3,5, 5', 6, 10
6	1.38(1H, m)	31.9	5, 5', 7, 7', 9	4, 5, 5', 7, 7',9
7	1.28 (1H, m)	31.1	6, 7', 8	6, 5, 5', 8, 9
7'	1.24-1.17 (2H, m)	31.1	6, 7, 8	6, 5, 5', 8, 9
5		40.0	4, 5', 6	3, 4, 6, 7, 7', 9, 10
5'	1.10 (1H, m)	40.0	4, 5, 6	3, 4, 6, 7, 7', 9, 10
$Si(CH_2\mathbf{CH_3})_3$	0.97(9H, t, J=8.0)	7.1	$Si(\mathbf{CH_2}CH_3)_3$	$Si(\mathbf{CH_2}CH_3)_3$
8	0.90-0.86(6H, m)	11.6,	7, 7'	6, 7, 7'
11		11.7	2	1, 1', 2,
10	0.85 (3H, d, J=6.8)	16.2	4	3, 4, 5, 5'
9	0.82(3H, d, J=6.5)	18.6	6	5, 5', 6, 7, 7'
$Si(\mathbf{CH_2}CH_3)_3$	0.62 (6H, q, J=8.0)	5.5	$Si(CH_2\mathbf{CH_3})_3$	$Si(CH_2\mathbf{CH_3})_3$

8.9 (2*S*,4*S*,5*R*,6*S*)-2,4,6-trimethyl-5-((triethylsilyl)oxy)octanal (59a)

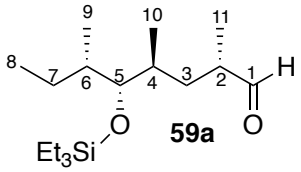

59a

Figure 8-8 Numbering of carbon atoms in compound **59a** for NMR assignment.

Table 8-8

Assigned NMR-shifts for compound **59a**, shown in **Figure 8-8** (600 MHz, $CDCl_3$). NMR-spectra given in appendix M.

Position	^{1}H [ppm] (int., multi., J[Hz])	^{13}C [ppm]	COSY	HMBC
1	9.63 (1H, d, J=1.7)	205.4	2	2, 3, 11
5	3.35 (1H, dd, J=5.4, J=4.0)	80.6	4, 6	4, 6, 7, 7', 9, 10
2	2.36 (1H, dsxt, J=6.9. J=1.5)	44.5	1, 3, 11	1, 3, 4, 11
4	1.68 (1H, spt, J=6.7)	34.3	3, 5	2, 3, 5,10
3	1.50-1.45 (3H, m)	32.8	2, 4	2, 4, 5, 10, 11
6		38.1	5, 7, 7'	4, 5, 7, 7', 8, 9
7	1.38 (1H, m)	27.3	6, 8	6, 8, 9
7'	1.19-1.11 (1H, m)			
11	1.06 (3H, d, J=6.9)	12.9	2	1, 2, 3
$Si(CH_2\mathbf{CH_3})_3$	0.96 (9H, t, J=7.9)	7.2	$Si(\mathbf{CH_2}CH_3)_3$	$Si(\mathbf{CH_2}CH_3)_3$
8	0.90-0.86 (6H, m)	12.1	7, 7'	6, 7, 7'
10		16.5	4	3, 4, 5
9	0.85 (3H, d, J=6.7)	14.1	6	5, 6, 7, 7'
$Si(\mathbf{CH_2}CH_3)_3$	0.61(6H, q, J=7.9)	5.6	$Si(CH_2\mathbf{CH_3})_3$	$Si(CH_2\mathbf{CH_3})_3$

8.10 (2*S*,4*R*,6*S*)-2,4,6-trimethyl-3-((triethylsilyl)oxy)octanal (59b)

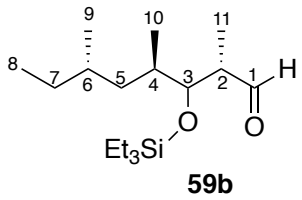

59b

Figure 8-9 Numbering of carbon atoms in compound **59b** for NMR assignment.

Table 8-9

Assigned NMR-shifts for compound **59b**, shown in **Figure 8-9** (600 MHz, $CDCl_3$). NMR-spectra given in appendix N.

Position	^{1}H [ppm] (int., multi., J[Hz])	^{13}C [ppm]	COSY	HMBC
1	9.73 (1H, s)	205.3	2	2, 3, 11
3	3.95 (1H, dd, J=5.7, J=3.9)	76.1	2, 4	2, 4, 10,11
2	2.49 (1H, m)	50.1	1, 3, 11	1, 3, 4, 11
4	1.71 (1H, m)	35.4	3, 5, 5', 10	2, 3, 5, 5', 6, 10
6	1.37 (1H, m)	31.8	5, 5', 7, 7', 9	4, 5, 5' 7, 7', 8, 9
7	1.31-1.25 (1H, m)	31.0	6, 8	5, 5', 6, 8, 9
7'	1.24-1.18 (1H, m)			
5	1.18- 1.12 (1H, m)	39.5	4, 6	3, 4, 6, 7, 7', 9, 10
11	1.11 (3H, d, J=6.9)	8.6	2	1, 2, 3
5'	1.10-1.05 (1H, m)	39.5	4, 6	3, 4, 6, 7, 7', 9, 10
$Si(CH_2\mathbf{CH_3})_3$	0.95 (9H, t, J=7.9)	7.0	$Si(\mathbf{CH_2}CH_3)_3$	$Si(\mathbf{CH_2}CH_3)_3$
8		11.5	7, 7'	6, 7, 7'
	0.89-0.85 (6H, m)			
10		15.7	4	3, 4, 5, 5'
9	0.81 (3H, d, J=6.4)	18.5	6	5, 5', 6, 7, 7'
$Si(\mathbf{CH_2}CH_3)_3$	0.59 (6H, q, J=7.9)	5.3	$Si(CH_2\mathbf{CH_3})_3$	$Si(CH_2\mathbf{CH_3})_3$

8.11 2-(trimethylsilyl)ethyl oct-7-ynoyl-*L*-valinate (72)

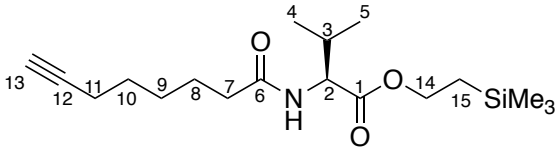

72

Figure 8-10 Numbering of carbon atoms in compound **72** for NMR assignment.

Table 8-10

Assigned NMR-shifts for compound **72**, shown in **Figure 8-10** (400 MHz, $CDCl_3$). NMR-spectra given in appendix U.

Position	^{1}H [ppm] (int., multi., J[Hz])	^{13}C [ppm]	COSY	HMBC
NH	5.90 (1H, d, J=8.6)	-	2	-
2	4.55 (1H, dd, J=8.8. J=4.8)	56.9	NH, 3	3, 4, 5
14	4.22 (2H, m)	63.7	15	15
7	2.25 (2H, t, J=7.7)	36.6	8	8
11	2.19 (2H, td, J=6.9, J=2.6)	18.3	10	10
3	2.17-2.11 (1H, m)	31.4	2, 4, 5	2, 4, 5
13	1.93 (1H, t, J=2.6)	68.3	11	11
8	1.67 (2H, qnt, J=7.6)	25.2	7, 9	7
10	1.55 (2H, qnt, J=7.0, H-10)	28.2	9, 11	9, 11, 12
9	1.45 (2H, m)	28.3	8, 10	8, 10
15	1.01 (2H, m)	17.5	14	14
4	0.94 (3H, d, J=6.8)	19.0	3	2, 3, 5
5	0.90 (3H, d, J=6.9)	17.8	3	2, 3, 4
$Si(CH_3)_3$)	0.05 (9H, s)	-1.5	-	-
12	-	84.4	-	10, 11
6	-	172.7	-	7, 8
1	-	172.4	-	2, 14

(*R*)-2-(1-(benzyloxy)propan-2-yl)-2-ethyl-1,3-dithiane (75)

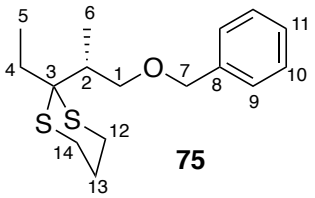

75

Figure 8-11 Numbering of carbon atoms in compound **75** for NMR assignment.

Table 8-10

Assigned NMR-shifts for compound **75**, shown in **Figure 8-11** (600 MHz, $CDCl_3$). NMR-spectra given in appendix V.

Position	^{1}H [ppm] (int., multi., J[Hz])	^{13}C [ppm]	COSY	HMBC
8	-	138.7	-	7, 7’
10	7.37-7.26 (5H, m)	128.7		
9		127.6		
11		127.5		
7, 7’	4.56 (1H, d, J=11.9)	73.2	-	1, 1’, ArH
	4.49(1H, d, J=11.9)			
1	4.04 (1H, dd, J=9.1, J=3.2)	72.9	2, 6	2, 6, 7, 7’
1’	3.44 (1H, t, J=9.0)			
12, 14	2.90-2.83 (2H, m)	25.6, 25.8	12’, 13, 13’, 14’	12’, 13, 13’, 14’
12’, 14’	2.78-2.67 (2H, m)	25.6, 25.8	12, 13, 13’, 14	12, 13, 13’, 14
2	2.29 (1H, m)	39.4	1, 1’, 6	1, 1’, 4, 4’, 6
4	2.05 (1H, sxt, J= 7.4)	28.7	5	5
4’		28.7	5	5
	2.01-1.94 (2H, m)			
13		25.3	12, 12’, 13’, 14’, 14	12, 12’, 14’, 14
13’	1.91-1.82 (1H, m)	25.3	12, 12’, 13, 14’, 14	12, 12’, 14’, 14
6	1.20 (3H, d, J=6.8)	13.0	2	1, 1’, 2
5	1.01(3H, t, J=7.3)	9.2	4, 4’	4, 4’
3	-	57.5	-	1, 1’, 2, 4, 5, 6, 12, 12’, 14, 14’

8.12 7-methoxy-7-oxoheptanoic acid (77)

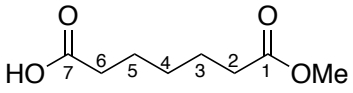

77

Figure 8-12 Numbering of carbon atoms in compound **77** for NMR assignment.

Table 8-11

Assigned NMR-shifts for compound **77**, shown in **Figure 8-12** (600 MHz, $CDCl_3$). NMR-spectra given in appendix Y.

Position	^{1}H [ppm] (int., multi., J[Hz])	^{13}C [ppm]	COSY	HMBC
OH	10.01 (s)	-	-	-
OCH_3	3.65 (3H, s)	51.6	-	-
2, 6	2.34 (4H, m)	33.8	3, 5	3, 4, 5
3, 5	1.64 (4H, qnt, J=7.6)	24.5, 24.3	2, 4, 6	2, 4, 6
4	1.36 (2H, m)	28.5	3, 5	2, 3, 5, 6
1	-	174.2	-	OCH_3, 2, 3
7	-	179.8	-	5, 6

9 Experimental Procedures

9.1 General Information

All reactions were carried out under N_2 atmosphere, in dry solvents and with oven (120 ℃) dried glassware, unless otherwise is specified. Dry dichloromethane (CH_2Cl_2), diethyl ether (Et_2O), tetrahydrofuran (THF), dimethylformamide (DMF) and acetonitrile (CH_3CN) were collected from a MBraun SPS-800 solventrenser. 99.8 % Anhydrous methanol (MeOH) and Toluene under Sure/Seal™ and the other reagents used are purchased from Merck. The reagents were used without further purification.

All reactions were monitored by TLC and were quenched when the reaction mixture showed full conversion of the starting material. TLC analysis was performed on Merck TLC Silica gel 60 F_{252} aluminum sheets. The compound spots were visualized by either UV-light (312/365 nm), vanillin, potassium permanganate or phosphor molybdic acid stain. Flash chromatography were performed on Silica Gel 40-63 μm. Flash chromatography dry loading was conducted with Florisil® <200 mesh. Filtration of the Pd-catalyzed reactions were aided by celite® 545.

For information for NMR analysis specifications, see section 8.1. The IR-spectra was recorded by Bruker Alpha FT-IR and the signals are reported in wavenumbers (cm^{-1}). Optical rotation measurements utilized Anton Paar Modular Circular Polarimeter 5100, with the wavelength of 589 nm, the optical rotation are given in units of 10^{-1} deg cm^2 $g^{-1.}$

For MS, accurate mass determination in positive and negative mode was performed on a "Synapt G2-S" Q-TOF instrument from Water TM. Samples were ionized by the use of ASAP probe (APCI) or ESI probe. No chromatographic separation was used previous to the mass analysis. Calculated exact mass and spectra processing was done by Waters TM Software Masslynx V4.1 SCN871.

Gas Chromatography–Mass Spectrometry (GC–MS). GC/MS analyses were carried out on a Gas Chromatograph 7890A equipped with a CTC PAL Autosampler and coupled with a mass spectrometer (inert XL EI/CI MSD with triple axis detector 5975). Helium was used as carrier gas. The sample was dissolved in dichloromethane. They were injected in Split mode 1 to 10. Separation of the different analytes was performed on a column a HP-PONA column (50m, ø0.2 and 0.5μm) from the method described in appendix O.

9.2 Methyl (*R*)-3-(benzyloxy)-2-methylpropanoate (50) (45, 81)

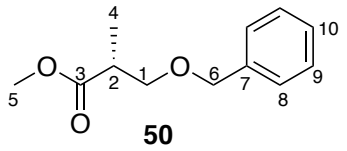

50

Figure 9-1 Numbering of carbon atoms in compound **50** for NMR assignment.

To a stirred solution of **24** (2.00 g, 16.9 mmol, 1.0 eq.) in CH_2Cl_2 (60 mL) a solution of benzyl 2,2,2-trichloroacetimidate (3.5 mL, 18.6 mmol, 1.1 eq.) in cyclohexane (120 mL) was added by cannula. Triflic acid (0.60 mL, 6.8 mmol, 0.4 eq.) was added dropwise which results in precipitation of trichloroacetamide as a white solid. The reaction mixture was monitored by TLC (15% EtOAc: hexane) and stirred at room temperature for 48 h. The precipitation was allowed to settle before the supernatant was decanted into a separating funnel and the precipitation was washed with hexane (2 x 30 mL). The organic phase was washed with $NaHCO_3$ (25 mL, saturated aqueous) and the aqueous phase was extracted with hexane (3 x 25 mL). The combined organic phases were washed with brine (25 mL, saturated aqueous) and dried over $MgSO_4$. The solvents were evaporated under reduced pressure. The remaining trichloroacetamide was precipitated by addition of hexane (40 mL) and was allowed to precipitate overnight. The supernatant was decanted into a filter and the crude product was concentrated *in vacuo*. The product was further purified by flash chromatography (5% EtOAc: pentane) which gave **50** as a colorless oil in a yield of 68.8% yield (2.43 g, 11.6 mmol). TLC (15% EtOAc: hexane) $\mathbf{R_f}$ = 0.43 $[\boldsymbol{\alpha}]_{\mathbf{D}}^{\mathbf{20}} = -11.1°$(c 1.35, $CHCl_3$).**^{1}H NMR** (400 MHz, $CDCl_3$) δ 7.37-7.27 (5H, m, ArH), 4.52 (2H, s, H-6), 3.69 (3H, s, H-5), 3.66 (1H, dd J=9.1, J=7.3, H-1), 3.49 (1H, dd J=9.1, J=5.9 , H-1), 2.78 (1H, m, H-2), 1.18 (3H, d J=7.1, H-4).**^{13}C NMR** (400 MHz, $CDCl_3$) δ 175.3(C-3), 138.1 (C-7), 128.4 (C-9), 127.6 (C-8), 127.6 (C-10), 73.1 (C-1), 72.0 (C-6), 51.7 (C-5), 40.2 (C-2), 14.0 (C-4). **IR** (thin film, cm^{-1}): 3027, 2979, 2949, 2845, 1735, 1453, 1434, 1361, 1197, 1174, 1090, 736, 697.

9.3 (*R*)-3-(benzyloxy)-*N*-methoxy-*N*,2-dimethylpropanamide (51) (45, 81)

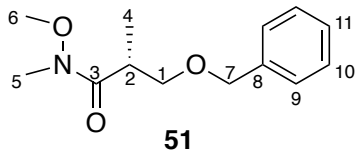

51

Figure 9-2 Numbering of carbon atoms in compound **51** for NMR assignment.

To a – 15 ℃ suspension of **50** (2.08 g, 9.98 mmol, 1.0 eq.) and *N*,*O*-dimethylhydroxylamine hydrochloride (1.60 g, 16.0 mmol, 1.6 eq.) in dry THF (20 mL) *iso*-propylmagnesium chloride (14.8 mL, 29.5 mmol 3.0 eq., 2M in THF) was added dropwise. After 4 h the reaction was quenched by addition of NH_4Cl (20 mL, saturated aqueous) and diluted with water (20 mL). The aqueous phase was extracted with Et_2O (3 x 20 mL), and the combined organic phases were then washed with brine (20 mL, saturated aqueous) and dried over $MgSO_4$, filtered and concentrated under reduced pressure. The crude product was purified by flash chromatography (20% EtOAc: pentane) to give **51** as a colorless oil in a yield of 83.8% (1.96 g, 8.24 mmol). TLC (15% EtOAc: hexane) $\mathbf{R_f}$ = 0.17.$[\boldsymbol{\alpha}]_{\mathbf{D}}^{\mathbf{20}} = -4.9°$ (c 3.9, $CHCl_3$). **^{1}H NMR** (400 MHz, $CDCl_3$) δ 7.36-7.24 (5H, m, ArH), 4.55 (1H, d, J=12.1, H-7), 4.48 (1H, d, J=12., H-7'), 3.72 (1H, m, H-1), 3.69 (3H, s, H-6), 3.43 (1H, dd, J=8.9, J=5.9, H-1'), 3.27 (1H, m, H-2), 3.21 (3H, s, H-5), 1.12 (3H, d, J=7.1, H-4). **^{13}C NMR** (400 MHz, $CDCl_3$) δ175.9 (C-3), 138.4(C-8), 128.6 (C-10), 127.5 (C-9), 127.5 (C-11), 73.2(C-1), 72.6(C-7), 61.5 (C-6), 35.9 (C-2), 32.1(C-5), 14.2 (C-4). **IR** (thin film, cm^{-1}): 2970, 2936, 2860, 1656, 1453, 1418, 1385, 1315, 1177, 1098,1076, 992, 738, 699.

9.4 (*R*)-1-(benzyloxy)-2-methylpentan-3-one (52) (45, 81)

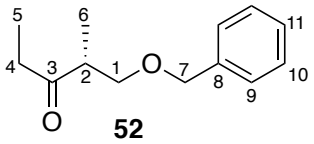

52

Figure 9-3 Numbering of carbon atoms in compound **52** for NMR assignment.

To a 0 ℃ solution of **51**(1.57 g, 6.61 mmol, eq.) in THF (65 mL) ethylmagnesium bromide (14.5 mL, 14.5 mmol, 2.2 eq., 1M in THF) was added dropwise. After 4 h the reaction was quenched with NH_4Cl (16 mL, saturated aqueous) and diluted with brine (16 mL, saturated aqueous). The aqueous phase was extracted with Et_2O (3 x 30 mL) and the combined organic phases was washed with brine (30 mL) and dried over $MgSO_4$, filtered and the solvent was evaporated under reduced pressure. The product was purified by flash chromatography (15% EtOAc: pentane) to give **52** as a colorless oil in a yield of 95.5% (1.30 g, 6.31mmol). TLC (15%

EtOAc: hexane) $\mathbf{R_f}$ = 0.51.$[\boldsymbol{\alpha}]_{\mathbf{D}}^{\mathbf{20}} = -28.1°$(c 8.0 $CHCl_3$).**^{1}H NMR** (400 MHz, $CDCl_3$) δ:7.37-7.27 (5H, m, ArH), 4.50 (1H, d, J=12.1, H-7), 4.46 (1H, d, J=12.1, H-7'), 3.63 (1H, dd, J=9.1, J=5.5, H-1), 3.46 (1H, J=9.0, J=7.9, H-1'), 2.89 (1H, ,H-2), 2.51 (2H, q, J=7.2, H-4), 1.10-1.02 (6H, m, H-5 and H-6).**^{13}C NMR** (400 MHz, $CDCl_3$) δ 213.7 (C-3), 138.2 (C-8), 128.4 (C-10), 127.6 (C-9), 127.6 (C-11), 73.2 (C-1), 72.4 (C-7), 46.2 (C-2), 35.3 (C-4), 13.6 (C-6), 7.6 (C-5). **IR** (thin film, cm^{-1}): 2973, 2936, 2876, 2856, 1712, 1454, 1361, 1092, 1027, 973, 736, 679.

9.5 (2*R*,4*R*,5*R*,6*S*)-1-(benzyloxy)-5-hydroxy-2,4,6-trimethyloctan-3-one (53) (45)

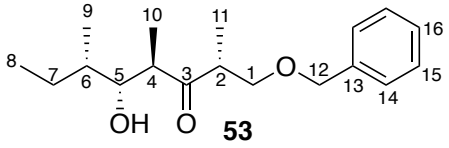

53

Figure 9-4 Numbering of carbon atoms in compound **53** for NMR assignment.

The ketone **52** (1.28 g, 6.23 mmol, 1.0 eq.) was dissolved in Et_2O (13 mL) and cooled to 0 ℃ before dicyclohexylboron chloride (9.3 mL, 9.3 mmol, 1.5 eq. 1M in hexane) was added, followed by dropwise addition of triethylamine (1.4 mL, 9.9 mmol, 1.6 eq.). Precipitation was observed upon the base addition. The reaction mixture was stirred at 0 ℃ for 2 h, before it was cooled to −78 ℃. The aldehyde **10** (2.8 g, 32.0 mmol, 5.1 eq.) was added dropwise at−78 ℃, and stirred at this temperature for 1 h, before it was stored overnight at −19 ℃. To quench the reaction pH buffer 7 was added (64 mL), it was transferred to a separation funnel and the water phase was extracted with Et_2O (4 x 64 mL), before it was concentrated under reduced pressure. To a 0 ℃ solution of the oil dissolved in MeOH (38 mL), it was treated with pH buffer 7 (38 mL) and a dropwise addition of hydrogen peroxide (32 mL, 30%). Stirring was continued at 0 ℃ for 1.5 h before it was diluted with water (64 mL), and extracted with CH_2Cl_2 (3 x 64 mL). The organic phase was washed with brine (64 mL, saturated aqueous) and dried over MgSO4, filtered and the solvent was evaporated under reduced pressure. The crude product was further purified by flash chromatography (15% EtOAc: pentane) to obtain the desired aldol product **53** in 91.5% yield (1.66 g, 5.69 mmol). TLC (15% EtOAc: hexane) $\mathbf{R_f}$ = 0.30. $[\boldsymbol{\alpha}]_{\mathbf{D}}^{\mathbf{20}} = -7.6°$ (c 1.0, $CHCl_3$). **^{1}H NMR** (600 MHz, $CDCl_3$) δ7.35-7.27 (5H, m, ArH), 4.51 (1H, d, J=12.2, H-12) 4.46 (1H, d, J=11.9, H-12'), 3.74-3.67 (2H, m, H-5 and H-1), 3.43 (1H, dd, J= 9.0, J= 4.9, H-1'), 3.13-3.06 (1H, m, H-2), 2.89-2.83 (1H, m, H-4), 2.46 (1H,m ,OH) 1.50-1.40 (2H, m, H-6 and H-7), 1.34-1.25 (1H, m, H-7'), 1.06 (3H, d, J=3.2, H-11), 1.04 (3H, d, J=3.2, H-10) 0.91 (3H, t, J=7.2, H-8), 0.86 (3H, d, J=6.7, H-9).**^{13}C NMR** (600 MHz, $CDCl_3$) δ 218.0(C-3), 137.9 (C-13), 128.4 (C-15) 127.7(C-14), 127.6(C-16),75.4 (C-5), 73.8 (C-12), 72.3 (C-1), 49.5(C-4),

45.6 (C-2), 36.3 (C-6), 26.9 (C-7), 13.8 (C-11), 13.3(C-10), 12.3 (C-9), 11.9 (C-8). **IR** (thin film, cm^{-1}): 3470, 2963, 2932, 2875, 1706, 1454, 1372, 1093, 985, 956, 734, 697. TOF **MS** ES^+ *m/z* $[M+Na]^+$ calc. for $C_{18}H_{28}O_3Na$ 315.1936, ion observed 315.1940.

9.6 (2*R*,4*R*,5*R*,6*S*)-1-(benzyloxy)-2,4,6-trimethyl-5-((triethylsilyl)oxy)octan-3-one (54)(82)

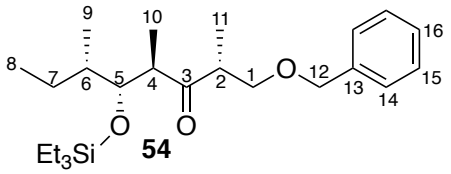

Figure 9-5 Numbering of carbon atoms in compound **54** for NMR assignment.

The aldol product **53** (1.32 g, 4.51 mmol, 1.0 eq.) was dissolved in CH_2Cl_2 (12 mL) and cooled to 0 ℃, to the solution 2,6-lutidine (0.6 mL, 5.4 mmol, 1.2 eq.) was added followed by dropwise addition of triethylsilyl trifloromethanesulfonate (1.1 mL, 5.0 mmol, 1.1 eq.). The reaction was stirred at 0 ℃ for 1 h, and quenched by addition of MeOH (5 mL). It was then washed with NH_4Cl (10 mL, saturated aqueous), the aqueous phase was extracted with Et2O (3 x 20 mL). The combined organic phase was dried over MgSO4, filtered and concentrated under reduced pressure. The crude product was purified via flash chromatography (3% EtOAc: pentane), giving **54** in 92.9% yield (1.70 g, 4.19 mmol). TLC (20% EtOAc: hexane) $\mathbf{R_f}$ = 0.71.$[\boldsymbol{\alpha}]_{\mathbf{D}}^{\mathbf{20}} = -27.0\,^\circ$ (c 1.0, $CHCl_3$). **^{1}H NMR** (600 MHz, $CDCl_3$) δ: 7.36-7.26 (5H, m, ArH), 4.52 (1H, d, J=12.0, H-12), 4.47 (1H, d, J=12.1, H-12'), 3.92 (1H, dd, J=8.5, J=1.9, H-5), 3.67 (1H, dd, J=9.0, J=6.7, H-1), 3.51 (1H, dd, J=9.1, J=5.5, H-1'), 2.98-2.86 (2H, m, H-2 and H-4), 1.42 (2H, m, H-6 and H-7), 1.19 (1H, qntd, J=7.2, J=2.9, H-7'), 1.08 (3H, d, J=7.0, H-11), 0.93 (15H, t, J=7.9,$Si(CH_2\mathbf{CH_3})_3$, H-8 and H-10), 0.85 (3H, d, J=6.8, H-9), 0.56 (6H, q, J=7.8, $Si(\mathbf{CH_2}CH_3)_3$). **^{13}C NMR** (600 MHz, $CDCl_3$) δ 214.7 (C-3), 138.3 (C-13), 128.3 (C-15), 127.5(C-14), 127.5 (C-16), 77.2 (C-5), 73.2 (C-12), 72.1 (C-1), 49.6 (C-4), 47.1(C-2), 38.1(C-6), 26.8 (C-7), 13.5, 13.1, 13.0, 12.4 (C-8, C-9, C-10, C-11) 7.1 ($Si(CH_2\mathbf{CH_3})_3$), 5.4 ($Si\mathbf{CH_2}CH_3)_3$). **IR** (thin film, cm^{-1}): 2957, 2935,2911, 2875, 1714, 1454, 1376, 1237, 1132, 1109,1057, 1005, 962, 812, 732, 696. TOF **MS** ES^+ *m/z* $[M+Na]^+$ calc. for $C_{24}H_{42}O_3SiNa$ 429.2801, ion observed 429.2799.

9.7 (2*R*,4*S*,5*R*,6*S*)-1-(benzyloxy)-2,4,6-trimethyl-5-((triethylsilyl)oxy)octan-3-ol (55)(104)

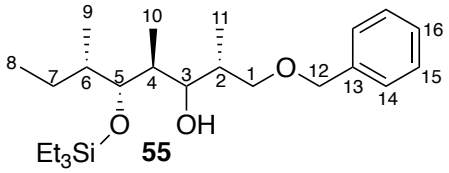

Figure 9-6 Numbering of carbon atoms in compound **55** for NMR assignment.

A solution of 1M LAH was prepared by dissolving LAH (259 mg, 6.8 mmol, 2.5 eq.) in THF (6.8 ml) at −78 C, then it was added dropwise to a solution of ketone **54** (1.10 g, mmol, 2.69 mmol, 1.0 eq.) in THF (48 mL) at −78 C. The reaction mixture was stirred at −78 C for 30 min, then quenched at this temperature by slow addition of MeOH (4.8 mL). The reaction was warmed to room temperature, added sodium potassium tartrate (72 mL, 10% aqueous) and the mixture was stirred for 1 h. The organic layer and the aqueous layer were separated, and the aqueous phase was extracted with Et_2O (3 x 50 mL). The combined organic layers were dried over MgSO4, filtered and concentrated in *vacuo*. Further purification was obtained via flash chromatography (25% EtOAc: pentane) to give the alcohol **55** as a colorless oil in 72.7% yield (800 mg, 1.96 mmol). TLC (20% EtOAc: hexane) $\mathbf{R_f} = 0.65$. $[\boldsymbol{\alpha}]_{\mathbf{D}}^{\mathbf{20}} = 0.0\,^{\circ}$ (c 1.0, $CHCl_3$)
^{1}H NMR (400 MHz, $CDCl_3$) δ: 7.37-7.26 (5H, m, ArH), 4.55 (1H, d, J=11.9, H-12), 4.51 (1H, d, J=12.0, H-12'), 3.81-3.70 (1H, m, H-3), 3.64-3.57 (2H, m, H-5 and H-1), 3.45 (1H, dd, J=8.8, J=6.0, H-1'), 2.00-1.87 (1H, m, H-2), 1.82-1.71 (1H, m, H-4), 1.54-1.39 (2H, m, H-7 and H-6), 1.31-1.11 (1H, m, H-7'), 0.98 (9H, t, J=7.8, $Si(CH_2\mathbf{CH_3})_3$), 0.94-0.87(9H, m, H-8, H-9 and H-11), 0.79 (3H, d, J=6.9, H-10), 0.66 (6H, q, J=7.8, $Si(\mathbf{CH_2}CH_3)_3$). **^{13}C NMR** (400 MHz, $CDCl_3$) δ:138.8 (C-13), 128.3 (C-15), 127.6 (C-14), 127.4 (C-16), 81.4 (C-5), 74.6 (C-1), 73.5 (C-3), 73.3(C-12), 40.2 (C-6), 39.5(C-4), 35.2 (C-2), 26.7 (C-7), 15.4(C-10), 14.2 (C-9), 12.3 (C-8), 9.3(C-11), 7.0 ($Si(CH_2\mathbf{CH_3})_3$), 5.2 ($Si(\mathbf{CH_2}CH_3)_3$). **IR** (thin film, cm^{-1}): 3520, 2980,2935, 2913, 2877, 1455, 1414, 1380, 1362, 1239, 1095, 1050, 1004, 842, 824, 797, 736, 697. TOF **MS** ES^+ *m/z* $[M+Na]^+$ calc. for $C_{24}H_{44}O_3SiNa$ 431.2957, ion observed 431.2955.

9.8 (((3*S*,4*R*,5*S*,7*S*)-8-(benzyloxy)-3,5,7-trimethyloctan-4-yl)oxy)triethylsilane (57a) and (((2*R*,4*R*,6*S*)-1-(benzyloxy)-2,4,6-trimethyloctan-3-yl)oxy)triethylsilane (57b)(55, 83)

The secondary alcohol **55** (700 mg, 1.71 mmol, 1.0 eq.) was dissolved in THF and NaHMDS (17.1 ml, 17.1 mmol, 1 M in THF, 10.0 eq.) was added dropwise to the −78 C solution. The reaction was stirred at this temperature for 30 min and CS_2 (6.9 ml, 34.3 mmol, 20.0 eq., 5 M in THF) was added. Stirring was continued at −78 C for 30 min and iodomethane (3.2 mL, 51.4 mmol, 30.0 eq.), it was stirred for 30 min before it was quenched by slow addition of water (10 mL) and extracted with EtOAc (3 x 30 mL). The organic phase was washed with water (8 mL) and brine (8 mL, saturated aqueous), then dried over $MgSO_4$, filtered and concentrated under reduced pressure. The crude product was purified by flash chromatography (1% EtOAc: pentane), which gave the mixture of the two isomers **56a** and **56b** as a colorless oil in 91.7% yield (784 mg, 1.57 mmol). TLC (3% EtOAc: hexane) $\mathbf{R_f}$ = 0.46 and 0.41. **IR** (thin film, cm^{-1}): 2956, 1454, 1412, 1381, 1221, 1107, 1047, 1004, 962, 838, 733, 697. TOF **MS** ES^+ *m/z* $[M+Na]^+$ calc. for $C_{26}H_{46}O_3SiS_2Na$ 521.2555, ion observed 521.2550.

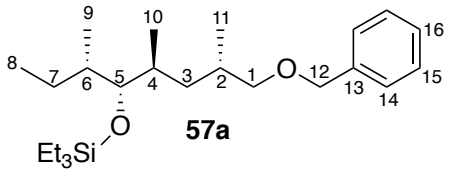

Figure 9-7 Numbering of carbon atoms in compound **57a** for NMR assignment.

To the solution of *S*-methyl carbonodithioate **56a** and **56b** (579 mg, 1.16 mmol, 1.0 eq.) in toluene (43 mL), tributyltin hydride (2.2 mL, 8.1 mmol, 7.0 eq.) was added followed by slow addition of triethyl borane (1.4 mL, 1.4 mmol, 1.2 eq., 1M in THF). The reaction was stirred at room temperature and was monitored by TLC. After 24 h, more tributyltin hydride (0.9 mL, 3.2 mmol, 2.8 eq.) and triethyl borane (0.6 mL, 0.6 mmol, 0.5 eq., 1M in THF) was added to ensure full consumption of starting material. After 48 h the reaction was quenched by addition of KF · $(H_2O)_2$ (1.64 g, 17.4 mmol, 15.0 eq.) and water (50 mL). The aqueous phase was separated and extracted with EtOAc (3 x 50 mL). The combined organic phases were washed with brine (64 mL) and dried over $MgSO_4$. Further purification by flash chromatography (20% CH_2Cl_2: pentane) afforded **57a** in 23.3% (106 mg, 0.270 mmol). TLC (20% CH_2Cl_2: pentane) $\mathbf{R_f}$ = 0.22. $[\boldsymbol{\alpha}]_{\mathbf{D}}^{\mathbf{20}} = -8.8$ ° (c 1.0, $CHCl_3$). ^{1}**H NMR** (600 MHz, $CDCl_3$) δ7.36-7.27 (5H, m, ArH), 4.51(2H, s, H-12), 3.32-3.29 (2H, m, H-1 and H-5), 3.25(1H, dd, J=9.0, 6.9, H-1), 1.87-1.80 (1H, m, H-2), 1.70-1.62 (1H, m, H-4), 1.50-1.44 (1H, m, H-6), 1.40-1.33 (1H, m, H-7), 1.27-1.21 (1H, m, H-3), 1.20-1.13 (2H, m, H-3', H-7'), 0.97 (9H, t, J=7.9, $Si(CH_2\mathbf{CH_3})_3$), 0.90-

0.86 (6H, m, H-8, H-11), 0.84 (3H, d, J=3.2, H-9), 0.83(3H, d, J=3.3, H-10), 0.60 (6H, q, J=7.9, Si(**C**$\mathbf{H_2}$CH$_3$)$_3$).^{13}**C NMR** (600 MHz, $CDCl_3$) δ 138.9 (C-13), 128.3 (C-15), 127.5 (C-14), 127.4 (C-16), 80.8 (C-5), 77.0 (C-1), 73.0 (C-12), 37.7 (C-6), 36.3 (C-3), 34.3 (C-4), 31.0 (C-2), 27.6 (C-7), 16.4 (C-11), 16.3, (C-10), 14.0 (C-9), 12.1 (C-8), 7.2 (Si(CH$_2$**C**$\mathbf{H_3}$)$_3$), 5.7 (Si(**C**$\mathbf{H_2}$CH$_3$)$_3$). IR (thin film, cm^{-1}):2956, 2913, 2875, 1454, 1414, 1378, 1363, 1242, 1097, 1028, 836, 734, 697. TOF **MS** ES$^+$ *m/z* [M+Na]$^+$ calc. for $C_{24}H_{44}O_2SiNa$ 415.3008, ion observed 414.3010.

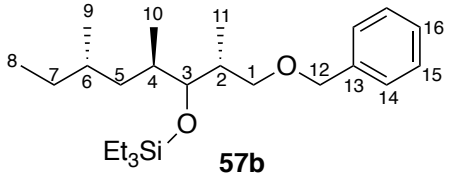

Figure 9-8 Numbering of carbon atoms in compound **57b** for NMR assignment.

57b was afforded in 58.2% yield (265 mg, 0.676 mmol). TLC (20% CH_2Cl_2: pentane) $\mathbf{R_f}$ = 0.39. ^{1}**H NMR** (600 MHz, $CDCl_3$) δ7.35-7.26 (5H, m, ArH), 4.52 (1H, d, J=12.0, H-12), 4.46 (1H, d, J=12, 12'), 3.55 (1H, dd, J=6.1, J=2.8, H-1), 3.38 (1H, dd, J=8.9, J=7.2, H-1'), 3.24 (1H, dd, 8.9, J=6.7, H-3), 1.98 (1H, dsxt, J=6.7, J=2.6, H-2), 1.64 (1H, m, H-4), 1.37(1H, m, H-6), 1.31-1.23 (1H, m, H-7), 1.22-1.14 (2H, m, H-7', H-5), 1.05 (1H, m, H-5), 0.95 (9H, t, J=8.0, Si(CH$_2$**C**$\mathbf{H_3}$)$_3$), 0.90 (6H, m, H-8, H-11), 0.82 (3H, d, J=6.8, H-10), 0.79 (3H, d, J=6.6, H-9), 0.58 (6H, dq, J=7.7, J=1.8, Si(**C**$\mathbf{H_2}$CH$_3$)$_3$).^{13}**C NMR** (600 MHz, $CDCl_3$) δ138. 75 (C-13), 128.3 (C-15), 127.6 (C-14), 127.4 (C-16), 77.1 (C-1), 74.3 (C-1), 72.9 (C-12), 40.0 (C-5), 35.9 (C-2), 35.2 (C-4) 31.8 (C-6), 31.0 (C-7), 18.6 (C-9), 15.8 (C-10), 11.6 (C-11), 11.6 (C-8), 7.1 (Si(CH$_2$**C**$\mathbf{H_3}$)$_3$), 5.6 (Si(**C**$\mathbf{H_2}$CH$_3$)$_3$).).**IR** (thin film, cm^{-1}): 2957, 2912, 2875, 1455, 1378, 1097, 1058, 1006, 963, 732, 696. TOF **MS** ES$^+$ *m/z* [M+Na]$^+$ calc. for $C_{24}H_{44}O_2SiNa$ 415.3008, ion observed 414.3011.

9.9 (2*S*,4*S*,5*R*,6*S*)-2,4,6-trimethyl-5-((triethylsilyl)oxy)octan-1-ol (58a) and (2*R*,4*R*,6*S*)-2,4,6-trimethyl-3-((triethylsilyl)oxy)octan-1-ol (58b)(45)

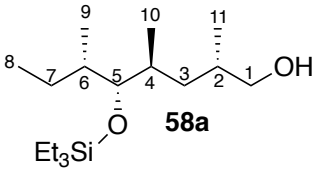

Figure 9-9 Numbering of carbon atoms in compound **58a** for NMR assignment.

The benzyl ether protected **57a** (0.1005 g, 0.2559 mmol) was dissolved in THF (7.5 mL) and $Pd(OH)_2$ (0.1495 g) was added slowly to the mixture. A H_2-balloon was attached to allow for hydrogen atmosphere, the reaction was stirred for 2 h at room temperature. The reaction mixture

was filtered on celite and the filtrate was evaporated under reduced pressure. The crude product was purified by flash chromatography (12% EtOAc: pentane) to afford the primary alcohol **58a** in 78.7% yield as a colorless oil (60.6 mg, 0.200 mmol). TLC (15% EtOAc: hexane) $\mathbf{R_f}$ = 0.40.$[\boldsymbol{\alpha}]_{\mathbf{D}}^{\mathbf{20}} = -24.3°$ (c 1.0, $CHCl_3$).**^{1}H NMR** (600 MHz, $CDCl_3$) δ3.48 (1H, m, H-1), 3.43 (1H, m, H-1'), 3.31 (1H, dd, J=5.5, J=3.9, H-5), 1.68 (2H, m, H-2, H-4), 1.48 (1H, m, H-6), 1.37 (1H, m, H-7), 1.29 (1H, t, J= 5.3, OH), 1.24 (1H, m, H-3), 1.20-1.15 (1H, m, H-7'), 1.12 (1H, m, H-3'), 0.96 (9H, t, J=8.0, $Si(CH_2\mathbf{CH_3})_3$), 0.90-0.86 (6H, m, H-8, H-11), 0.84 (6H, d, J=6.9, H-9, H-10), 0.61 (6H, q, J=8.0, $Si(\mathbf{CH_2}CH_3)_3$).**^{13}C NMR** (600 MHz, $CDCl_3$) δ 80.9 (C-5), 69.6 (C-1), 37.8 (C-6), 35.8 (C-3), 34.2 (C-4), 33.4 (C-2), 27.5 (C-7), 16.4 (C-10), 15.8 (C-11), 14.1 (C-9), 12.1 (C-8), 7.2 ($Si(CH_2\mathbf{CH_3})_3$), 5.7 ($Si(\mathbf{CH_2}CH_3)_3$)**IR** (thin film, cm^{-1}): 3339, 2959, 2935, 2913, 2876, 1461, 1415, 1380, 1238, 1109, 1058, 1009, 736, 726. TOF **MS** ES^+ *m/z* $[M+Na]^+$ calc. for $C_{17}H_{38}O_2SiNa$ 325.2439, ion observed 325.241.

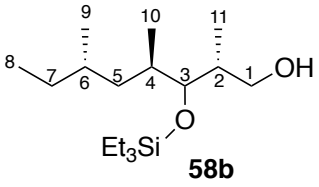

58b

Figure 9-10 Numbering of carbon atoms in compound **58b** for NMR assignment.

The same procedure was followed for preparation of **58b** form **57b** (44.2 mg, 0.113 mmol). **58b** was afforded in 94.6 % yield (32.2 mg, 0.106 mmol). TLC (15% EtOAc: hexane) R_f = 0.51. **^{1}H NMR** (600 MHz, $CDCl_3$) δ 3.61-3.56 (2H, m, H-1, H-3), 3.48 (1H, m, H-1'), 1.87 (1H, dsxt, J=7.0, J=2.9, H-2), 1.70 (2H, m, OH, H-4), 1.38 (1H, m, H-6), 1.28 (1H, m, H-7), 1.24-1.17 (2H, m, H-7', H-5), 1.10 (1H, m, H-5), 0.97 (9H, t, J=8.0, $Si(CH_2\mathbf{CH_3})_3$), 0.90-0.86 (6H, m, H8, H-11), 0.85 (3H, d, J=6.8, H-10), 0.82 (3H, d, J=6.5, H-9), 0.62 (6H, q, J=8.0, $Si(\mathbf{CH_2}CH_3)_3$)**^{13}C NMR** (600 MHz, $CDCl_3$) δ78.0 (C-3), 66.9 (C-1), 40.0 (C-5), 38.6 (C-2), 34.6 (C-4), 31.9 (C-6), 31.1 (C-7), 18.6 (C-9), 16.2 (C-10), 11.7 (C-11), 11.6 (C-8), 7.1($Si(CH_2\mathbf{CH_3})_3$),), 5.5 ($Si(\mathbf{CH_2}CH_3)_3$). **IR** (thin film, cm^{-1}):3329, 2957, 2933, 2911, 2876, 1458, 1414, 1379, 1237, 1099, 1016, 964, 831, 812, 724

9.10 (2*S*,4*S*,5*R*,6*S*)-2,4,6-trimethyl-5-((triethylsilyl)oxy)octanal (59a) and (2*S*,4*R*,6*S*)-2,4,6-trimethyl-3-((triethylsilyl)oxy)octanal (59b)(60)

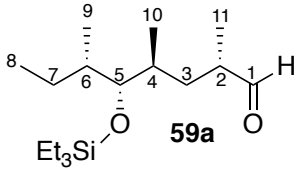

Figure 9-11 Numbering of carbon atoms in compound **59a** for NMR assignment.

The primary alcohol **58a** (59.5 mg, 0.197 mmol, 1.0 eq.) was dissolved in CH_3CN (3.3 mL), before $[Cu(MeCN)_4]OTf$ (14.8 mg, 0.039 mmol, 0.2 eq.), bpy (6.1 mg, 0.039 mmol, 0.2 eq.), TEMPO (6.5 mg, 0.039 mmol, 0.2 eq.) and N-methyl imidazole (6.3 μL, 0.079 mmol, 0.4 eq.) was added to the mixture. The reaction was stirred at room temperature for 2 days under O_2-atmosphere. During the reaction time the color of the mixture changed from dark brown to green. The solvent was evaporated *in vaccu* before it was purified by flash chromatography (10 % EtOAc: pentane). The titled compound **59a** was given as a colorless oil (47.9 mg, 0.159 mmol, 81.0%). TLC (15% EtOAc: hexane) $\mathbf{R_f} = 0.90$. $[\boldsymbol{\alpha}]_{\mathbf{D}}^{\mathbf{20}} = -11.7°$ (c 1.0, $CHCl_3$). **^{1}H NMR** (600 MHz, $CDCl_3$) δ 9.63 (1H, d, J=1.7, H-1), 3.35 (1H, dd, J=5.4, J=4.0, H-5), 2.36 (1H, dsxt, J=6.9. J=1.5, H-2), 1.68 (1H, spt, J=6.7, H-4), 1.50-1.45 (3H, m, H-3), 1.38 (1H, m, H-7), 1.19-1.11 (1H, m, H-7'), 1.06 (3H, d, J=6.9, H-11), 0.96 (9H, t, J=7.9, $Si(CH_2\mathbf{CH_3})_3$), 0.90-0.86 (6H, m, H-8, H-10), 0.85 (3H, d, J=6.7, H-9), 0.61(6H, q, J=7.9, $Si(\mathbf{CH_2}CH_3)_3$). **^{13}C NMR** (600 MHz, $CDCl_3$) δ 205.4 (C-1), 80.6 (C-5), 44.5 (C-2), 38.1 (C-6), 34.3 (C-4), 32.8 (C-3) 27.3 (C-7), 16.5 (C-10), 14.1 (C-9), 12.9 (C-11) 12.1 (C-8), 7.2 ($Si(CH_2\mathbf{CH_3})_3$), 5.6 ($Si(\mathbf{CH_2}CH_3)_3$). **IR** (thin film, cm^{-1}):2960, 2936, 2914, 2877, 2704, 1729, 1460, 1380, 1238.7, 1107, 1061, 1008, 737, 726. TOF **MS** ASAP$^+$ *m/z* $[M- H^-]^+$ calc. for $C_{17}H_{35}O_2Si$ 299.2406, ion observed 299.2412.

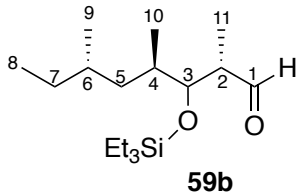

Figure 9-12 Numbering of carbon atoms in compound **59b** for NMR assignment.

The same procedure was followed for preparation of **58b** form **59b** (133 mg, 0.439 mmol). **59b** was afforded in 85.7% yield (113 mg, 0.376 mmol). TLC (15% EtOAc: hexane) $\mathbf{R_f} = 0.96$. **^{1}H NMR** (600 MHz, $CDCl_3$) δ9.73 (1H, s, H-1), 3.95 (1H, dd, J=5.7, J=3.9, H-3), 2.49 (1H, m, H-2), 1.71 (1H, m, H-4), 1.37 (1H, m, H-6), 1.31-1.25 (1H, m, H-7), 1.24-1.18 (1H, m, H-7'), 1.18- 1.12 (1H, m, H-5), 1.11 (3H, d, J=6.9, H-11), 1.10-1.05 (1H, m, 5'), 0.95 (9H, t, J=7.9, $Si(CH_2\mathbf{CH_3})_3$), 0.89-0.85 (6H, m, H-8, H-10), 0.81 (3H, d, J=6.4, H-9), 0.59 (6H, q, J=7.9, $Si(\mathbf{CH_2}CH_3)_3$). **^{13}C NMR** (600 MHz, $CDCl_3$) δ205.3 (C-1), 76.1 (C-3), 50.1 (C-2), 39.5 (C-5),

35.4 (C-4), 31.8 (C-6), 31-0 (C-7), 18.5 (C-9), 15.7 (C-10), 11.5 (C-8), 8.6 (C-11), 7.0 ($Si(CH_2\mathbf{CH_3})_3$), 5.3 ($Si(\mathbf{CH_2}CH_3)_3$).**IR** (thin film, cm^{-1}): 2957, 2935, 2911, 2876, 2701, 1725, 1457, 1414, 1379, 1238, 1100, 1007, 963, 808, 790, 737, 688.TOF **MS** ASAP$^+$ *m/z* [M- H$^\cdot$]$^+$ calc. for $C_{17}H_{35}O_2Si$ 299.2406, ion observed 299.2412.

9.11 (*S*)-2-methylbutanal (10)(60)

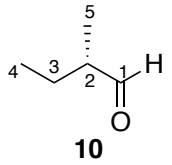

10

Figure 9-13 Numbering of carbon atoms in compound **10** for NMR assignment.

The primary alcohol **65** (5.23 g, 59.4 mmol, 1.0 eq.) was dissolved in CH_3CN (200 mL) was first added $[Cu(MeCN)_4]OTf$ (1.11 g, 3.0 mmol, 0.05 eq) and bpy (464 mg, 3.0 mmol, 0.05 eq.) which colored the solution dark brown. Further TEMPO (464 mg, 3.0 mmol, 0.05 eq.) and *N*-methyl imidazole (0.50 mL, 5.9 mmol, 0.1 eq.) was added. The reaction was stirred at room temperature for 24 hours under O_2- atmosphere. During the reaction time the color of the mixture changed from dark brown to green. The reaction was quenched by addition of HCl (15 mL, 1 M) and diluted with water (500 mL). The product was extracted out of the water phase with pentane (10 x 50 mL). The combined organic phases were washed with $Na_2S_2O_3$ (3 x 30 mL, saturated aqueous), dried over $MgSO_4$ and filtrated. To remove pentane, the reaction was distilled at pentanes boiling point, the product yield was then calculated from the product to pentane ratio by ^{1}H-NMR, which gave the product **10** in 54.0% yield (2.76 g, 32.0 mmol). TLC (15% EtOAc: hexane) $\mathbf{R_f}$ = 0.38. **^{1}H NMR** (MHz, $CDCl_3$) δ: 9.65 (1H, d, J=1.8, H-1), 2.31 (1H, sxtd, J=6.9, J=1.7, H-2), 1.78 (1H, hpt, J=7.5, H-3), 1.47 (1H, hpt, J=7.2, H-3), 1.12 (2H, d, J=7.0, H-5), 0.98 (3H, t, J=7.5, H-4).**^{13}C NMR** (MHz, $CDCl_3$) δ:204.8 (C-1), 47.2 (C-2), 23.0 (C-3), 12.3 (C-5), 10.8 (C-4). **GC-MS**: Retention time average 6.540-6.663 min, molecular weight 57.1 for $C_5H_{10}O$, match factor 897.

9.12 2-(trimethylsilyl)ethyl ((benzyloxy)carbonyl)-*L*-valinate (66)(111)

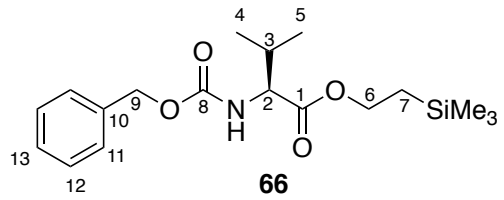

66

Figure 9-14 Numbering of carbon atoms in compound **66** for NMR assignment.

To a solution of **31** (2.11 g, 8.4 mmol, 1 eq.) in CH_2Cl_2 (86 mL), 2-trimethylsilylethanol (1.6 mL, 10.7 mmol, 1.3 eq.), EDC (1.9 mL, 10.7 mmol, 1.3 eq.) and DMAP (10.0 mg, 0.08 mmol, 0.01 eq.) were added and the reaction was stirred at room temperature overnight. The reaction was washed with HCl (3 x 100 mL, 1M), $NaHCO_3$ (3 x 100 mL, saturated aqueous) and brine (100 mL, saturated aqueous). The organic phase was dried over $MgSO_4$, filtered and concentrate in *vacuo*. The crude product was purified by flash chromatography (12% EtOAc: pentane), the protected **66** was afforded as a clear oil in 46.9% yield (1.30 g, 3.69 mmol). TLC (20% EtOAc: hexane) $\mathbf{R_f}$ = 0.62. $[\boldsymbol{\alpha}]_{\mathbf{D}}^{\mathbf{20}} = +2.9°$ (c 1.0, $CHCl_3$).$^{\mathbf{1}}$**H NMR** (400 MHz, $CDCl_3$) δ:7.39-7.29 (5H, m, ArH), 5.27 (1H, d, J=8.9, NH), 5.11 (2H, s, H-9), 4.32-4.17 (3H, m, H-2 and H-6), 2.17 (1H, m, H-3), 1.01 (2H, m, H-7) 0.97 (3H, d, J=6.8, H-4), 0.89 (3H, d, J=6.9, H-5), 0.05 (9H, s, $Si(CH_3)_3$).$^{\mathbf{13}}$**C NMR** (400 MHz, $CDCl_3$) δ 172.2(C-1), 156.2 (C-8), 136.4 (C-10), 128.5 (C-12), 128.2 (C-11), 128.1 (C-13), 67.0 (C-9), 63.6 (C-6), 59.1 (C-2), 32.3 (C-3), 19.0 (C-7), 17.5 (C-4), 17.5 (C-5), -1.5 ($Si(CH_3)_3$). **IR** (thin film, cm^{-1}): 3348, 2958, 2899, 1726, 1510, 1250, 1218, 860, 838, 697. TOF **MS** ES^+ *m/z* $[M+Na]^+$ calc. for $C_{18}H_{29}NO_4SiNa$ 374.1764, ion observed 374.1763.

9.13 2-(trimethylsilyl)ethyl *L*-valinate (67)(111)

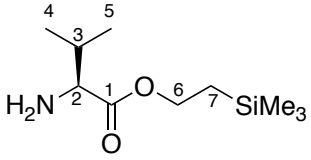

67

Figure 9-15 Numbering of carbon atoms in compound **67** for NMR assignment.

66 (780 mg, 2.22 mmol, 1.0 eq.) was dissolved in dry MeOH (56 mL) and Pd-C (280 mg, 10%) was slowly added to the mixture. The reaction was bubbled with hydrogen gas for 2 h at room temperature before it was filtered through celite. The solvent was evaporated under reduced pressure and further purification was done by flash chromatography (2% MeOH: CH_2Cl_2) where the desired amine **67** was obtained as a clear oil (350 mg, 1.61 mmol, 72.5%). TLC (2% MeOH: CH_2Cl_2) $\mathbf{R_f}$ = 0.28. $[\alpha]_D^{20} = +24.0°$ (c 1.0, $CHCl_3$). $^{\mathbf{1}}$**H NMR** (400 MHz, $CDCl_3$) δ:

4.20 (2H, m, H-6), 3.24 (1H, d, J=5.0, H-2), 2.02 (1H, m, H-3), 1.42 (2H, s, NH_2), 1.00 (2H, m, H-7), 0.97 (3H, d, J=6.9, H-4), 0.90 (3H, d, J=6.9, H-5), 0.05 (9H, s, $Si(CH_3)_3$). **^{13}C NMR** (400 MHz, $CDCl_3$) δ 175.7 (C-1), 62.9 (C-6), 60.1 (C-2), 32.1 (C-3), 19.4 (C-7), 17.5 (C-4), 17.2 (C-5), -1.5 ($Si(CH_3)_3$. **IR** (thin film, cm^{-1}): 3386, 3310, 2956, 2898, 2875, 1728, 1605, 1468, 1389, 1368, 1250, 1225, 1168, 1042, 980, 933, 857, 834, 761, 694. TOF **MS** ASAP$^+$ *m/z* $[M\text{-}CH_2+H]^+$ calc. for $C_9H_{22}NO_2Si$ 204.1420, ion observed 204.1420.

9.14 Methyl 7-oxoheptanoate (69)(112)

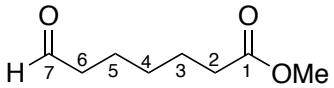

69

Figure 9-16 Numbering of carbon atoms in compound **68** for NMR assignment.

Cycloheptene **68** (1.57 g, 16.3 mmol, 1.0 eq.) and $NaHCO_3$ (410 mg, 4.9 mmol, 0.3 eq.) was dissolved in dry CH_2Cl_2 (39 mL) and dry MeOH (12 mL), at −78 ℃ the solution was bubbled with ozone for 20 min when a blue color appeared, it was then bubbled with ozone for 5 more min. The mixture was then bubbled with O_2 gas and then N_2 gas until the blue color disappeared. The reaction was allowed to warm to room temperature, it was then filtered and benzene was added (20 mL) before it was concentrated under reduced pressure to about 30 mL with water bath at room temperature. The mixture was diluted with CH_2Cl_2 (50 mL) and cooled to 0 ℃, acetic anhydride (4.5 mL, 47.2 mmol, 2.9 eq) and triethyl amine (3.4 mL, 24.5 mmol, 1.5 eq.) were added and the reaction was stirred at 0 ℃ for 2 h. The reaction was then washed with $NaHCO_3$ (30 ml, saturated aqueous) and brine (30 ml, saturated aqueous). The organic phase was dried over $MgSO_4$, filtered and the solvent was evaporated under reduced pressure. Purification via flash chromatography (15% EtOAc: pentane) resulted in the desired product **68** as clear liquid (2.05 g, 12.9 mmol 79.2%). TLC (20% EtOAc: hexane) $\mathbf{R_f}$ = 0.41. **^{1}H NMR** (400 MHz, $CDCl_3$) δ: 9.75 (1H, t, J=1.6, H-7), 3.66 (3H, s, OCH_3), 2.44 (2H, td, J=7.3, J=1.6, H-6), 2.31 (2H, t, J=7.5, H-2), 1.64 (4H, qnt, J=7.7, H-5 and H-3), 1.34 (2H, m, H-4).**^{13}C NMR** (400 MHz, $CDCl_3$) δ 202.5 (C-7), 174.0 (C-1), 51.5 (OCH_3), 43.6 (C-6), 33.8 (C-2), 28.6 (C-4), 24.6 (C-3), 21.7 (C-5). **IR** (thin film, cm^{-1}):2950, 2866, 1737, 1708, 1437, 1202, 1174. TOF **MS** ES$^+$ *m/z* $[M+Na]^+$ calc. for $C_8H_{14}O_3Na$ 181.0841, ion observed 181.0842.

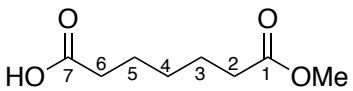

77

Figure 9-17 Numbering of carbon atoms in compound **77** for NMR assignment.

When the aldehyde **69** is stored the compound is oxidized to carboxylic acid **77**. **^{1}H NMR** (400 MHz, $CDCl_3$) δ10.01 (s, OH), 3.65 (3H, s, OCH_3), 2.34 (4H, m, H-2,6), 1.64 (4H, qnt, J=7.6, H-3, H-5), 1.36 (2H, m, H-4).**^{13}C NMR** (400 MHz, $CDCl_3$) δ 179.8(C-7), 174.2(C-1), 51.6(OCH_3), 33.8 (C-2, C-6), 28.5 (C-4), 24.5, 24.3(C-3, C-5).**IR** (thin film, cm^{-1}): 3176, 2945,2864,1733, 1705, 1436, 1416, 1363, 1198, 1172, 1087, 1007, 858, 738. TOF **MS** ES^+ *m/z* $[M+Na]^+$ calc. for $C_8H_{14}O_4Na$ 197.0790, ion observed 197.0793.

9.15 Methyl oct-7-ynoate (70)(114, 115)

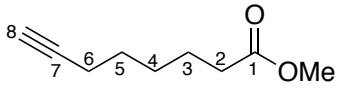

70

Figure 9-18 Numbering of carbon atoms in compound **70** for NMR assignment.

A solution of diethyl 1-diazo-2-oxopropylphosphonate (8.2 mL, 4.3 mmol, 1.1 eq., 10% in CH_3CN) in MeOH (30 mL) was added K_2CO_3 (1.4 g, 10.1 mmol, 2.6 eq.) at 0 ℃ and was stirred for 0.5 h. Then **69** (613 mg, 3.88 mmol, 1.0 eq.) was added slowly to the mixture over 1 h. The reaction was stirred for 1 h at 0 ℃ before the cooling bath was removed and the reaction was stirred at room temperature overnight. The mixture was added Et_2O (150 mL) and was washed with a $NaHCO_3$ (50 mL, 5% aqueous). The aqueous phase was extracted with Et_2O (20 mL), the combined organic phases were again washed with $NaHCO_3$ (3 x 30 mL, 5% aqueous) and brine (30 mL). The organic phase was dried over $MgSO_4$, filtered and concentrated under reduced pressure. Purification by flash chromatography (5% EtOAc: pentane) gave the desired product **70** in 38.7% yield (232 mg, 1.50 mmol).TLC (20% EtOAc: hexane) $\mathbf{R_f}$ = 0.71.**^{1}H NMR** (400 MHz, $CDCl_3$) δ: 3.66 (3H, s, OCH_3), 2.32 (2H, t, J=7.5 H-2), 2.22 (2H, td, J=6.9, J=2.6, H-6), 1.93 (1H, t, J=2.6, H-8), 1.64 (2H, qnt, J=7.7, H-3), 1.64 (2H, qnt, J=7.1, H-5), 1.44 (2H, m, H-4).**^{13}C NMR** (400 MHz, $CDCl_3$) δ:174.1 (C-1), 84.3 (C-7), 68.3(C-8), 51.5 (OCH_3), 33.9 (C-2), 28.2 (C-4), 28.1 (C-5), 24.4 (C-3), 18.2 (C-6). **IR** (thin film, cm^{-1}): 3293, 2940, 2862, 2116, 1735, 1435, 1362, 1324, 1252, 1201, 1172, 1123, 1087, 1071, 1007, 638. TOF **MS** $ASAP^+$ *m/z* $[M+H]^+$ calc. for $C_9H_{15}O_2$ 155.1072, ion observed 155.1070.

9.16 Oct-7-ynoic acid (71)(115)

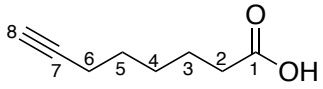

71

Figure 9-19 Numbering of carbon atoms in compound **71** for NMR assignment.

A solution of **70** (106 mg, 0.671 mmol, 1.0 eq.) in 4:1 THF-water (2.2: 0.54 mL) was cooled to 0 ℃ and added LiOH (0.05 g, 2.1 mmol, 3.0 eq.). The cooling bath was removed and the reaction was stirred over night at room temperature. The reaction was added EtOAc (30 mL), and acidified with $KHSO_4$ (10 mL, 5% aqueous) until pH 2 was reached. The two layers were separated and the aqueous phase was extracted with EtOAc (3 x 20 mL). The combined organic phases were washed with brine and dried over $MgSO_4$, filtered and concentrated in *vacuo*. The desired product **71** was obtained in 98.7% yield (92.9 mg, 0.663 mmol) without further purification. TLC (5% MeOH: CH_2Cl_2) $\mathbf{R_f} = 0.33$. **^{1}H NMR** (400 MHz, $CDCl_3$) δ: 9.72 (1H, s, OH), 2.37 (2H, t, J=7.4, H-2), 2.20 (2H, td, J=6.8, J=2.6, H-6), 1.94 (1H, t, J=2.6, H-8), 1.66 (2H, qnt, J=7.6, H-3), 1.56 (2H, qnt, J=7.0, H-5), 1.47 (2H, m, H-4).**^{13}C NMR** (400 MHz, $CDCl_3$) δ: 179.7 (C-1), 84.3 (C-7), 68.4 (C-8), 33.8 (C-2), 28.1 (C-4), 28.1 (C-5), 24.1 (C-3), 18.2 (C-6). **IR** (thin film, cm^{-1}):3298, 3042, 2941, 2865, 1708, 1413, 1279, 1227, 938, 636. TOF **MS** ES^- *m/z* $[M-H]^-$ calc. for $C_8H_{11}O_2$ 139.0759, ion observed 139.0760.

9.17 2-(trimethylsilyl)ethyl oct-7-ynoyl-*L*-valinate (72)(120)

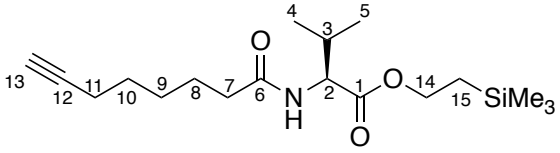

72

Figure 9-20 Numbering of carbon atoms in compound **72** for NMR assignment.

71 (193 mg, 1.37 mmol. 1.0 eq.) was dissolved in DMF (39 mL) and cooled to 0 ℃ before **67** (407 mg, 1.87 mmol, 1.4 eq), DIPEA (7.5 mL, 43.3 mmol, 31.5 eq.) and HATU (1.65 g, 4.3 mmol, 3.2 eq.) was added. The cooling bath was removed and the reaction was stirred at room temperature for 4 h. Once HATU was added the reaction changed color to bright yellow, the color of the reaction slowly changed to red/orange over the reaction period. When the reaction showed full consumption of **71**, the solvent was evaporated under reduced pressure to give a purple oil. Further purification with flash chromatography (20% EtOAc: pentane) to give the desired amide **72** in 91.9% yield (430 mg, 1.27 mmol). TLC (15% EtOAc: hexane) $\mathbf{R_f} = 0.23$. $[\boldsymbol{\alpha}]_{\mathbf{D}}^{\mathbf{20}} = +9.7°$ (c 1.0, $CHCl_3$).**^{1}H NMR** (MHz, $CDCl_3$) δ 5.90 (1H, d, J=8.6, NH), 4.55 (1H,

dd, J=8.8. J=4.8, H-2), 4.22 (2H, m, H-14), 2.25 (2H, t, J=7.7, H-7), 2.19 (2H,td, J=6.9, J=2.6, H-11), 2.17-2.11 (1H, m, H-3), 1.93 (1H, t, J=2.6, H-13), 1.67 (2H, qnt, J=7.6, H-8), 1.55 (2H, qnt, J=7.0, H-10), 1.45 (2H, m, H-9), 1.01 (2H, m, H-15), 0.94 (3H, d, J=6.8, H-4), 0.90 (3H, d, J=6.9, H-5), 0.05 (9H, s, $Si(CH_3)_3$).**^{13}C NMR** (MHz, $CDCl_3$) δ: 172.7 (C-6), 172.4 (C-1), 84.4 (C-12), 68.3 (C-13), 63.7 (C-14), 56.9 (C-2), 36.6 (C-7) 31.4 (C-3), 28.3 (C-9), 28.2 (C-10), 25.2 (C-8), 19.0 (C-4), 18.3 (C-11), 17.8 (C-5), 17.5 (C-15), -1.5 ($Si(CH_3)_3$). **IR** (thin film, cm^{-1}): 3312, 3058, 2955, 2937, 2863, 2117, 1736, 1647, 1536, 1250, 1179, 1152, 1042, 935, 859, 837, 760, 694, 628. TOF **MS** ES^+ *m/z* $[M+Na]^+$ calc. for $C_{18}H_{33}NO_3SiNa$ 362.2127, ion observed 362.2131.

10 References

1. Holohan C, Van Schaeybroeck S, Longley DB, Johnston PG. Cancer drug resistance: an evolving paradigm. Nat. Rev. Cancer. **2013**;13(10):714-26.
2. Dong J, Qin Z, Zhang W-D, Cheng G, Yehuda AG, Ashby Jr CR, et al. Medicinal chemistry strategies to discover P-glycoprotein inhibitors: An update. Drug Resistance Updates. **2020**;49:100681.
3. Liu C-P, Xie C-Y, Zhao J-X, Ji K-L, Lei X-X, Sun H, et al. Dysoxylactam a: a macrocyclolipopeptide reverses p-glycoprotein-mediated multidrug resistance in cancer cells. J. Am. Chem. Soc.. **2019**;141(17):6812-6.
4. Yang M, Peng W, Guo Y, Ye T. Total Synthesis of Dysoxylactam A. Org. Lett.. **2020**;22(5):1776-9.
5. Prabhakar Reddy D, Yu B. Total Synthesis of Macrocyclic Dysoxylactam A. Chemistry–An Asian Journal. **2020**.
6. Chandankar SS, Raghavan S. Stereoselective Synthesis of Dysoxylactam A. Org. Lett.. **2020**;22(2):653-5.
7. Waghray D, Zhang Q. Inhibit or Evade Multidrug Resistance P-Glycoprotein in Cancer Treatment. J. Med. Chem. . **2018**;61(12):5108-21.
8. Patrick GL. An introduction to medicinal chemistry: Oxford university press; **2013**.
9. Dean M, Hamon Y, Chimini G. The human ATP-binding cassette (ABC) transporter superfamily. J. Lipid Res.. **2001**;42(7):1007-17.
10. Gottesman MM, Ling V. The molecular basis of multidrug resistance in cancer: the early years of P-glycoprotein research. FEBS Lett.. **2006**;580(4):998-1009.

11. Cole S, Bhardwaj G, Gerlach J, Mackie J, Grant C, Almquist K, et al. Overexpression of a transporter gene in a multidrug-resistant human lung cancer cell line. Science. 1992;258(5088):1650-4.
12. Rabindran SK, Ross DD, Doyle LA, Yang W, Greenberger LM. Fumitremorgin C reverses multidrug resistance in cells transfected with the breast cancer resistance protein. Cancer Res.. **2000**;60(1):47-50.
13. Doyle LA, Yang W, Abruzzo LV, Krogmann T, Gao Y, Rishi AK, et al. A multidrug resistance transporter from human MCF-7 breast cancer cells. P. Natl. A.. **1998**;95(26):15665-70.
14. Schinkel A, Smit J, van Tellingen m, Beijnen J, Wagenaar E, Van Deemter L, et al. Disruption of the mouse mdr1a P-glycoprotein gene leads to a deficiency in the blood-brain barrier and to increased sensitivity to drugs. Cell. **1994**;77(4):491-502.
15. Fojo AT, Ueda K, Slamon DJ, Poplack D, Gottesman M, Pastan I. Expression of a multidrug-resistance gene in human tumors and tissues. P. Natl. A.. **1987**;84(1):265-9.
16. AJ Darby R, Callaghan R, M McMahon R. P-glycoprotein inhibition: the past, the present and the future. Curr. Drug Metab.. **2011**;12(8):722-31.
17. Lavie Y, Cao H-t, Volner A, Lucci A, Han T-Y, Geffen V, et al. Agents that reverse multidrug resistance, tamoxifen, verapamil, and cyclosporin A, block glycosphingolipid metabolism by inhibiting ceramide glycosylation in human cancer cells. J. Biol. Chem.. **1997**;272(3):1682-7.
18. Fellner S, Bauer B, Miller DS, Schaffrik M, Fankhänel M, Spruß T, et al. Transport of paclitaxel (Taxol) across the blood-brain barrier in vitro and in vivo. J. Clin. Invest.. **2002**;110(9):1309-18.
19. Friedenberg WR, Rue M, Blood EA, Dalton WS, Shustik C, Larson RA, et al. Phase III study of PSC-833 (valspodar) in combination with vincristine, doxorubicin, and dexamethasone (valspodar/VAD) versus VAD alone in patients with recurring or refractory multiple myeloma (E1A95) A trial of the Eastern Cooperative Oncology Group. Cancer. **2006**;106(4):830-8.
20. Hyafil F, Vergely C, Du Vignaud P, Grand-Perret T. In vitro and in vivo reversal of multidrug resistance by GF120918, an acridonecarboxamide derivative. Cancer Res.. **1993**;53(19):4595-602.
21. Roe M, Folkes A, Ashworth P, Brumwell J, Chima L, Hunjan S, et al. Reversal of P-glycoprotein mediated multidrug resistance by novel anthranilamide derivatives. Bioorg. Med. Chem. Lett.. **1999**;9(4):595-600.

22. Shepard RL, Cao J, Starling JJ, Dantzig AH. Modulation of P-glycoprotein but not MRP1-or BCRP-mediated drug resistance by LY335979. Int. J. Cancer. **2003**;103(1):121-5.
23. Dantzig AH, Shepard RL, Cao J, Law KL, Ehlhardt WJ, Baughman TM, et al. Reversal of P-glycoprotein-mediated multidrug resistance by a potent cyclopropyldibenzosuberane modulator, LY335979. Cancer Res.. **1996**;56(18):4171-9.
24. Choi J-S, Han H-K. Enhanced oral exposure of diltiazem by the concomitant use of naringin in rats. Int. J. Pharm.. **2005**;305(1-2):122-8.
25. Li X, Choi J-S. Effect of genistein on the pharmacokinetics of paclitaxel administered orally or intravenously in rats. Int. J. Pharm.. **2007**;337(1-2):188-93.
26. Jin J, Bi H, Hu J, Zhong G, Zhao L, Huang Z, et al. Enhancement of oral bioavailability of paclitaxel after oral administration of Schisandrol B in rats. Biopharm. Drug Dispos.. **2010**;31(4):264-8.
27. Lakshmi V, Pandey K, Agarwal S. Bioactivity of the compounds in genus Dysoxylum. Acta Ecologica Sinica. **2009**;29(1):30-44.
28. Qifeng Z, Shide L, Huiying W. Dammarane triterpenoids from Dysoxylum hongkongense. Acta Botanica Yunnanica. **1998**;20(3):362-8.
29. Zhao J-X, Yu Y-Y, Wang S-S, Huang S-L, Shen Y, Gao X-H, et al. Structural Elucidation and Bioinspired Total Syntheses of Ascorbylated Diterpenoid Hongkonoids A–D. J. Am. Chem. Soc.. **2018**;140(7):2485-92.
30. Schneider T, Müller A, Miess H, Gross H. Cyclic lipopeptides as antibacterial agents–potent antibiotic activity mediated by intriguing mode of actions. Int. J. Med. Microbiol.. **2014**;304(1):37-43.
31. Dewick PM. Medicinal natural products: a biosynthetic approach: John Wiley & Sons; **2002**.
32. Millan Delgado A, Grigol Martínez P, Aggarwal V. Stereocontrolled Synthesis of Polypropionate Fragments based on a Building Block Assembly Strategy using Lithiation-Borylation Methodologies. Chem. Eur. J. , 24 (3), 730-735. Chem. Eur. J. . **2018**;24(3):730-5.
33. Prabhakar Reddy D, Yu B. Total Synthesis of Macrocyclic Dysoxylactam A. Chemistry–An Asian Journal. **2020**;15(16):2467-9.
34. Nakajima N, Horita K, Abe R, Yonemitsu O. MPM (4-methoxybenzyl) protection of hydroxy functions under mild acidic conditions. Tetrahedron Lett.. **1988**;29(33):4139-42.

35. Eckenberg P, Groth U, Huhn T, Richter N, Schmeck C. A useful application of benzyl trichloroacetimidate for the benzylation of alcohols. Tetrahedron. **1993**;49(8):1619-24.
36. Feldman B. The Nobel Prize: a history of genius, controversy, and prestige: Arcade Publishing; **2000**.
37. Rieke RD. Preparation of organometallic compounds from highly reactive metal powders. Science. **1989**;246(4935):1260-4.
38. Carey FA, Sundberg RJ. Advanced organic chemistry: part B: reaction and synthesis: Springer Science & Business Media; **2007**.
39. Rogers HR, Hill CL, Fujiwara Y, Rogers RJ, Mitchell HL, Whitesides GM. Mechanism of formation of Grignard reagents. Kinetics of reaction of alkyl halides in diethyl ether with magnesium. J. Am. Chem. Soc.. **1980;**102(1):217-26.
40. Nahm S, Weinreb SM. N-Methoxy-N-methylamides as effective acylating agents. Tetrahedron Lett.. **1981**;22(39):3815-8.
41. Williams JM, Jobson RB, Yasuda N, Marchesini G, Dolling U-H, Grabowski EJ. A new general method for preparation of N-methoxy-N-methylamides. Application in direct conversion of an ester to a ketone. Tetrahedron Lett.. **1995**;36(31):5461-4.
42. Brown HC, Dhar RK, Bakshi RK, Pandiarajan PK, Singaram B. Major effect of the leaving group in dialkylboron chlorides and triflates in controlling the stereospecific conversion of ketones into either [E]-or [Z]-enol borinates. J. Am. Chem. Soc.. **1989;**111(9):3441-2.
43. Evans D, Nelson J, Vogel E, Taber T. Stereoselective aldol condensations via boron enolates. J. Am. Chem. Soc.. **1981**;103(11):3099-111.
44. Franklin AS, Paterson I. Recent developments in asymmetric aldol methodology. Contemporary Organic Synthesis. **1994**;1(5):317-38.
45. Paterson I, Steadman neé Doughty VA, McLeod MD, Trieselmann T. Stereocontrolled total synthesis of (+)-concanamycin F: the strategic use of boron-mediated aldol reactions of chiral ketones. Tetrahedron. **2011**;67(52):10119-28.
46. Greene T, Greene P. Wuts, Protective Groups in Organic Synthesis. Wiley & Sons; **1991**.
47. Shimizu N, Takesue N, Yasuhara S, Inazu T. Prediction of structural effects of trialkylsilyl groups on reactivity toward nucleophilic displacement at silicon. Chem. Lett.. **1993**;22(10):1807-10.

48. Shimizu N, Takesue N, Yamamoto A, Tsutsumi T, Yasuhara S, Tsuno Y. A quantitative scale for the structural effect on reactivity toward nucleophilic displacement at silicon. Chem. Lett.. **1992**;21(7):1263-6.
49. Aitken RA, Thomas AW. Heterocyclic acyl and formyl anion equivalents. Adv. Heterocycl. Chem. . **2001**;79:89-114.
50. Reddy CP, Rao RB. Mechanism of cyclic acetal formation. Tetrahedron. **1982**;38(12):1825-6.
51. Oikawa Y, Tanaka T, Horita K, Yonemitsu O. Selective hydrogenolysis of the benzyl protecting group for hydroxy function with raney nickel in the presence of the MPM (4-methoxybenzyl) and DMPM (3,4-dimethoxybenzyl) protecting groups. Tetrahedron Lett.. **1984**;25(47):5397-400.
52. Rickborn B, Wuesthoff MT. Kinetics, stereochemistry, and mechanism of the sodium borohydride reduction of alkyl-substituted cyclohexanones. J. Am. Chem. Soc.. **1970**;92(23):6894-904.
53. Barton DHR, McCombie SW. A new method for the deoxygenation of secondary alcohols. J. Chem. Soc., Perkin Transactions 1. **1975**(16):1574-85.
54. Zhou S, Zhu R, Hu J, Zhang L, Lu Q, Yu X. Economical Process for Preparation of the 19-nor A Ring of Paricalcitol from (−)-Shikimic Acid. Org. Process. Rev. Dev.. **2019**;23(9):1887-91.
55. Reddy KM, Shashidhar J, Ghosh S. A concise approach for the synthesis of bitungolides: total syntheses of (−)-bitungolide B & E. Org. Biomol. Chem.. **2014**;12(23):4002-12.
56. O'Mahony G. Triethylborane (Et3B). Synlett. **2004**;2004(03):572-3.
57. Forbes J, Zard S. A novel radical chain reaction of xanthic anhydrides. Further observations on the intermediacy of alkoxy-thiocarbonyl radicals in the Barton-McCombie reaction. Tetrahedron Lett.. **1989**;30(33):4367-70.
58. Hartung WH, Simonoff R. Hydrogenolysis of benzyl groups attached to oxygen, nitrogen, or sulfur. Org. Reactions. **2004**;7:263-326.
59. Grossman RB, Grossman R. The art of writing reasonable organic reaction mechanisms: Springer; **2003**.
60. Hoover JM, Stahl SS. Highly Practical Copper(I)/TEMPO Catalyst System for Chemoselective Aerobic Oxidation of Primary Alcohols. J. Am. Chem. Soc.. **2011**;133(42):16901-10.

61. Hoover JM, Ryland BL, Stahl SS. Mechanism of copper (I)/TEMPO-catalyzed aerobic alcohol oxidation. J. Am. Chem. Soc.. **2013**;135(6):2357-67.
62. Steves JE, Stahl SS. Copper(I)/ABNO-Catalyzed Aerobic Alcohol Oxidation: Alleviating Steric and Electronic Constraints of Cu/TEMPO Catalyst Systems. J. Am. Chem. Soc.. **2013**;135(42):15742-5.
63. Frantz D, Fässler R, Tomooka C, Carreira E. The discovery of novel reactivity in the development of C− C bond-forming reactions: in situ generation of zinc acetylides with ZnII/R3N. Accounts. Chem. Res.. **2000**;33(6):373-81.
64. Frantz DE, Fässler R, Carreira EM. Facile enantioselective synthesis of propargylic alcohols by direct addition of terminal alkynes to aldehydes. J. Am. Chem. Soc.. **2000**;122(8):1806-7.
65. Zani L, Bolm C. Direct addition of alkynes to imines and related C N electrophiles: A convenient access to propargylamines. Chem. Commun.. **2006**(41):4263-75.
66. Neises B, Steglich W. Simple method for the esterification of carboxylic acids. Angew. Chem., Int. Ed. Engl.. **1978**;17(7):522-4.
67. Valeur E, Bradley M. Amide bond formation: beyond the myth of coupling reagents. Chem. Soc. Rev. . **2009**;38(2):606-31.
68. Hikota M, Tone H, Horita K, Yonemitsu O. Chiral synthesis of polyketide-derived natural products. 27. Stereoselective synthesis of erythronolide A via an extremely efficient macrolactonization by the modified Yamaguchi method. J. Org. Chem.. **1990**;55(1):7-9.
69. Johnson S, Morrison DL. Kinetics and mechanism of decarboxylation of N-arylcarbamates. Evidence for kinetically important zwitterionic carbamic acid species of short lifetime. J. Am. Chem. Soc.. **1972**;94(4):1323-34.
70. Bailey PS. The reactions of ozone with organic compounds. Chem. Rev.. **1958**;58(5):925-1010.
71. Lattimer RP, Kuczkowski RL, Gillies CW. Mechanism of ozonolysis.(a) Microwave spectra, structures, and dipole moments of propylene and trans-2-butene ozonides.(b) Orbital symmetry analysis. J. Am. Chem. Soc.. **1974**;96(2):348-58.
72. Nangia PS, Benson SW. Thermochemistry and kinetics of ozonation reactions. J. Am. Chem. Soc.. **1980**;102(9):3105-15.
73. Henne AL, Hill P. The Preparation of Aldehydes, Ketones, and Acids by Ozone Oxidation. J. Am. Chem. Soc.. **1943**;65(5):752-4.

74. Keaveney WP, Berger MG, Pappas JJ. Direction of cleavage of primary ozonides in the methanolic ozonolyses of styrene, propenylbenzene, and 2-methylpropenylbenzene. J. Org. Chem.. **1967**;32(5):1537-42.
75. Gilbert JC, Weerasooriya U. Diazoethenes: their attempted synthesis from aldehydes and aromatic ketones by way of the Horner-Emmons modification of the Wittig reaction. A facile synthesis of alkynes. J. Org. Chem.. **1982**;47(10):1837-45.
76. Seyferth D, Marmor RS, Hilbert P. Reactions of dimethylphosphono-substituted diazoalkanes. (MeO)2P(O)CR transfer to olefins and 1,3-dipolar additions of (MeO)2P(O)C(N2)R. J. Org. Chem.. **1971**;36(10):1379-86.
77. Ohira S. Methanolysis of dimethyl (1-diazo-2-oxopropyl) phosphonate: generation of dimethyl (diazomethyl) phosphonate and reaction with carbonyl compounds. Synthetic commun.. **1989**;19(3-4):561-4.
78. Müller S, Liepold B, Roth GJ, Bestmann HJ. An improved one-pot procedure for the synthesis of alkynes from aldehydes. Synlett. **1996**;1996(6):521-2.
79. Roth GJ, Liepold B, Mueller SG, Bestmann HJ. Further improvements of the synthesis of alkynes from aldehydes. Synthesis. **2004**;2004(01):59-62.
80. Day J, Ingold C. Mechanism and kinetics of carboxylic ester hydrolysis and carboxyl esterification. T. Faraday Soc.. **1941**;37:686-705.
81. Paterson I, Norcross RD, Ward RA, Romea P, Lister MA. Studies in Macrolide Synthesis: A Stereocontrolled Synthesis of Oleandolide Employing Reagent- and Substrate-Controlled Aldol Reactions of (S)-1-(Benzyloxy)-2-methylpentan-3-one. J. Am. Chem. Soc.. **1994**;116(25):11287-314.
82. Evans DA, Fitch DM. Enantioselective Synthesis of the Elaiophylin Aglycon. J. Org. Chem.. **1997**;62(3):454-5.
83. Anderl T, Nicolas L, Münkemer J, Baro A, Sasse F, Steinmetz H, et al. Gephyronic acid, a missing link between polyketide inhibitors of eukaryotic protein synthesis (part II): Total synthesis of gephyronic acid. Angew. Chem. Int. Ed. **2011**;50(4):942-5.
84. Sidera M, Fletcher SP. Cu-catalyzed asymmetric addition of sp 2-hybridized zirconium nucleophiles to racemic allyl bromides. Chem. Commun.. **2015**;51(24):5044-7.
85. Firouzabadi H, Iranpoor N, Hazarkhani H. Iodine Catalyzes Efficient and Chemoselective Thioacetalization of Carbonyl Functions, Transthioacetalization of O,O- and S,O-Acetals and Acylals. J. Org. Chem.. **2001**;66(22):7527-9.
86. Das S, Borah R, Devi RR, Thakur AJ. Molecular iodine in protection and deprotection chemistry. Synlett. **2008**;2008(18):2741-62.

87. Lipshutz BH, Keith J. Selective deprotection of alkyl vs. aryl silyl ethers. Tetrahedron Lett.. **1998**;39(17):2495-8.
88. Cruickshank FR, Benson SW. Carbon-hydrogen bond dissociation energy in methanol. J. Phys. Chem.. **1969**;73(3):733-7.
89. Vaino AR, Szarek WA. A mild and efficient method for the deprotection of tert-butyldimethylsilyl ethers using iodine in methanol. Chem. Commun.. **1996**(20):2351-2.
90. Kelly DR, Roberts SM, Newton RF. The Cleavage of t-Butyldimethylsilyl Ethers with Boron Trifluoride Etherate. Synthetic commun.. **1979**;9(4):295-9.
91. Kawahara S-i, Wada T, Sekine M. 1:1 and 1:2 complexes of Bu4NF and BF3·Et2O: Unique properties as reagents for cleavage of silyl ethers. Tetrahedron Lett.. **1996**;37(4):509-12.
92. Granberg KL, Edvinsson KM, Nilsson K. Retro-aldol cleavage of bafilomycin derivatives. Tetrahedron Lett.. **1999**;40(4):755-8.
93. Kumar V, Dev S. Titanium tetrachloride, an efficient and convenient reagent for thioacetalization1,1. Tetrahedron Lett.. **1983**;24(12):1289-92.
94. Eustache F, Dalko PI, Cossy J. Synthesis of the C14−C25 Subunit of Bafilomycin A1. J. Org. Chem.. **2003**;68(26):9994-10002.
95. Iida A, Okazaki H, Misaki T, Sunagawa M, Sasaki A, Tanabe Y. Efficient Method for the Deprotection of tert-Butyldimethylsilyl Ethers with TiCl4−Lewis Base Complexes: Application to the Synthesis of 1β-Methylcarbapenems. J. Org. Chem.. **2006;**71(14):5380-3.
96. Tietze LF, Weigand B, Wulff C. A mild and efficient method for the preparation of 1, 3-dithianes from aldehydes and ketones. Synthesis. **2000**;2000(01):69-71.
97. Lu T-N, Chang C-C. Synthesis of 3-Deoxy-l-ketohexoses through Group Transfer. J. Org. Chem.. **2016**;81(2):469-75.
98. Han BY, Lam NYS, MacGregor CI, Goodman JM, Paterson I. A synthesis-enabled relative stereochemical assignment of the C1–C28 region of hemicalide. Chem. Commun.. **2018**;54(26):3247-50.
99. de Vries EF, Brussee J, Van der Gen A. Intramolecular reductive cleavage of tert-butyldimethylsilyl ethers. Selective mono-deprotection of bis-silyl-protected diols. J. Org. Chem.. **1994**;59(23):7133-7.
100. Li D, Zhao Y, Ye L, Chen C, Zhang J. A Formal Total Synthesis of Fostriecin by a Convergent Approach. Synthesis. **2010**;2010(19):3325-31.

101. Xie J, Ma Y, Horne DA. Total synthesis of the proposed structure of iriomoteolide-1a. Tetrahedron. **2011**;67(39):7485-501.
102. Crouch RD. Selective deprotection of silyl ethers. Tetrahedron. **2013**;69(11):2383-417.
103. Lister T, Perkins MV. A Retro-Claisen Approach to Dolabriferol. Org. Lett.. **2006**;8(9):1827-30.
104. Paterson I, Coster MJ, Chen DYK, Aceña JL, Bach J, Keown LE, et al. The stereocontrolled total synthesis of altohyrtin A/spongistatin 1: the southern hemisphere EF segment. Org. Biomol. Chem.. **2005**;3(13):2420-30.
105. Oves D, Díaz M, Fernández S, Ferrero M, Gotor V. Synthesis of imidazoylthiocarbonyl intermediates for the radical deoxygenation of hindered secondary alcohols. Synthetic commun.. **2001**;31(15):2335-43.
106. Crimmins MT, Wang Z, McKerlie LA. Double Diastereoselection in Intramolecular Photocycloadditions: A Radical Rearrangement Approach to the Total Synthesis of the Spirovetivane Phytoalexin (±)-Lubiminol. J. Am. Chem. Soc.. **1998**;120(8):1747-56.
107. Enders D, Vicario JL, Job A, Wolberg M, Müller M. Asymmetric total synthesis of (−)-callystatin A and (−)-20-epi-callystatin A employing chemical and biological methods. Chem. Eur. J. . **2002**;8(18):4272-84.
108. Morozova V, Skotnitzki J, Moriya K, Karaghiosoff K, Knochel P. Preparation of Optically Enriched Secondary Alkyllithium and Alkylcopper Reagents—Synthesis of (−)-Lardolure and Siphonarienal. Angew. Chem. Int. Ed. **2018**;57(19):5516-9.
109. Boyall D, López F, Sasaki H, Frantz D, Carreira E. Enantioselective Addition of 2-Methyl-3-butyn-2-ol to Aldehydes: Preparation of 3-Hydroxy-1-butynes. Org. Lett.. **2000**;2(26):4233-6.
110. Fortner KC, Kato D, Tanaka Y, Shair MD. Enantioselective Synthesis of (+)-Cephalostatin 1. J. Am. Chem. Soc.. **2010**;132(1):275-80.
111. Freire F, Gellman SH. Macrocyclic design strategies for small, stable parallel β-sheet scaffolds. J. Am. Chem. Soc.. **2009**;131(23):7970-2.
112. Egger J, Bretscher P, Freigang S, Kopf M, Carreira EM. Discovery of a Highly Potent Anti-inflammatory Epoxyisoprostane-Derived Lactone. J. Am. Chem. Soc.. **2014**;136(50):17382-5.
113. Vanoye L, Favre-Réguillon A, Aloui A, Philippe R, de Bellefon C. Insights in the aerobic oxidation of aldehydes. RSC Adv.. **2013**;3(41):18931-7.

114. Sønderskov J, Tungen JE, Palmas F, Dalli J, Serhan CN, Stenstrøm Y, et al. Stereoselective synthesis of MaR2n-3 DPA. Tetrahedron Lett.. **2020**;61(7):151510.
115. Chen H, Feng Y, Xu Z, Ye T. The total synthesis and reassignment of stereochemistry of dragonamide. Tetrahedron. **2005**;61(47):11132-40.
116. Basha A, Lipton M, Weinreb SM. A mild, general method for conversion of esters to amides. Tetrahedron Lett.. **1977**;18(48):4171-2.
117. Dubois N, Glynn D, McInally T, Rhodes B, Woodward S, Irvine DJ, et al. On DABAL-Me3 promoted formation of amides. Tetrahedron. **2013**;69(46):9890-7.
118. Novak A, Humphreys LD, Walker MD, Woodward S. Amide bond formation using an air-stable source of AlMe3. Tetrahedron Lett.. **2006**;47(32):5767-9.
119. Cornella J, Zarate C, Martin R. Metal-catalyzed activation of ethers via C–O bond cleavage: a new strategy for molecular diversity. Chem. Soc. Rev. . **2014**;43(23):8081-97.
120. Bowsher M, Hiebert S, Li R, Wang AX, Friborg J, Yu F, et al. The discovery and optimization of naphthalene-linked P2-P4 Macrocycles as inhibitors of HCV NS3 protease. Bioorg. Med. Chem. Lett.. **2018**;28(1):43-8.
121. Linstadt RT, Peterson CA, Lippincott DJ, Jette CI, Lipshutz BH. Stereoselective silylcupration of conjugated alkynes in water at room temperature. Angew. Chem. Int. Ed. **2014**;53(16):4159-63.
122. Trost BM, Ball ZT, Jöge T. Regioselective hydrosilylation of propargylic alcohols: an aldol surrogate. Angew. Chem.. **2003**;115(29):3537-40.
123. Anand NK, Carreira EM. A Simple, Mild, Catalytic, Enantioselective Addition of Terminal Acetylenes to Aldehydes. J. Am. Chem. Soc.. **2001**;123(39):9687-8.
124. Trost BM, Weiss AH, Jacobi von Wangelin A. Dinuclear Zn-Catalyzed Asymmetric Alkynylation of Unsaturated Aldehydes. J. Am. Chem. Soc.. **2006**;128(1):8-9.
125. Wolf C, Liu S. Bisoxazolidine-Catalyzed Enantioselective Alkynylation of Aldehydes. J. Am. Chem. Soc.. **2006**;128(34):10996-7.
126. Takita R, Yakura K, Ohshima T, Shibasaki M. Asymmetric Alkynylation of Aldehydes Catalyzed by an In(III)/BINOL Complex. J. Am. Chem. Soc.. **2005**;127(40):13760-1.

A Methyl (*R*)-3-(benzyloxy)-2-methylpropanoate (50)
A.1 ^{1}H-NMR for 50, 400 MHz, $CDCl_3$ (ppm)

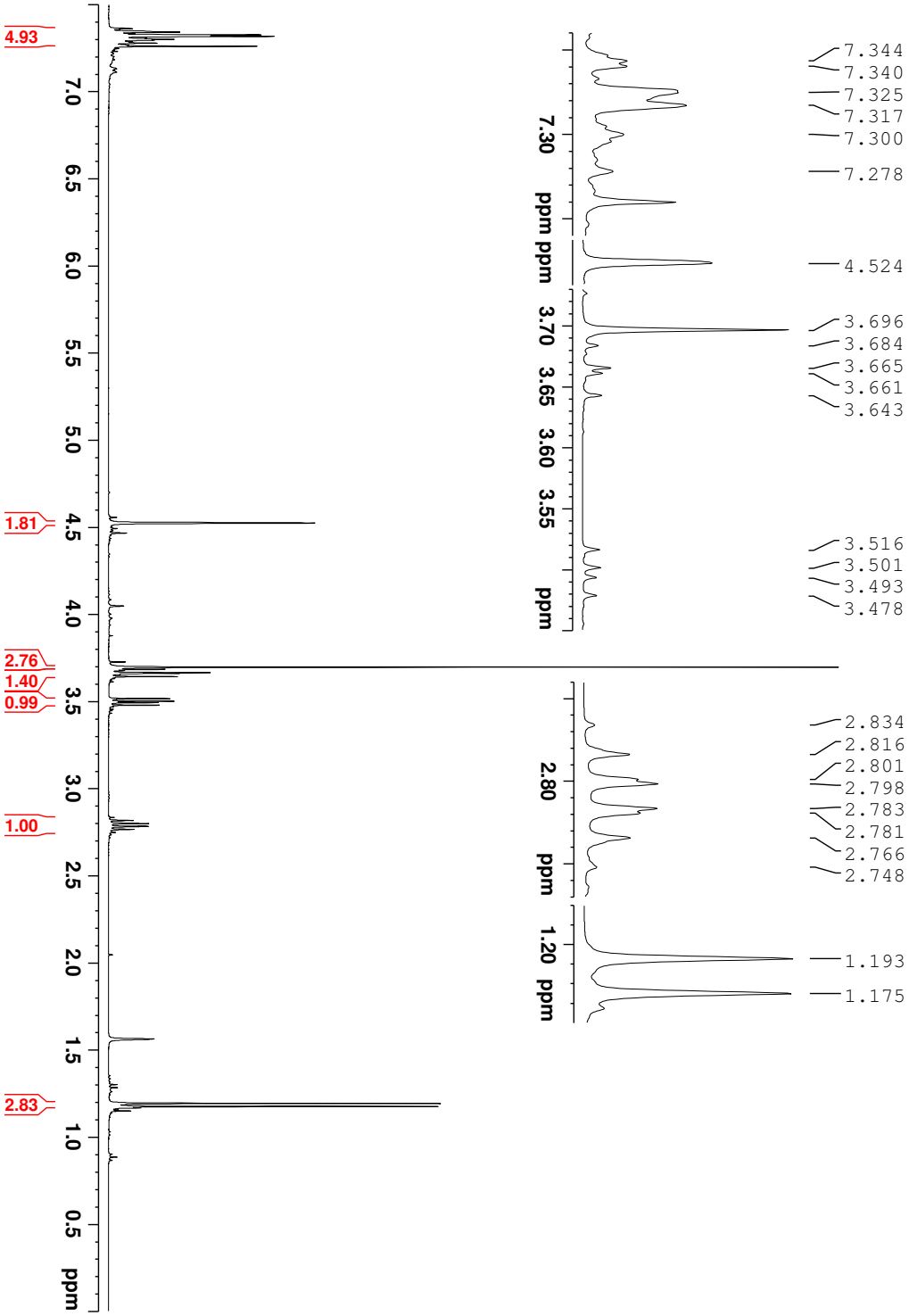

A.2 ^{1}H-NMR for 50, 400 MHz, $CDCl_3$ (Hz)

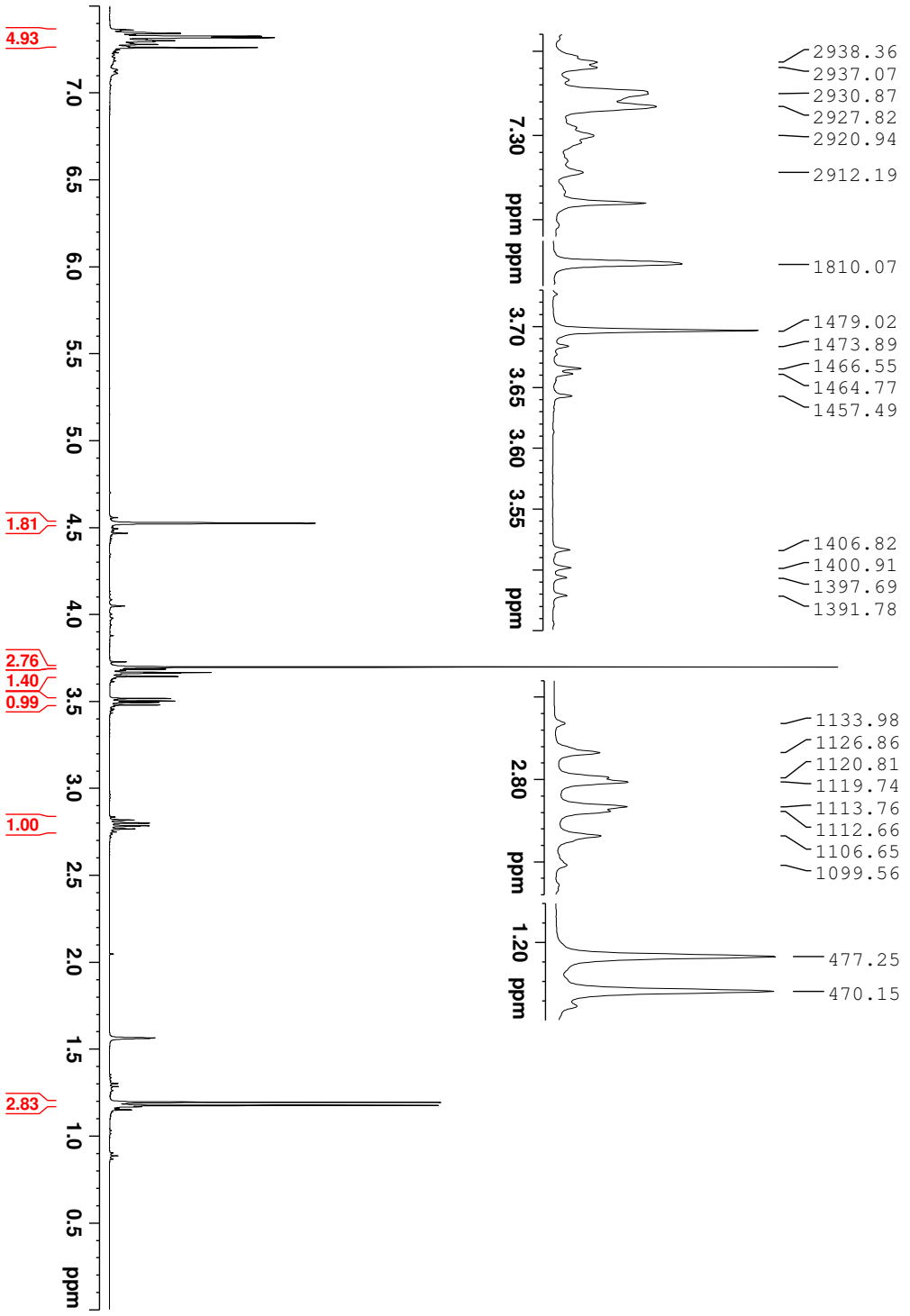

A.3 ^{13}C-NMR for 50, 400 MHz, $CDCl_3$ (ppm)

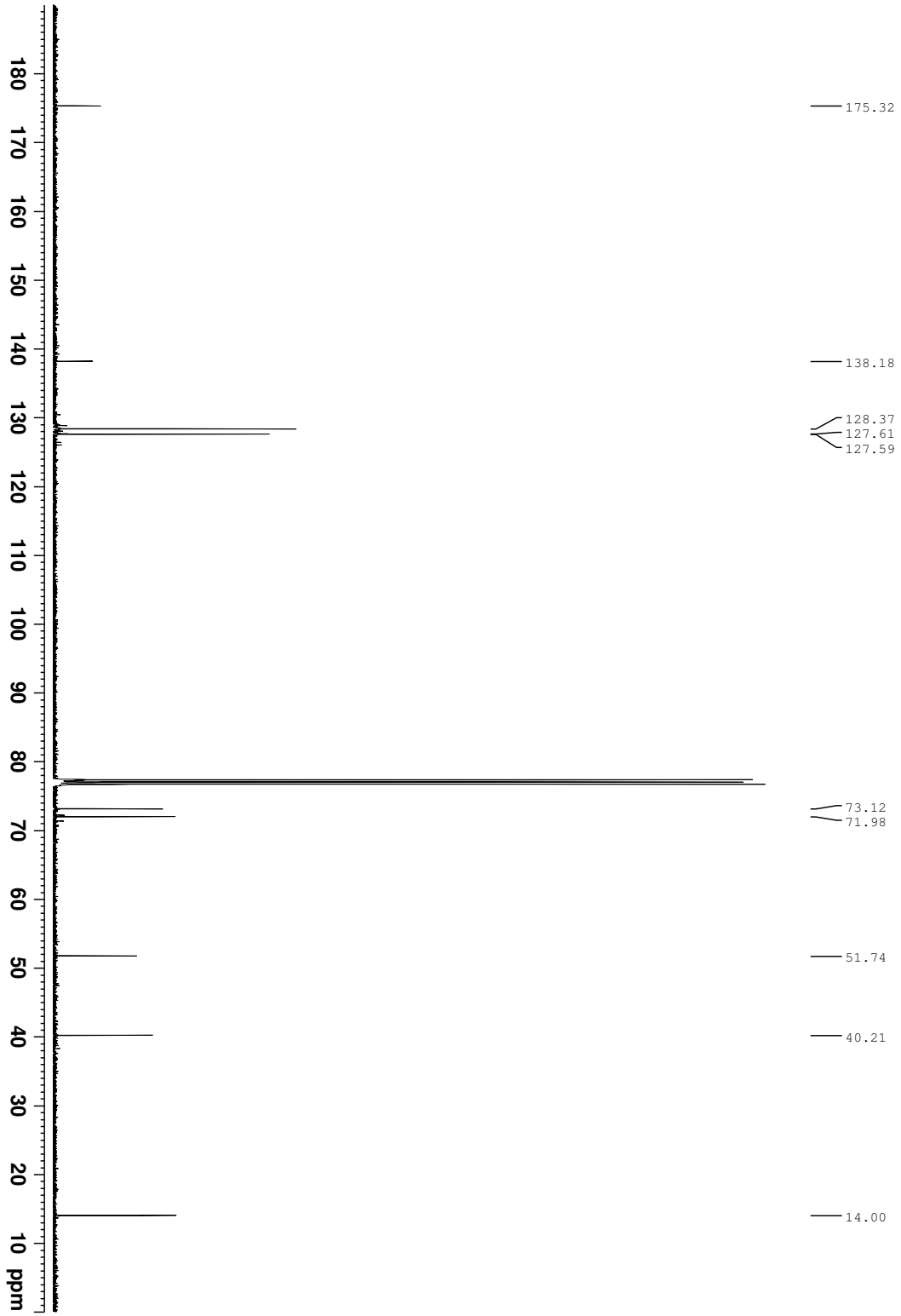

A.4 IR Spectrum (cm^{-1}) of 50

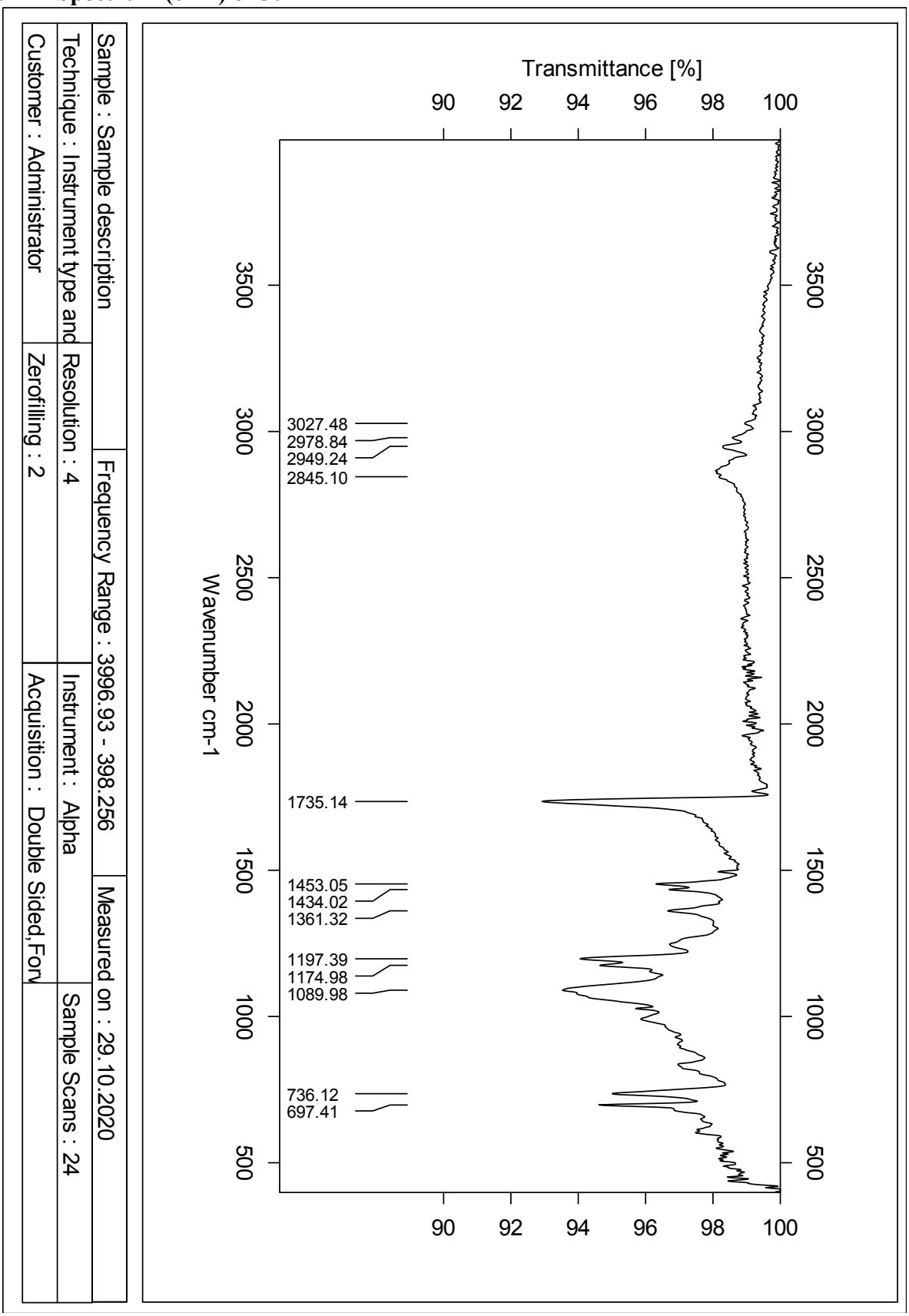

B (R)-3-(benzyloxy)-N-methoxy-N,2-dimethylpropanamide (51)
B.1 ^{1}H-NMR Spectrum of 51, 400 MHz, $CDCl_3$ (ppm)

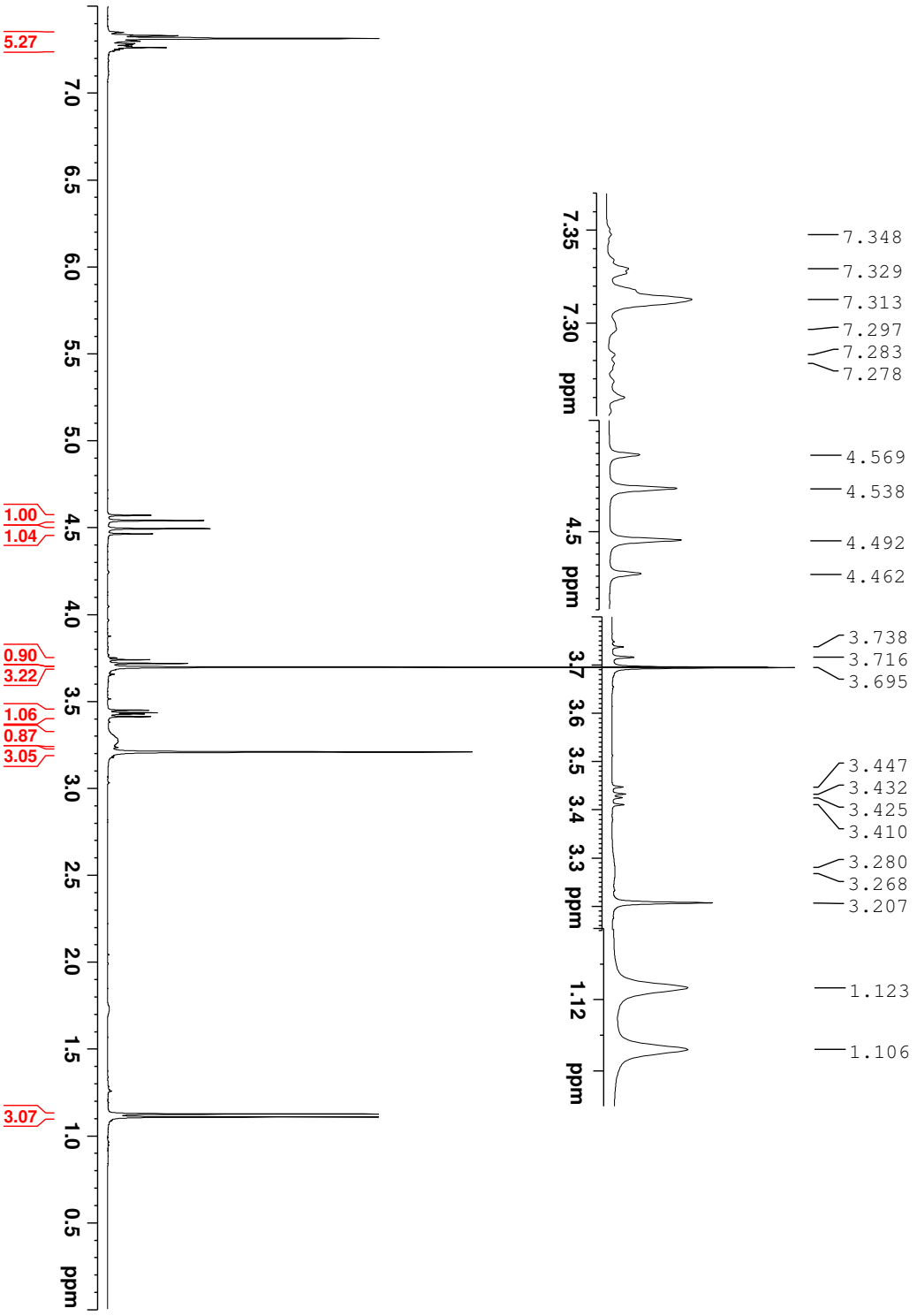

B.2 ^{1}H-NMR for 51, 400 MHz, $CDCl_3$ (Hz)

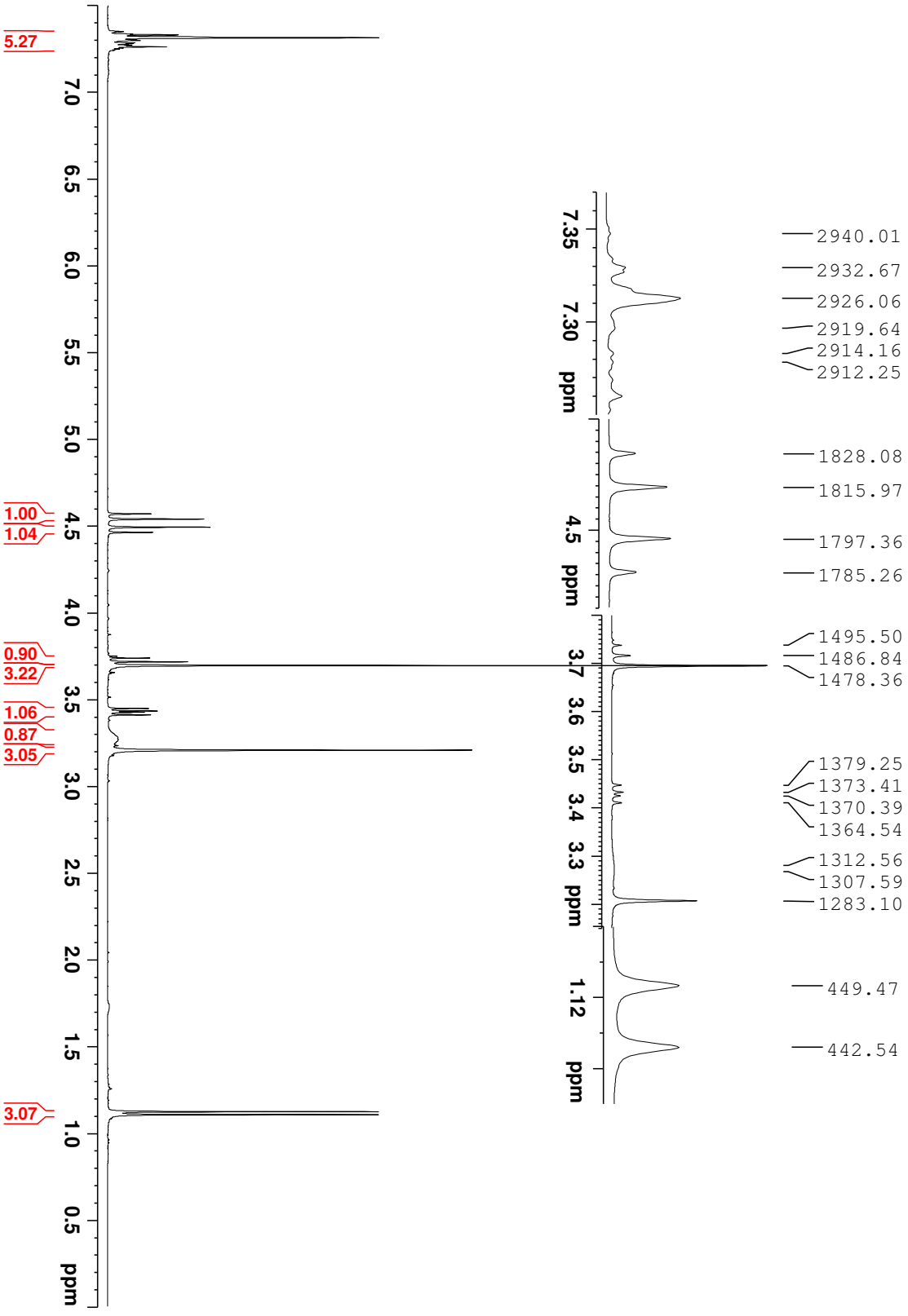

B.3 ^{13}C-NMR for 51, 400 MHz, $CDCl_3$ (ppm)

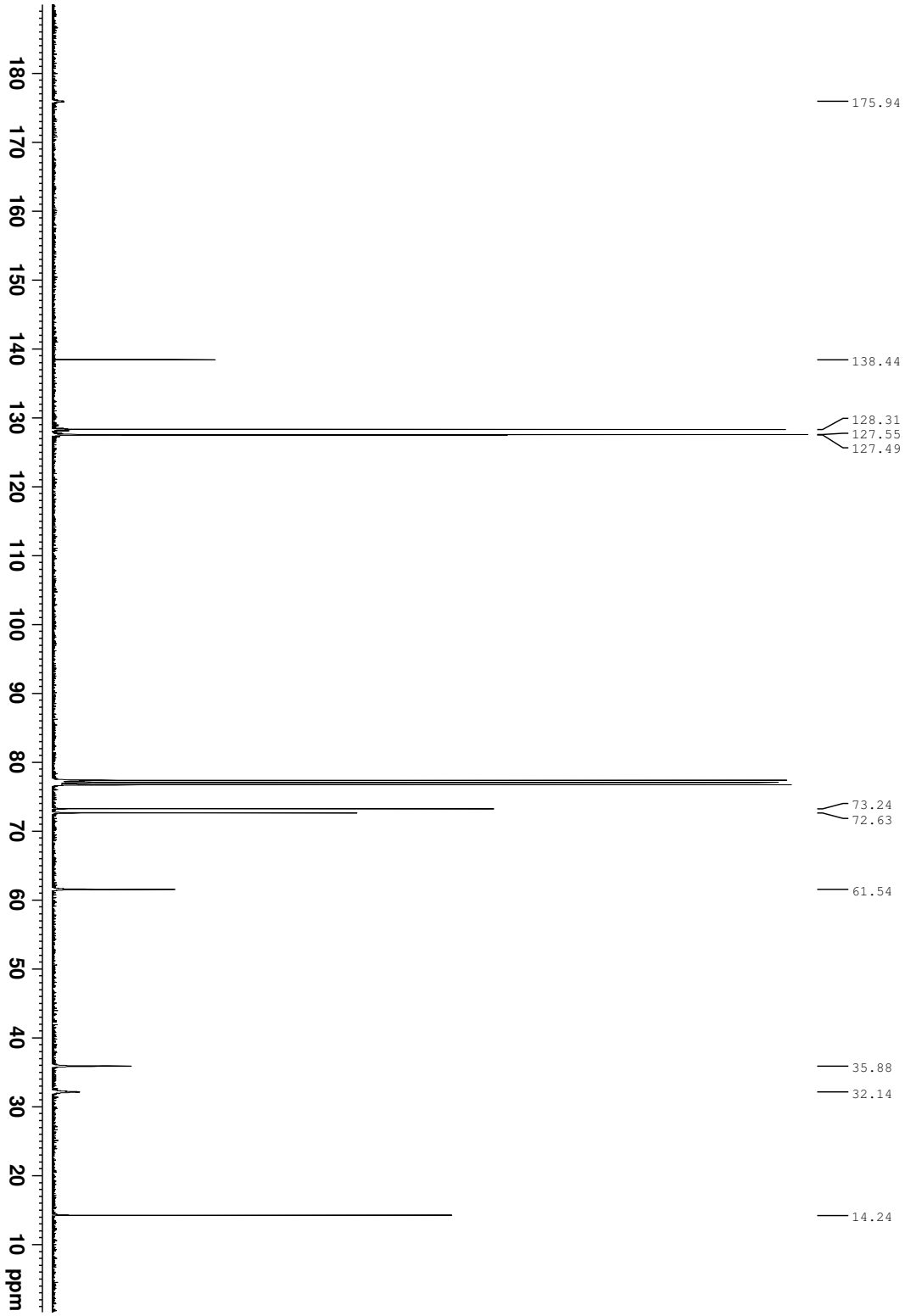

B.4 IR Spectrum (cm^{-1}) of 51

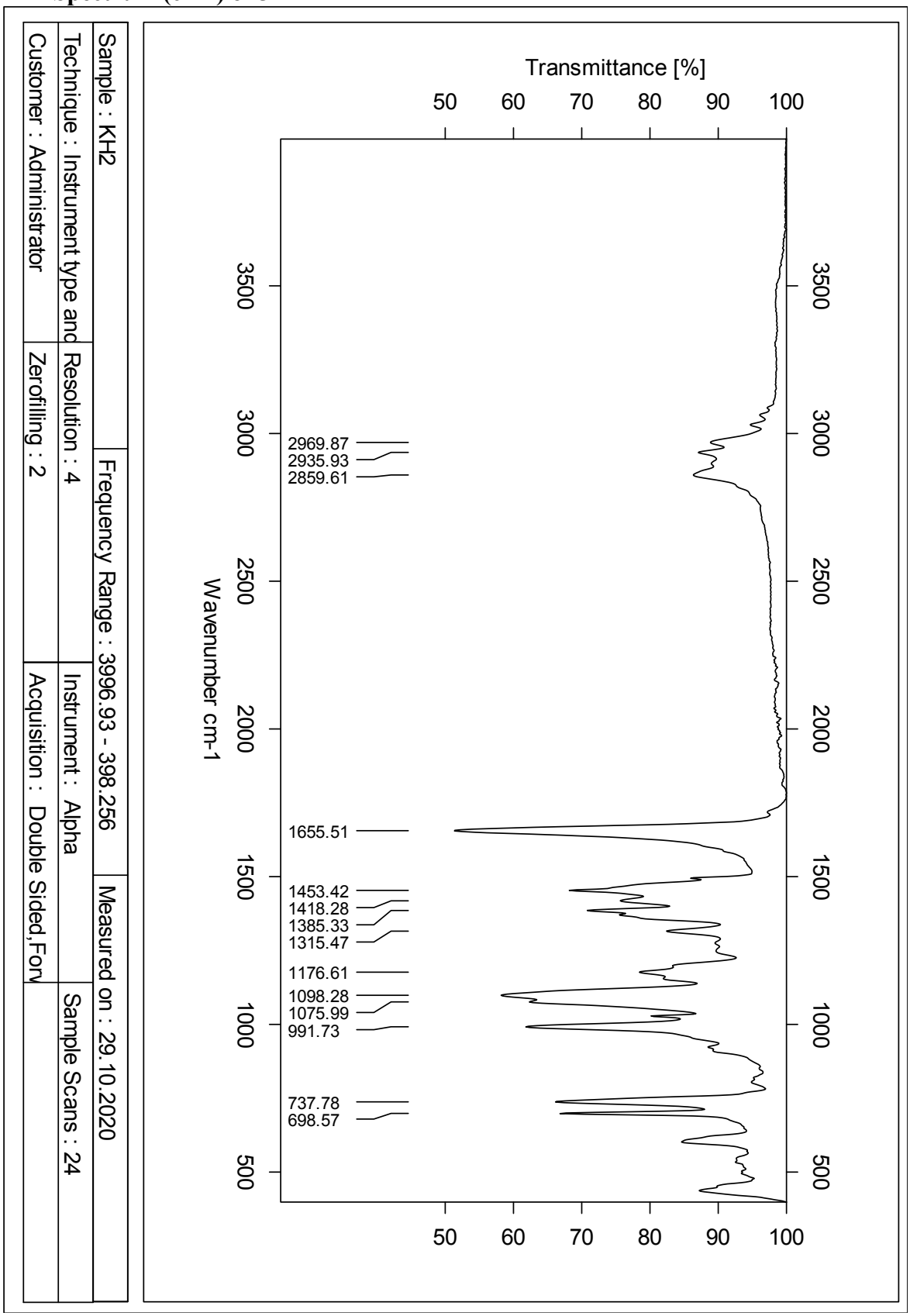

C (R)-1-(benzyloxy)-2-methylpentan-3-one (52)
C.1 ^{1}H-NMR for 52, 400 MHz, $CDCl_3$ (ppm)

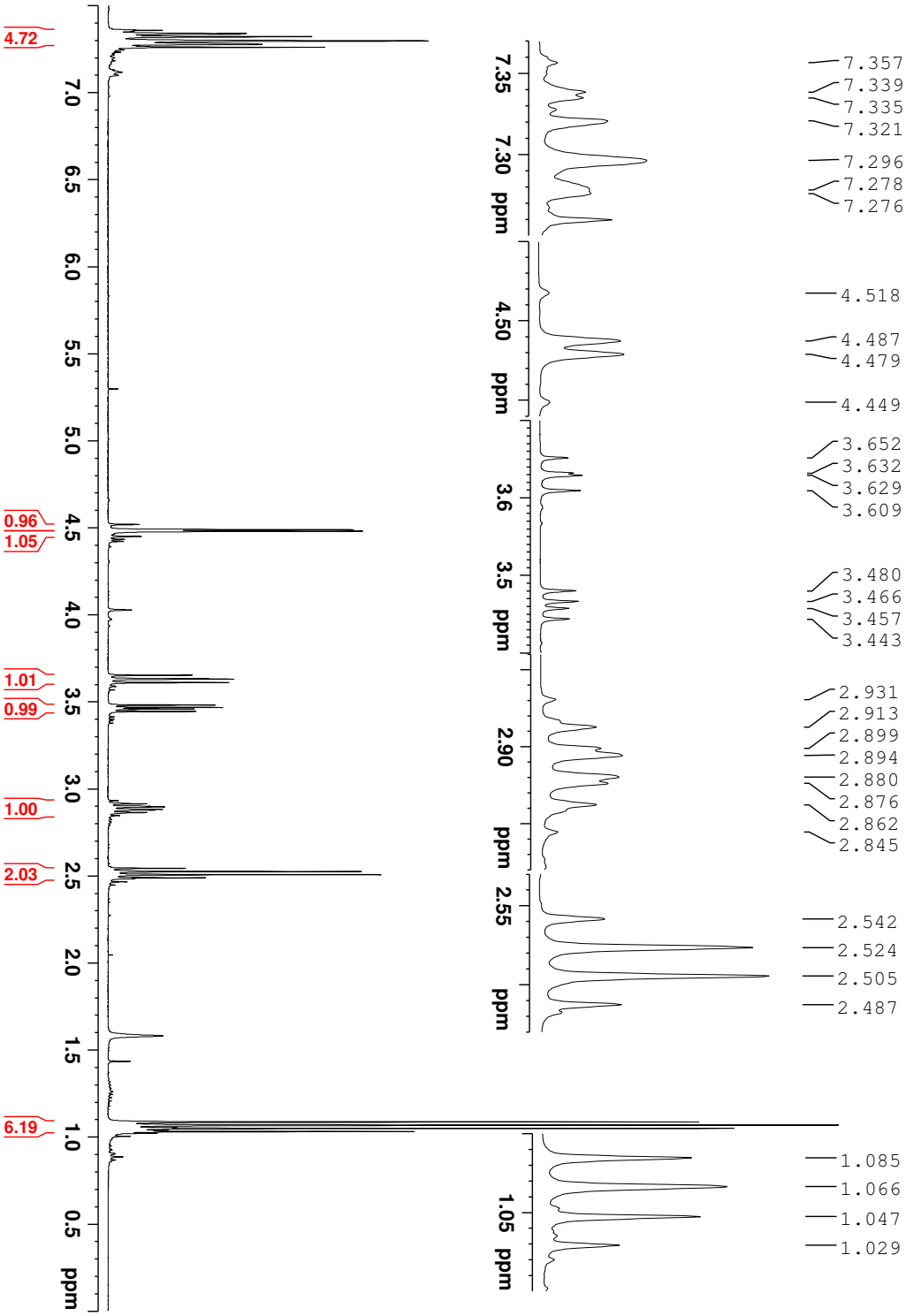

C.2 ^{1}H-NMR for 52, 400 MHz, $CDCl_3$ (Hz)

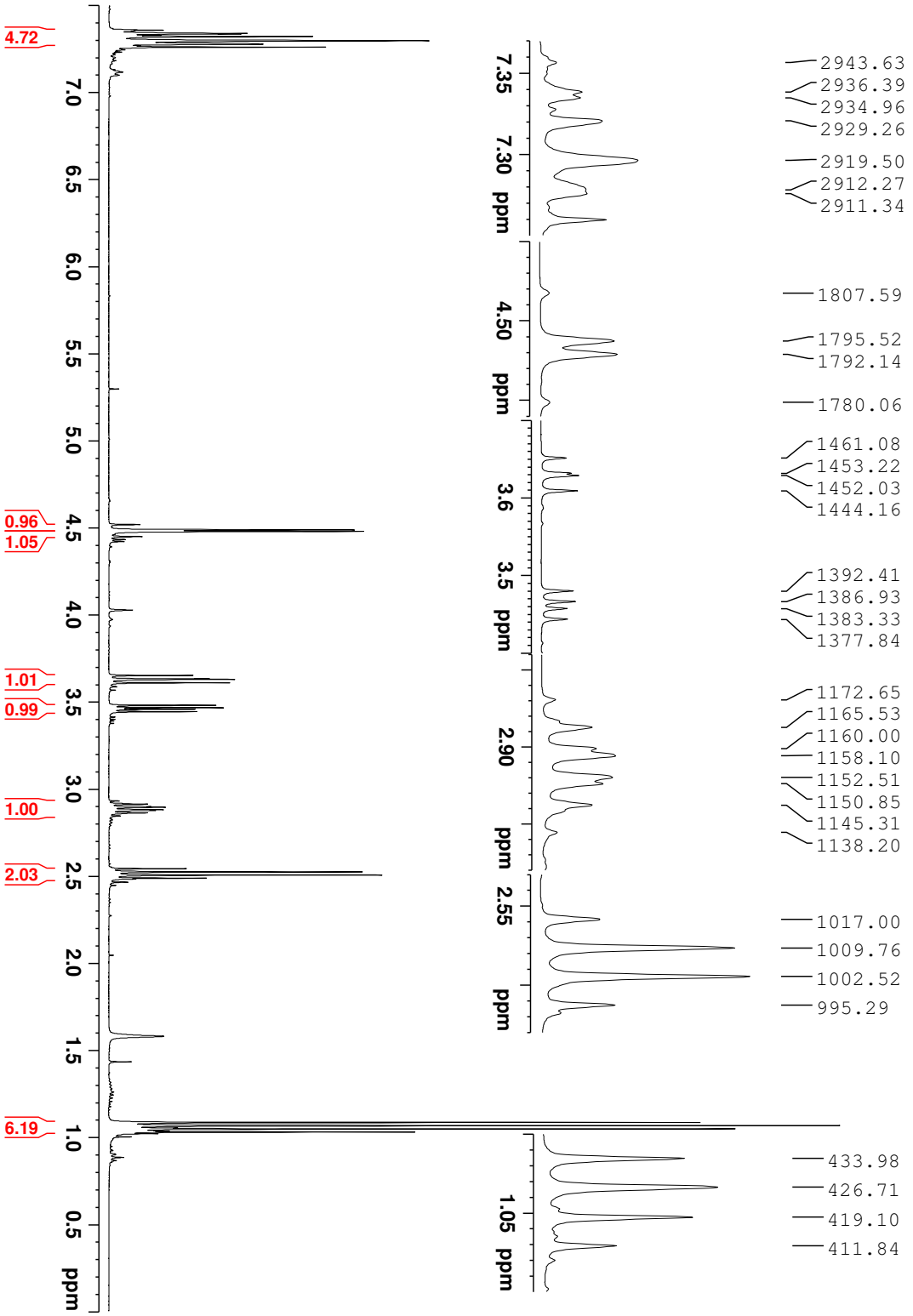

C.3 ^{13}C-NMR for 52, 400 MHz, $CDCl_3$ (shifts in ppm)

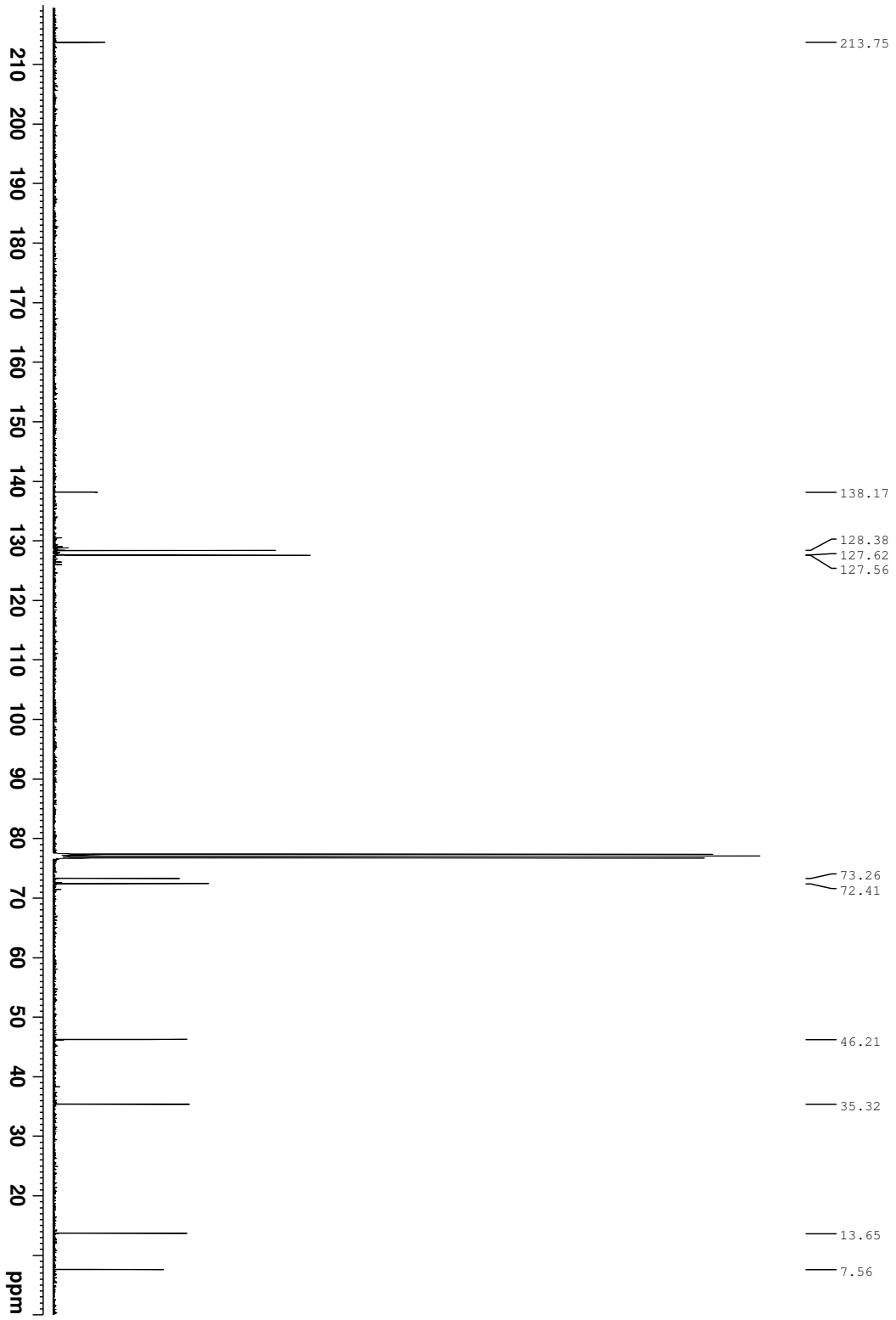

C.4 IR Spectrum (cm^{-1}) of 52

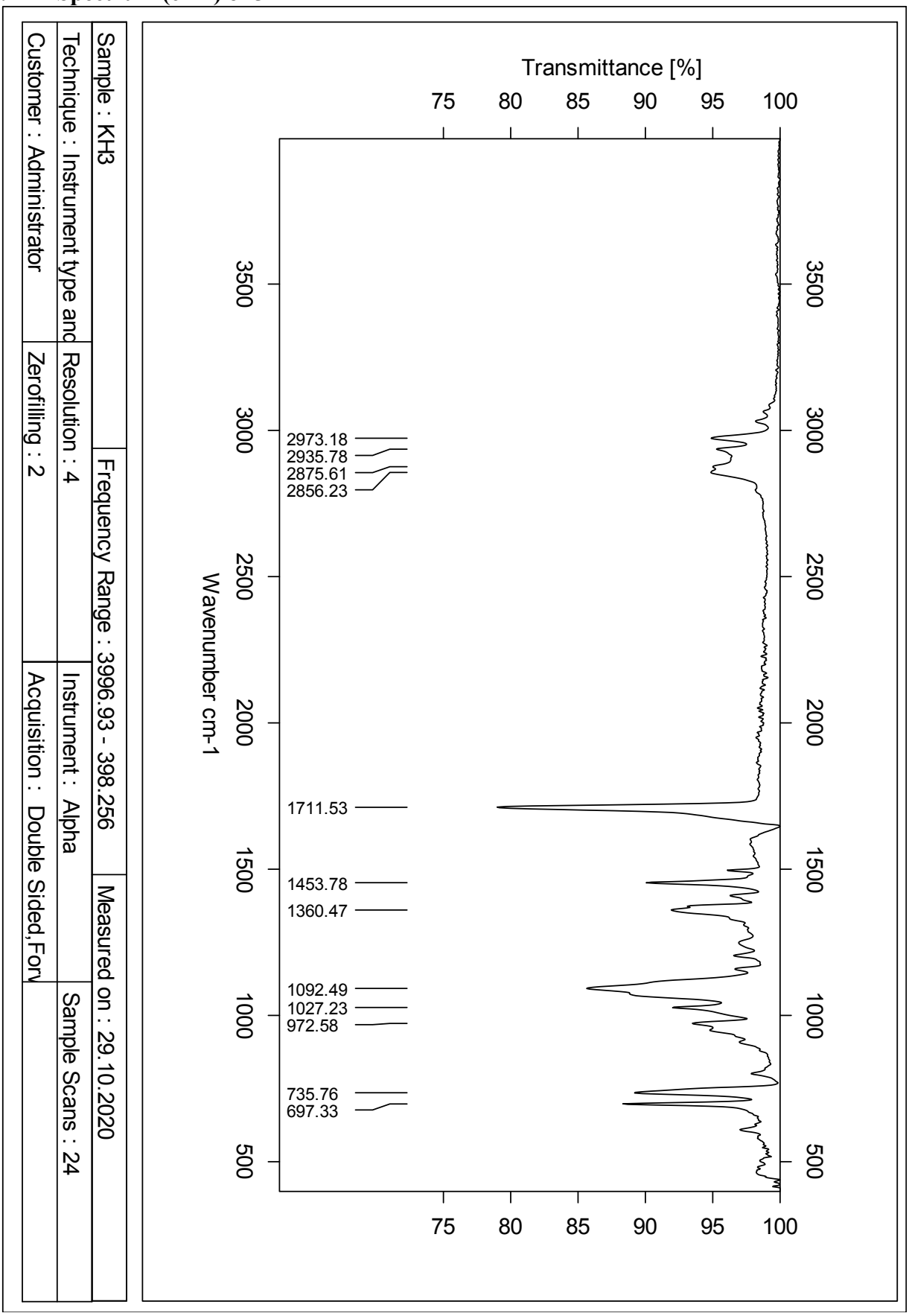

D (2*R*,4*R*,5*R*,6*S*)-1-(benzyloxy)-5-hydroxy-2,4,6-trimethyloctan-3-one (53)
D.1 ^{1}H-NMR for 53, 600 MHz, $CDCl_3$ (ppm)

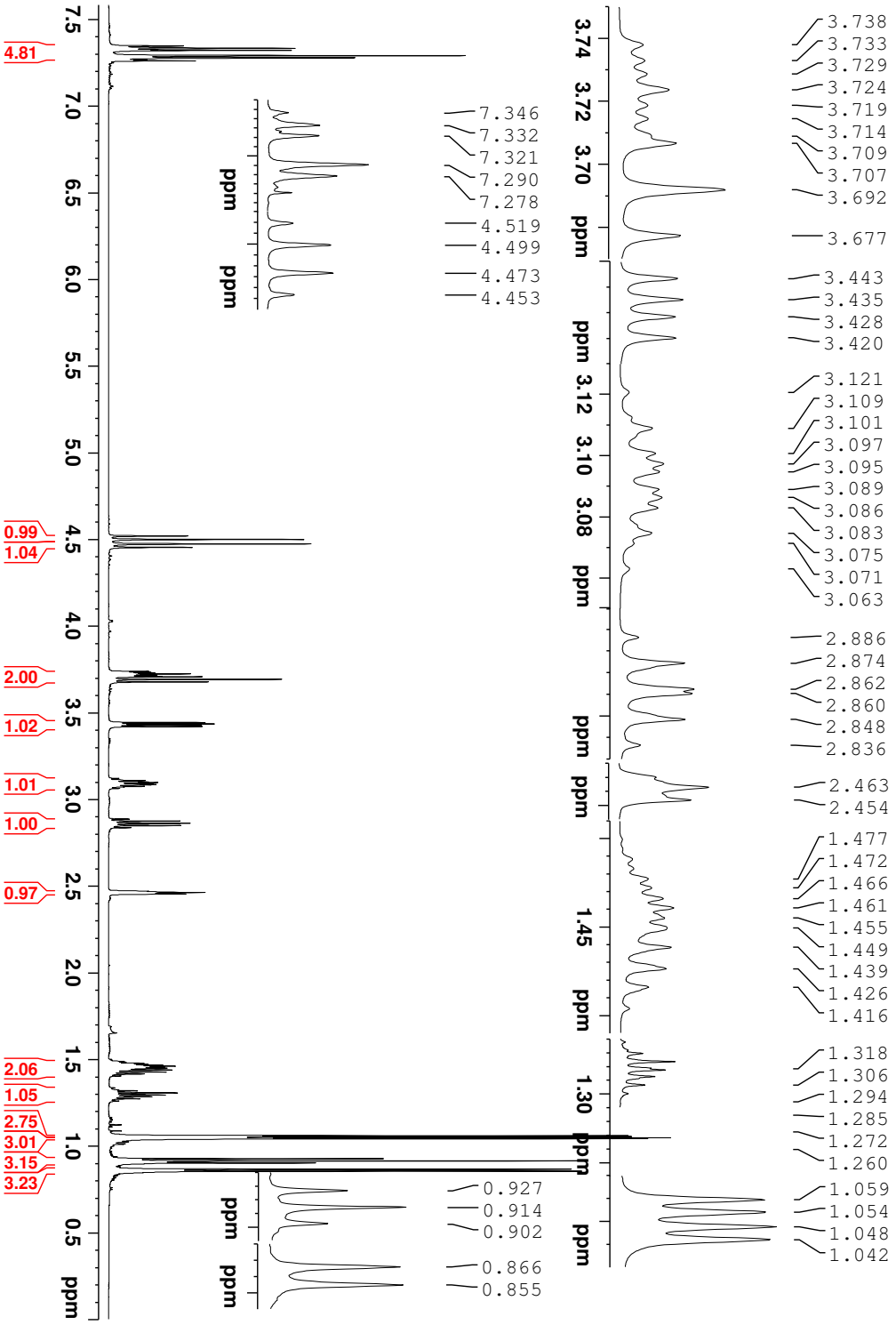

D.2 ^{1}H-NMR for 53, 600 MHz, $CDCl_3$ (Hz)

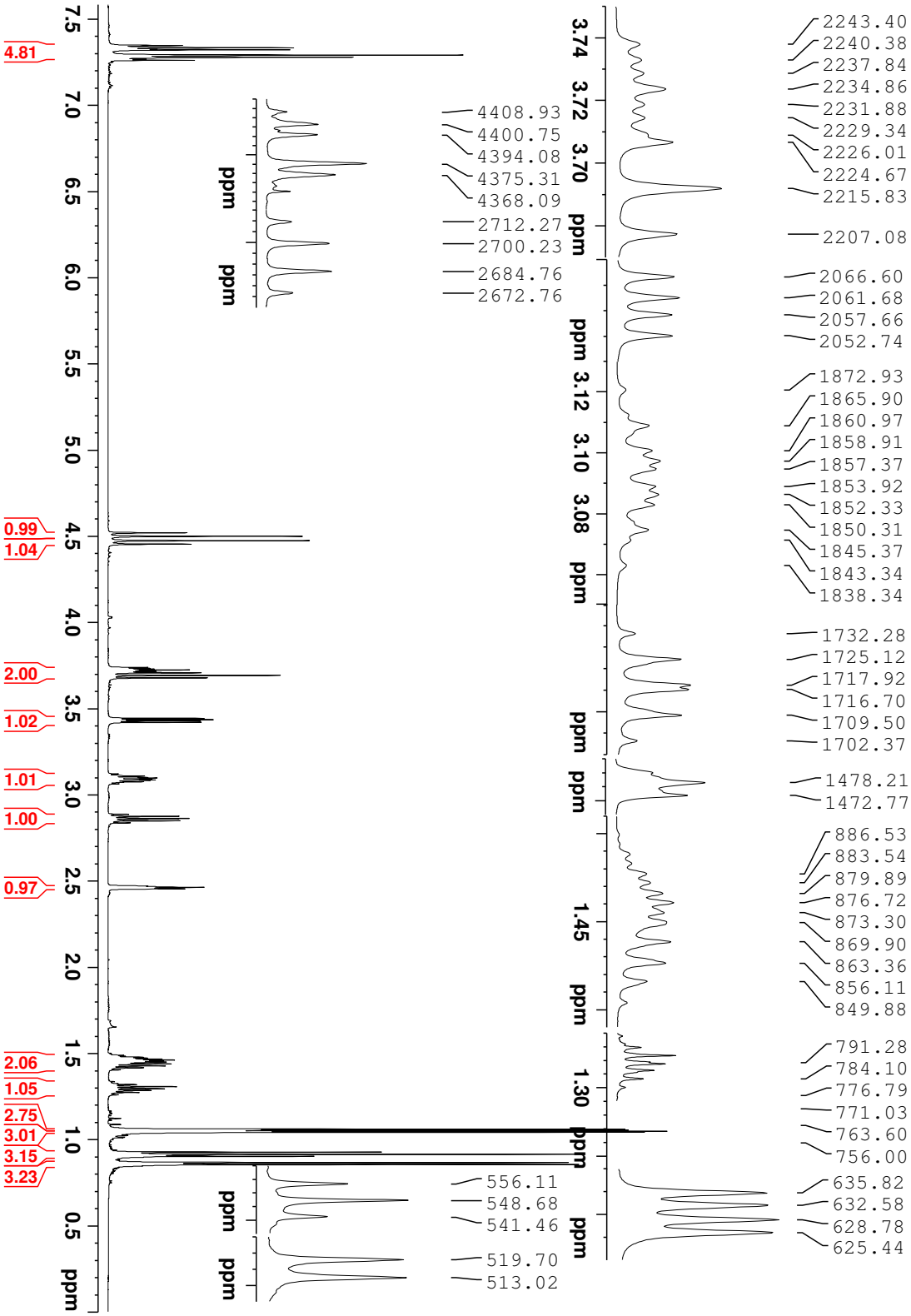

D.3 ^{13}C-NMR for 53, 600 MHz, $CDCl_3$ (ppm)

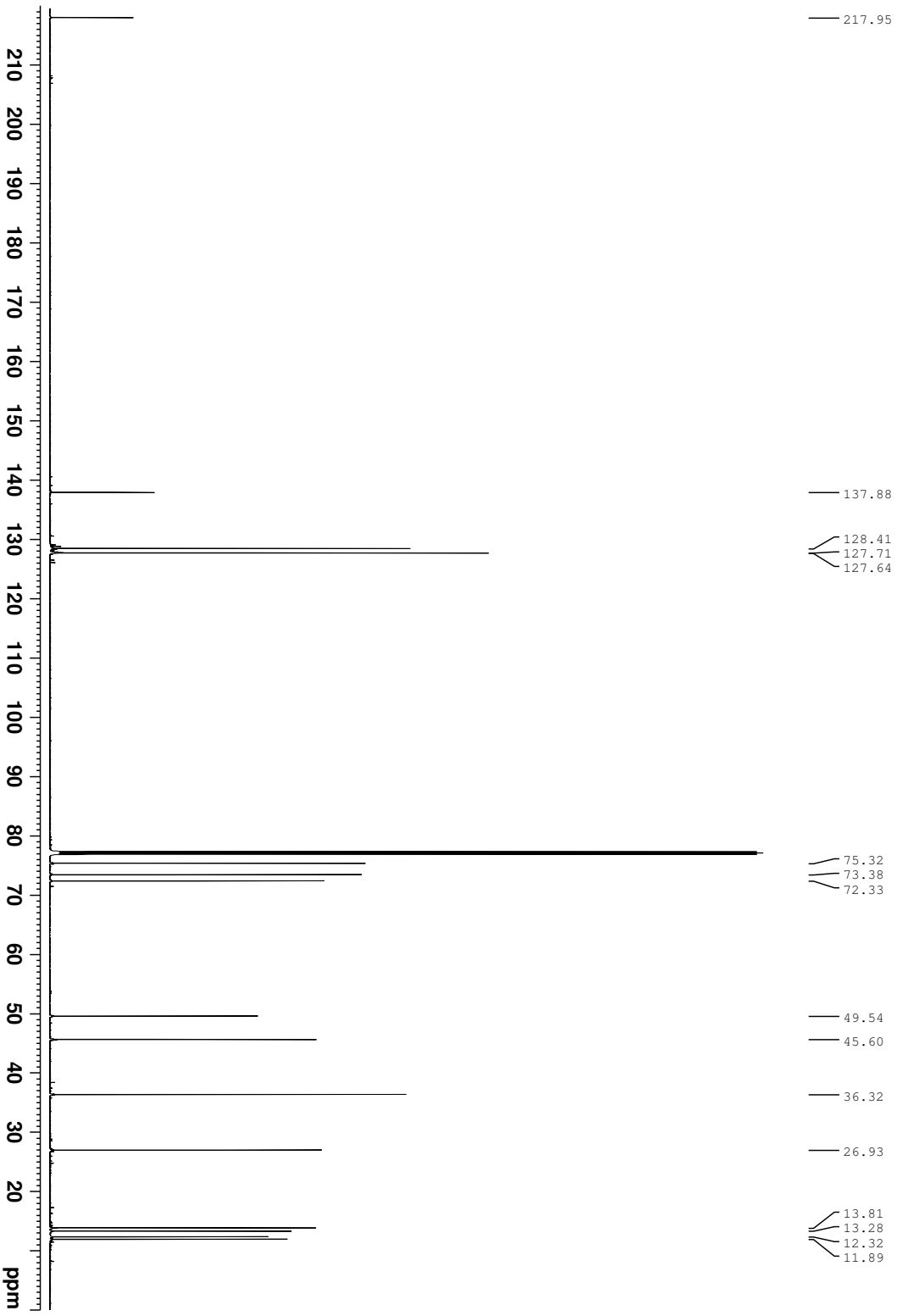

D.4 ^{1}H-^{1}H-COSY for 53, 600 MHz, $CDCl_3$

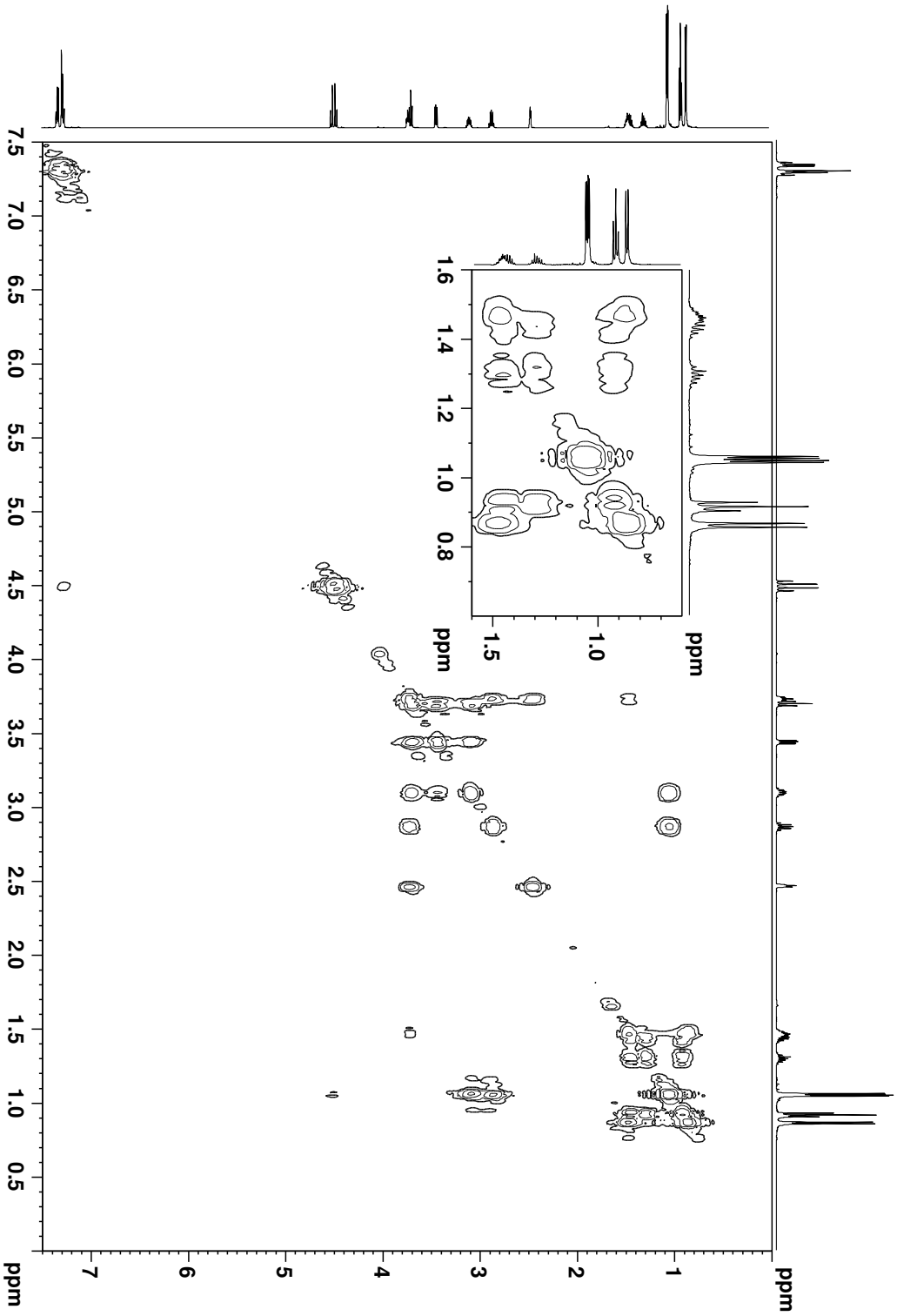

D.5 ^{1}H-^{13}C HSQC for 53, 600 MHz, $CDCl_3$

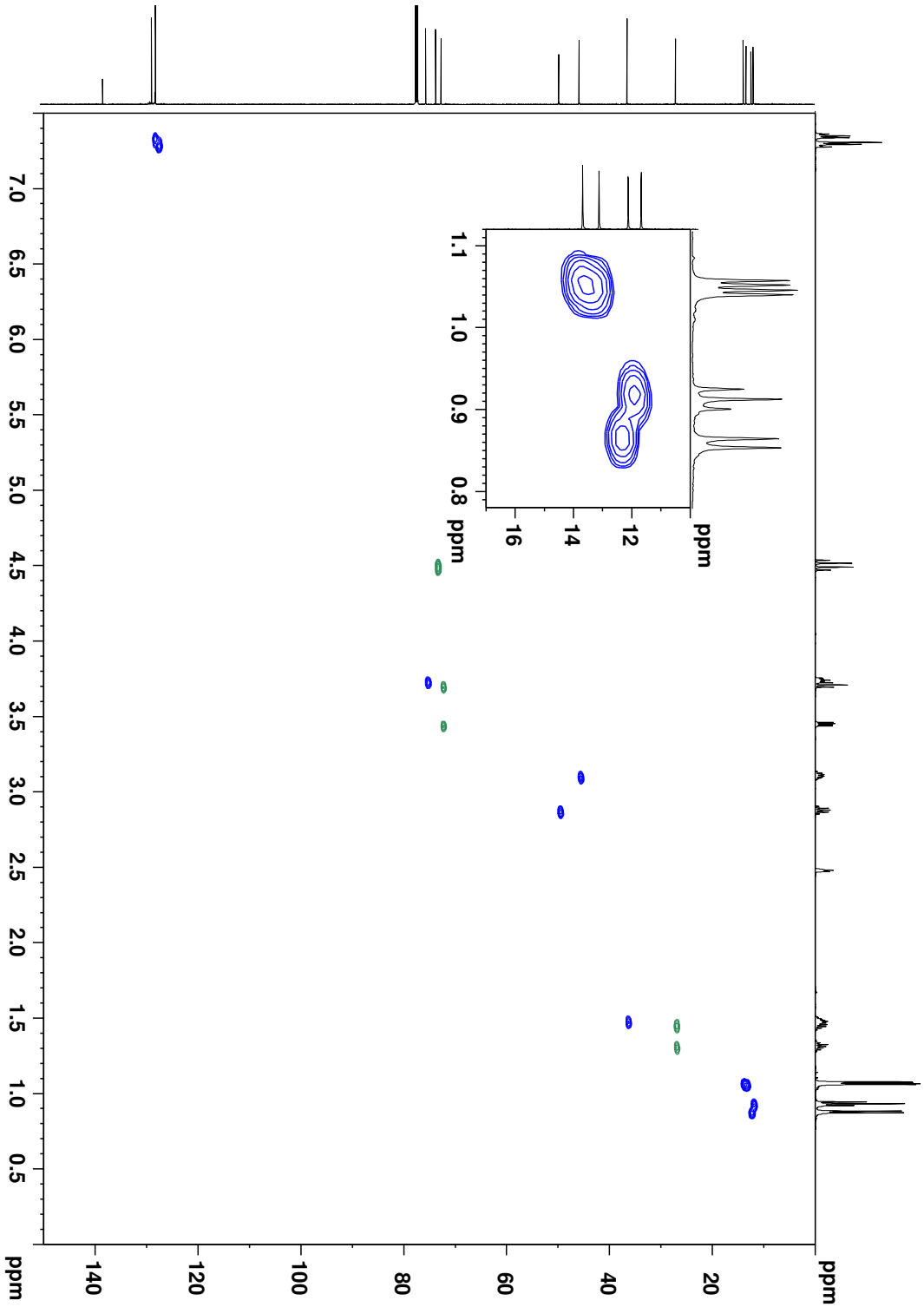

D.6 ^{1}H-^{13}C HMBC for 53, 600 MHz, $CDCl_3$

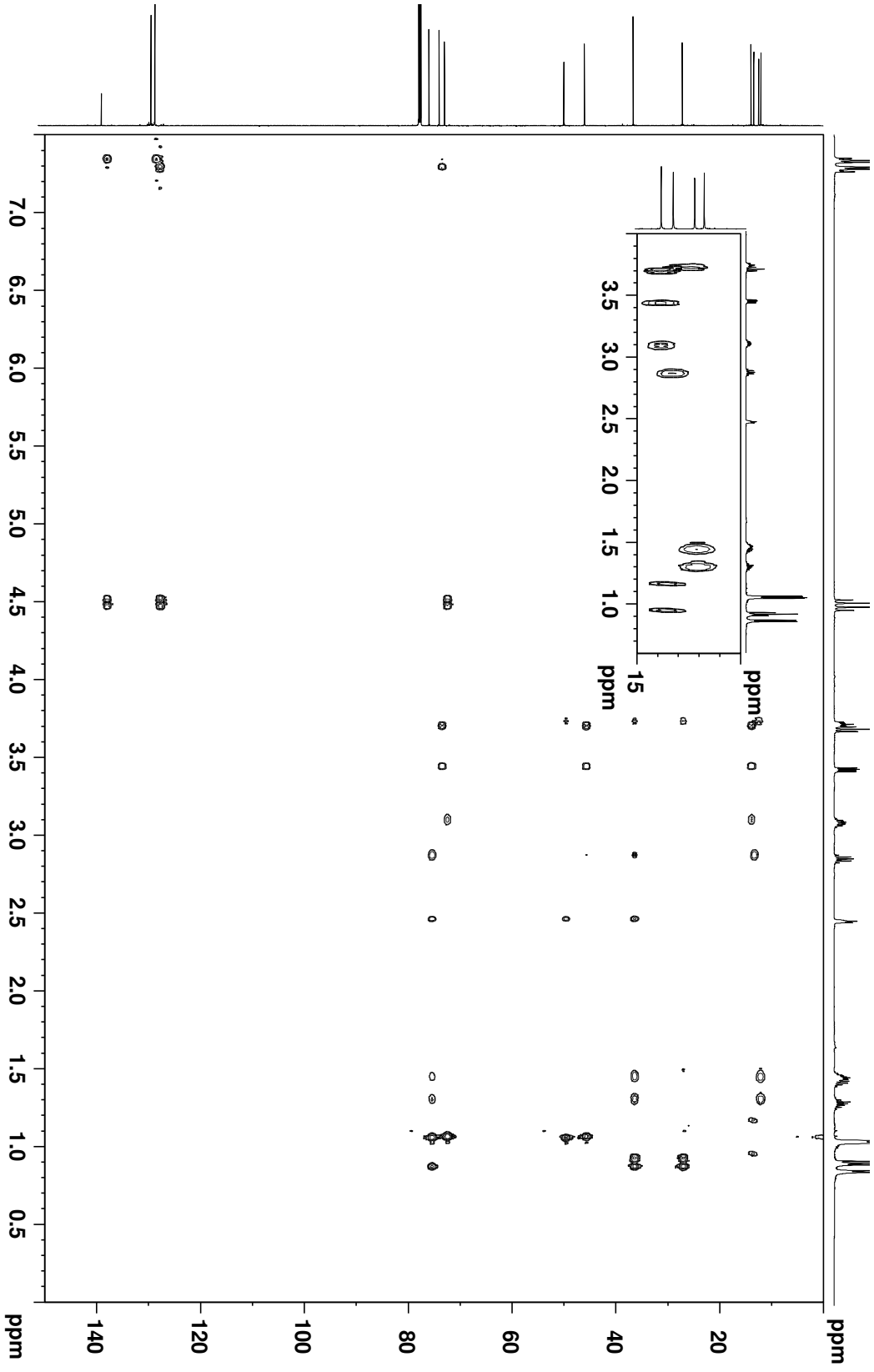

D.7 IR Spectrum of 53 (cm^{-1})

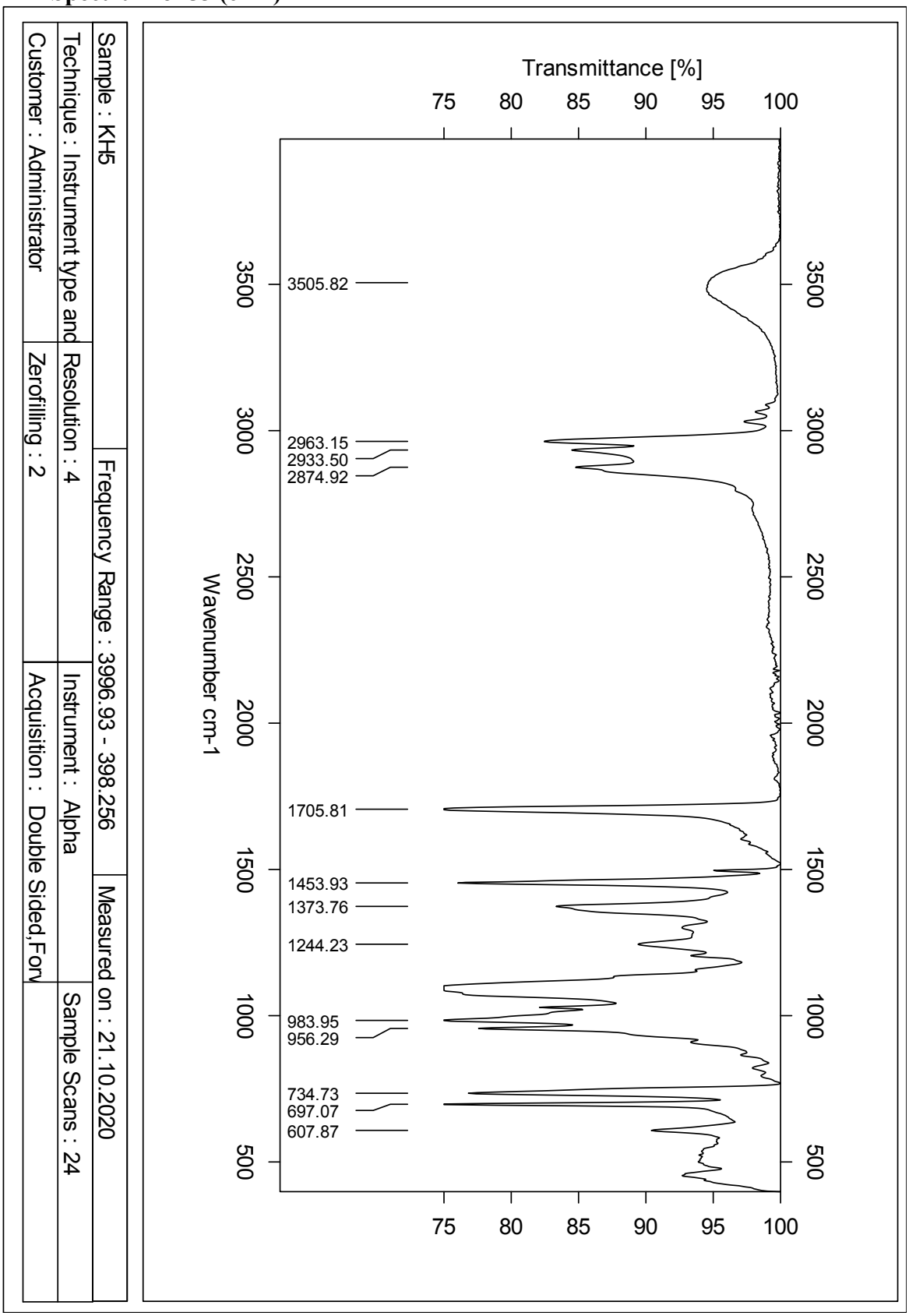

Elemental Composition Report

Single Mass Analysis

Tolerance = 2.1 PPM / DBE: min = -1.5, max = 50.0
Element prediction: Off
Number of isotope peaks used for i-FIT = 3

Monoisotopic Mass, Even Electron Ions
134 formula(e) evaluated with 1 results within limits (up to 50 closest results for each mass)
Elements Used:
C: 0-500 H: 0-1000 O: 0-10 Na: 0-1 I: 0-2

JA_20210218_55 146 (1.379) AM2 (Ar,35000.0,0.00,0.00); Cm (135:146)
1: TOF MS ES+

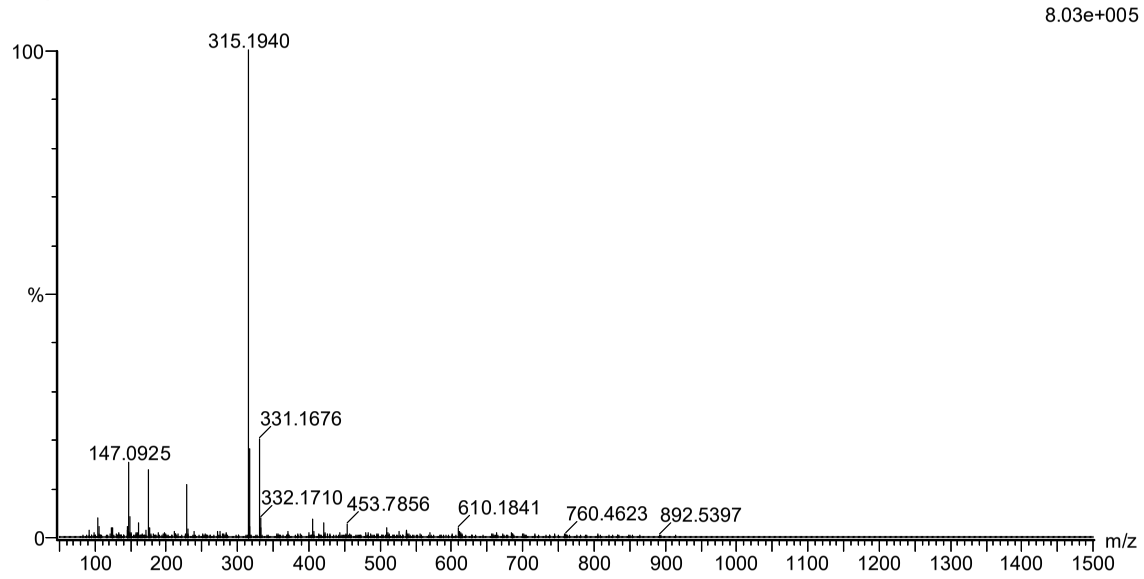

Minimum:				-1.5				
Maximum:		5.0	2.1	50.0				
Mass	Calc. Mass	mDa	PPM	DBE	i-FIT	Norm	Conf(%)	Formula
315.1940	315.1936	0.4	1.3	4.5	1110.8	n/a	n/a	C18 H28 O3 Na

XX

E (2R,4R,5R,6S)-1-(benzyloxy)-2,4,6-trimethyl-5-((triethylsilyl)oxy)octan-3-one (54)
E.1 ^{1}H-NMR for 54, 600 MHz, $CDCl_3$ (ppm)

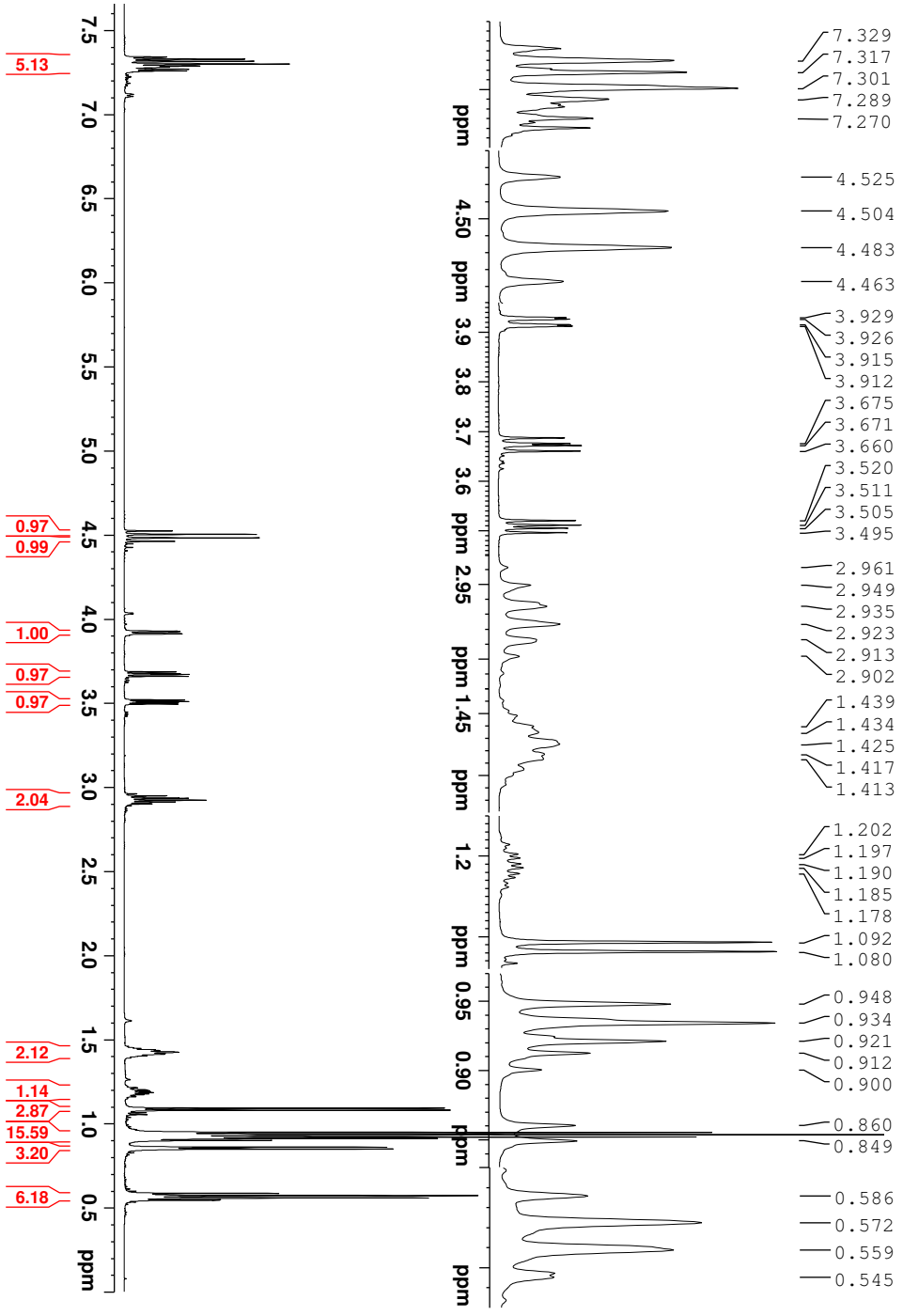

E.2 ^{1}H-NMR for 54, 600 MHz, $CDCl_3$ (Hz)

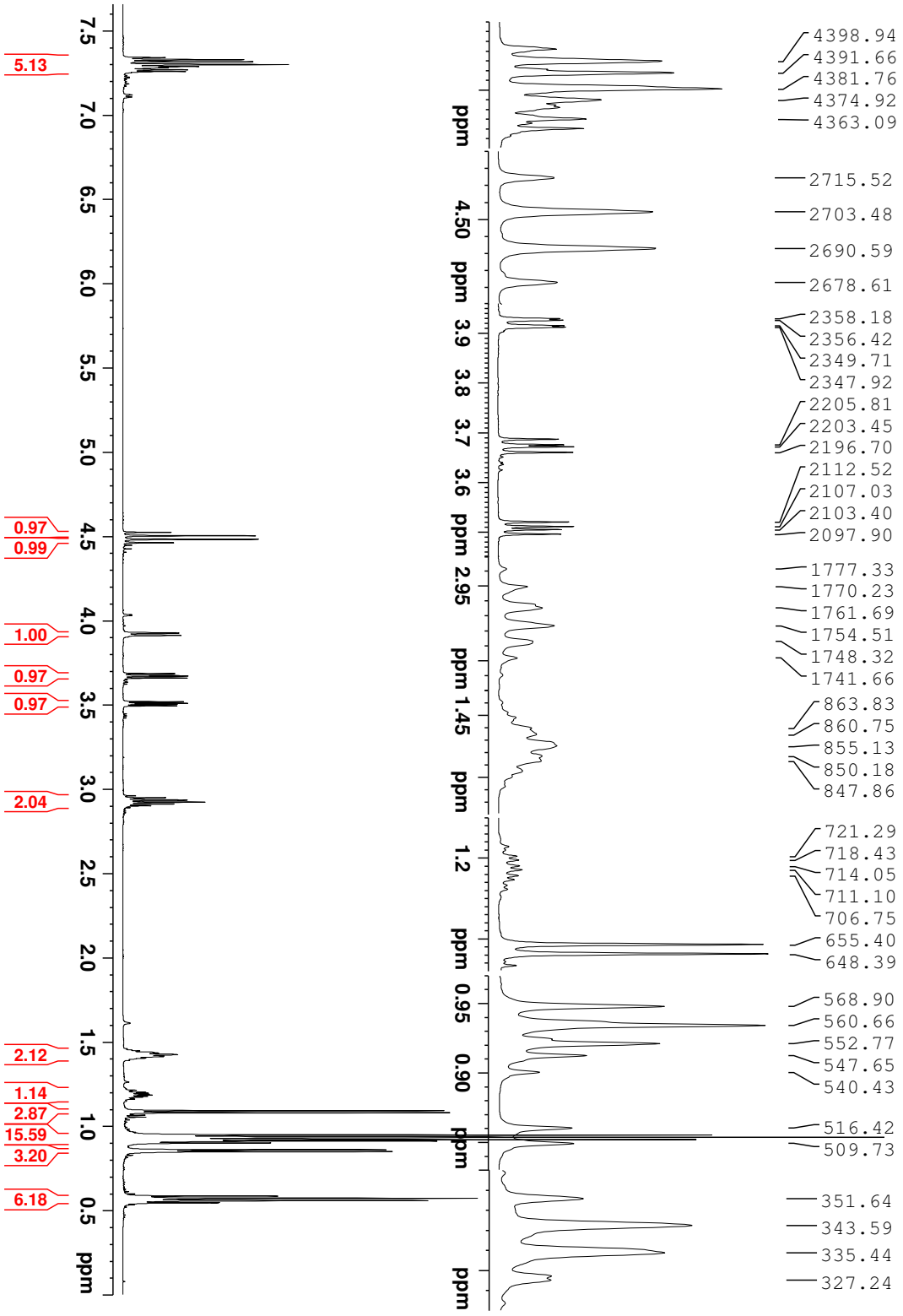

E.3 ^{13}C-NMR for 54, 600 MHz, $CDCl_3$ (ppm)

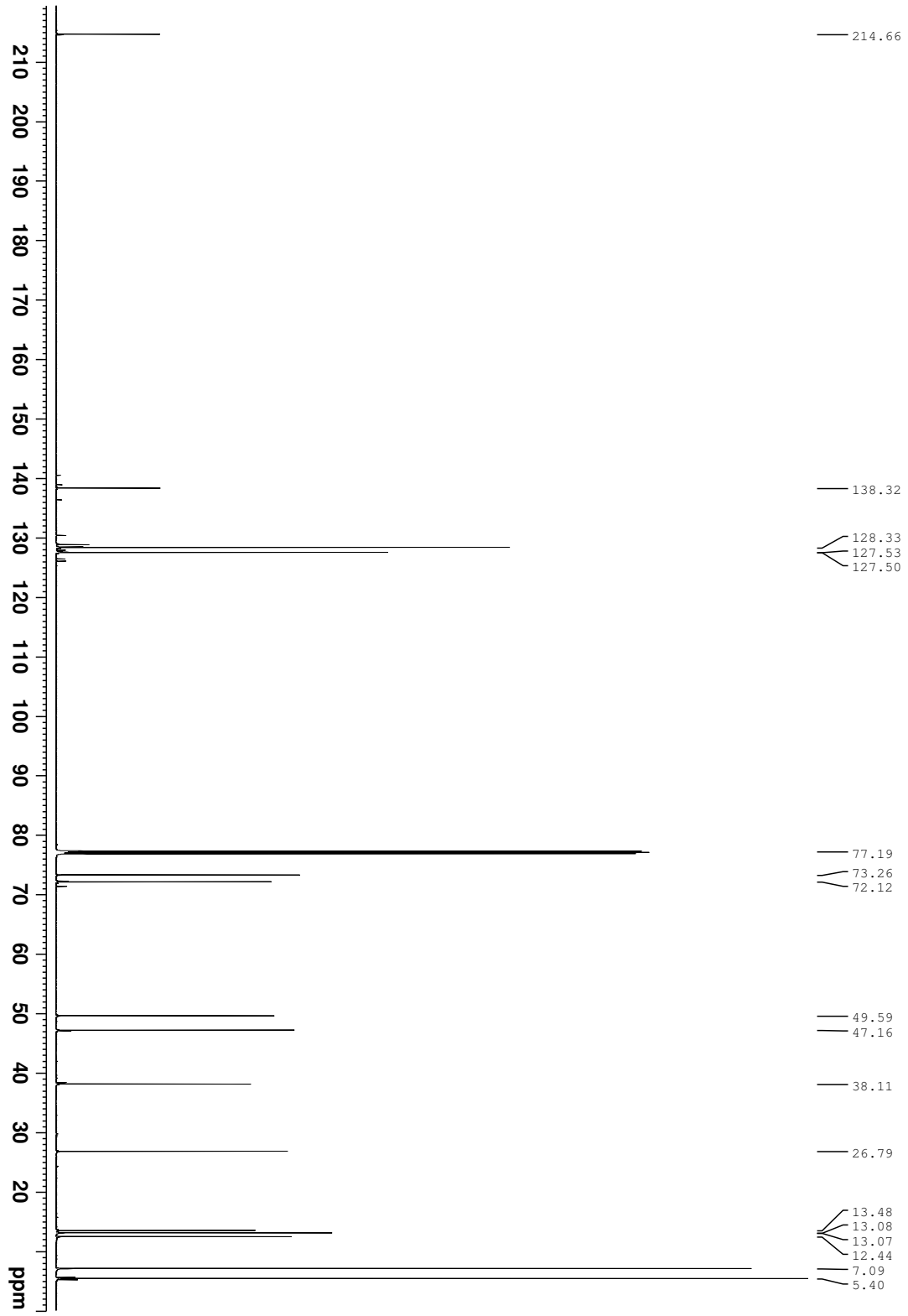

E.4 ^{1}H-^{1}H-COSY for 54, 600 MHz, $CDCl_3$

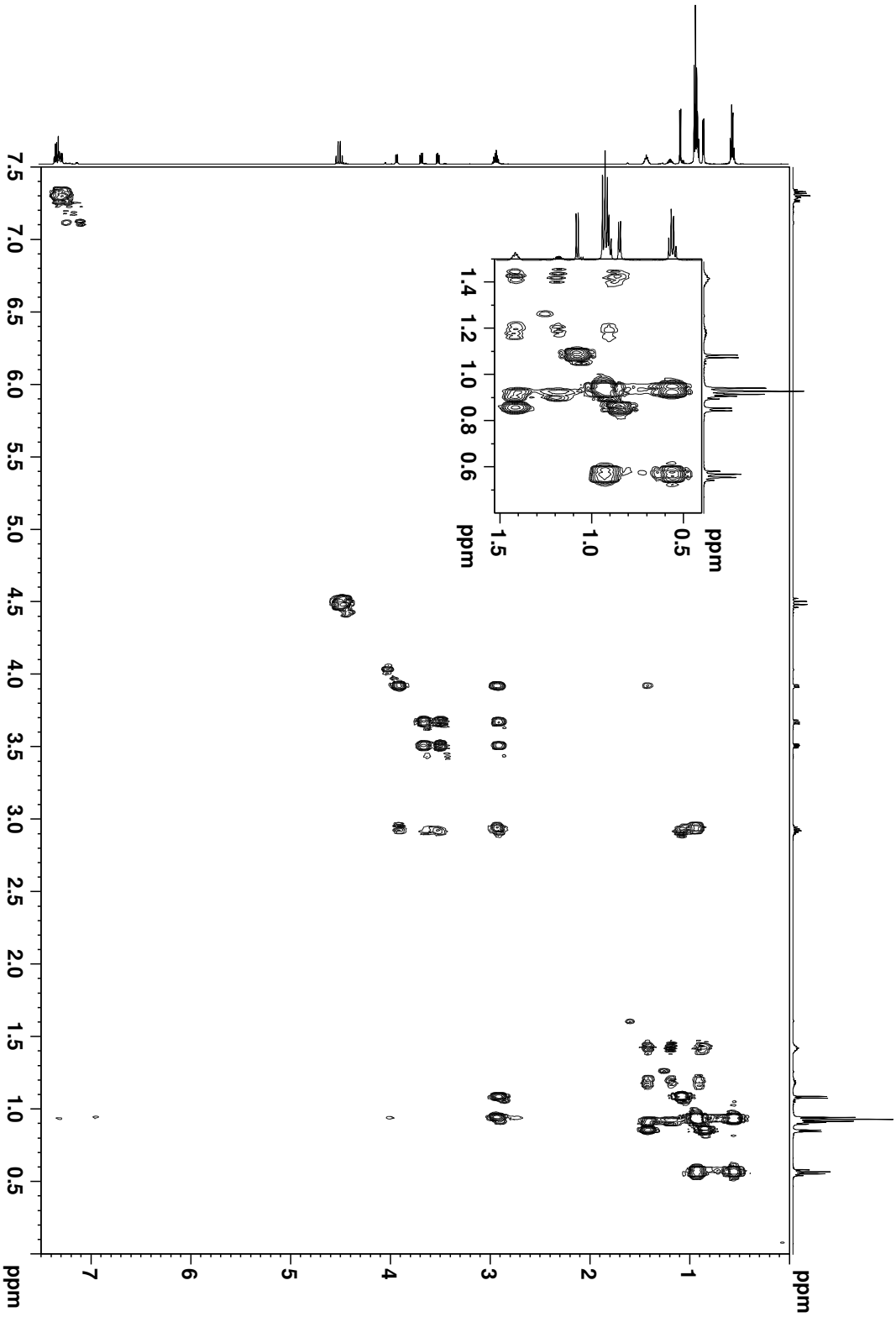

E.5 ^{1}H-^{13}C HSQC for 54, 600 MHz, $CDCl_3$

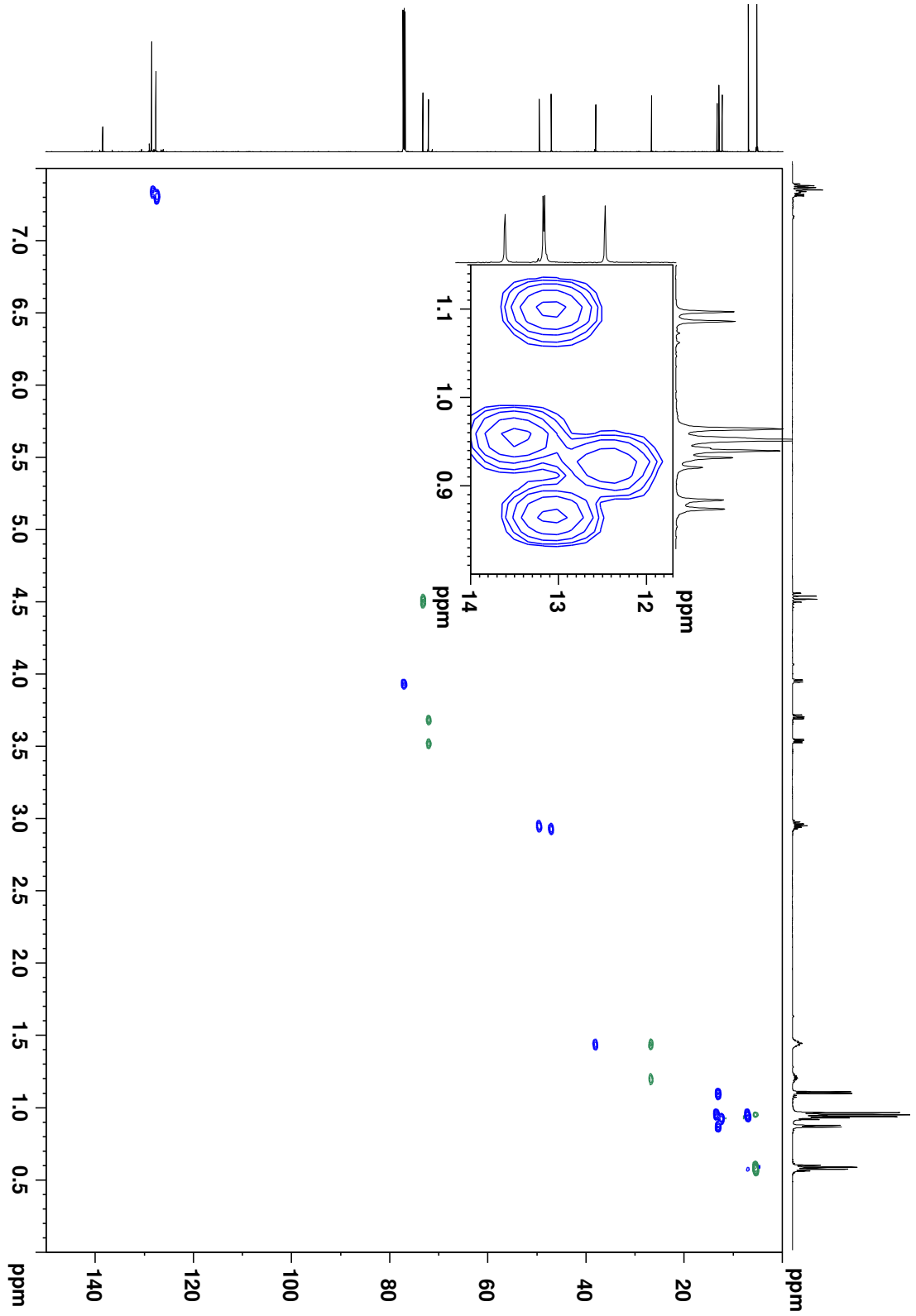

E.6 ^{1}H-^{13}C HMBC for 54, 600 MHz, $CDCl_3$

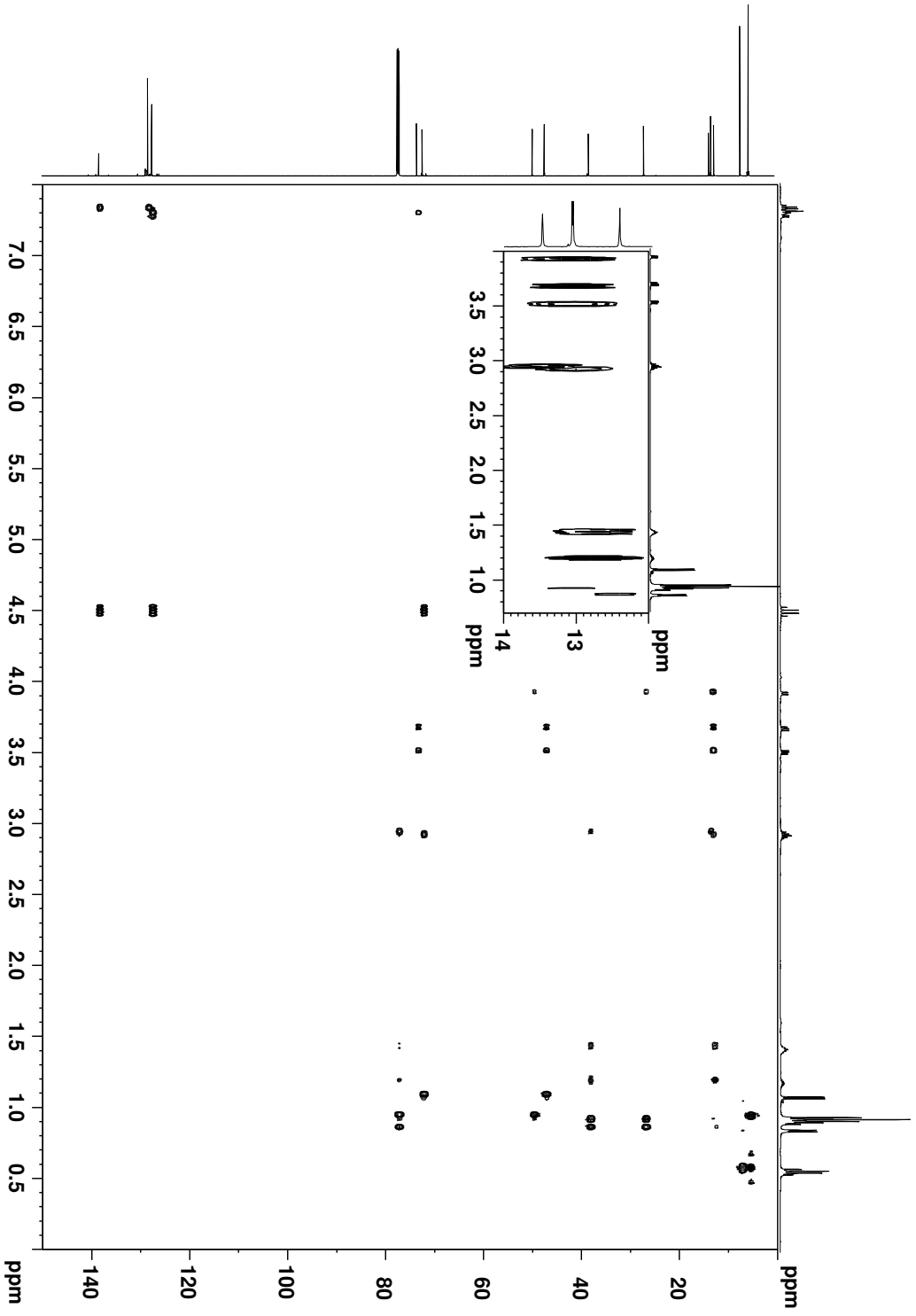

E.7 IR Spectrum of 54 (cm^{-1})

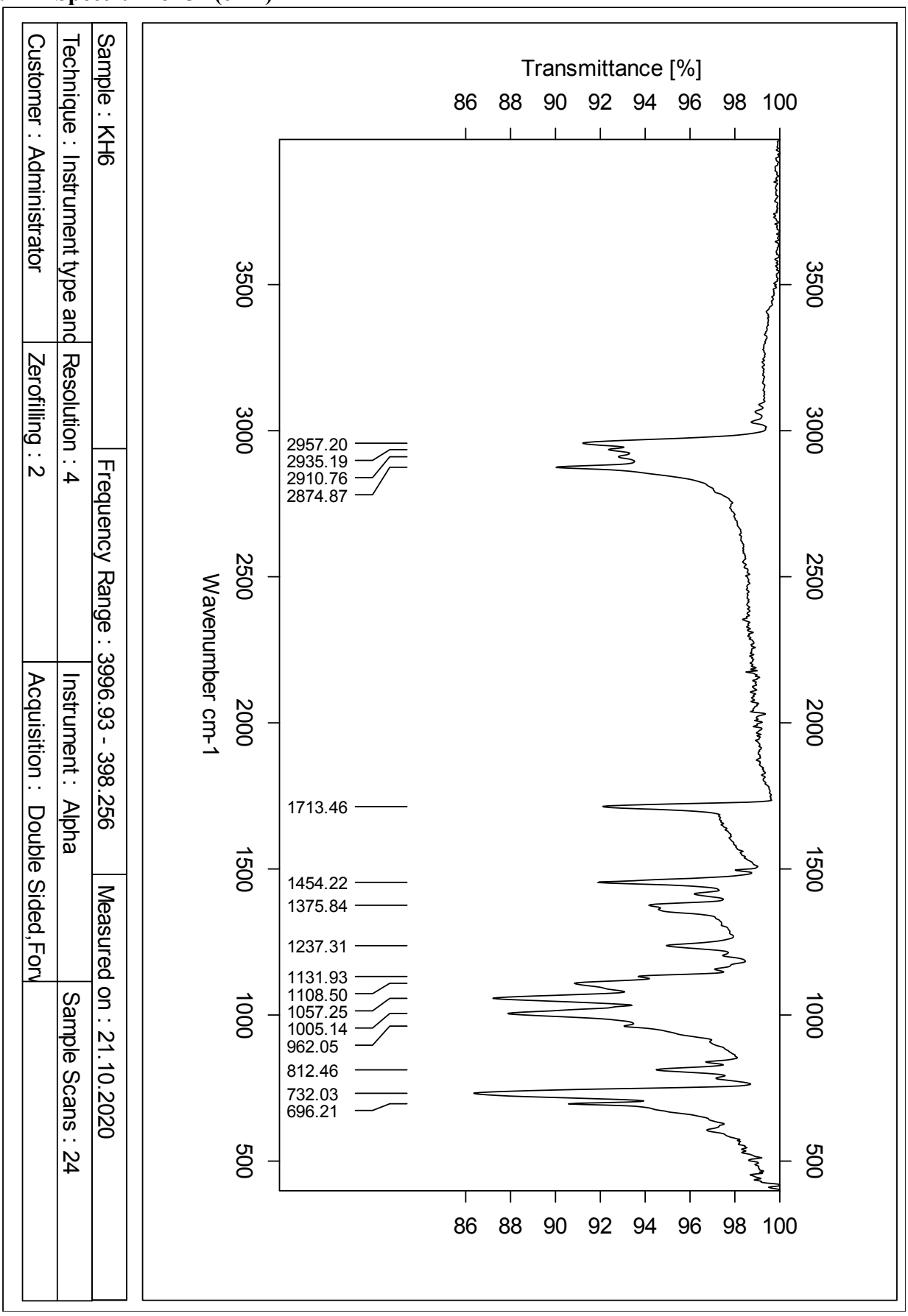

Elemental Composition Report

Single Mass Analysis

Tolerance = 3.0 PPM / DBE: min = -10.0, max = 50.0
Element prediction: Off
Number of isotope peaks used for i-FIT = 6

Monoisotopic Mass, Even Electron Ions
914 formula(e) evaluated with 2 results within limits (all results (up to 1000) for each mass)
Elements Used:
C: 0-100 H: 0-100 N: 0-3 O: 0-5 Na: 0-1 Si: 0-2

JA_20210218_56 95 (0.900) AM2 (Ar,35000.0,0.00,0.00); Cm (95:105)
1: TOF MS ES+

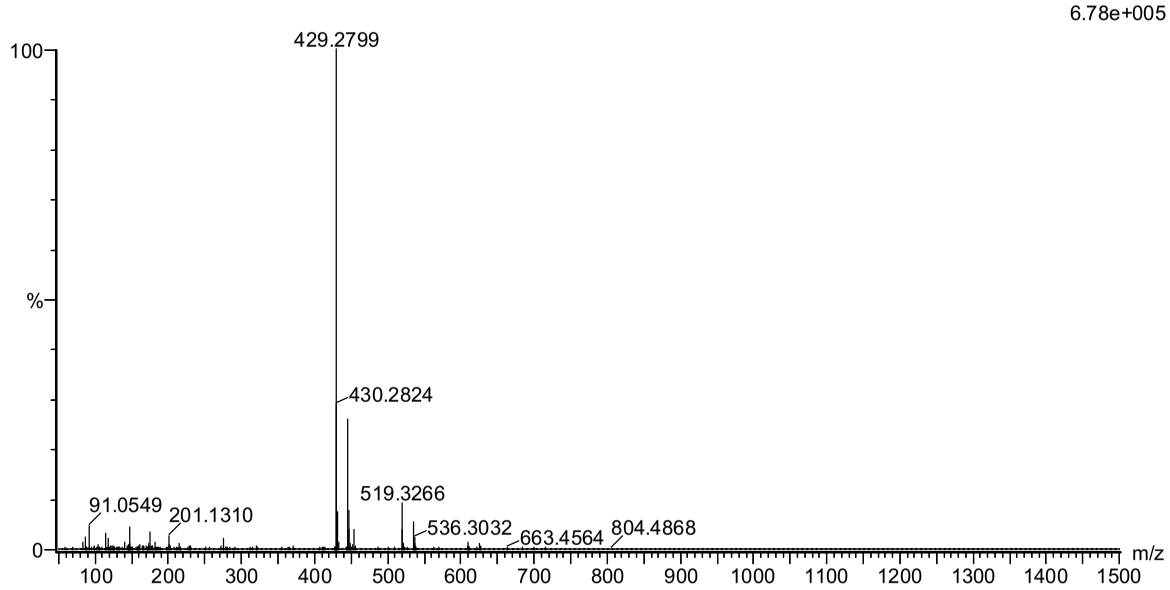

Minimum:				-10.0				
Maximum:		5.0	3.0	50.0				
Mass	Calc. Mass	mDa	PPM	DBE	i-FIT	Norm	Conf(%)	Formula
429.2799	429.2801	-0.2	-0.5	4.5	1671.1	0.000	99.98	C24 H42 O3 Na Si
	429.2794	0.5	1.2	12.5	1679.6	8.527	0.02	C30 H37 O2

F (2*R*,4*S*,5*R*,6*S*)-1-(benzyloxy)-2,4,6-trimethyl-5-((triethylsilyl)oxy)octan-3-ol (55)
F.1 ^{1}H-NMR of 55, 400 MHz, $CDCl_3$ (ppm)

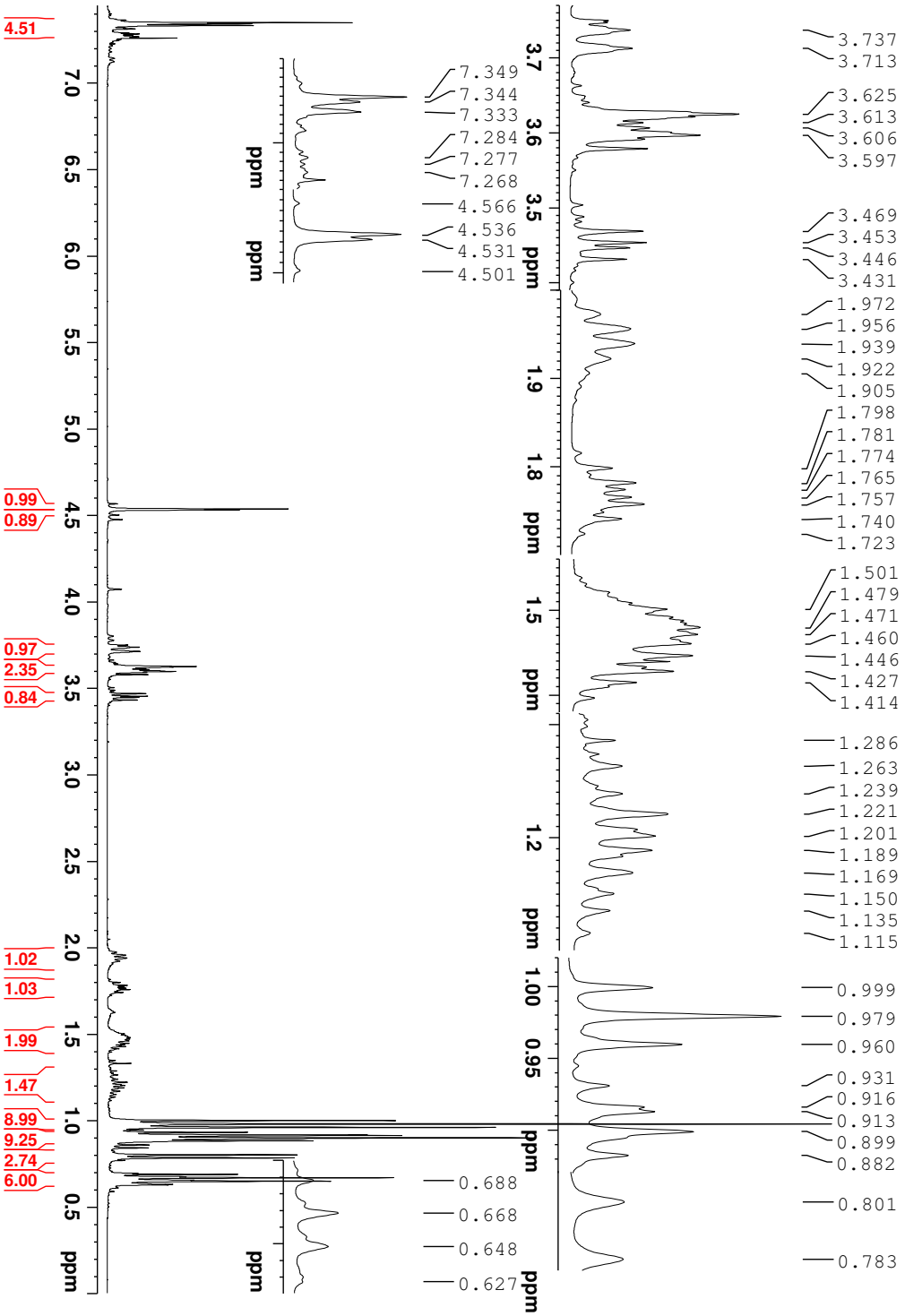

F.2 ^{1}H-NMR of 55, 400 MHz, $CDCl_3$ (Hz)

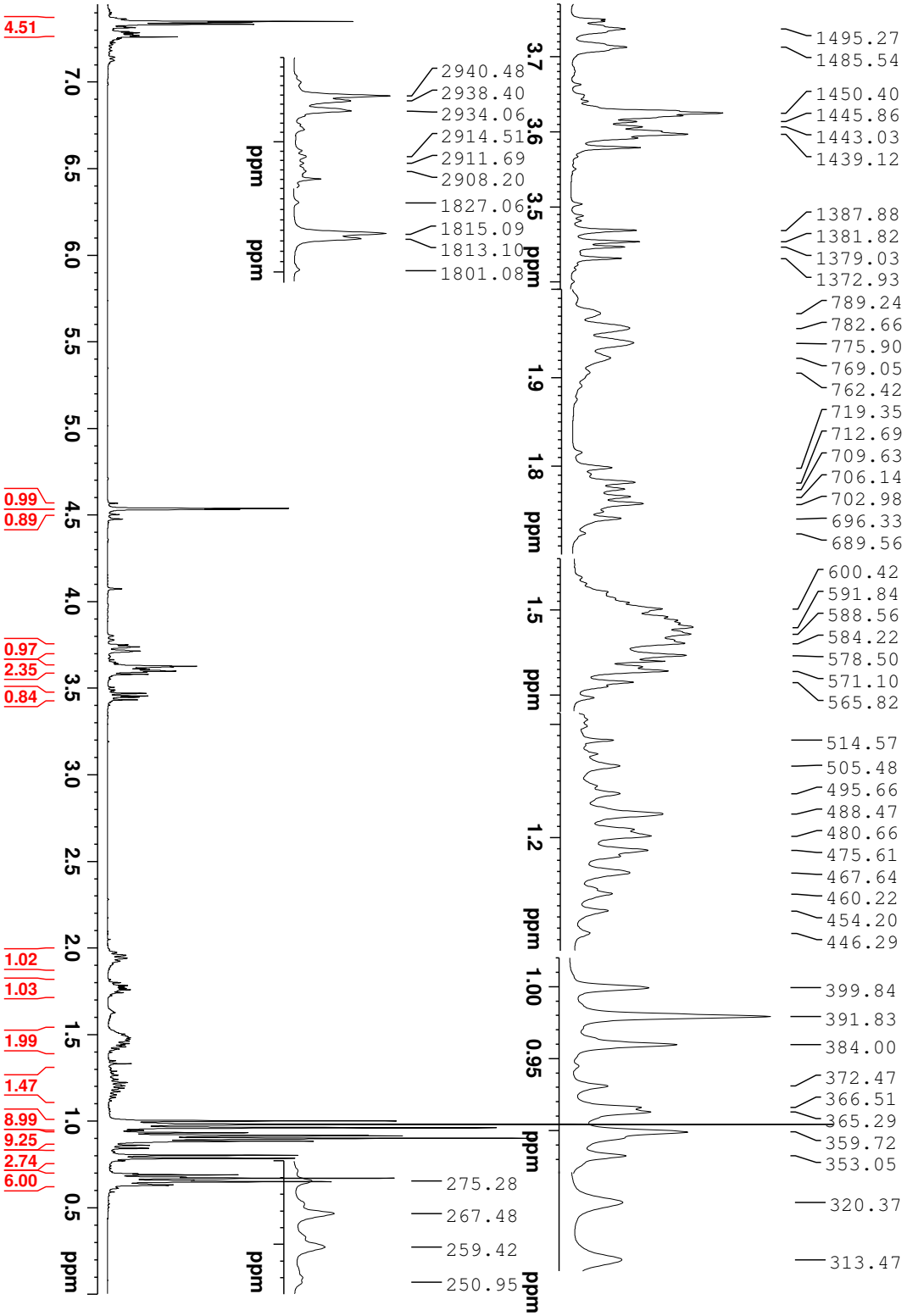

F.3 ^{13}C-NMR of 55, 400 MHz, $CDCl_3$ (ppm)

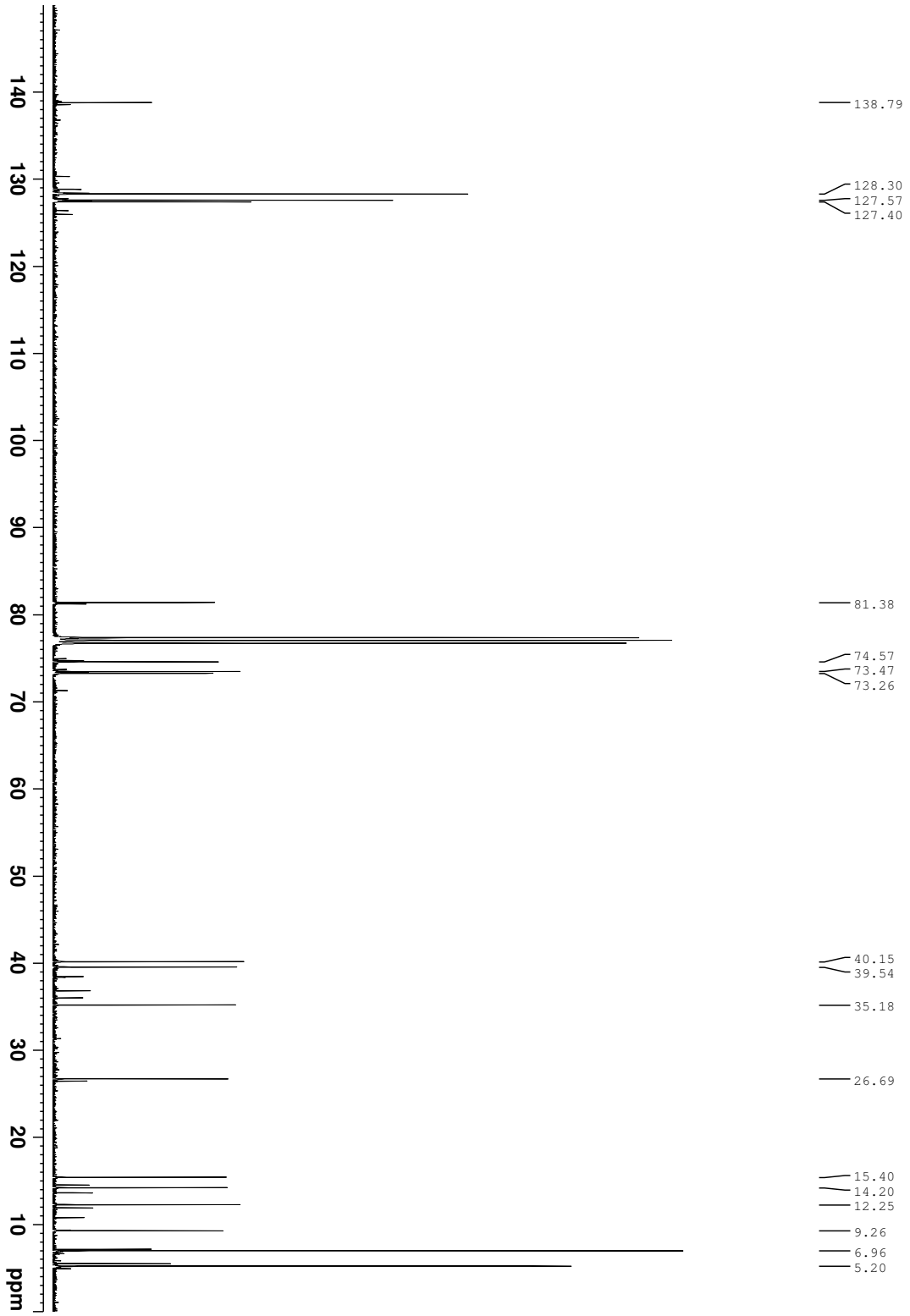

F.4 ^{1}H-^{1}H-COSY for 55, 400 MHz, $CDCl_3$

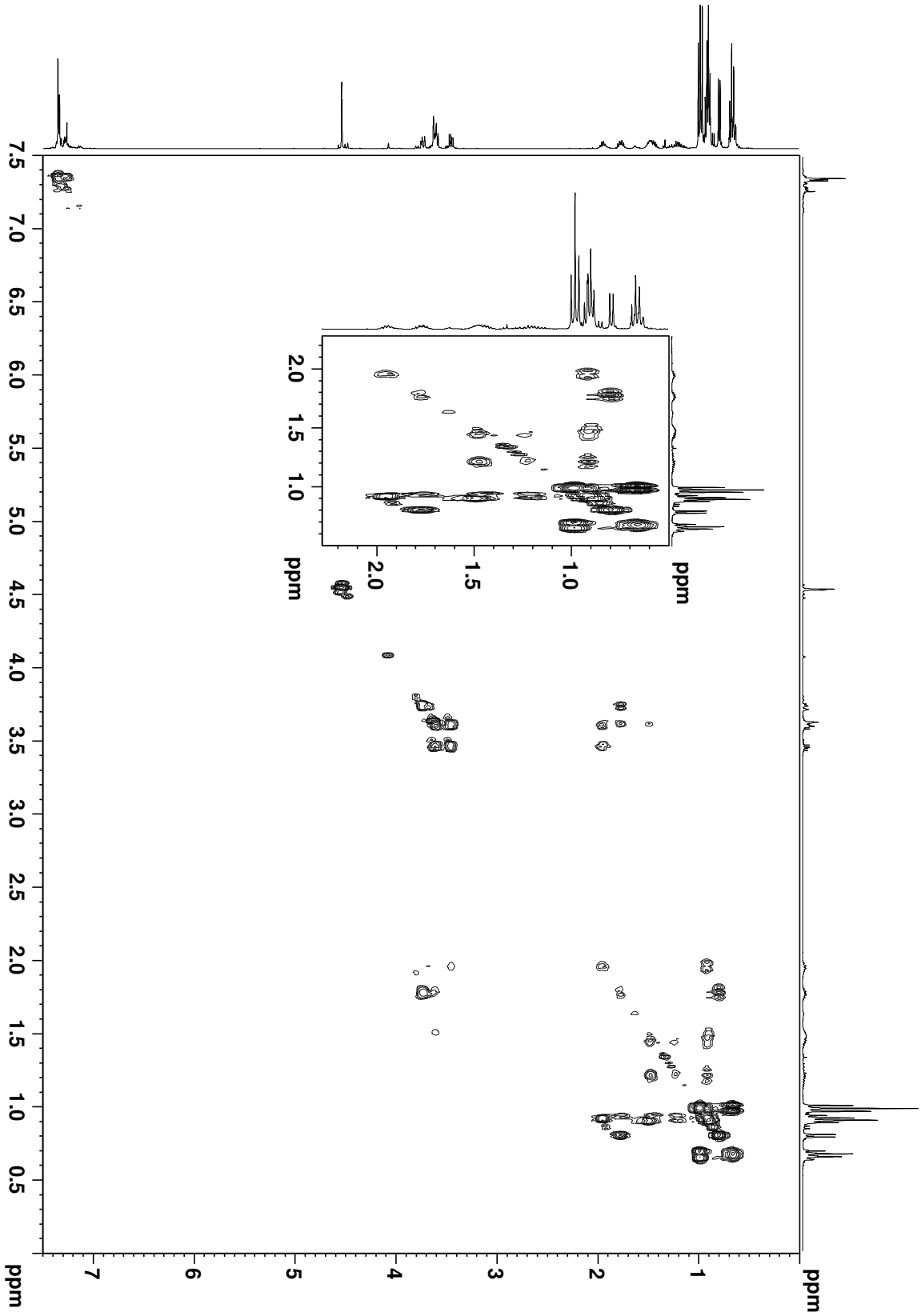

F.5 ^{1}H-^{13}C HSQC for 55, 400 MHz, $CDCl_3$

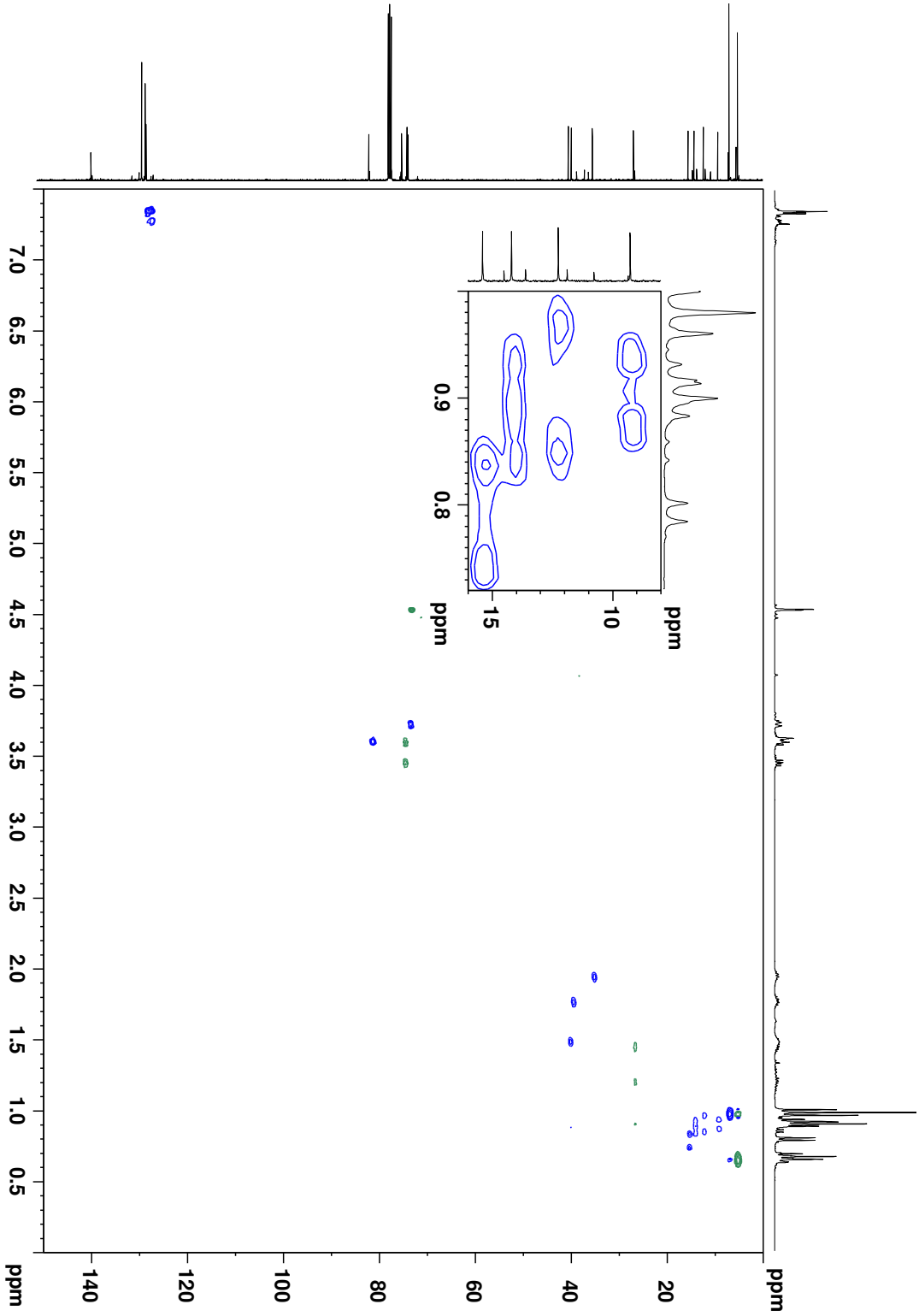

F.6 ^{1}H-^{13}C HMBC for 55, 400 MHz, $CDCl_3$

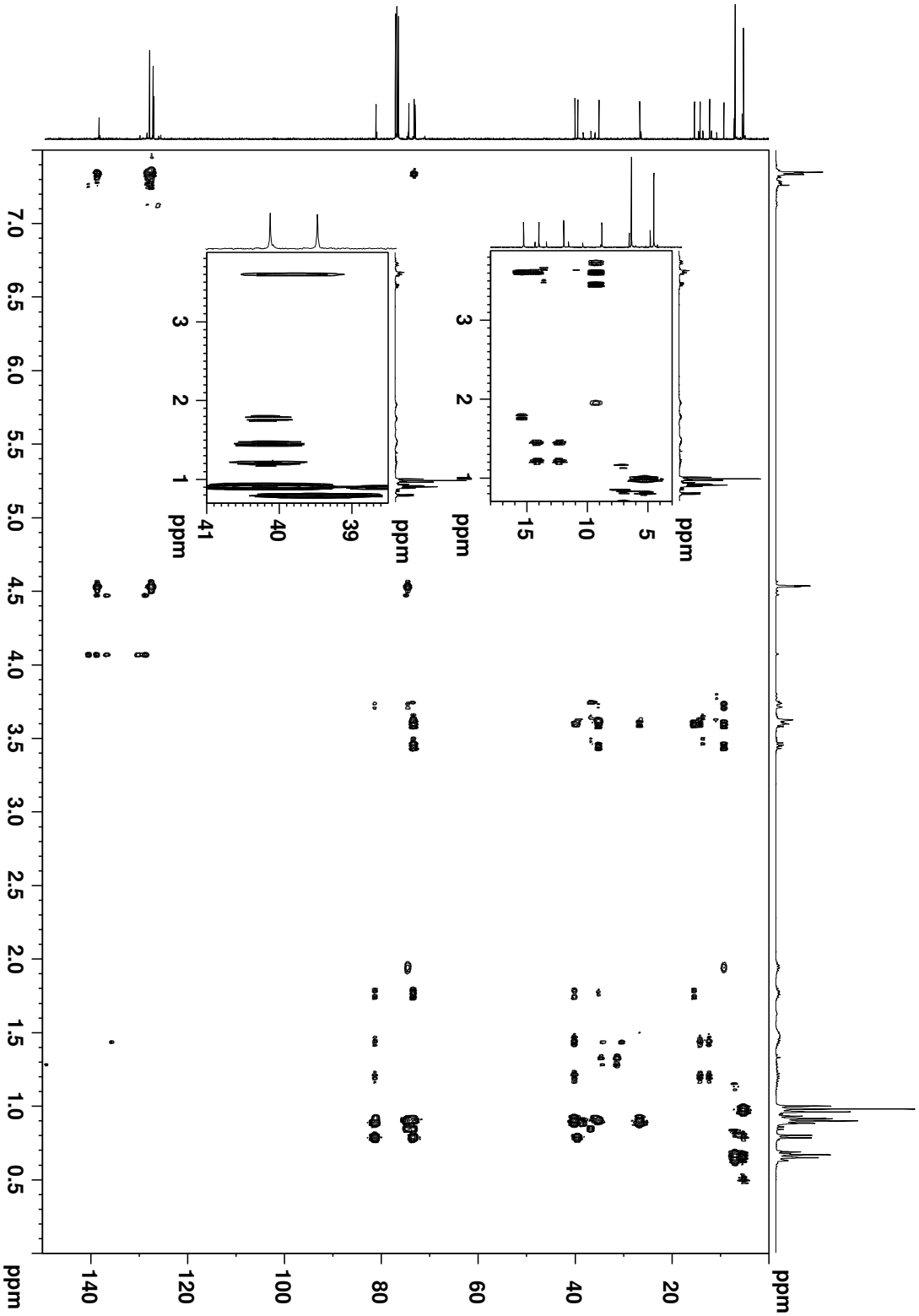

F.7 IR Spectrum of 55 (cm^{-1})

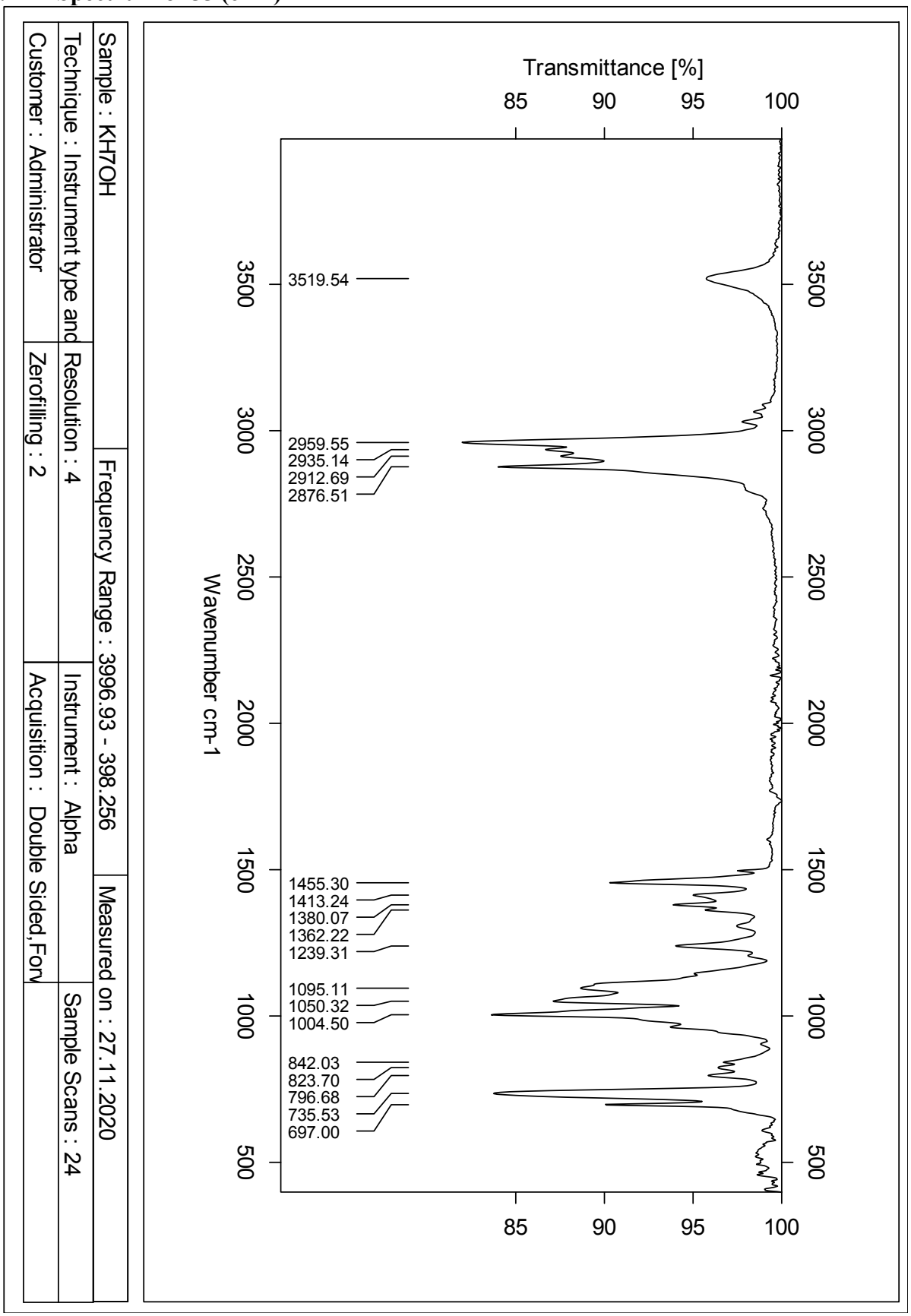

Elemental Composition Report

Single Mass Analysis

Tolerance = 3.0 PPM / DBE: min = -10.0, max = 50.0
Element prediction: Off
Number of isotope peaks used for i-FIT = 6

Monoisotopic Mass, Even Electron Ions
918 formula(e) evaluated with 2 results within limits (all results (up to 1000) for each mass)
Elements Used:
C: 0-100 H: 0-100 N: 0-3 O: 0-5 Na: 0-1 Si: 0-2

JA_20210218_57 79 (0.752) AM2 (Ar,35000.0,0.00,0.00); Cm (79:87)
1: TOF MS ES+

1.45e+006

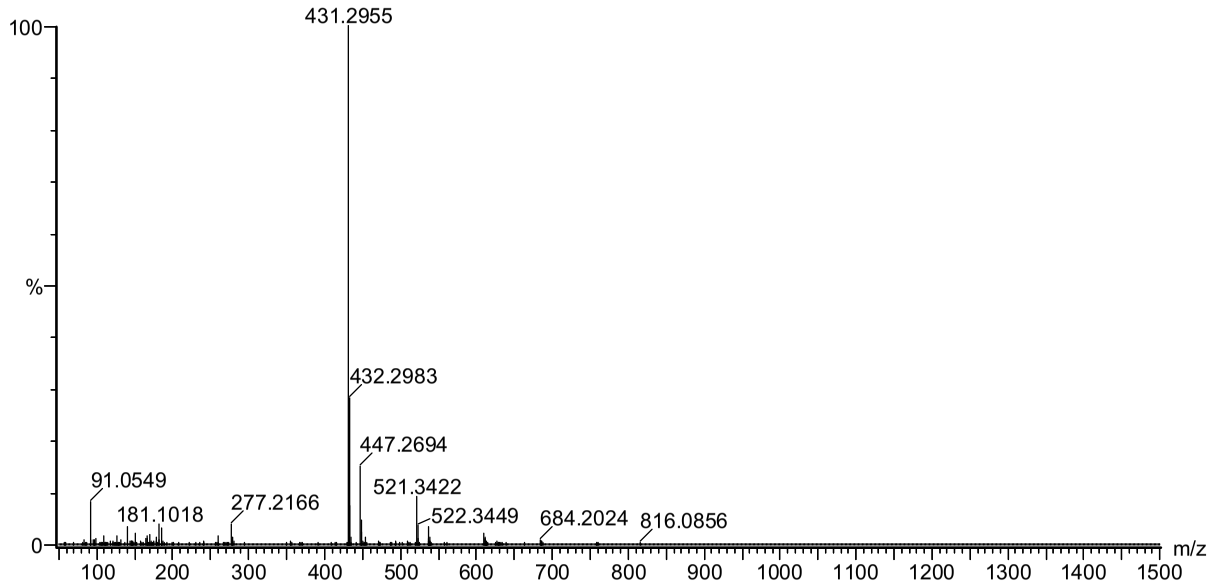

Minimum:				-10.0				
Maximum:		5.0	3.0	50.0				
Mass	Calc. Mass	mDa	PPM	DBE	i-FIT	Norm	Conf(%)	Formula
431.2955	431.2957	-0.2	-0.5	3.5	1897.9	0.000	100.00	C24 H44 O3 Na Si
	431.2950	0.5	1.2	11.5	1908.7	10.820	0.00	C30 H39 O2

G Mixture of *O*-((2*R*,4*S*,5*R*,6*S*)-1-(benzyloxy)-2,4,6-trimethyl-5-((triethylsilyl)oxy)octan-3-yl) *S*-methyl carbonodithioate (56a) and *O*-((3*S*,4*R*,5*R*,7*R*)-8-(benzyloxy)-3,5,7-trimethyl-6-((triethylsilyl)oxy)octan-4-yl) *S*-methyl carbonodithioate (56b)

G.1 ^{1}H-NMR Spectrum of the mixture of 56a and 56b, 400 MHz, $CDCl_3$

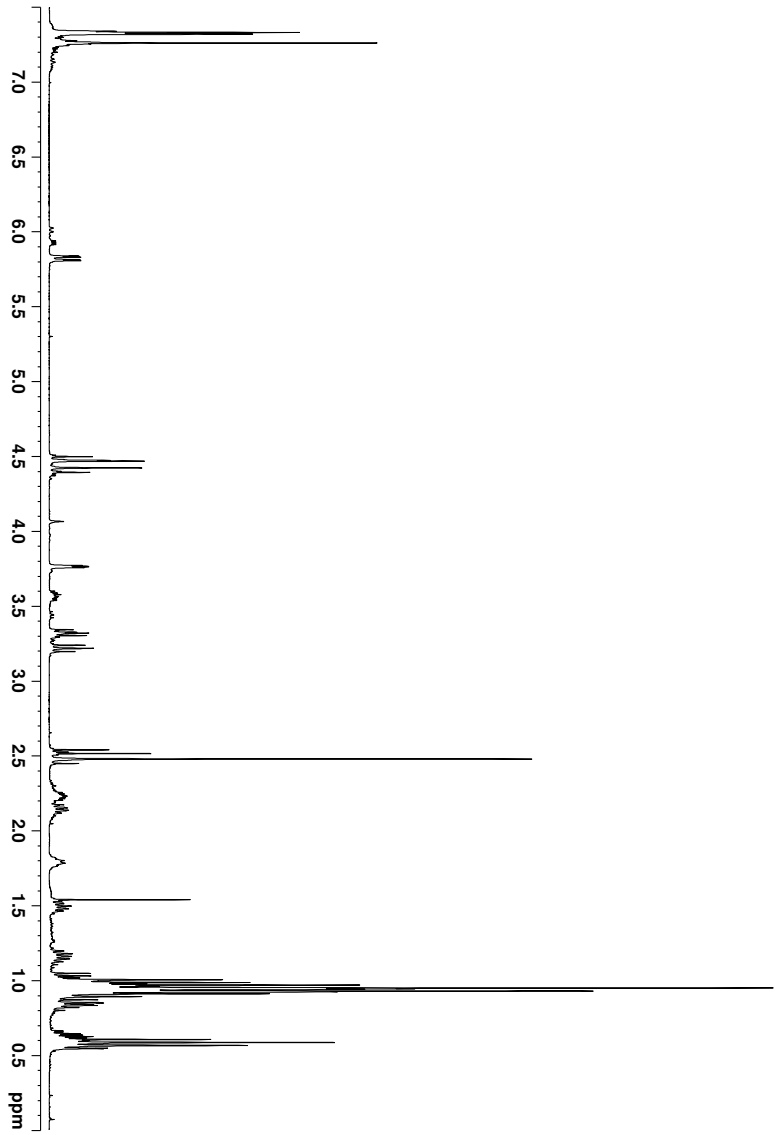

G.2 IR Spectrum of the mixture of 56a and 56b (cm^{-1})

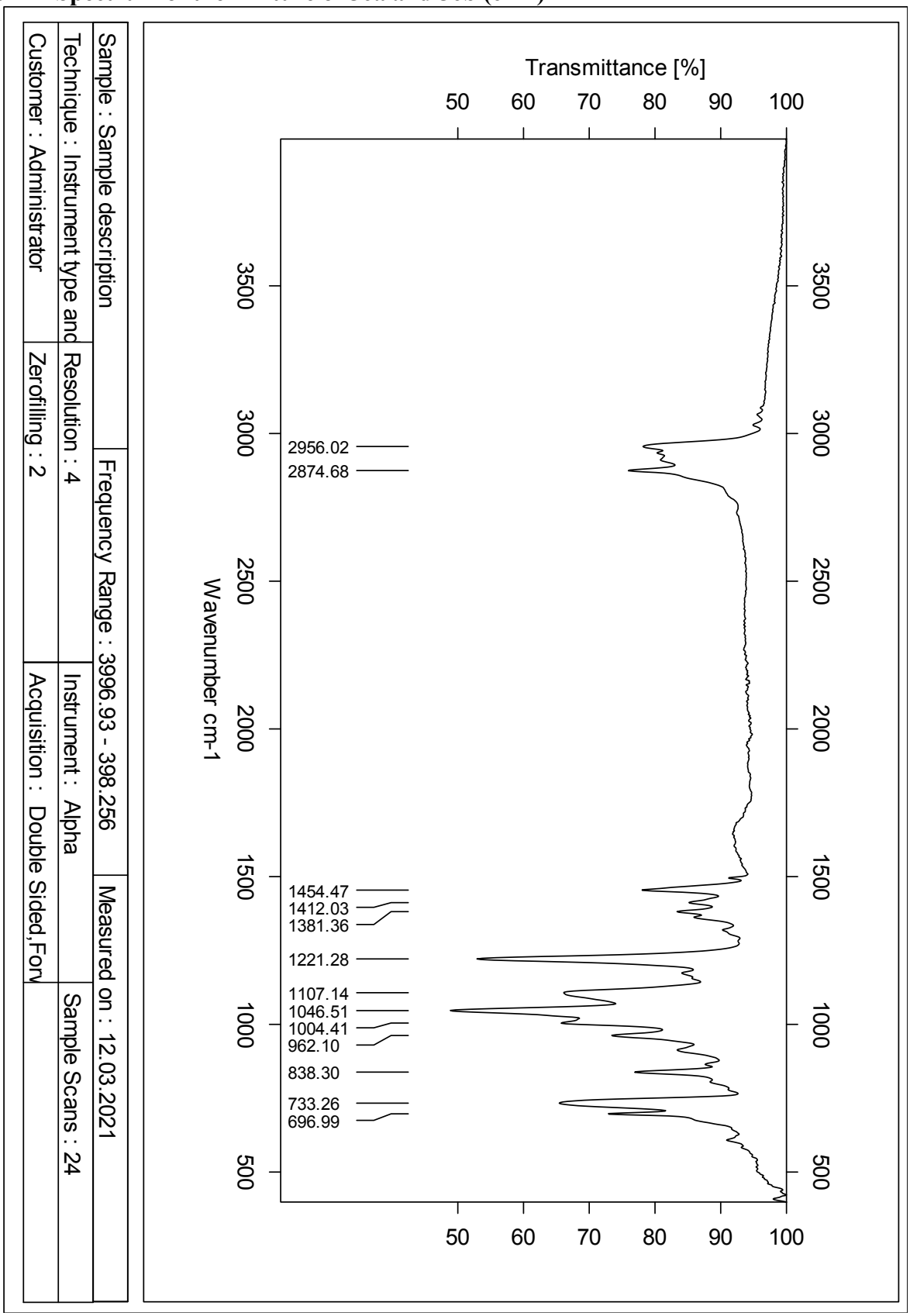

Elemental Composition Report

Single Mass Analysis

Tolerance = 2.0 PPM / DBE: min = -10.0, max = 50.0
Element prediction: Off
Number of isotope peaks used for i-FIT = 6

Monoisotopic Mass, Even Electron Ions
3854 formula(e) evaluated with 12 results within limits (all results (up to 1000) for each mass)
Elements Used:
C: 0-100 H: 0-100 O: 0-10 Na: 0-1 S: 0-3 I: 0-2 Si: 0-2

2021-83 46 (0.526) AM2 (Ar,35000.0,0.00,0.00); Cm (46:50)
1: TOF MS ES+

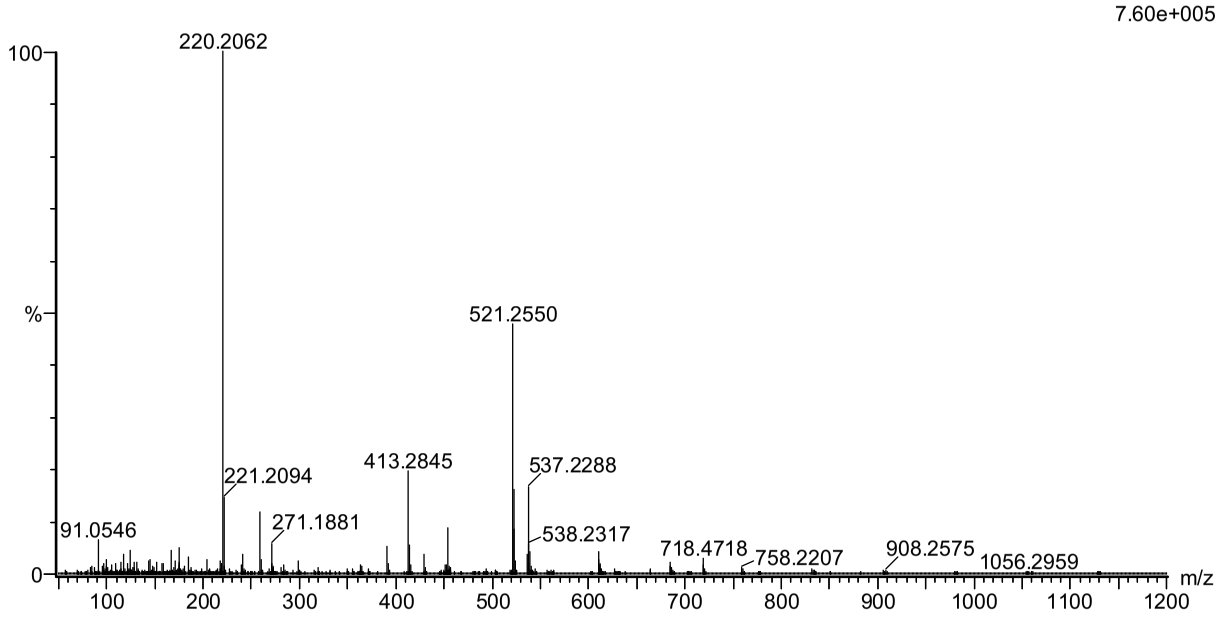

Minimum:				-10.0				
Maximum:		5.0	2.0	50.0				
Mass	Calc. Mass	mDa	PPM	DBE	i-FIT	Norm	Conf(%)	Formula
521.2550	521.2555	-0.5	-1.0	4.5	1499.2	0.096	90.85	C26 H46 O3 Na S2 Si

H MS spectrum of the Mixture of 56a/56b and 57a/57b

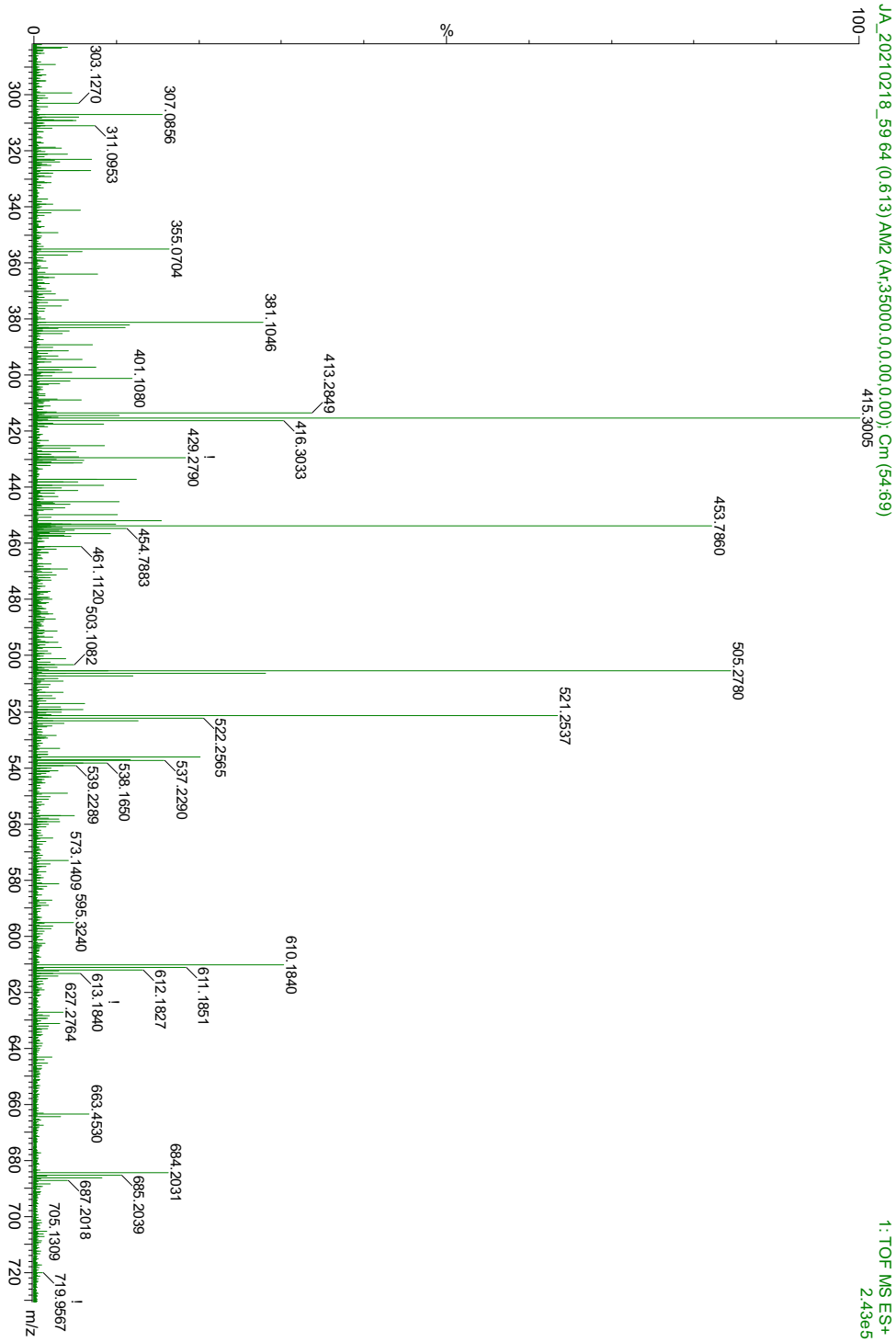

I (((3*S*,4*R*,5*S*,7*S*)-8-(benzyloxy)-3,5,7-trimethyloctan-4-yl)oxy)triethylsilane (57a)
I.1 ^{1}H-NMR for 57a, 600 MHz, $CDCl_3$ (ppm)

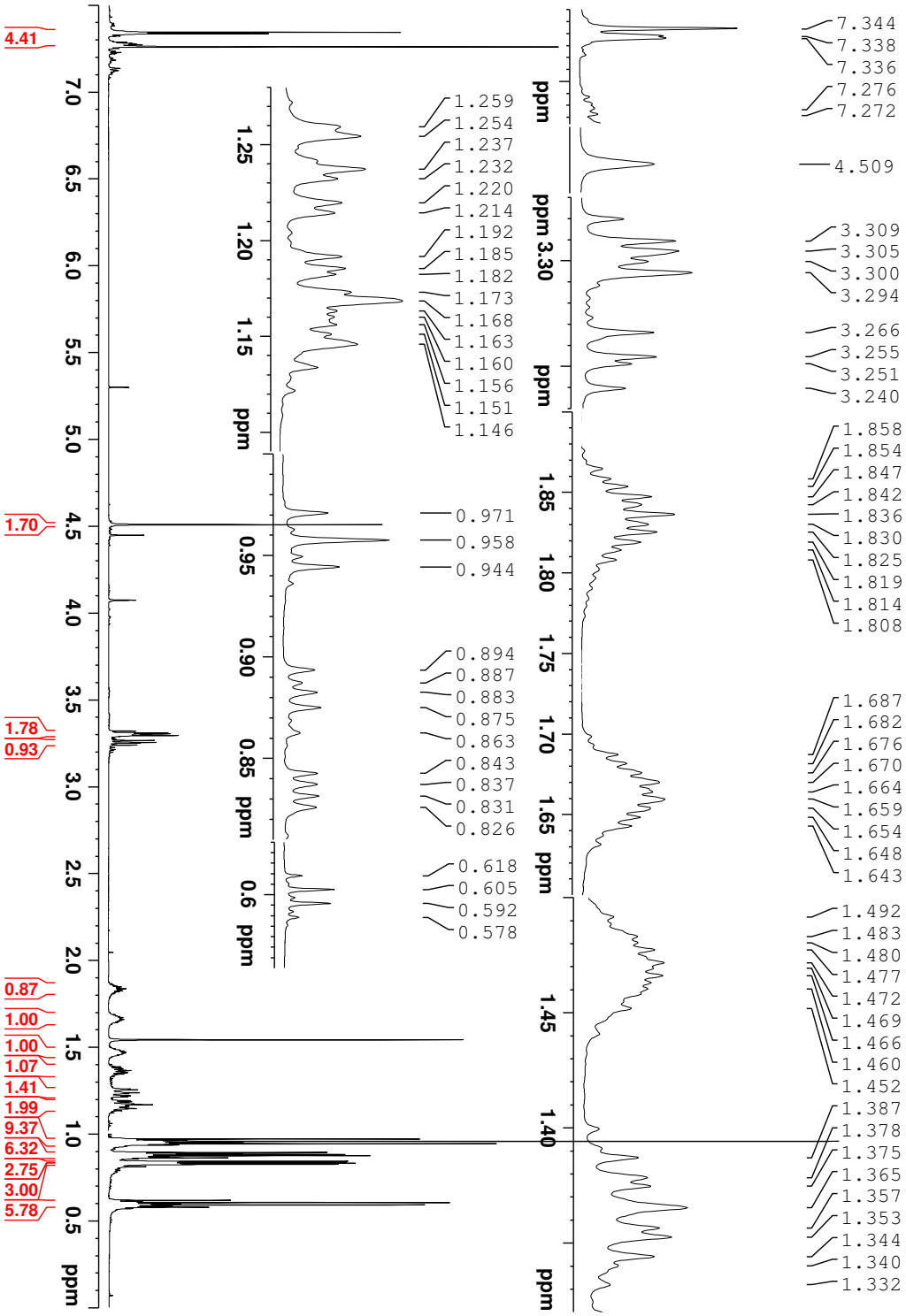

I.2 ^{1}H-NMR for 57a, 600 MHz, $CDCl_3$ (Hz)

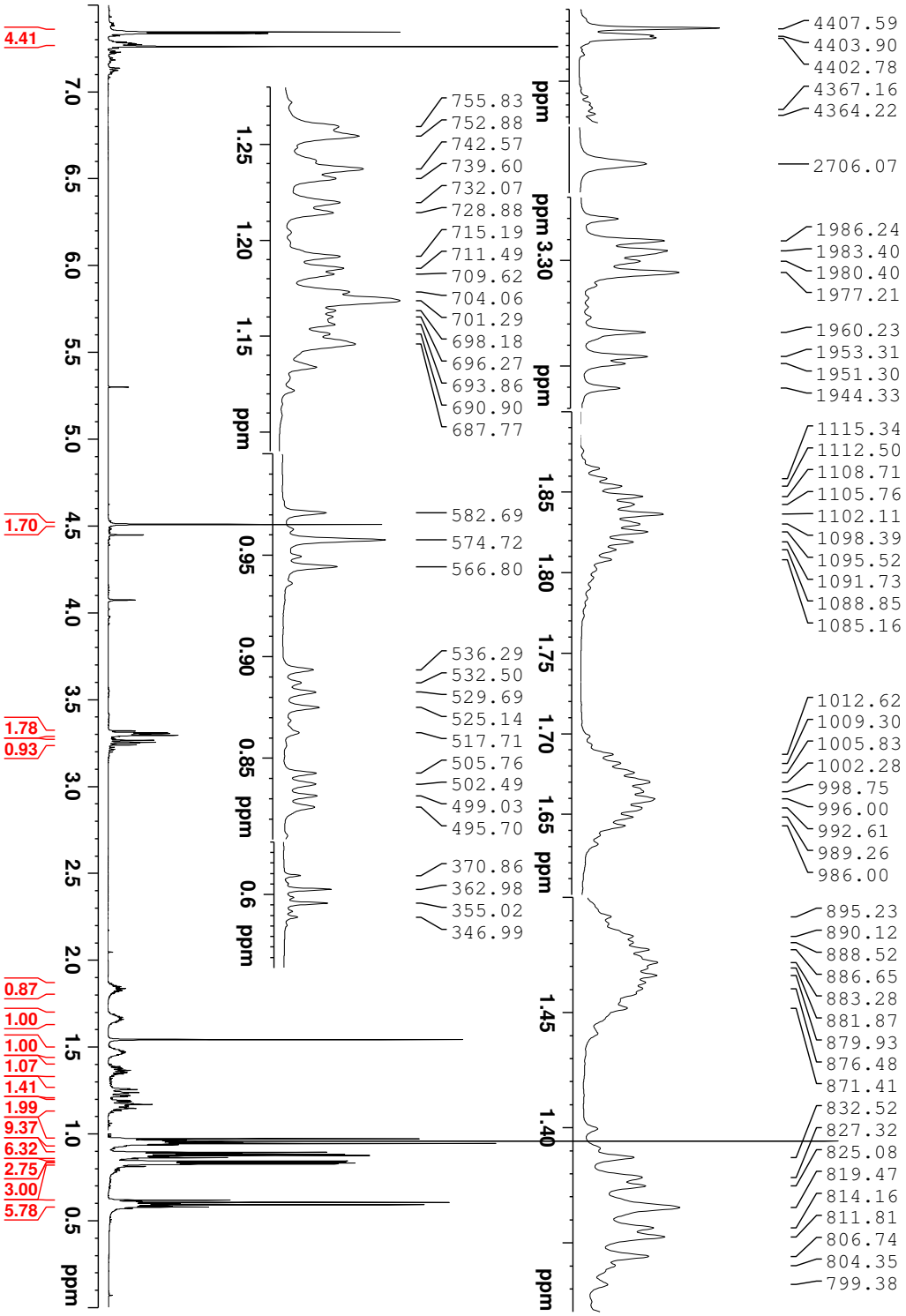

I.3 ^{13}C-NMR for 57a, 600 MHz, $CDCl_3$ (ppm)

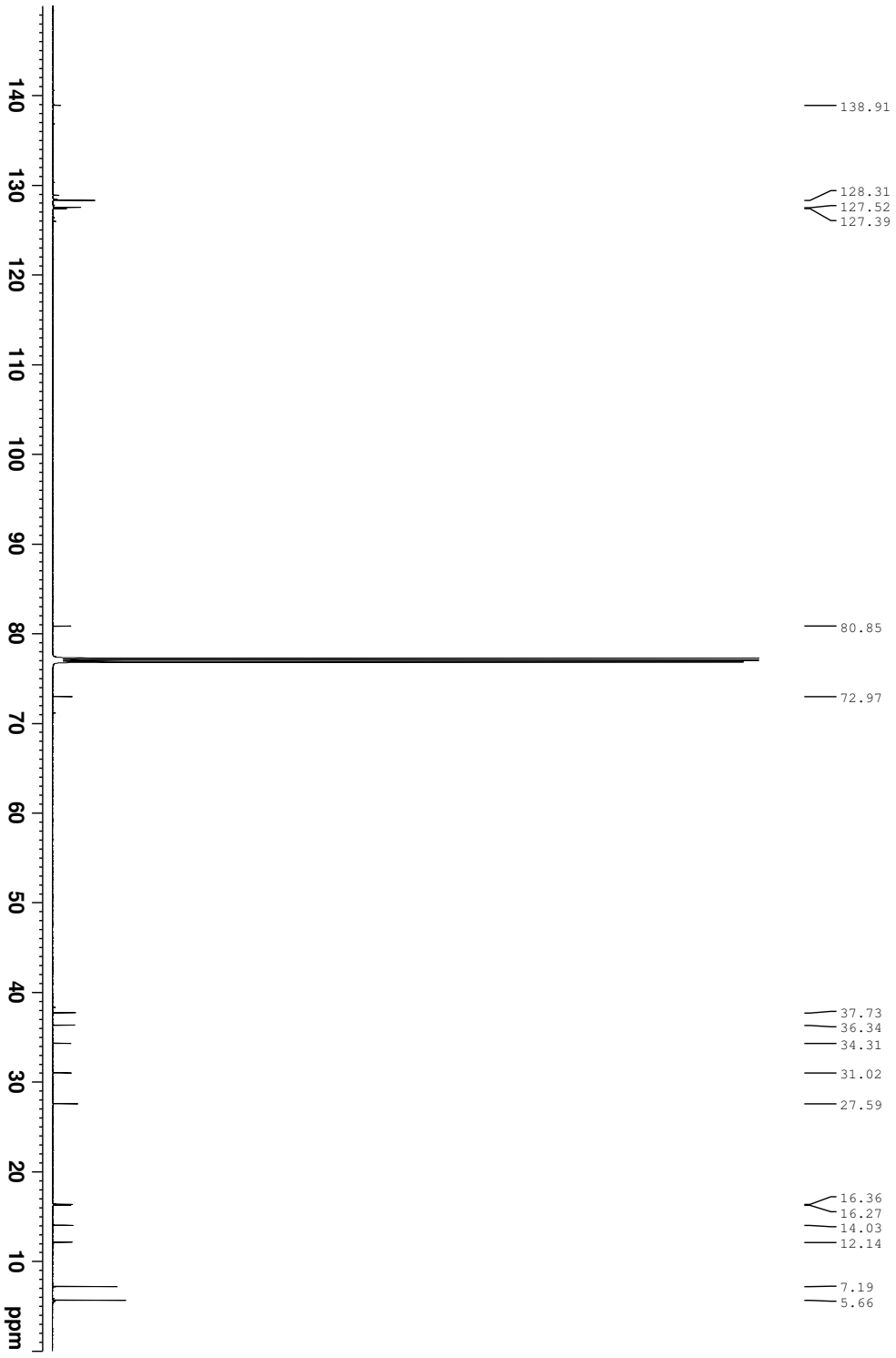

I.4 ^{1}H-^{1}H-COSY for 57a, 600 MHz, $CDCl_3$

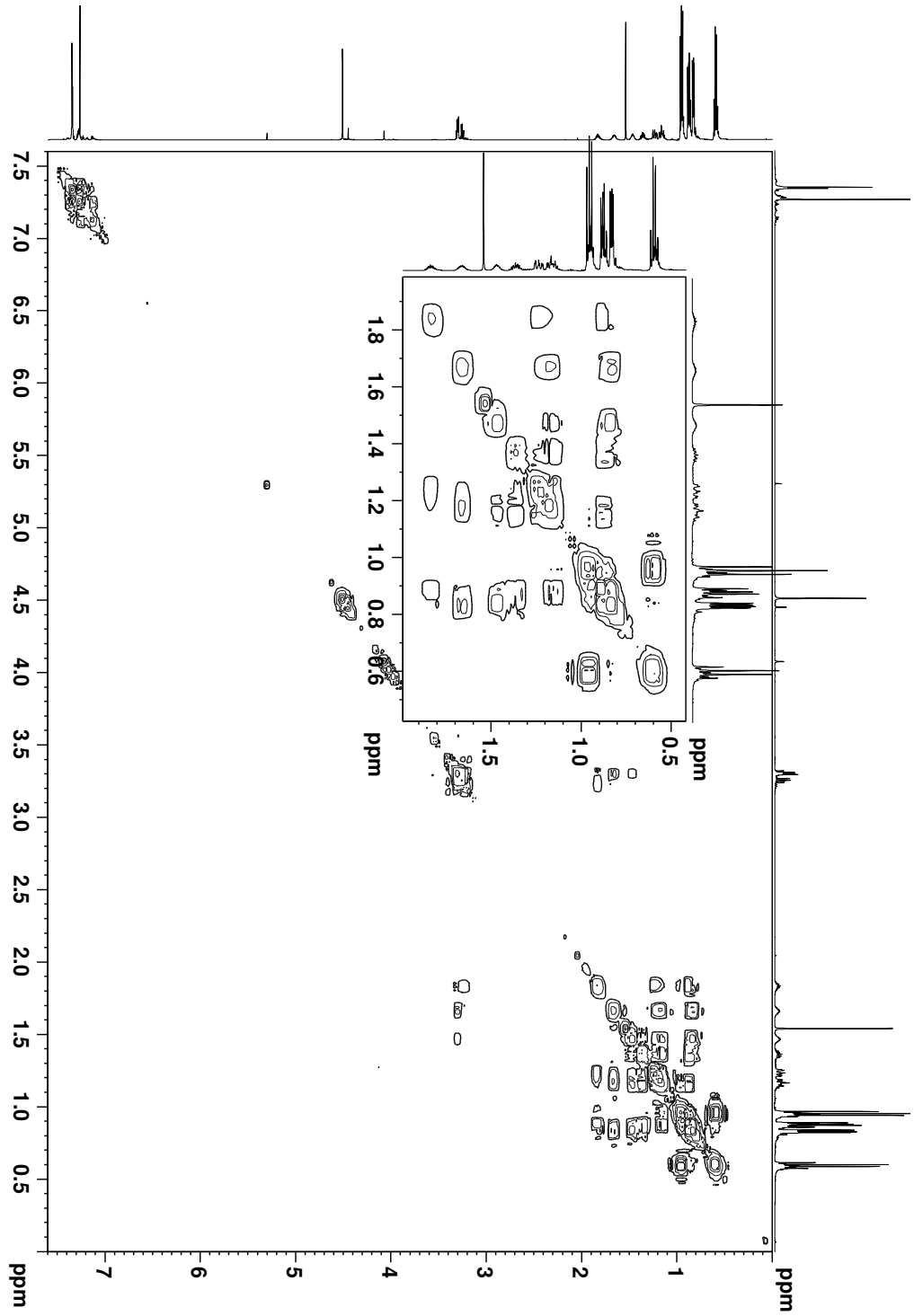

I.5 ^{1}H-^{13}C HSQC for 57a, 600 MHz, $CDCl_3$

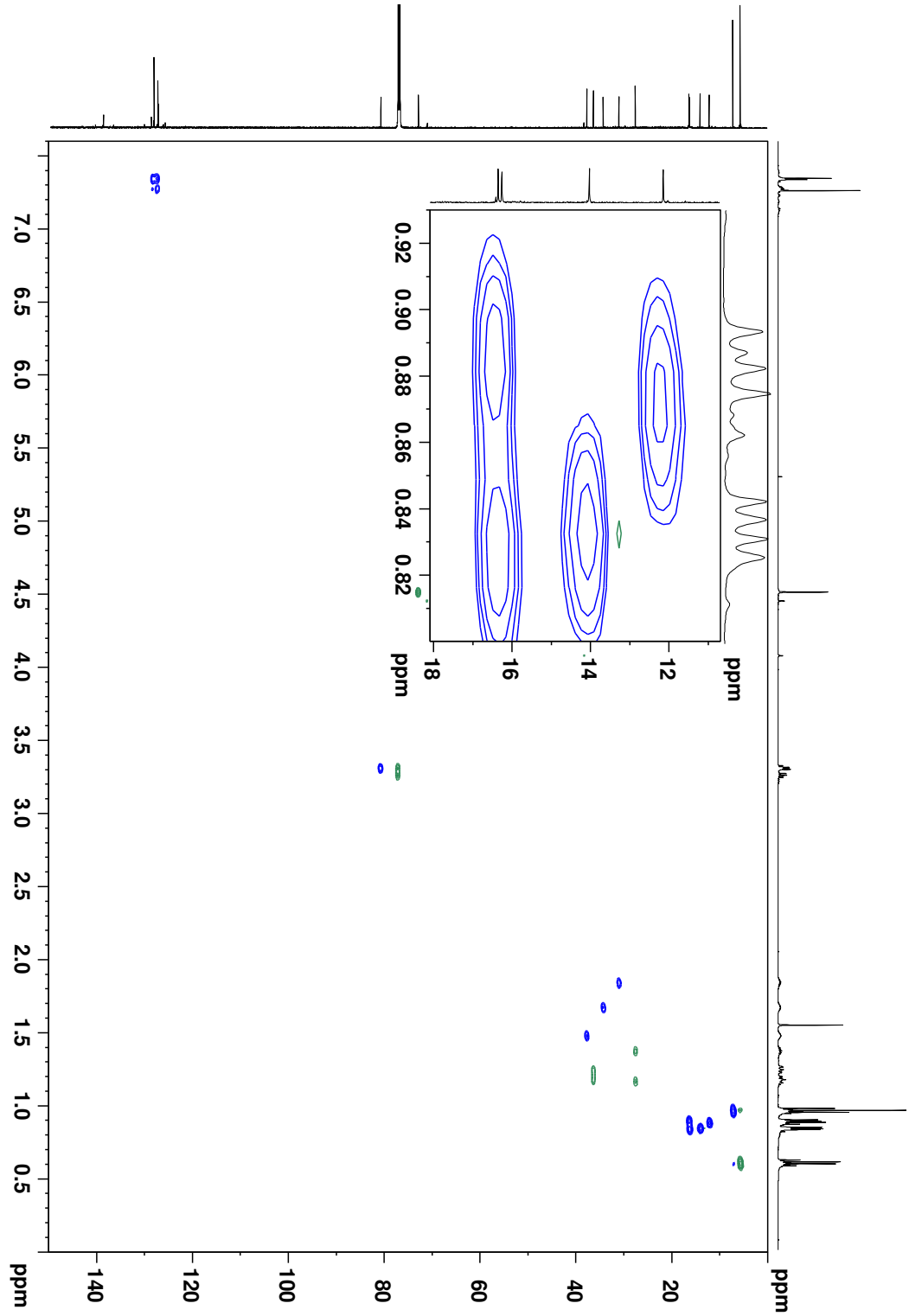

I.6 ^{1}H-^{13}C HMBC for 57a, 600 MHz, $CDCl_3$

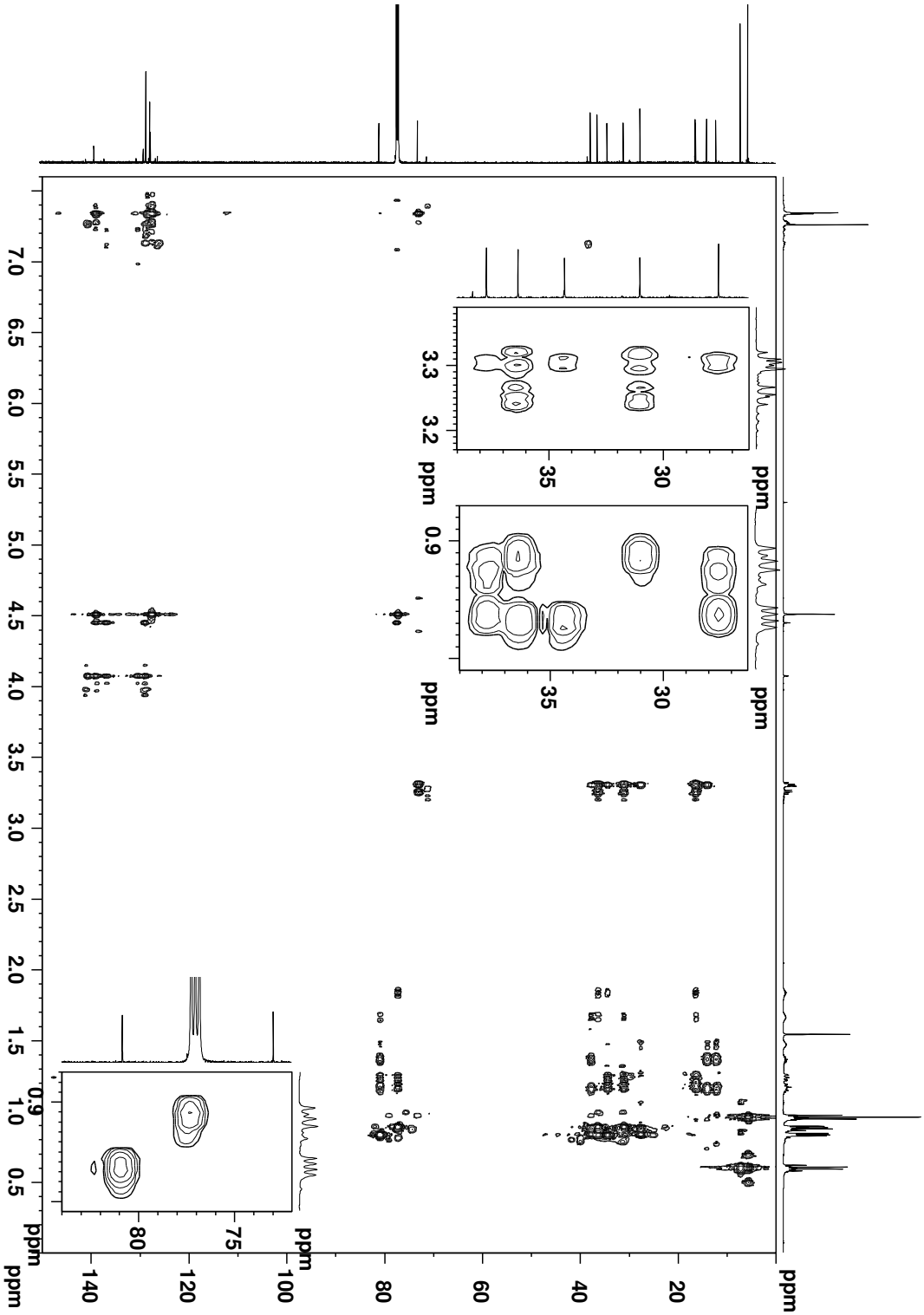

I.7 IR Spectrum of 57a (cm^{-1})

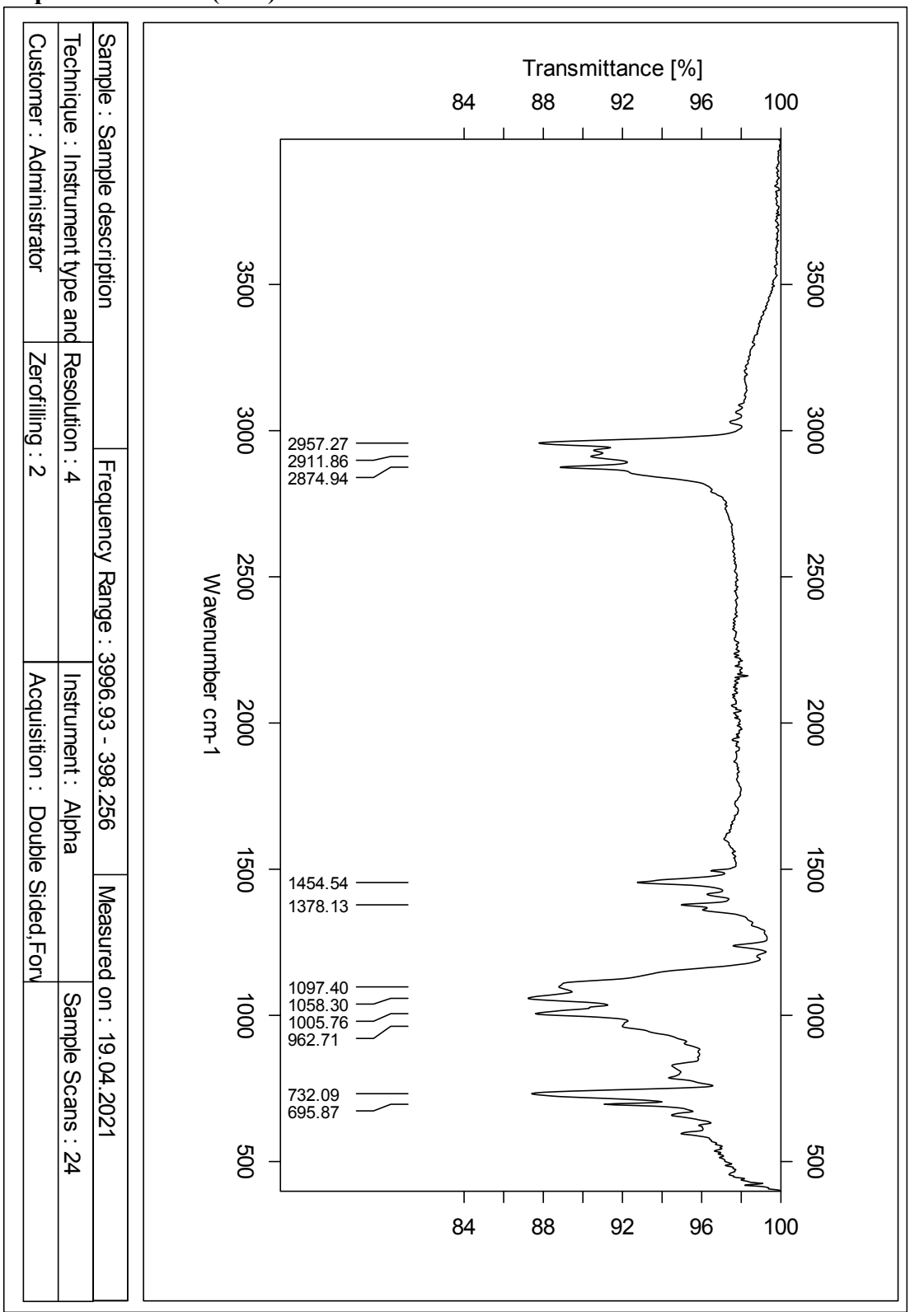

Elemental Composition Report

Single Mass Analysis

Tolerance = 2.0 PPM / DBE: min = -10.0, max = 50.0
Element prediction: Off
Number of isotope peaks used for i-FIT = 6

Monoisotopic Mass, Even Electron Ions
1512 formula(e) evaluated with 1 results within limits (all results (up to 1000) for each mass)
Elements Used:
C: 0-100 H: 0-100 N: 0-5 O: 0-6 Na: 0-1 Si: 0-2

2021-236 56 (0.535) AM2 (Ar,35000.0,0.00,0.00); Cm (51:56)
1: TOF MS ES+

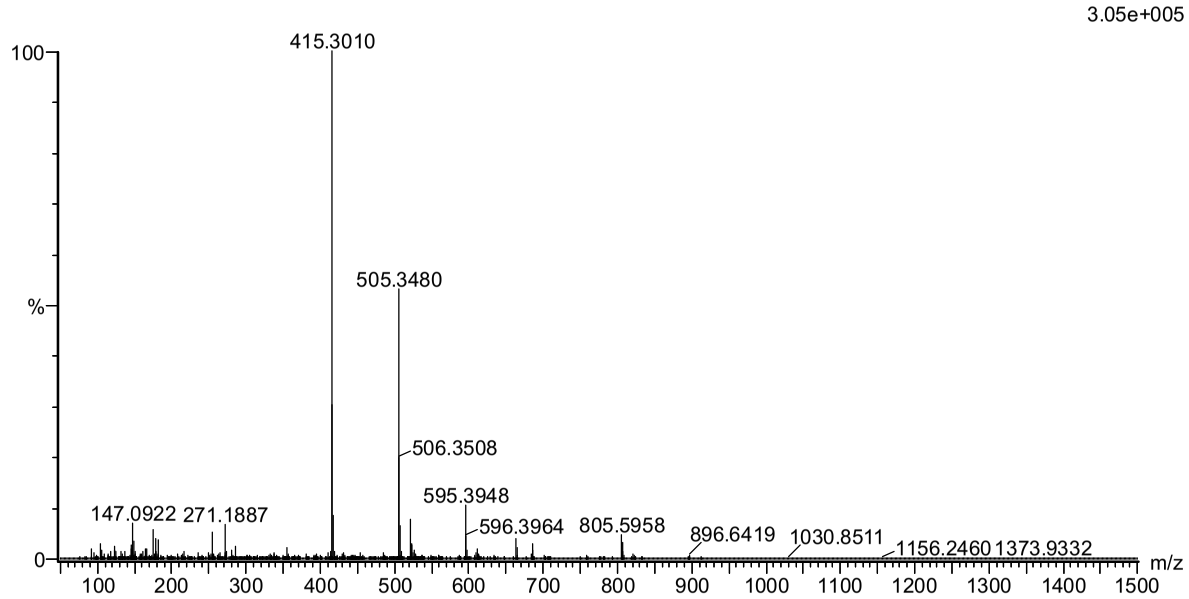

Minimum:				-10.0				
Maximum:		5.0	2.0	50.0				
Mass	Calc. Mass	mDa	PPM	DBE	i-FIT	Norm	Conf(%)	Formula
415.3010	415.3008	0.2	0.5	3.5	1666.3	n/a	n/a	C24 H44 O2 Na Si

I.8 MS Spectrum of 57a

J (((2*R*,4*R*,6*S*)-1-(benzyloxy)-2,4,6-trimethyloctan-3-yl)oxy)triethylsilane (57b)
J.1 ^{1}H-NMR for 57b, 600 MHz, $CDCl_3$ (ppm)

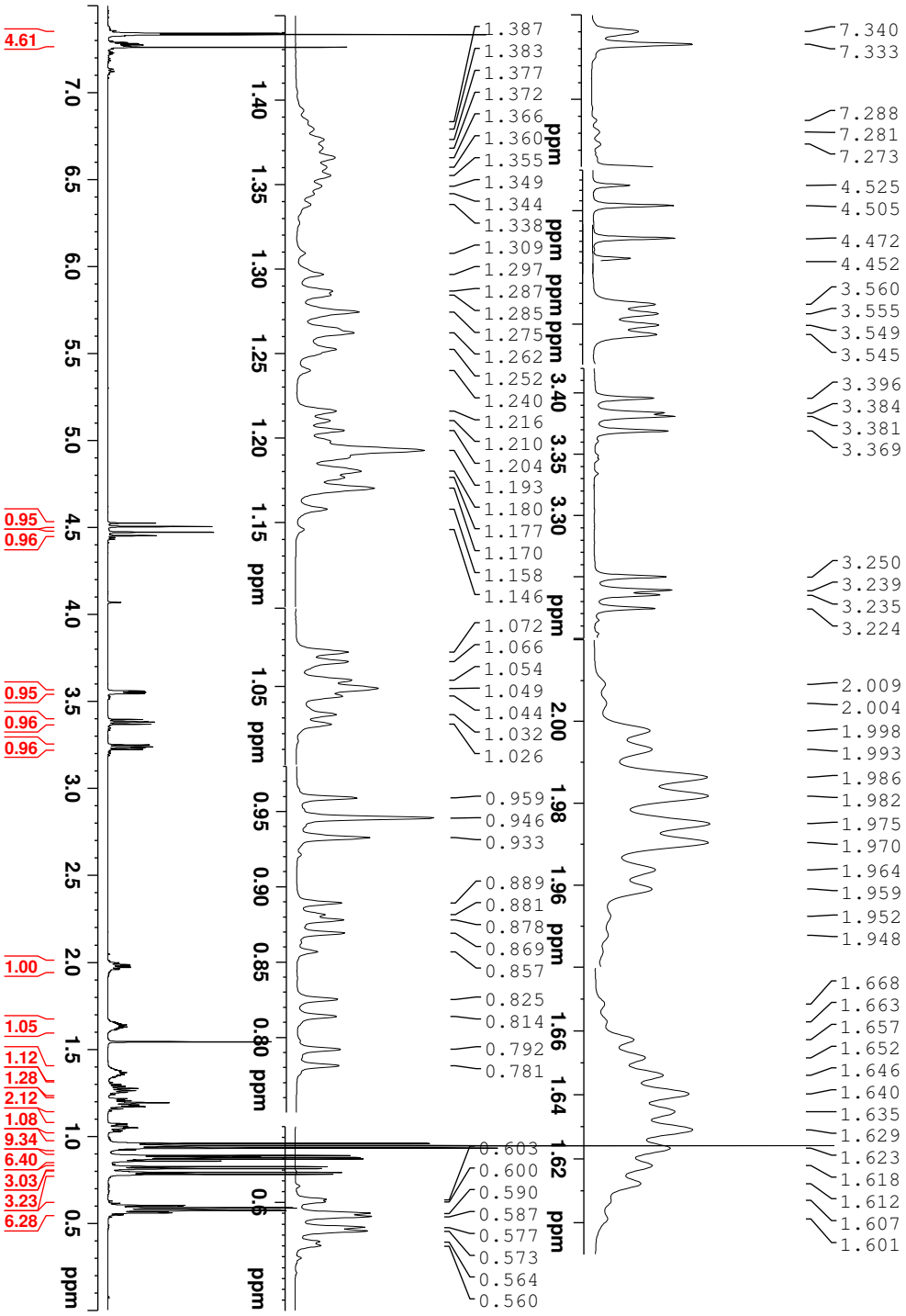

J.2 ^{1}H-NMR for 57b, 600 MHz, $CDCl_3$ (Hz)

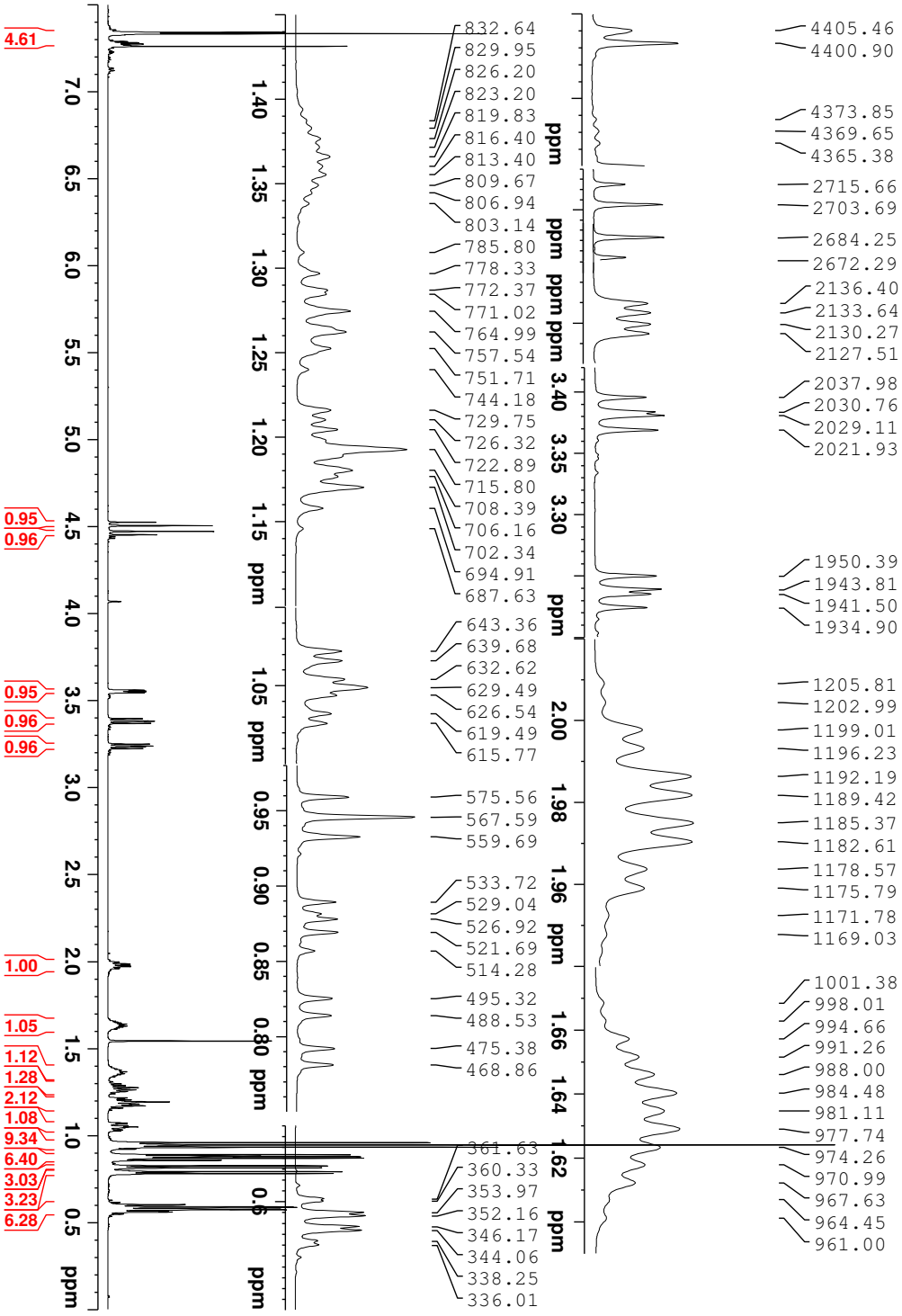

J.3 ^{13}C-NMR for 57b, 600 MHz, $CDCl_3$ (ppm)

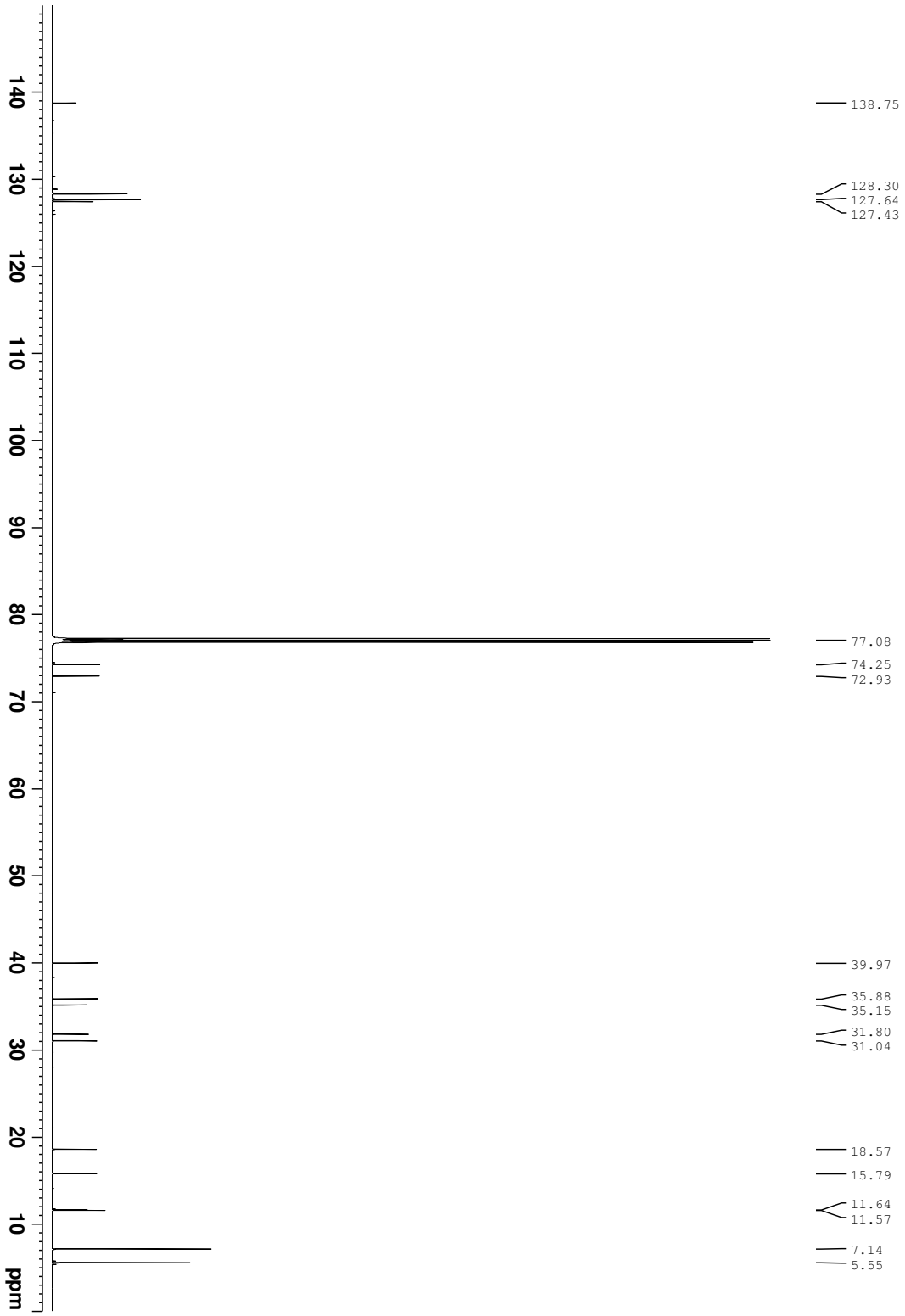

J.4 ^{1}H-^{1}H-COSY for 57b, 600 MHz, $CDCl_3$

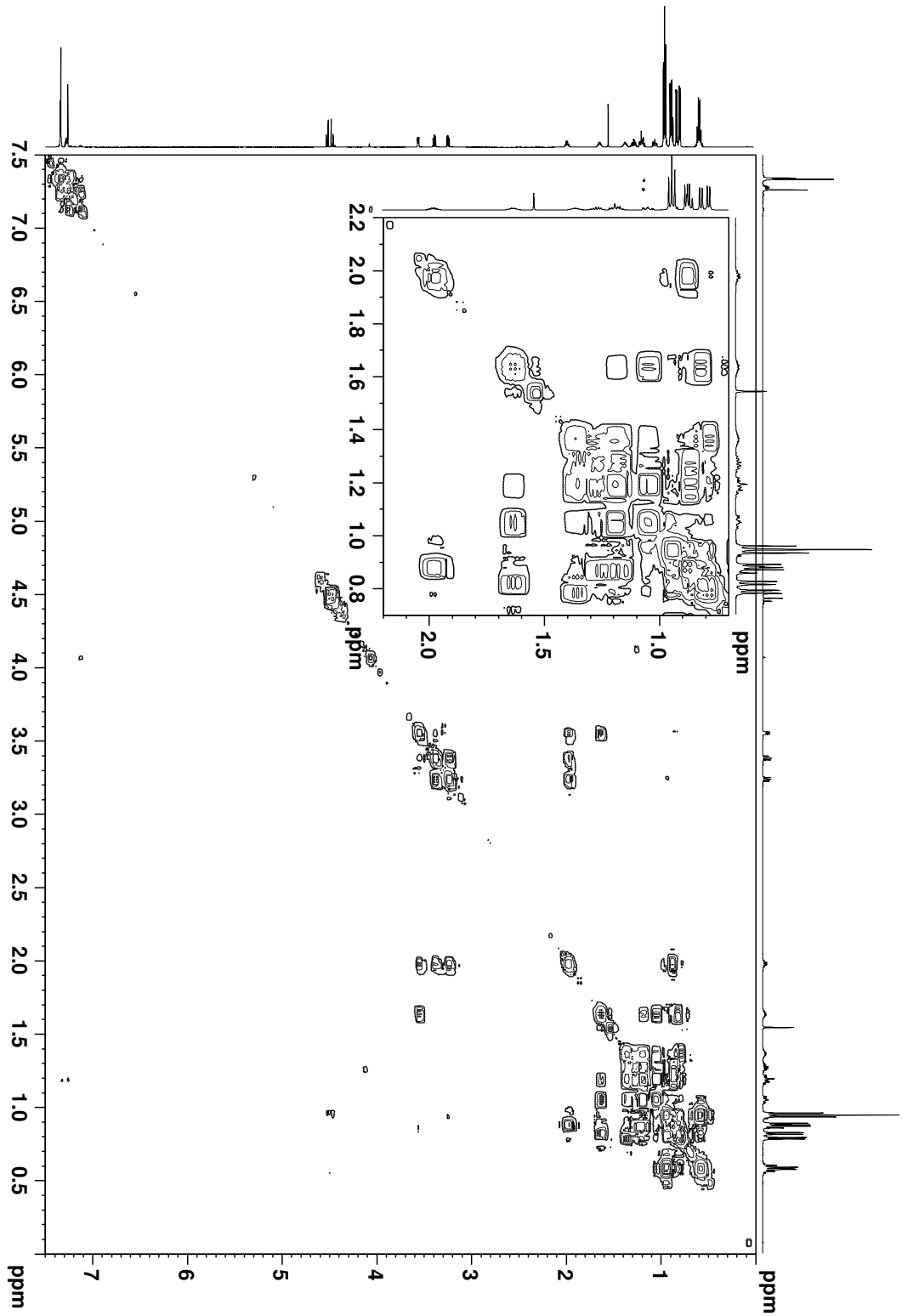

J.5 ^{1}H-^{13}C HSQC for 57b, 600 MHz, $CDCl_3$

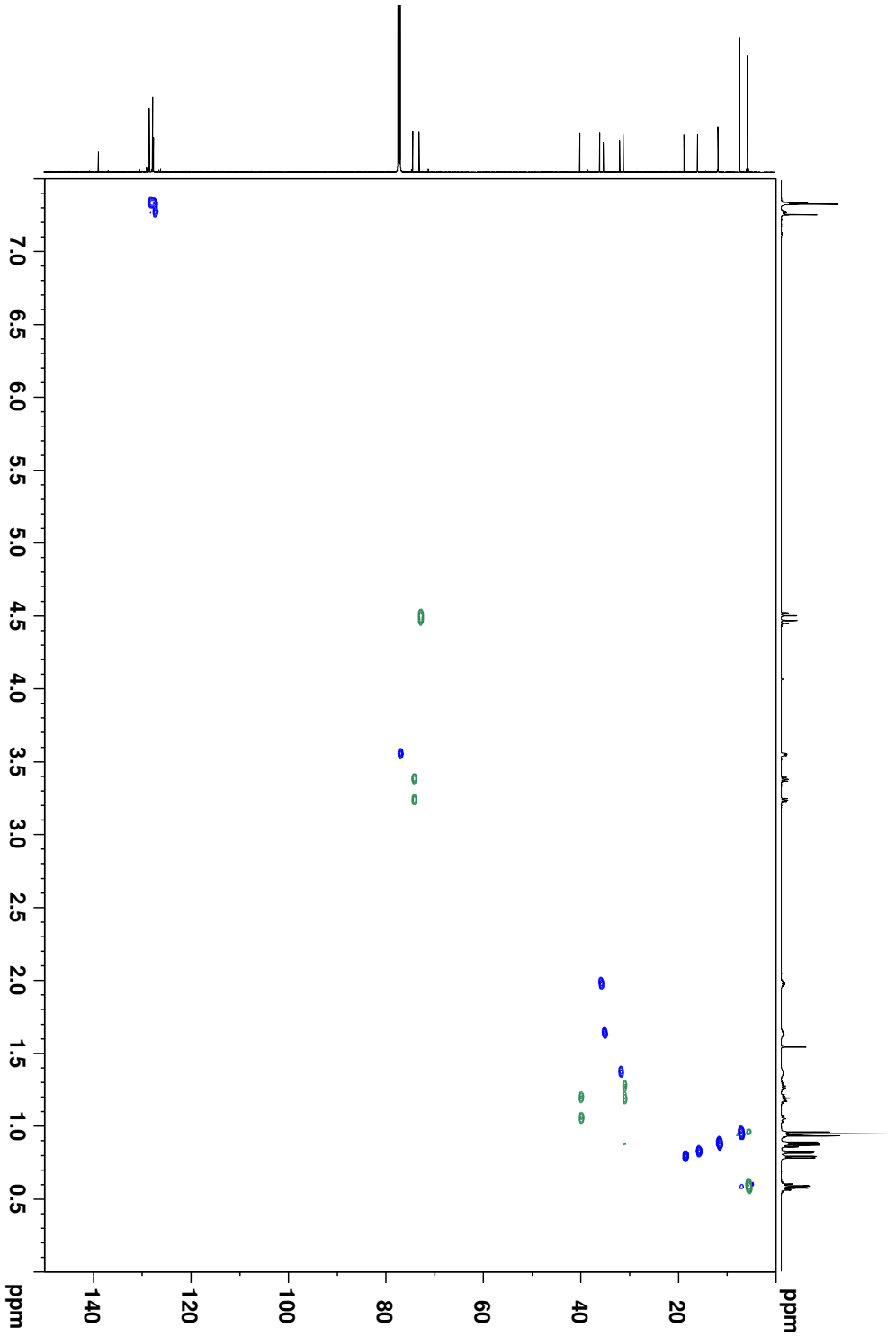

J.6 ^{1}H-^{13}C HMBC for 57b, 600 MHz, $CDCl_3$

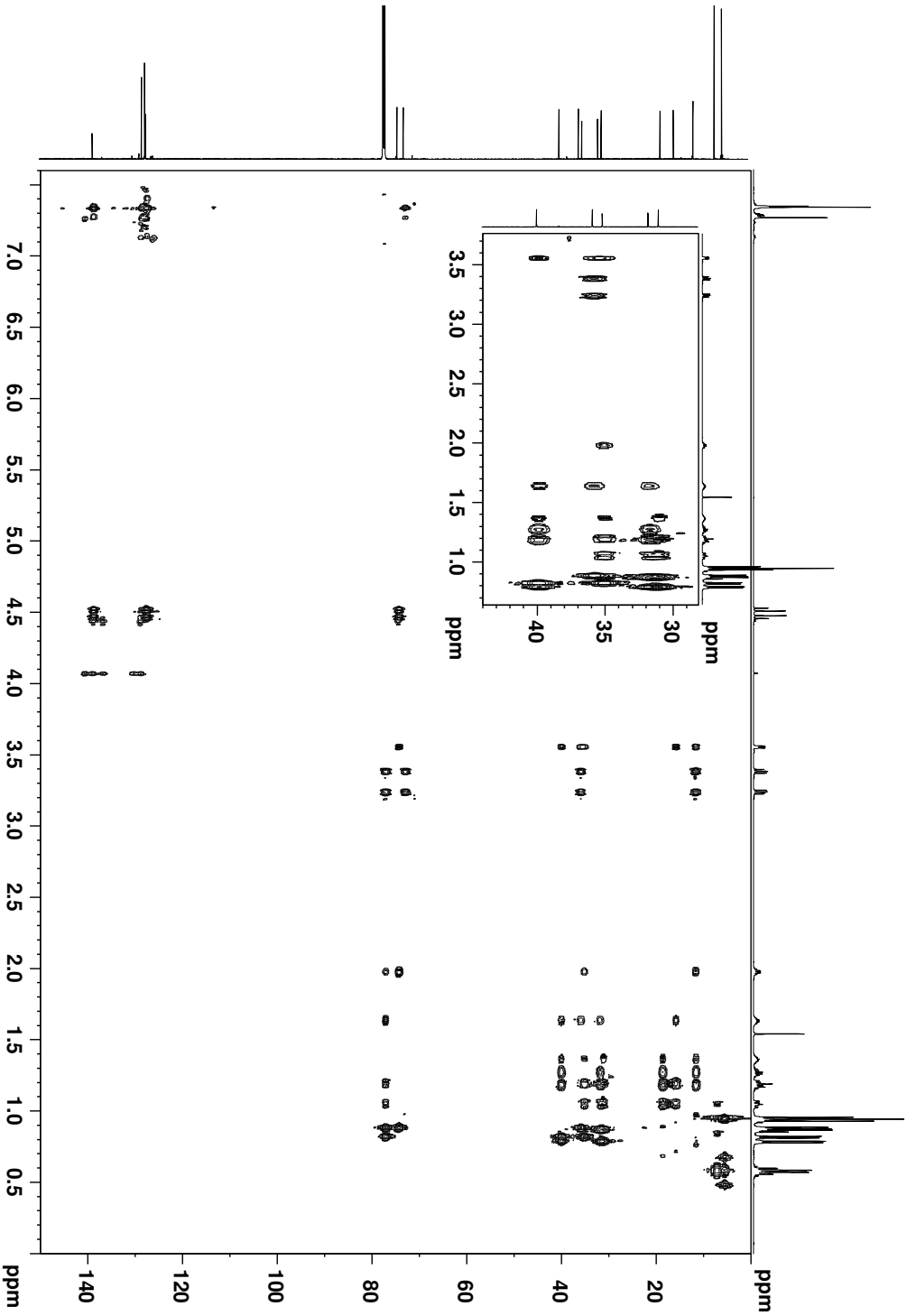

J.7 IR Spectrum of 57b (cm^{-1})

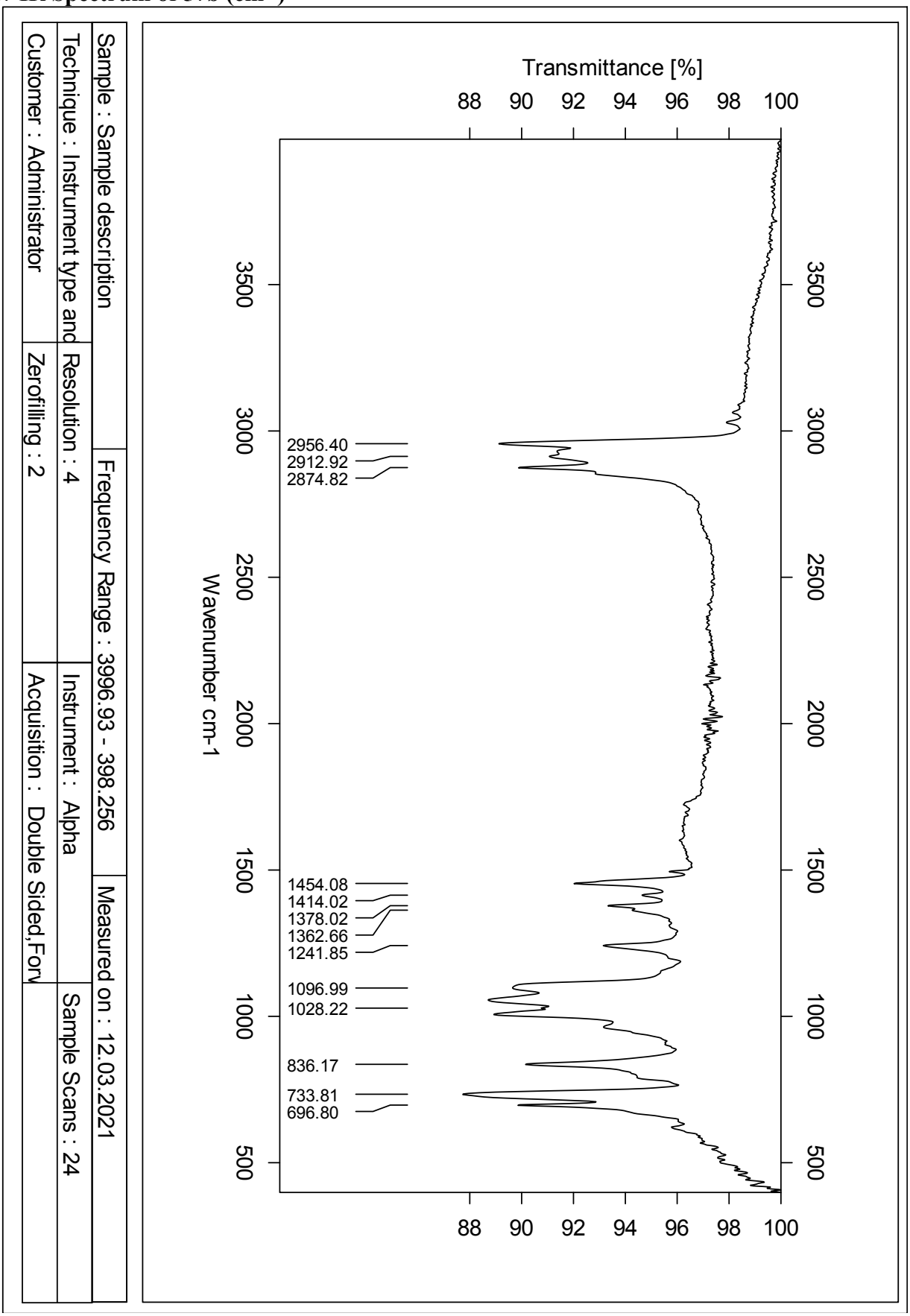

Elemental Composition Report

Single Mass Analysis

Tolerance = 2.0 PPM / DBE: min = -10.0, max = 50.0
Element prediction: Off
Number of isotope peaks used for i-FIT = 6

Monoisotopic Mass, Even Electron Ions
450 formula(e) evaluated with 1 results within limits (all results (up to 1000) for each mass)
Elements Used:
C: 0-100 H: 0-100 O: 0-12 Na: 0-1 Si: 0-2
2021_268 58 (0.552) AM2 (Ar,35000.0,0.00,0.00); Cm (58)
1: TOF MS ES+

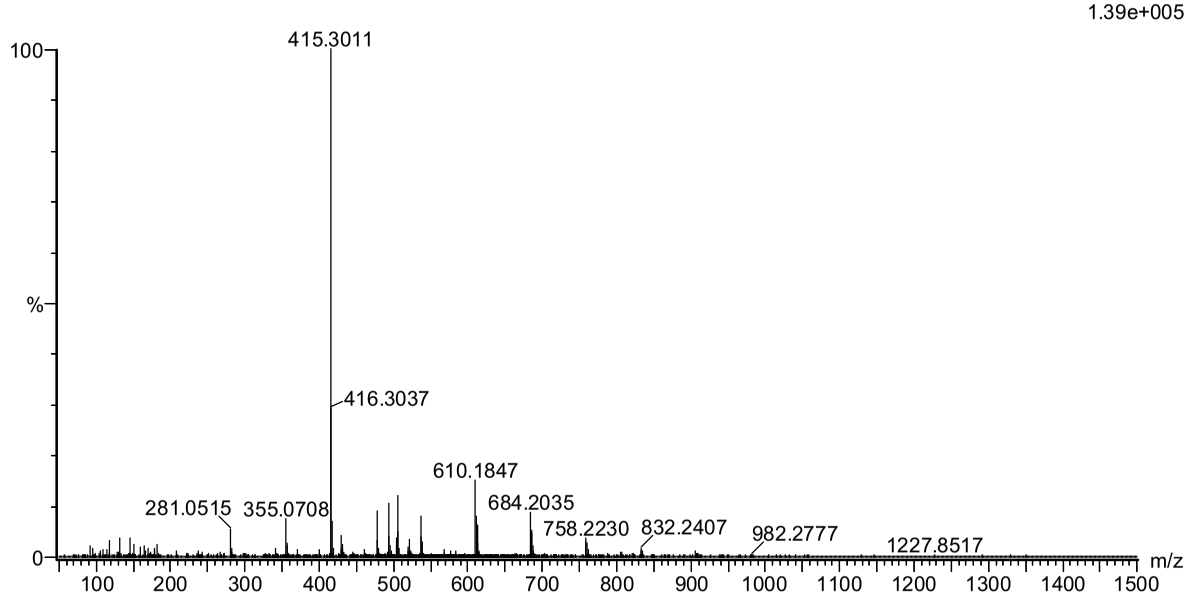

Minimum:				-10.0				
Maximum:		5.0	2.0	50.0				
Mass	Calc. Mass	mDa	PPM	DBE	i-FIT	Norm	Conf(%)	Formula
415.3011	415.3008	0.3	0.7	3.5	1455.9	n/a	n/a	C24 H44 O2 Na Si

J.8 MS Spectrum of 57b

K (2*S*,4*S*,5*R*,6*S*)-2,4,6-trimethyl-5-((triethylsilyl)oxy)octan-1-ol (58a)
K.1 ^{1}H-NMR for 58a, 600 MHz, $CDCl_3$ (ppm)

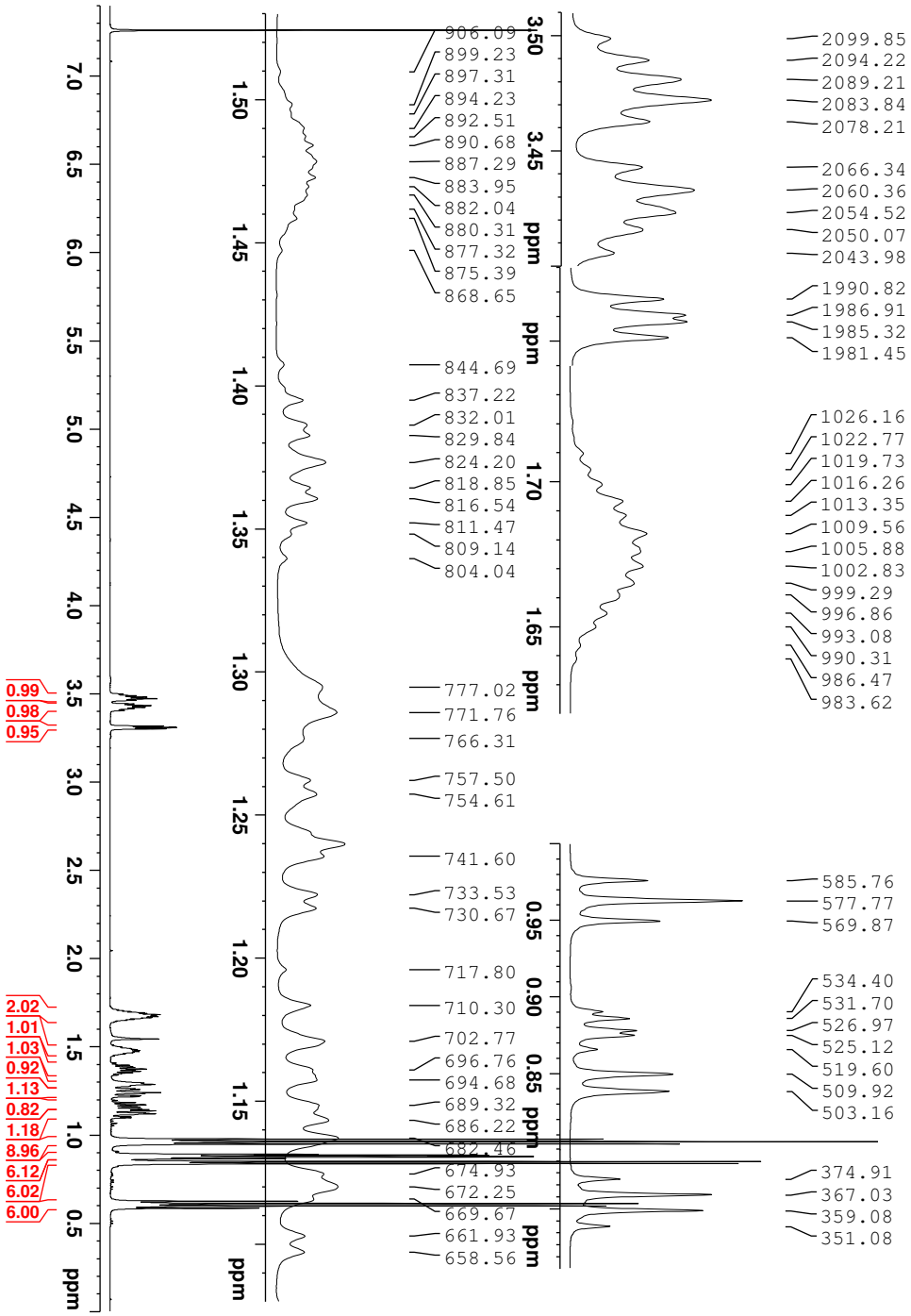

K.2 ^{1}H-NMR of 58a, 600 MHz, $CDCl_3$ (Hz)

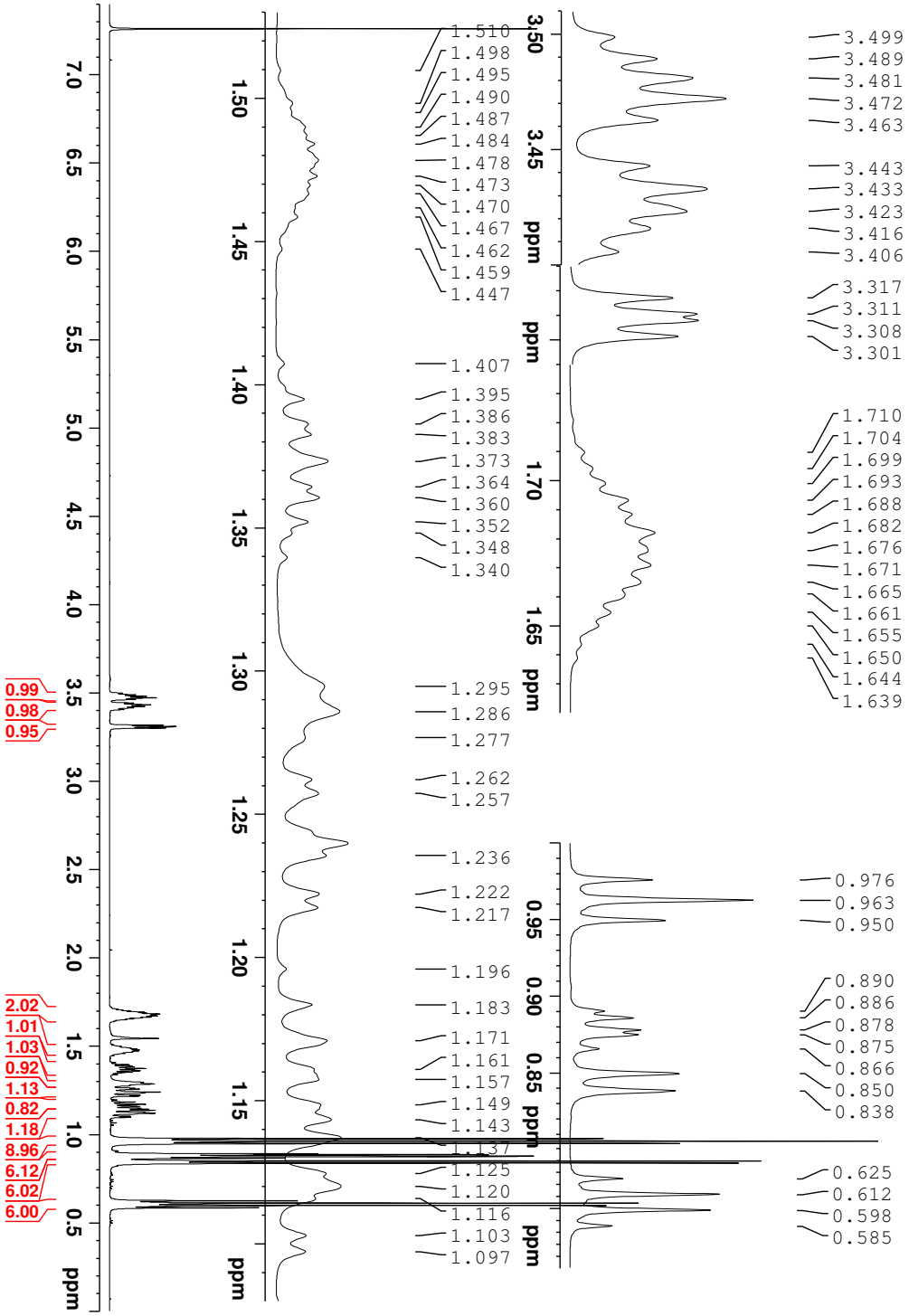

K.3 ^{13}C-NMR of 58a, 600 MHz, $CDCl_3$ (ppm)

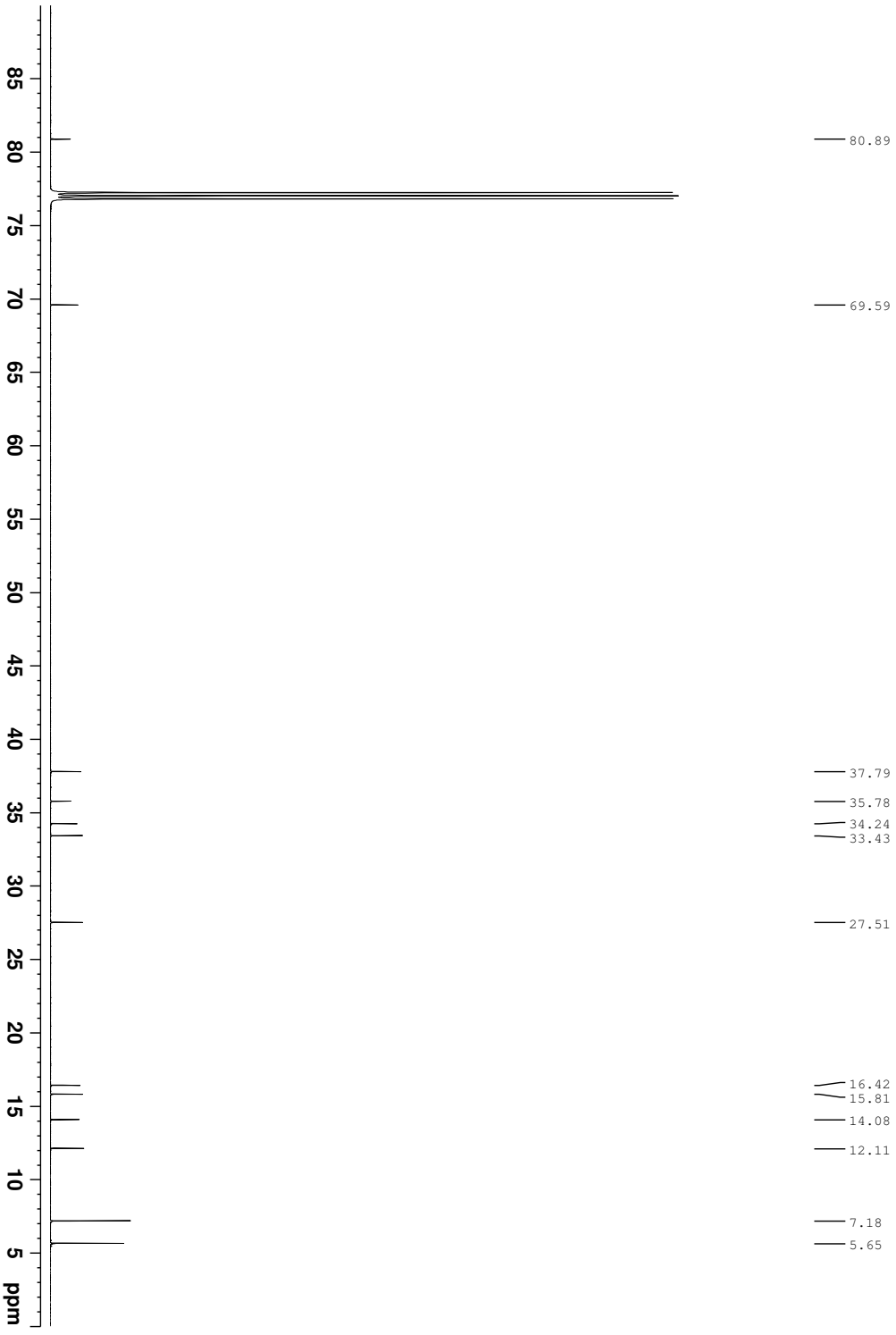

K.4 ^{1}H-^{1}H-COSY for 58a, 600 MHz, $CDCl_3$

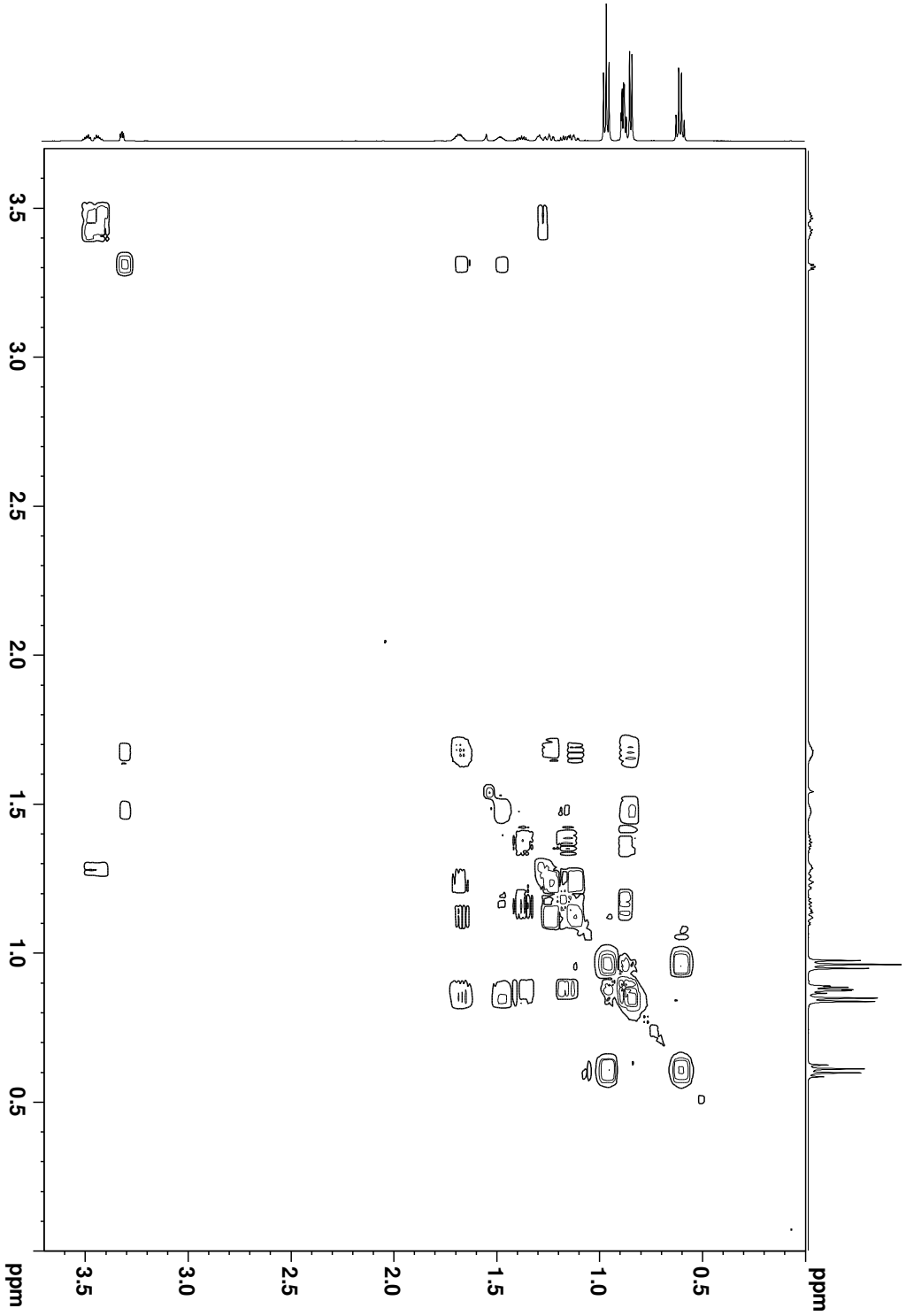

K.5 ^{1}H-^{13}C HSQC for 58a, 600 MHz, $CDCl_3$

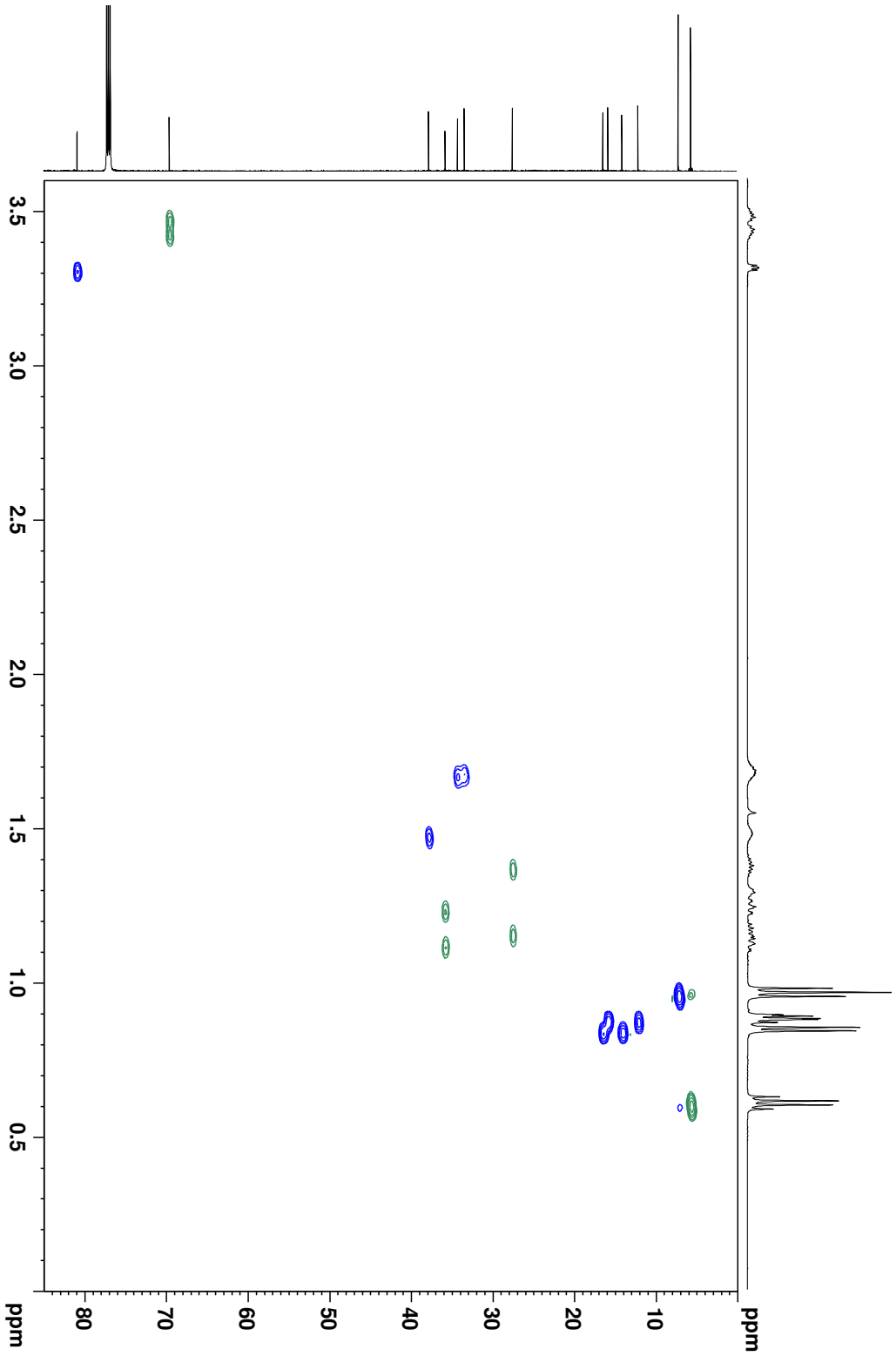

K.6 ^{1}H-^{13}C HMBC for 58a, 600 MHz, $CDCl_3$

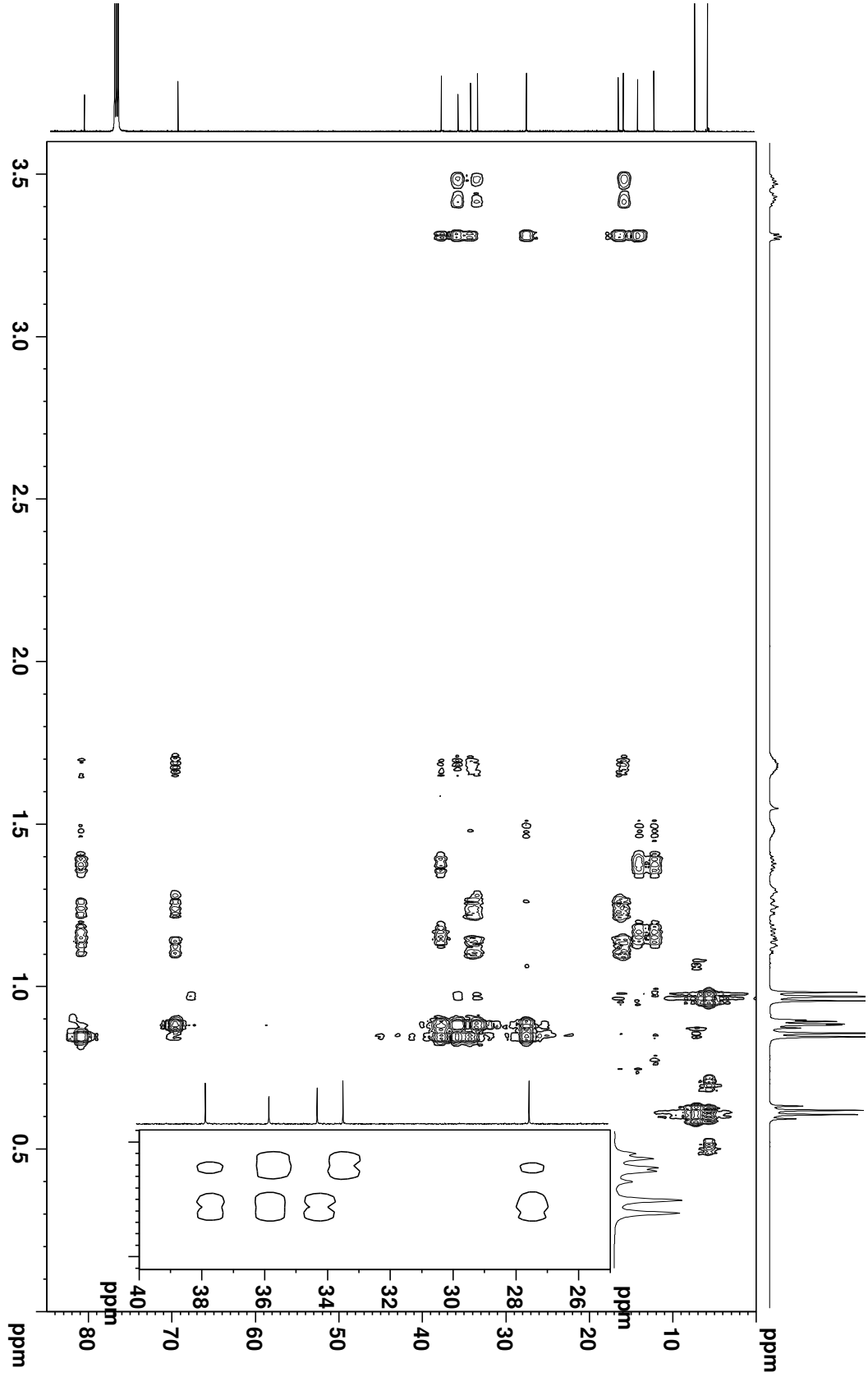

K.7 IR Spectrum of 58a (cm^{-1})

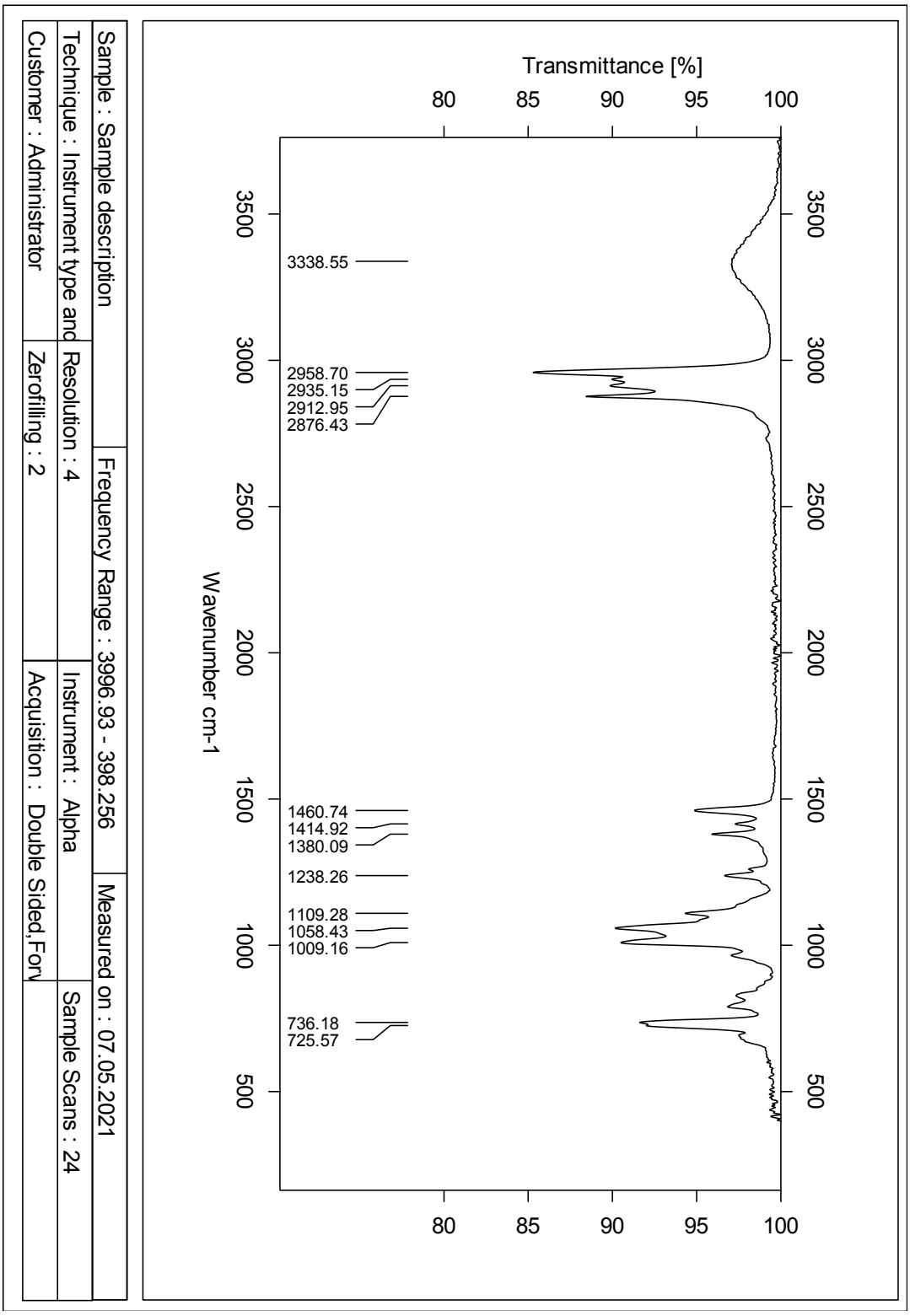

Elemental Composition Report **Page 1**

Single Mass Analysis

Tolerance = 3.0 PPM / DBE: min = -10.0, max = 50.0
Element prediction: Off
Number of isotope peaks used for i-FIT = 6

Monoisotopic Mass, Even Electron Ions
250 formula(e) evaluated with 2 results within limits (all results (up to 1000) for each mass)
Elements Used:
C: 0-100 H: 0-100 O: 0-3 Si: 0-2 Cl: 0-1 Na: 0-1

2021-293 77 (0.734) AM2 (Ar,35000.0,0.00,0.00); Cm (65:82)
1: TOF MS ES+

4.10e+005

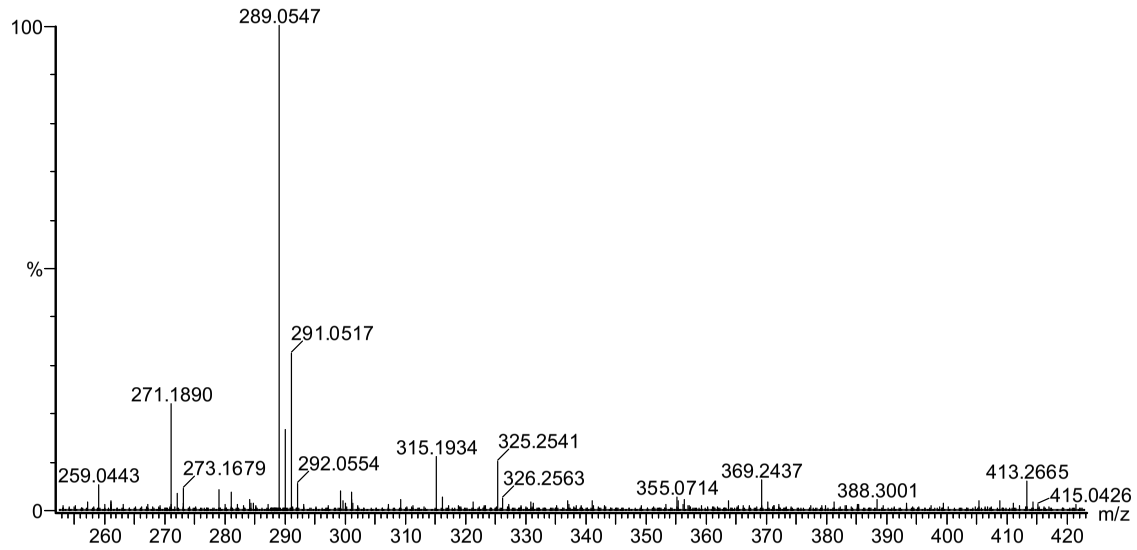

Minimum:				-10.0				
Maximum:		5.0	3.0	50.0				
Mass	Calc. Mass	mDa	PPM	DBE	i-FIT	Norm	Conf(%)	Formula
325.2541	325.2539	0.2	0.6	-0.5	2403.4	0.225	79.84	C17 H38 O2 Si Na

K.8 MS Spectrum of 58a

L (2*R*,4*R*,6*S*)-2,4,6-trimethyl-3-((triethylsilyl)oxy)octan-1-ol (58b)
L.1 ^{1}H-NMR for 58b, 600 MHz, $CDCl_3$ (ppm)

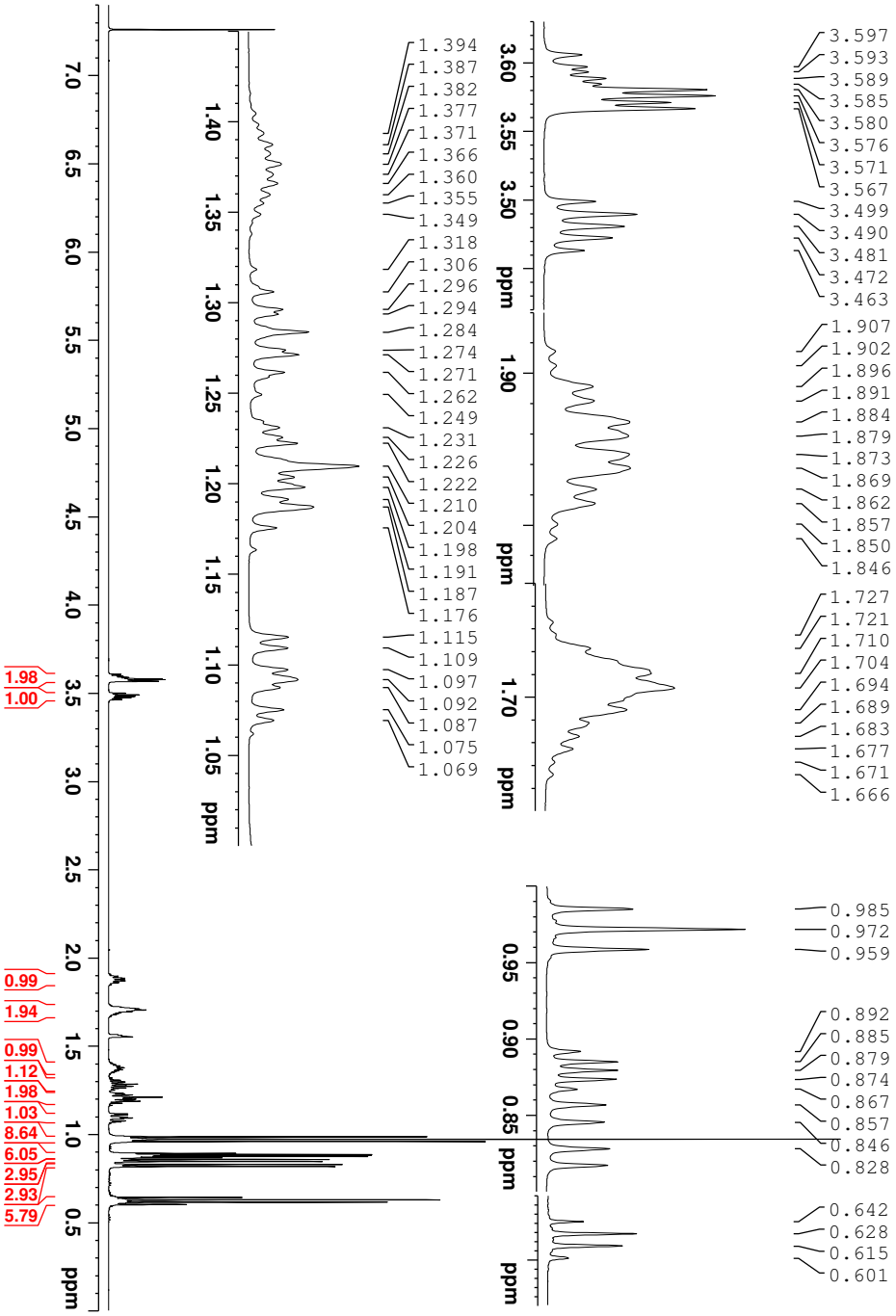

L.2 ^{1}H-NMR for 58b, 600 MHz, $CDCl_3$ (Hz)

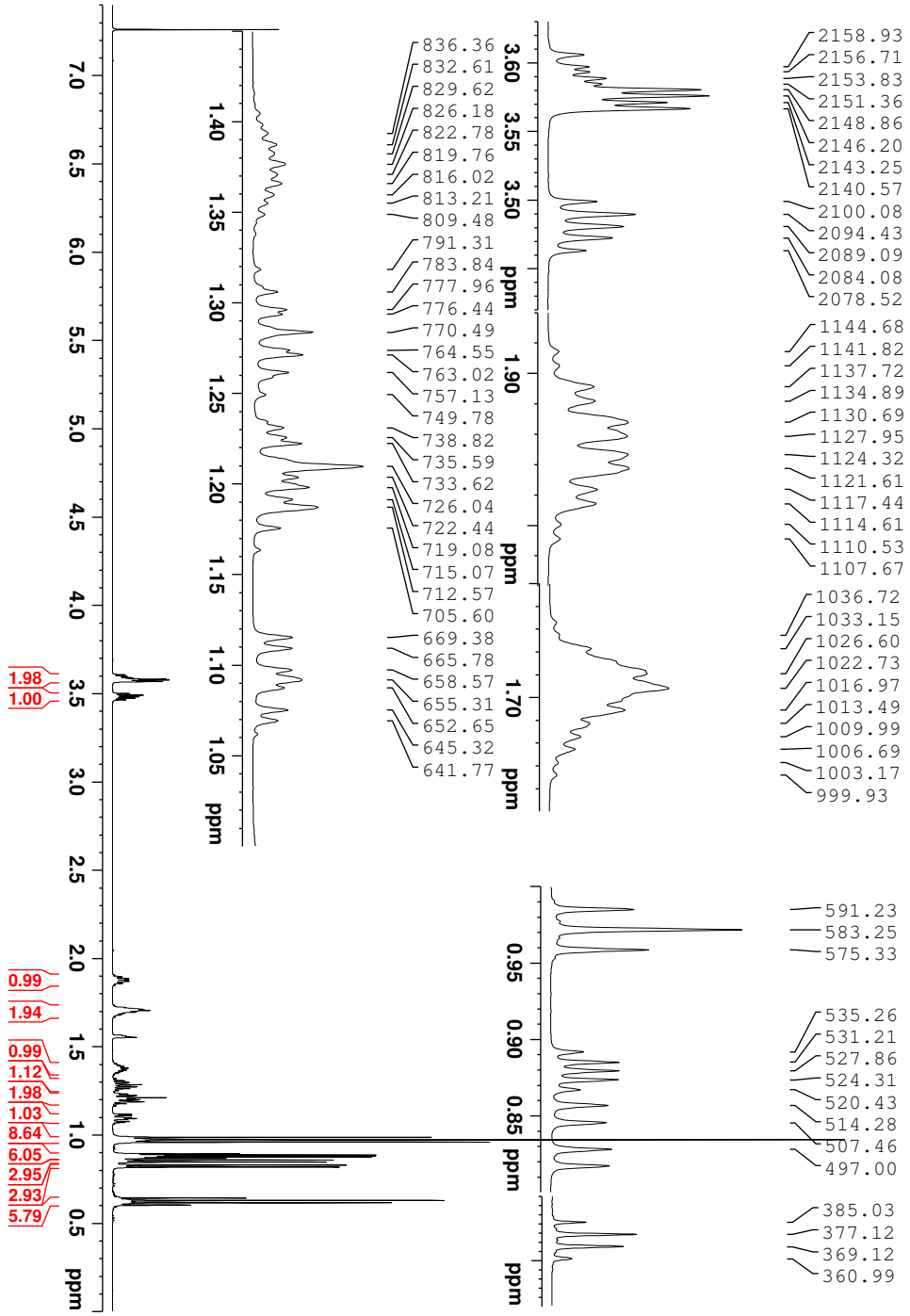

L.3 ^{13}C-NMR Spectrum of 58b, 600 MHz, $CDCl_3$ (ppm)

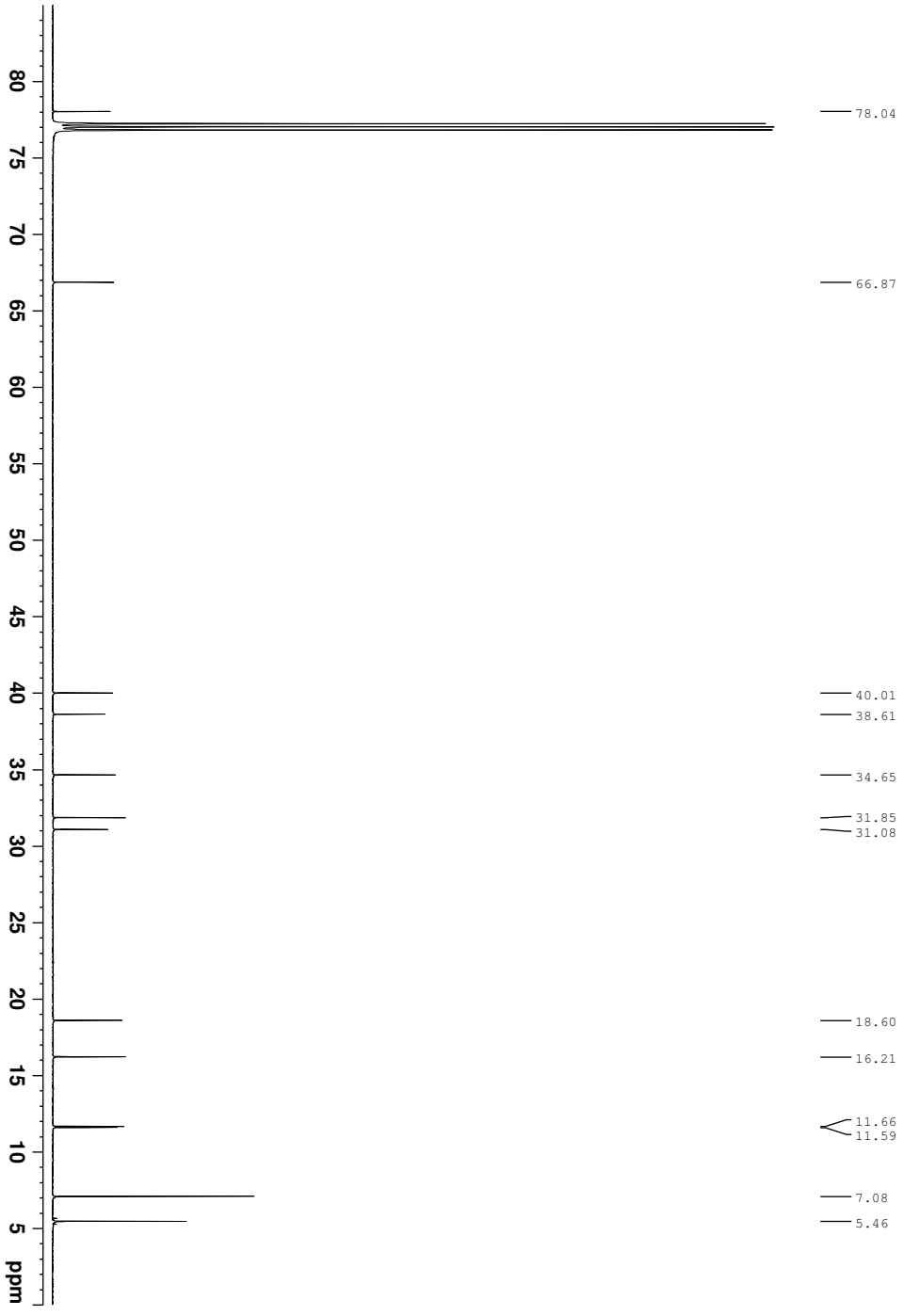

L.4 ^{1}H-^{1}H-COSY for 58b, 600 MHz, $CDCl_3$

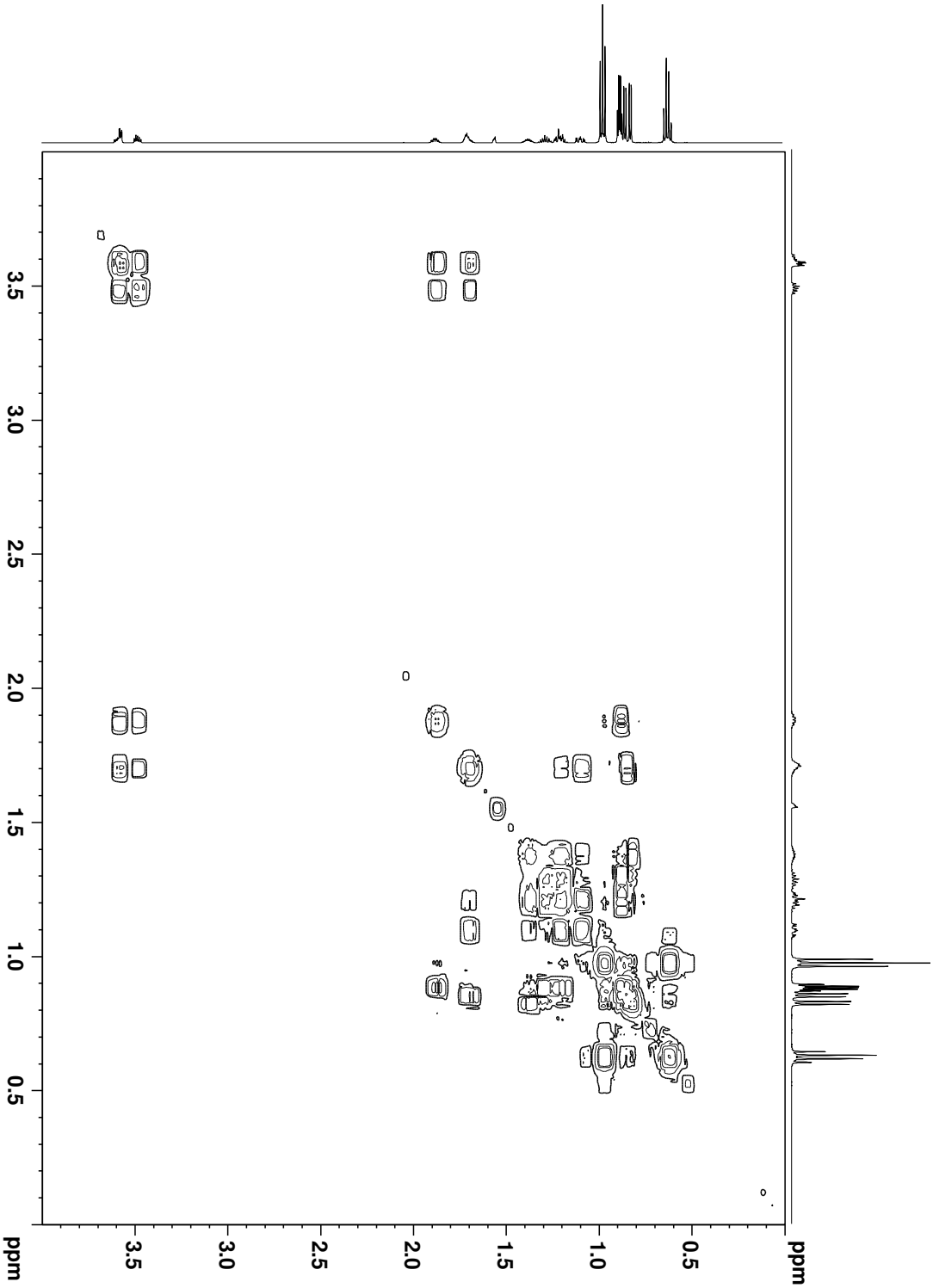

L.5 ^{1}H-^{13}C HSQC for 58b, 600 MHz, $CDCl_3$

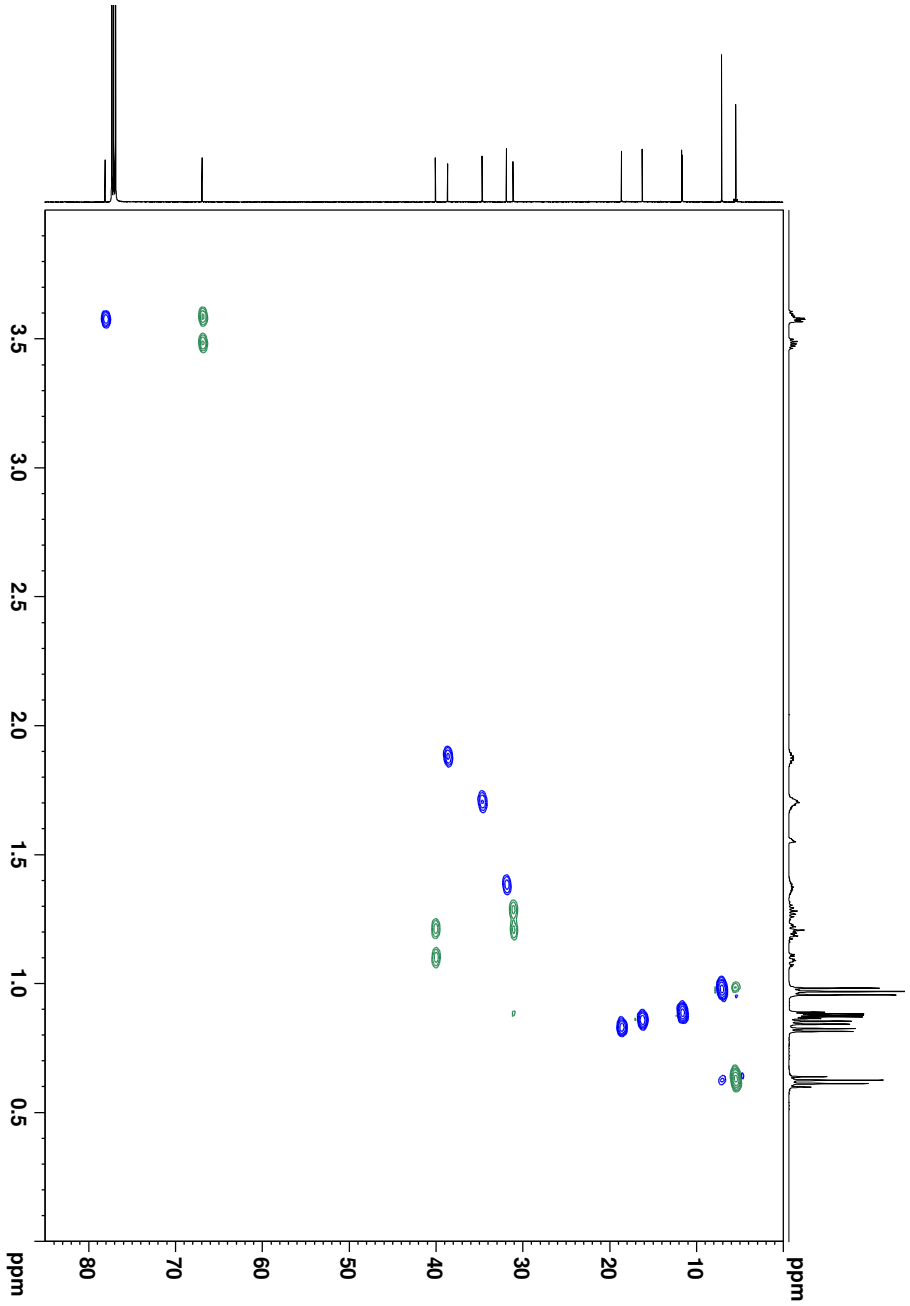

L.6 ^{1}H-^{13}C HMBC for 58b, 600 MHz, $CDCl_3$

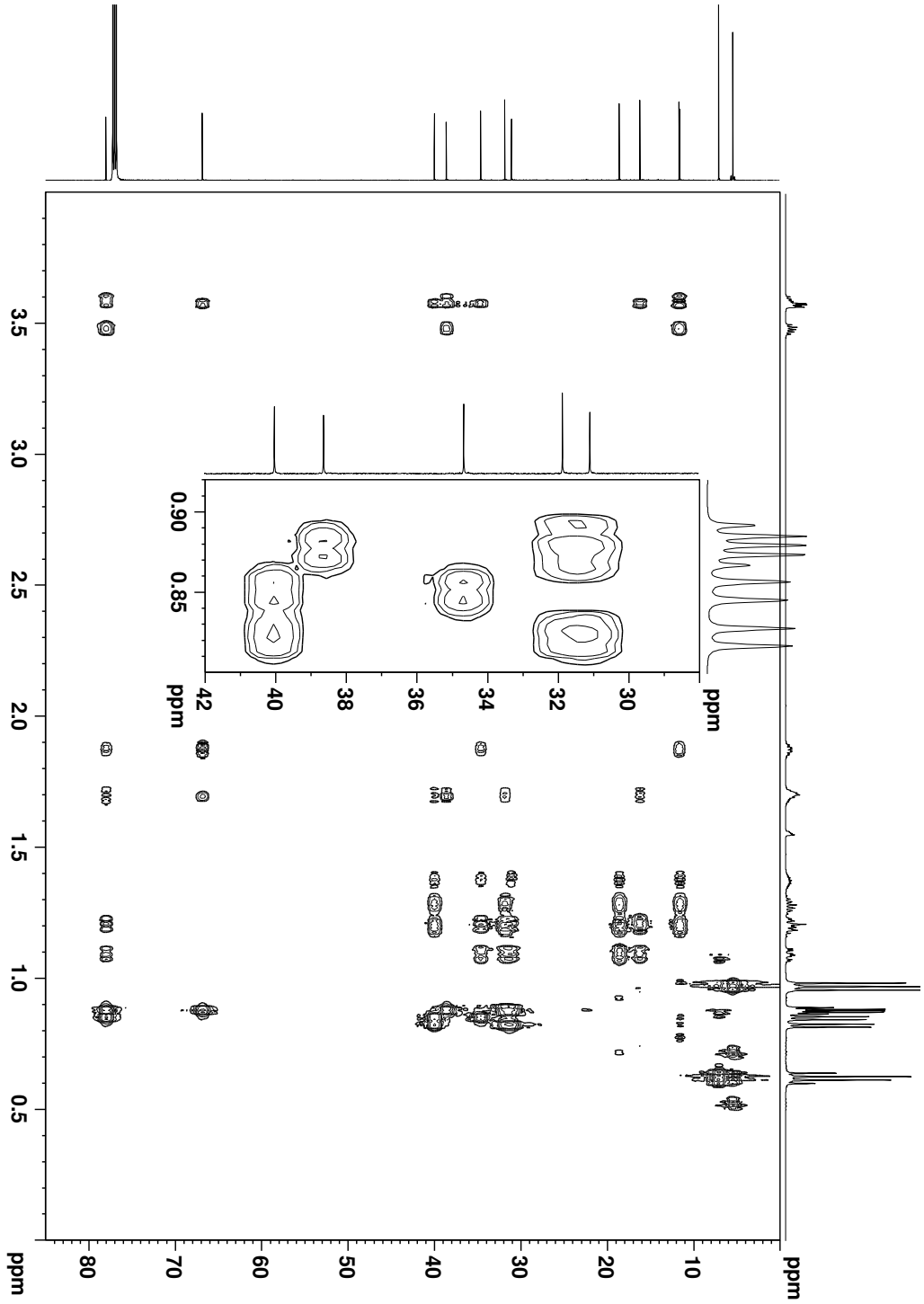

L.7 IR Spectrum of 58b (cm^{-1})

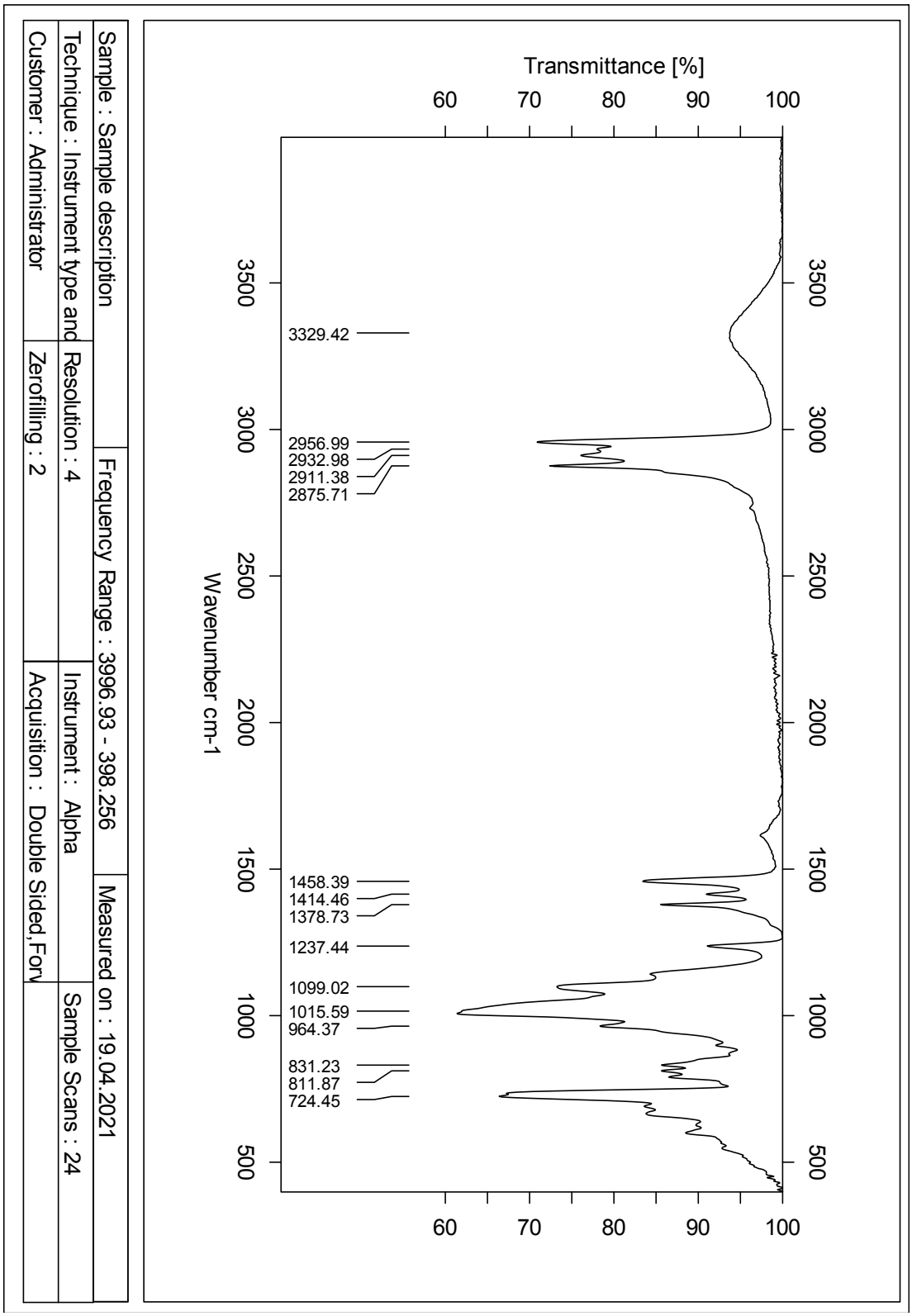

M (2*S*,4*S*,5*R*,6*S*)-2,4,6-trimethyl-5-((triethylsilyl)oxy)octanal (59a)
M.1 ^{1}H-NMR for 59a, 600 MHz, $CDCl_3$ (ppm)

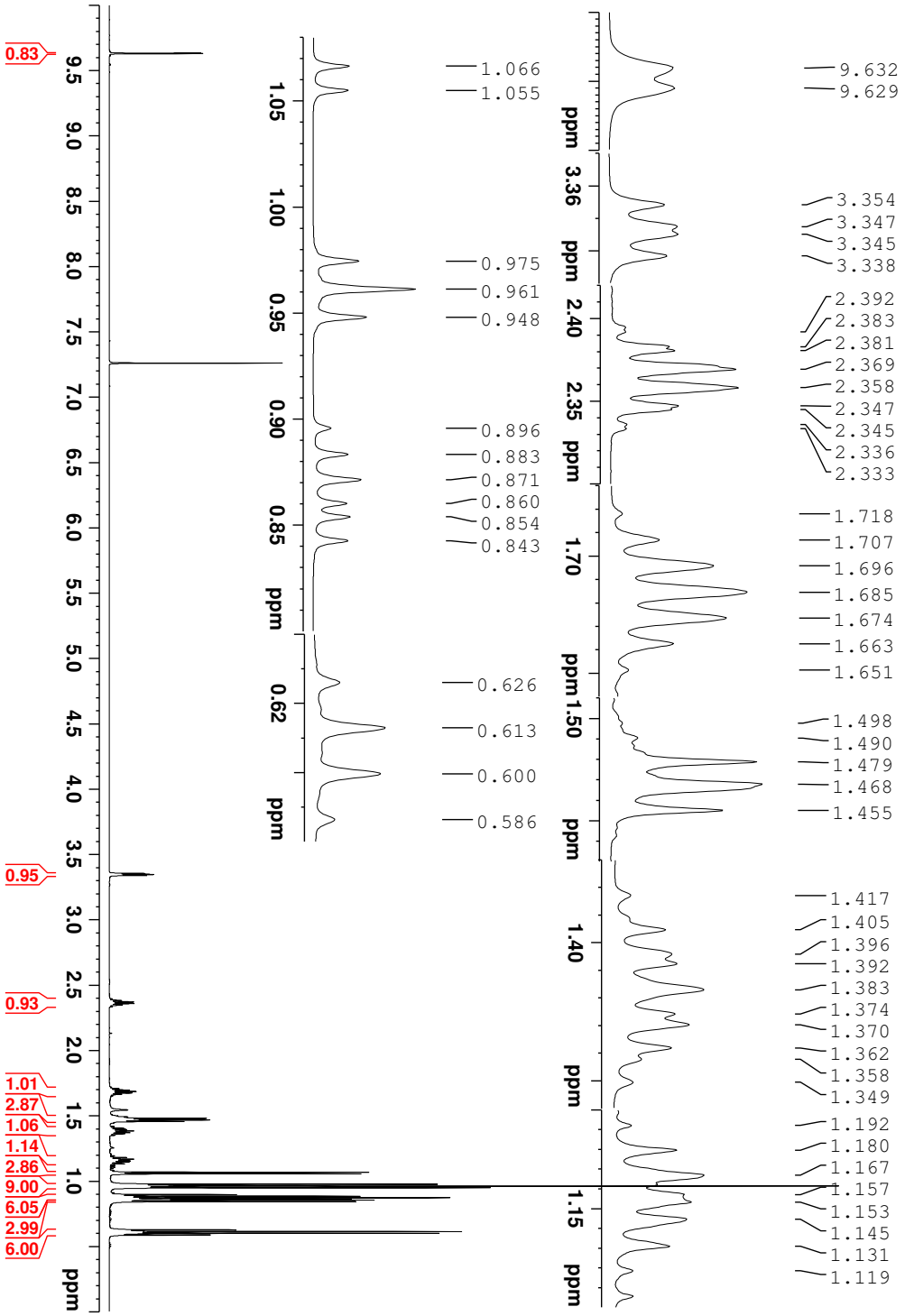

M.2 ^{1}H-NMR for 59a, 600 MHz, $CDCl_3$ (Hz)

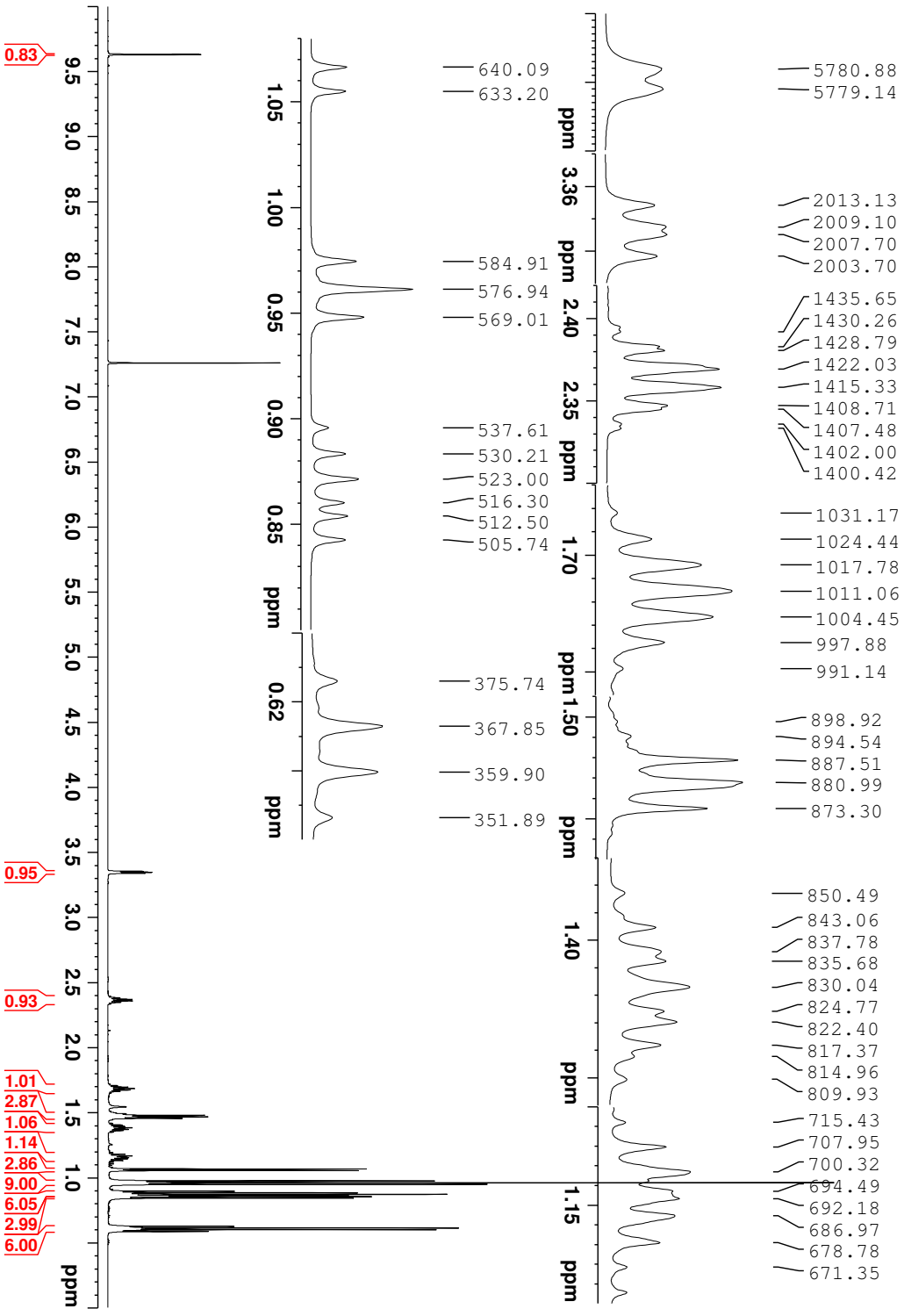

M.3 ^{13}C-NMR for 59a, 600 MHz, $CDCl_3$

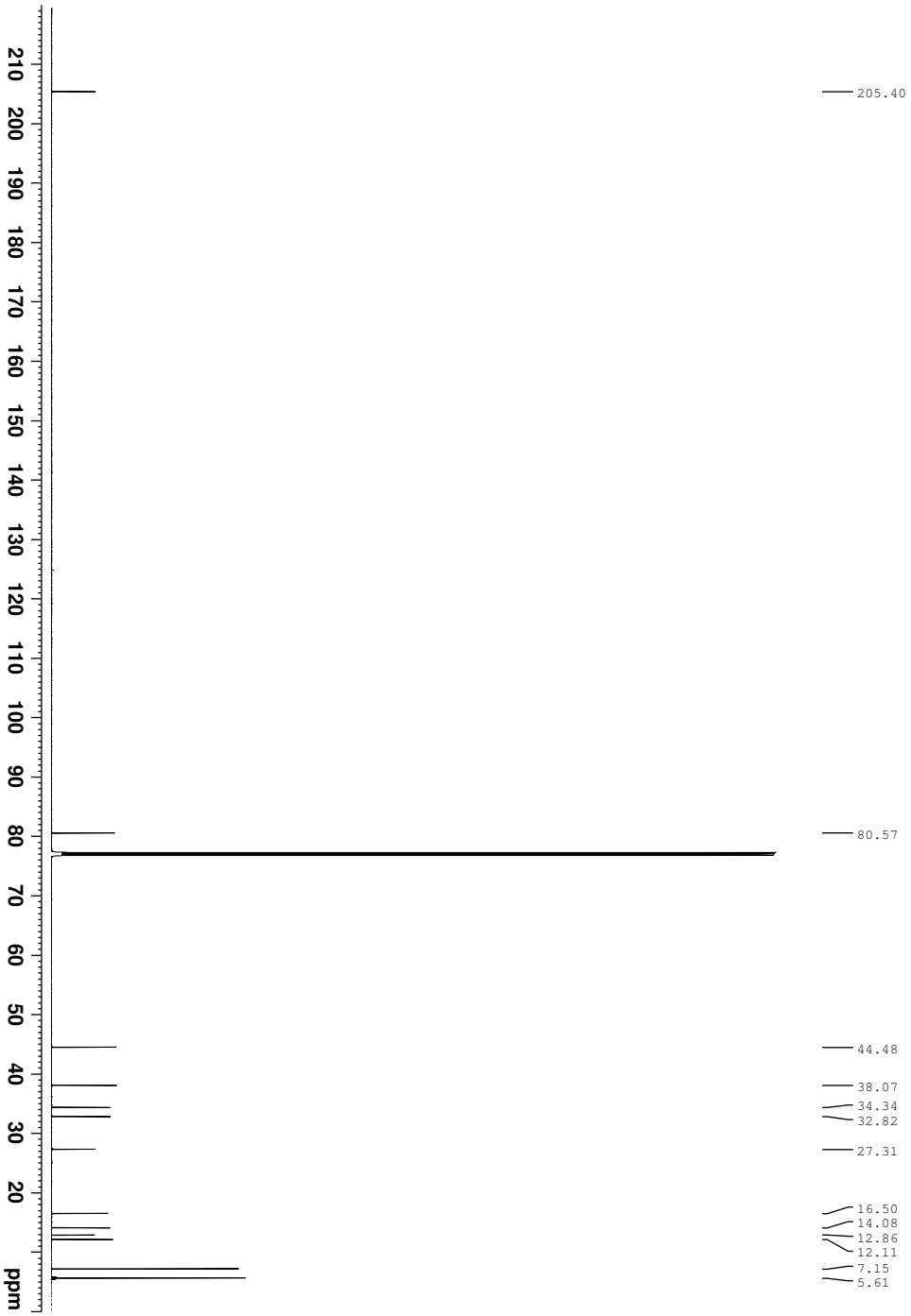

M.4 ^{1}H-^{1}H-COSY for 59a, 600 MHz, $CDCl_3$

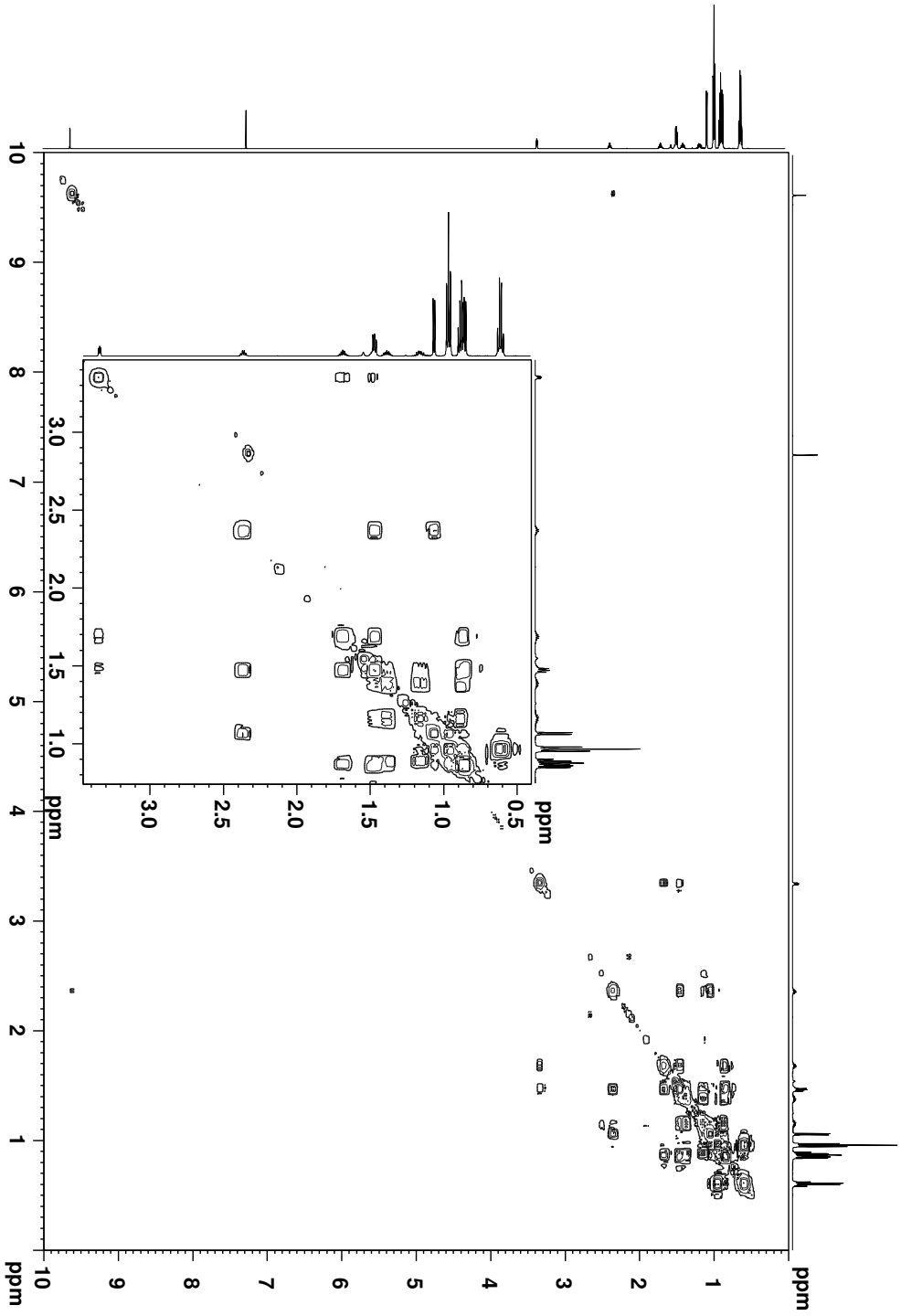

M.5 ^{1}H-^{13}C HSQC for 59a, 600 MHz, $CDCl_3$

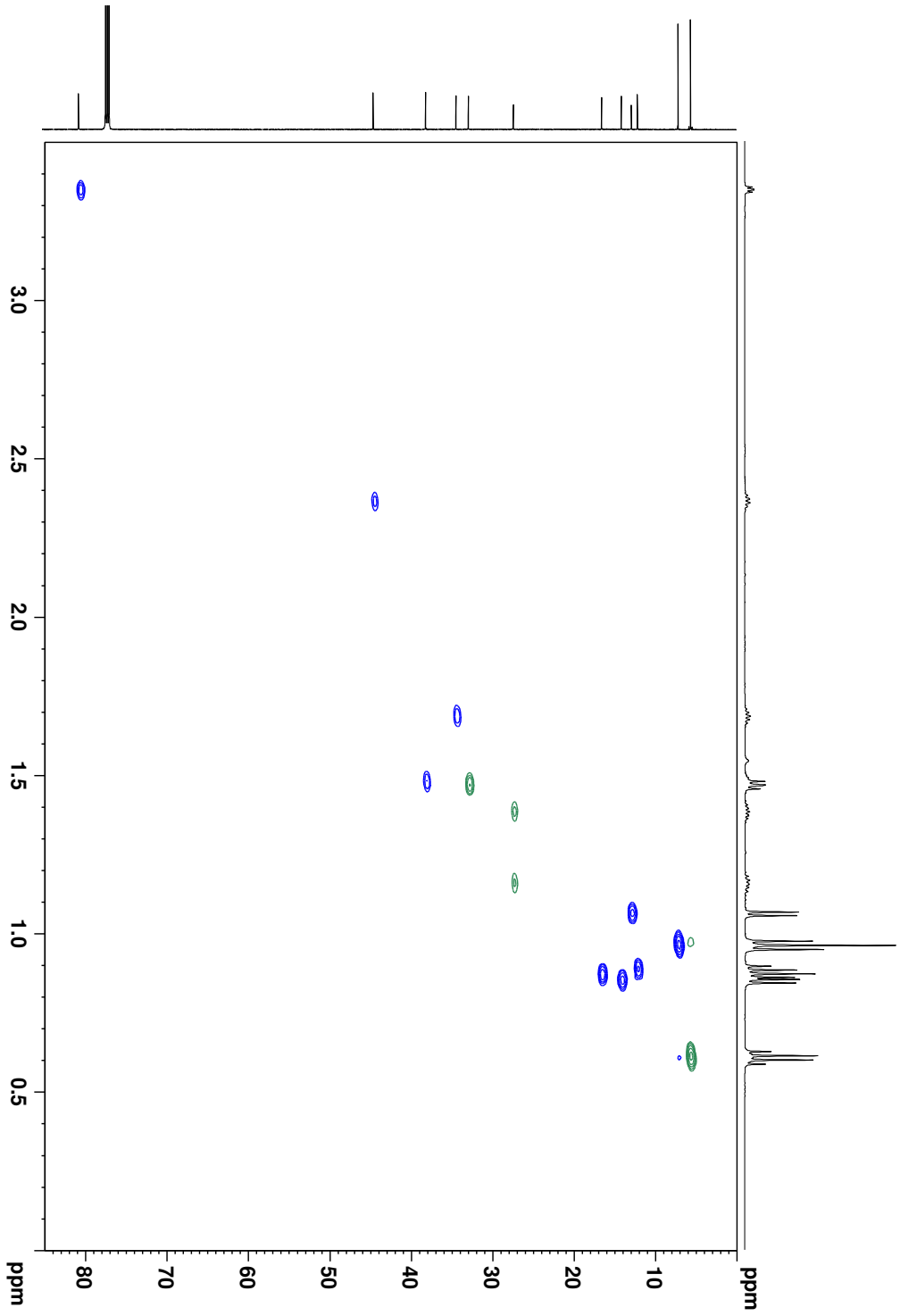

M.6 ^{1}H-^{13}C HMBC for 59a, 600 MHz, $CDCl_3$

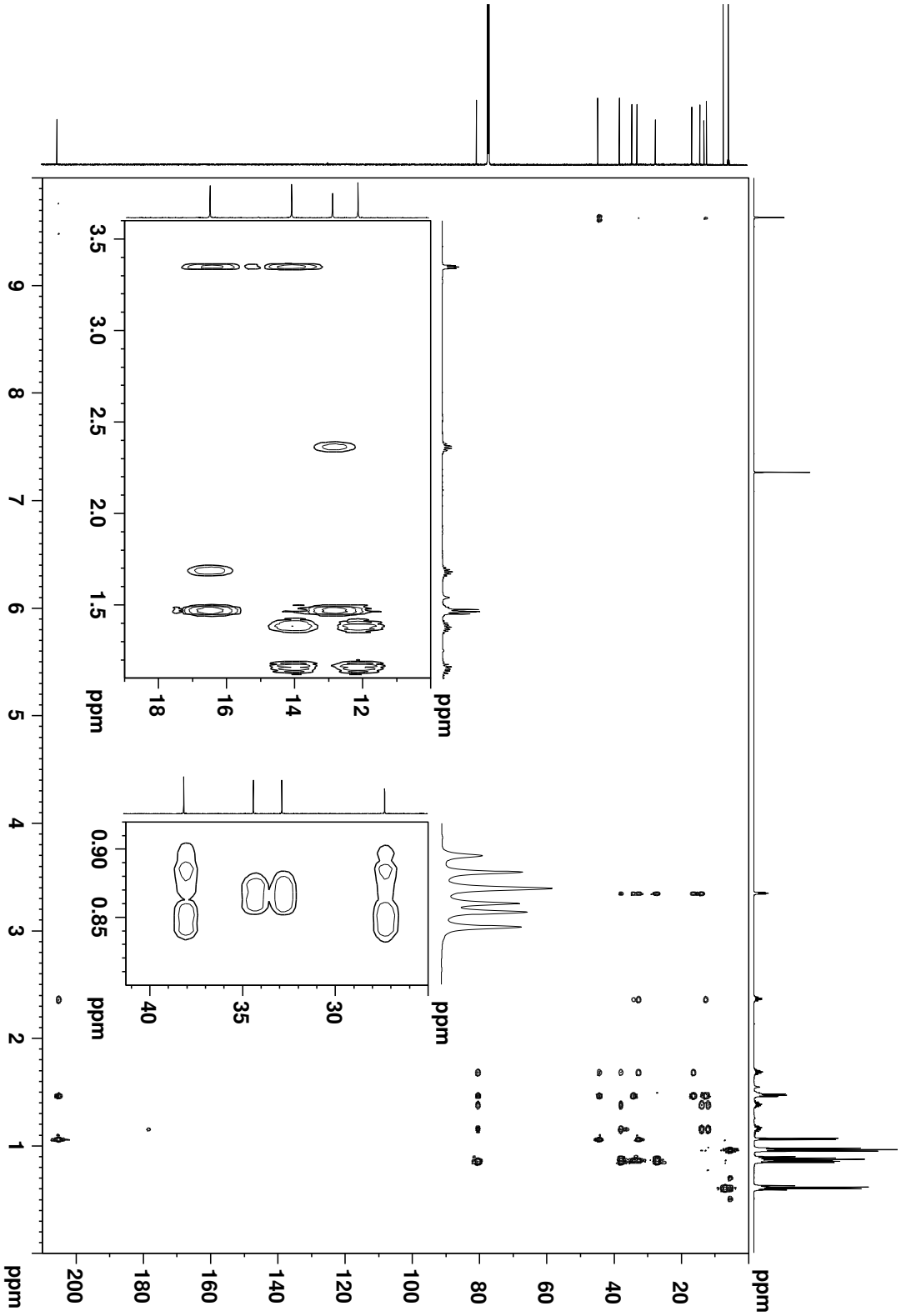

M.7 IR Spectrum of 59a (cm^{-1})

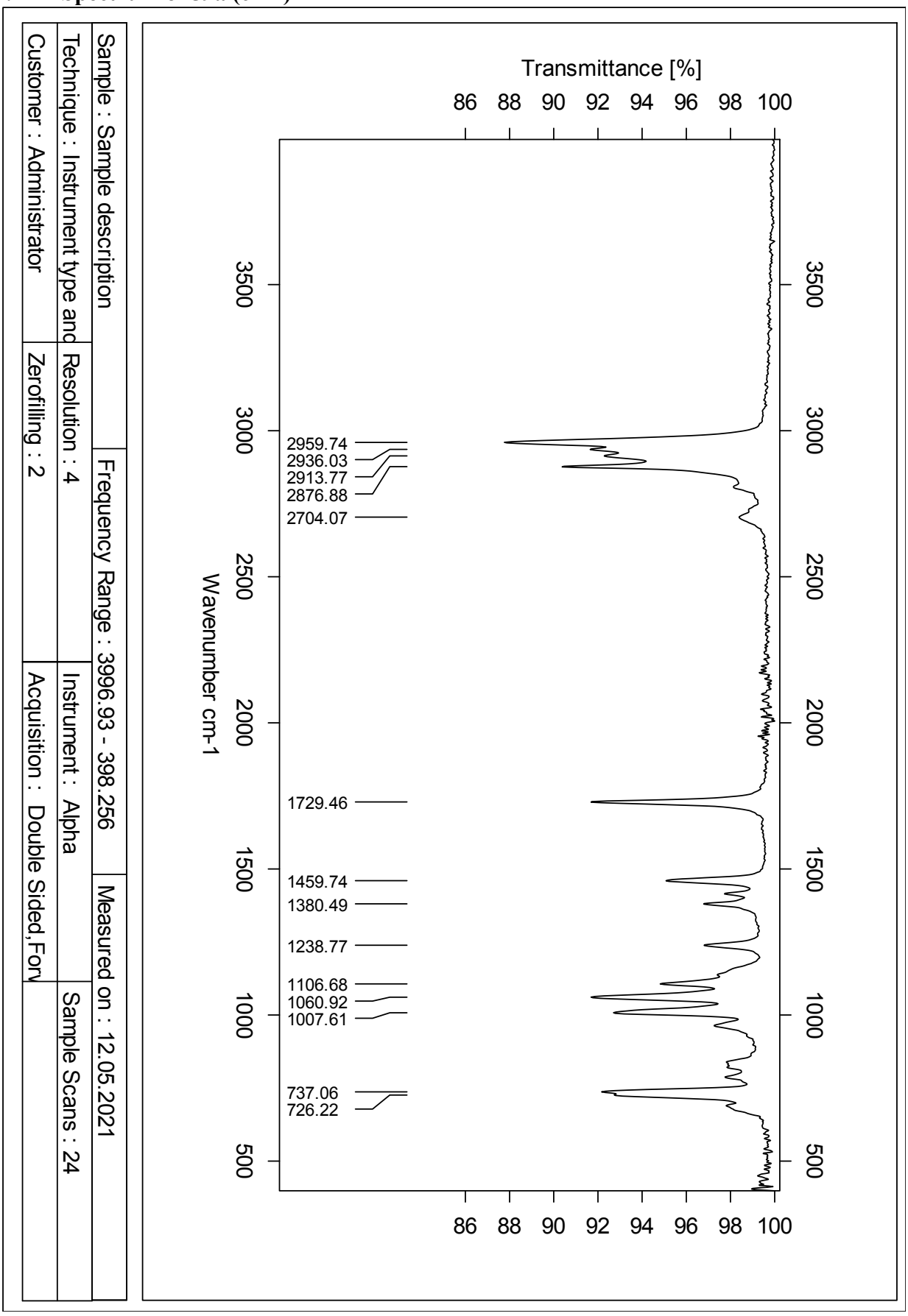

Single Mass Analysis

Tolerance = 2.1 PPM / DBE: min = -10.0, max = 50.0
Element prediction: Off
Number of isotope peaks used for i-FIT = 6

Monoisotopic Mass, Even Electron Ions
647 formula(e) evaluated with 2 results within limits (all results (up to 1000) for each mass)
Elements Used:
C: 0-100 H: 0-100 N: 0-10 O: 0-3 Si: 0-2

2021-karolineekstra 64 (1.257) AM2 (Ar,35000.0,0.00,0.00)
1: TOF MS ASAP+

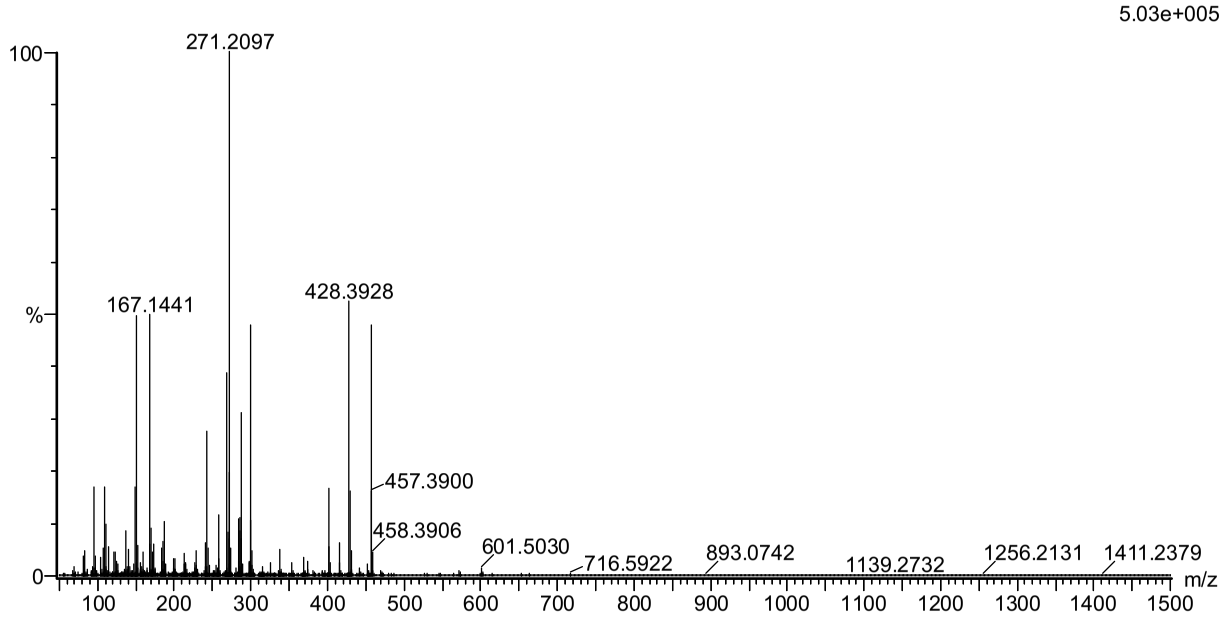

Minimum:				-10.0				
Maximum:		5.0	2.1	50.0				
Mass	Calc. Mass	mDa	PPM	DBE	i-FIT	Norm	Conf(%)	Formula
299.2412	299.2411	0.1	0.3	-2.5	2561.7	0.034	96.62	C9 H35 N6 O Si2
	299.2406	0.6	2.0	1.5	2565.1	3.387	3.38	C17 H35 O2 Si

N (2*S*,4*R*,6*S*)-2,4,6-trimethyl-3-((triethylsilyl)oxy)octanal (59b)
N.1 ^{1}H-NMR for 59b, 600 MHz, $CDCl_3$ (ppm)

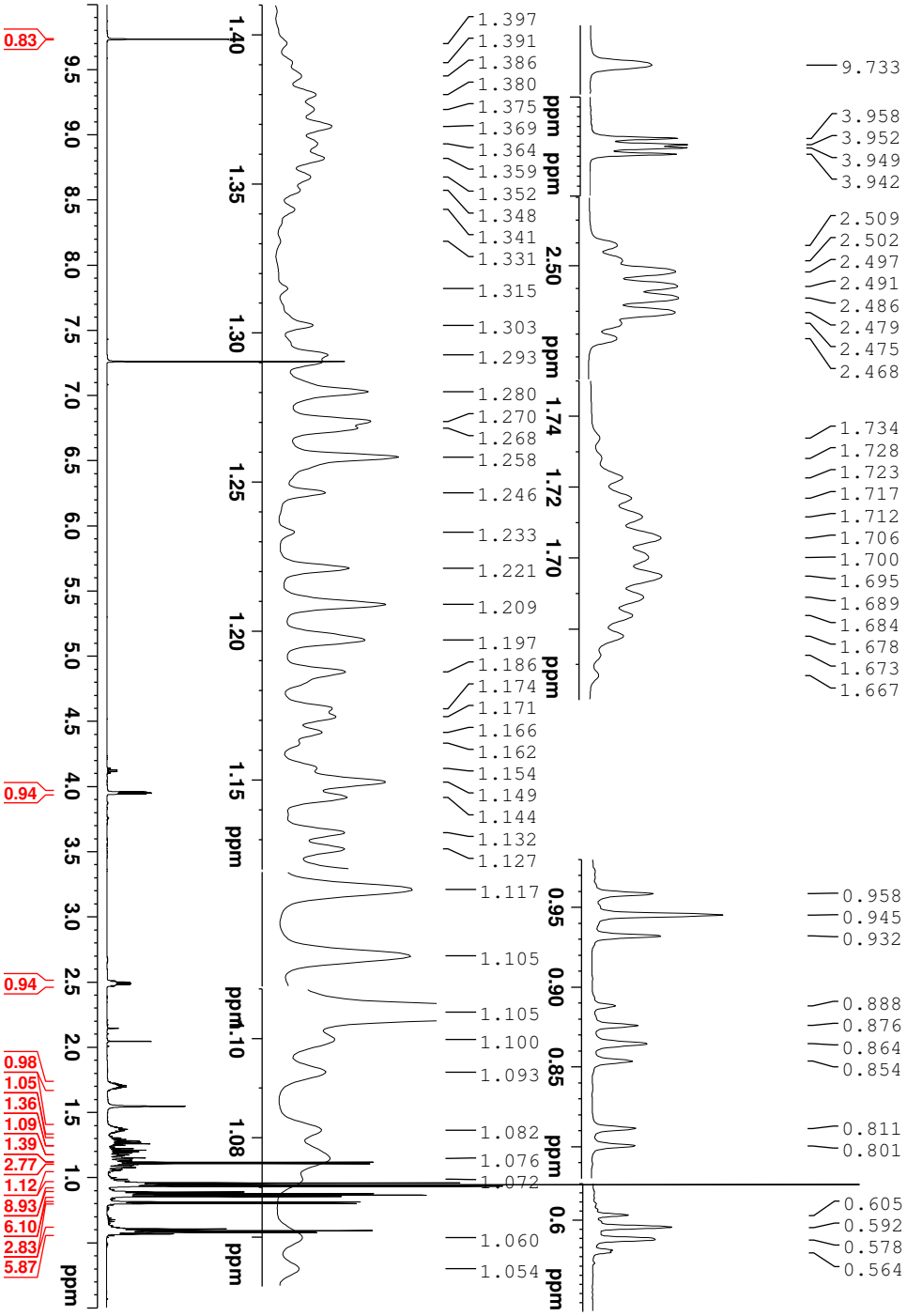

N.2 ^{1}H-NMR for 59b, 600 MHz, $CDCl_3$ (Hz)

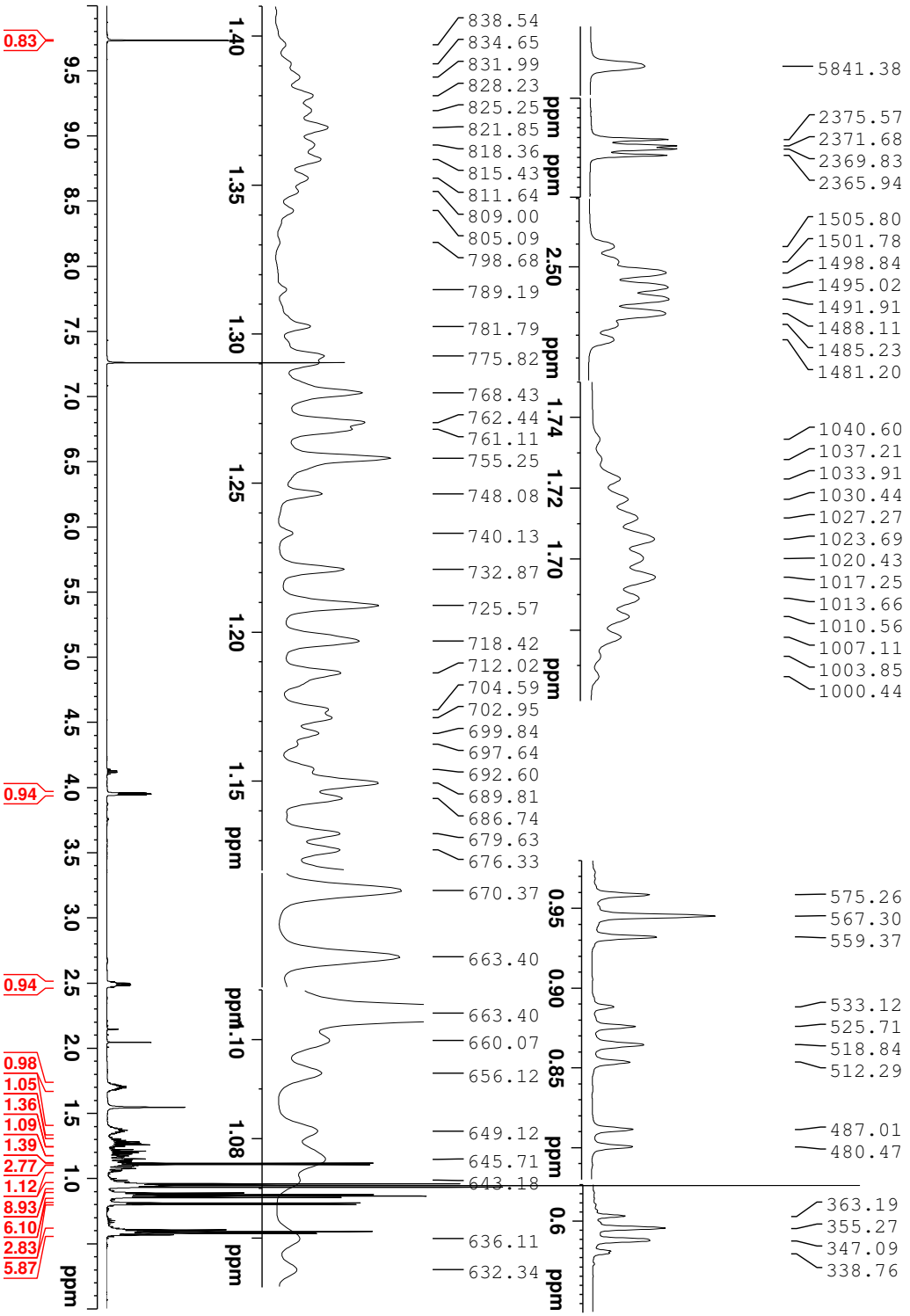

N.3 ^{13}C-NMR for 59b 600 MHz, $CDCl_3$ (ppm)

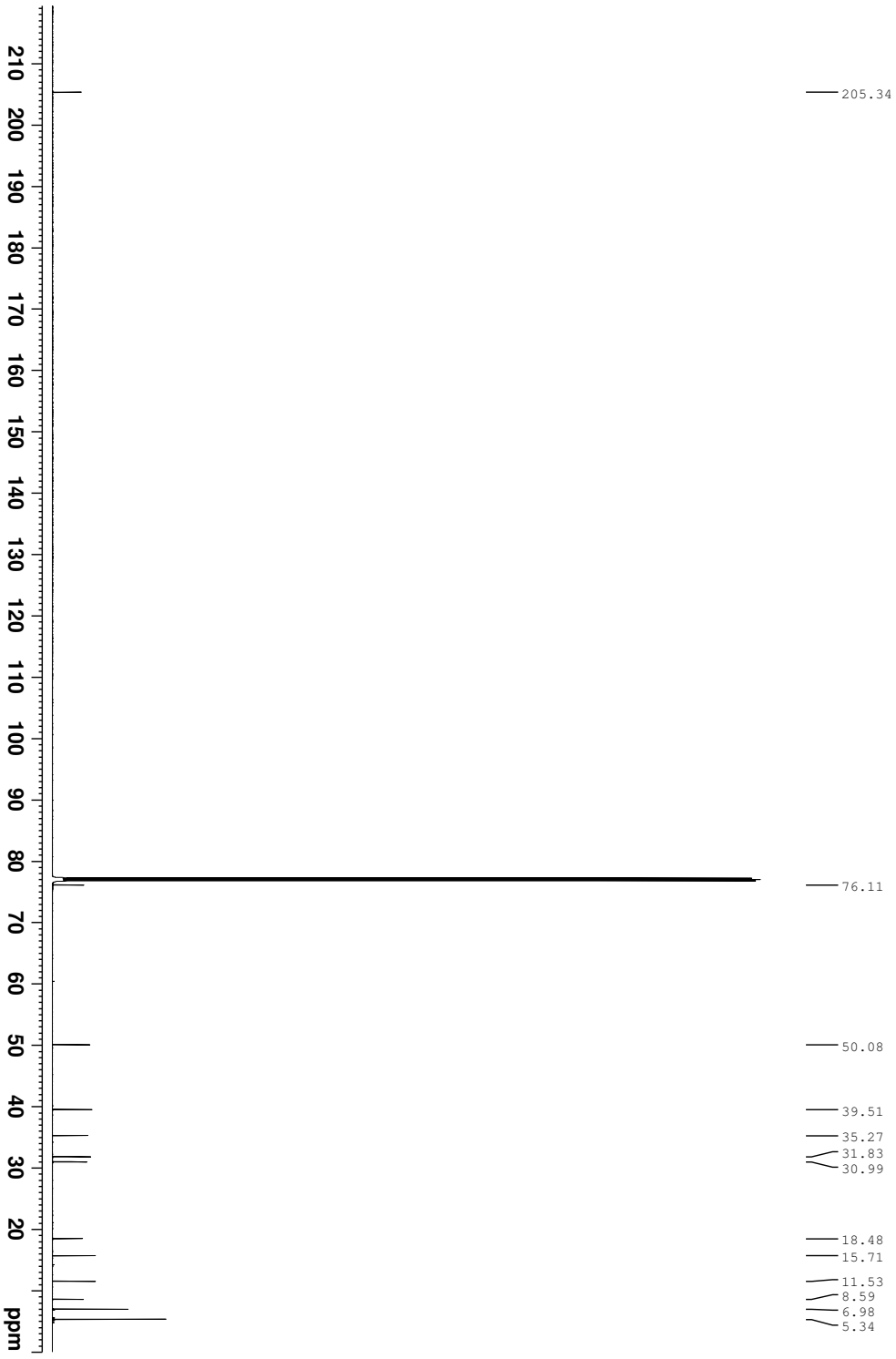

N.4 ^{1}H-^{1}H-COSY for 59b, 600 MHz, $CDCl_3$

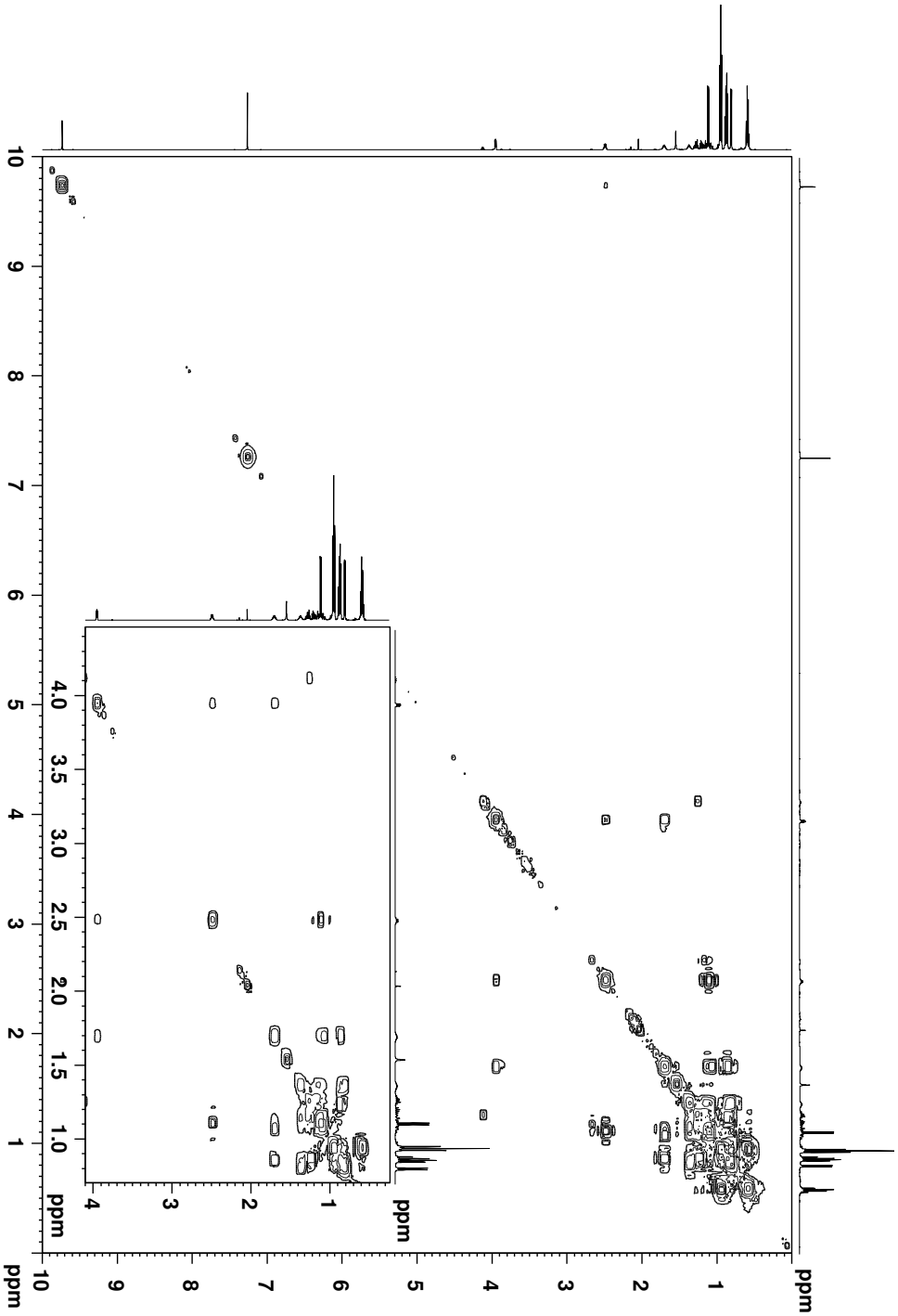

N.5 ^{1}H-^{13}C HSQC for 59b, 600 MHz, $CDCl_3$

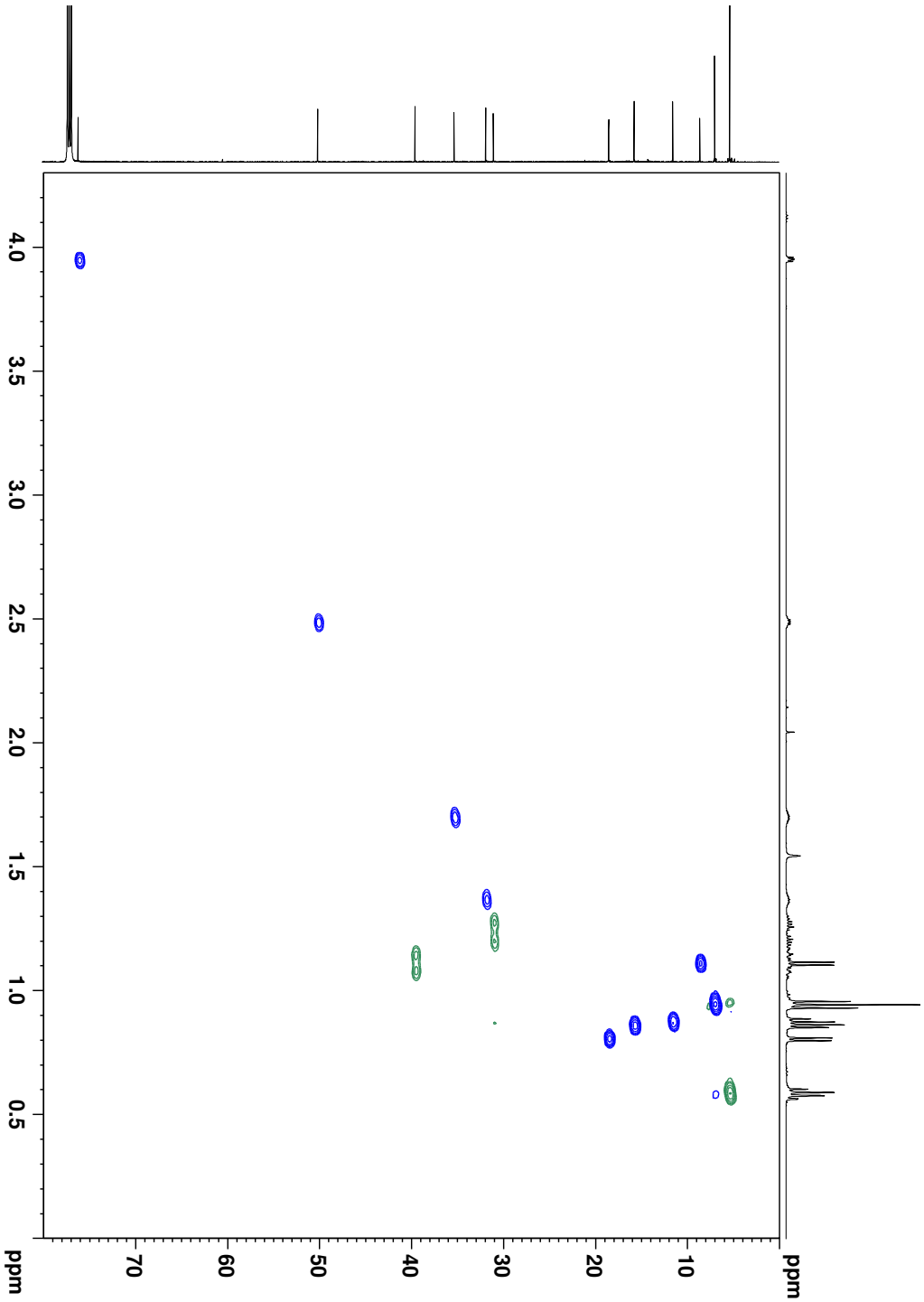

N.6 ^{1}H-^{13}C HMBC for 59b, 600 MHz, $CDCl_3$

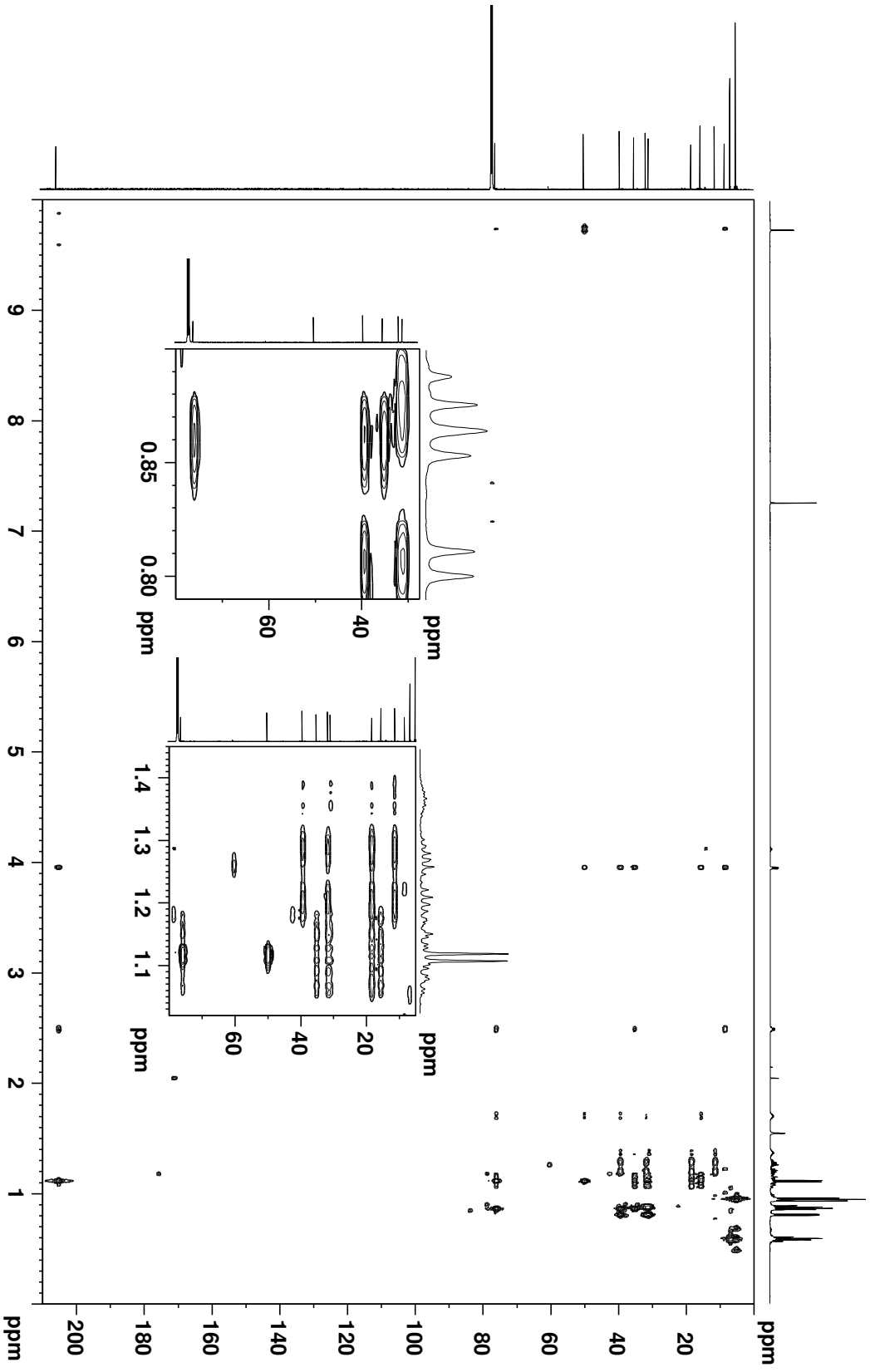

N.7 IR Spectrum of 59b (cm^{-1})

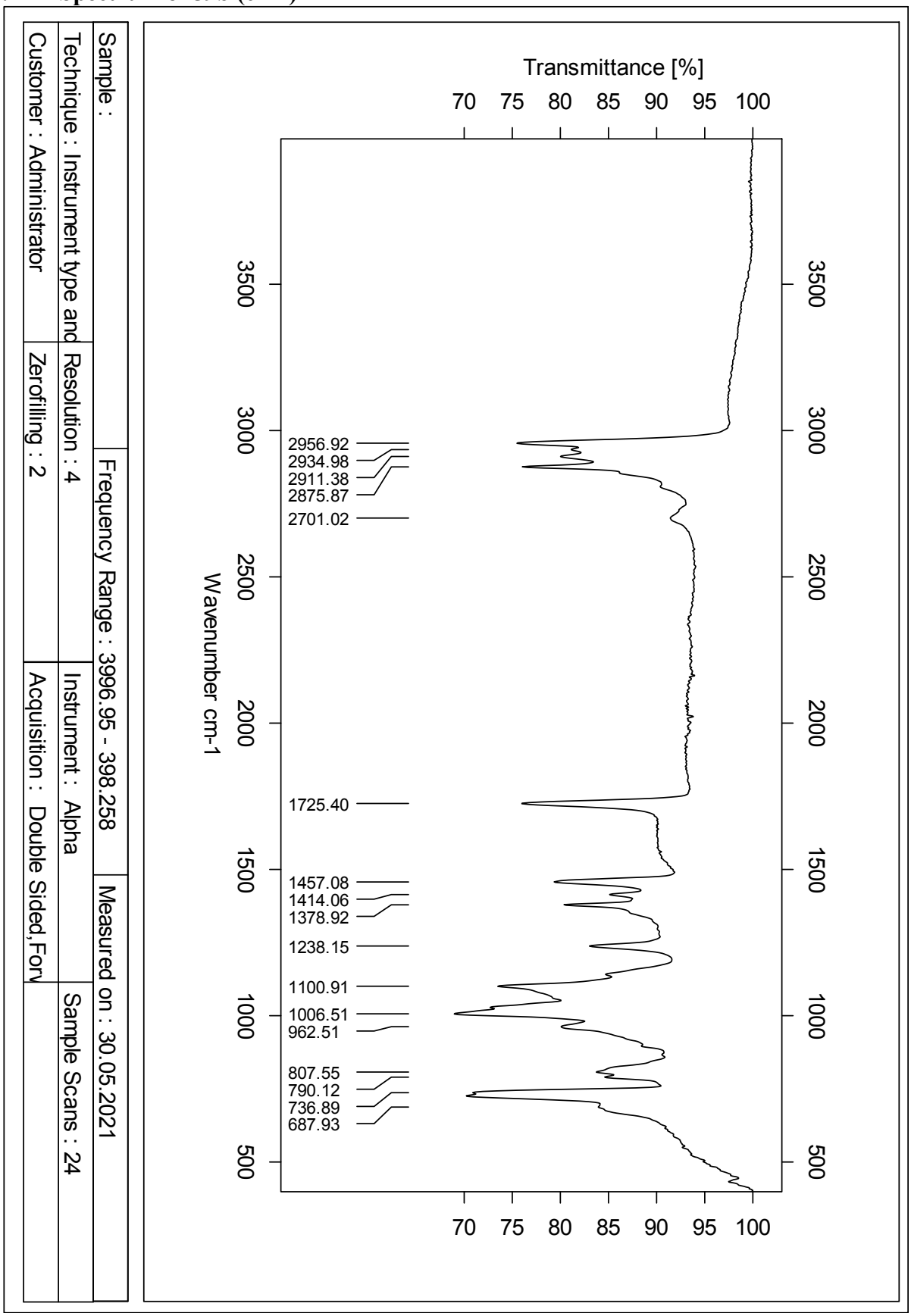

Elemental Composition Report

Single Mass Analysis

Tolerance = 2.1 PPM / DBE: min = -10.0, max = 50.0
Element prediction: Off
Number of isotope peaks used for i-FIT = 6

Monoisotopic Mass, Even Electron Ions
647 formula(e) evaluated with 2 results within limits (all results (up to 1000) for each mass)
Elements Used:
C: 0-100 H: 0-100 N: 0-10 O: 0-3 Si: 0-2

2021-292oil 31 (0.620) AM2 (Ar,35000.0,0.00,0.00); Cm (28:31)
1: TOF MS ASAP+

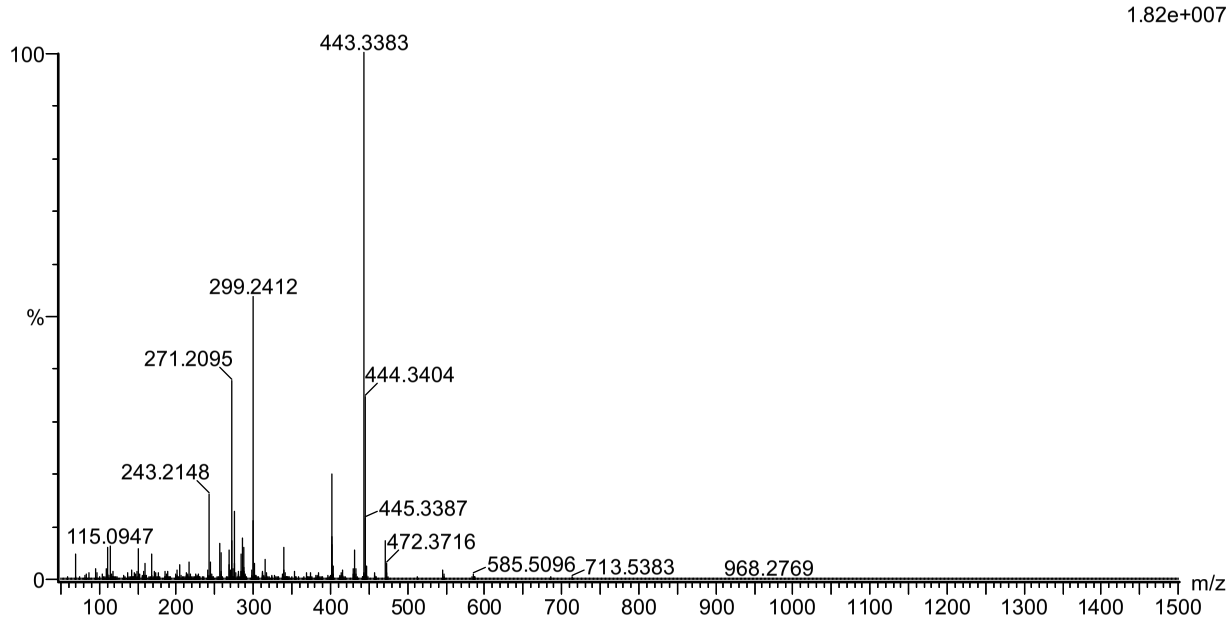

Minimum:				-10.0				
Maximum:		5.0	2.1	50.0				
Mass	Calc. Mass	mDa	PPM	DBE	i-FIT	Norm	Conf(%)	Formula
299.2412	299.2406	0.6	2.0	1.5	3687.8	0.000	100.00	C17 H35 O2 Si

N.8 MS Spectrum of 59b

O (*S*)-2-methylbutanal (10)

O.1 ^{1}H-NMR for 10, 400 MHz, $CDCl_3$ (ppm)

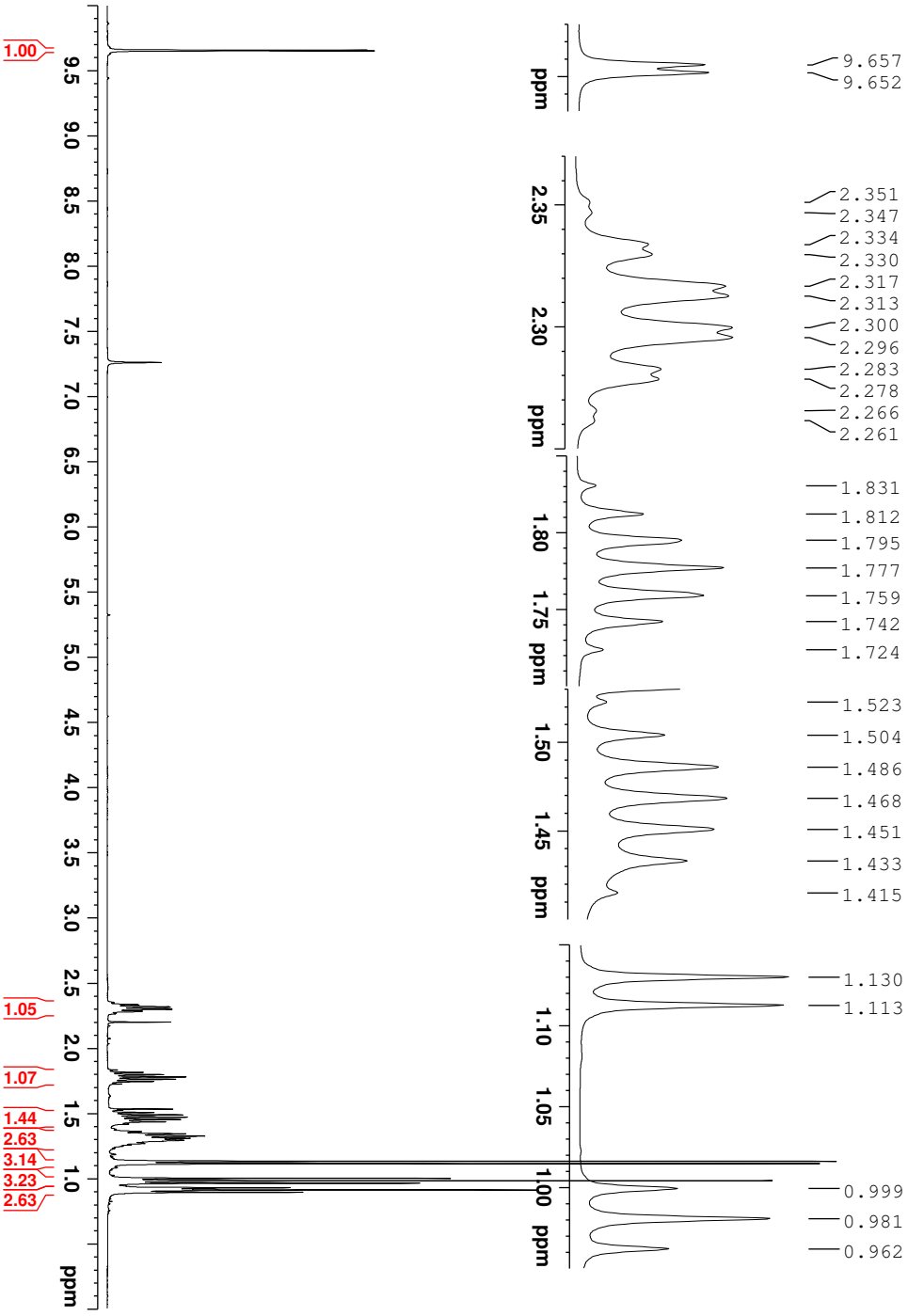

O.2 ^{1}H-NMR for 10, 400 MHz, $CDCl_3$ (Hz)

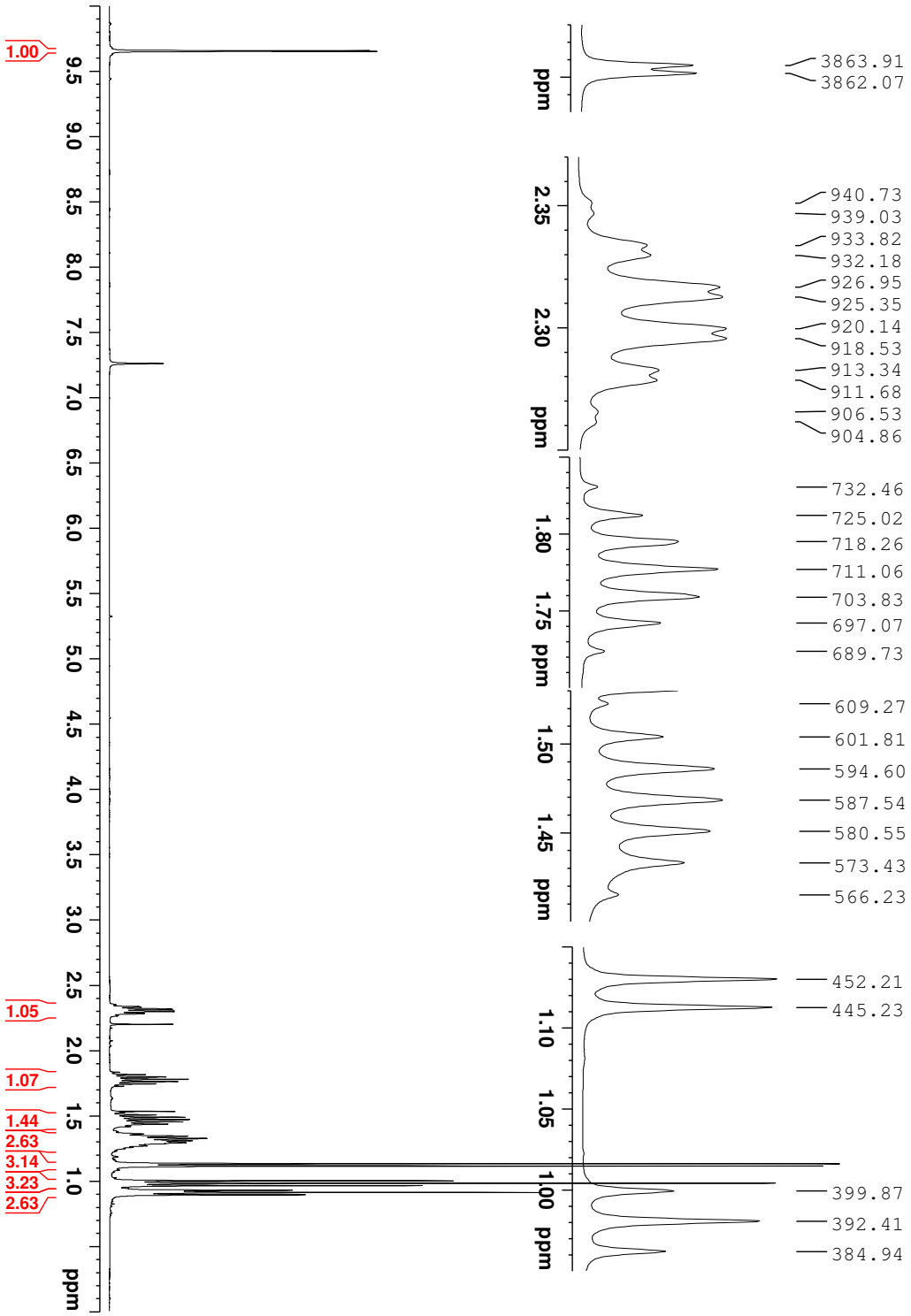

O.3 ^{13}C-NMR for 10, 400 MHz, $CDCl_3$ (ppm)

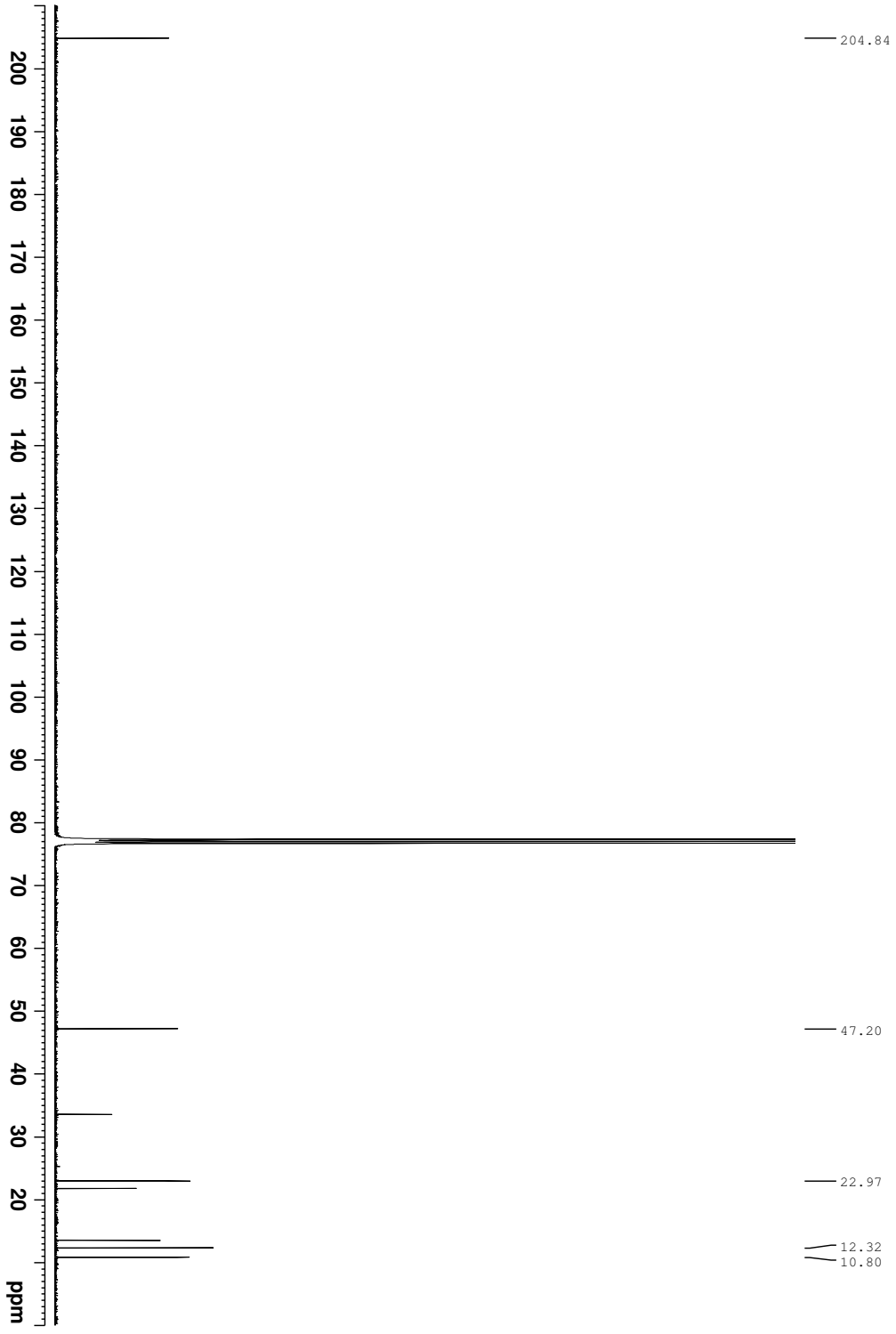

O.4 GC MS of 10

```
                                INSTRUMENT CONTROL PARAMETERS:    GCMS2
                                --------------------------------------

   C:\MSDCHEM\3\METHODS\WAXExtract_Nikolas_Sintef_HPpona.M
      Tue May 11 15:26:47 2021

Control Information
------- -----------

Sample Inlet      :  GC
Injection Source  :  CTC PAL ALS
Mass Spectrometer :  Enabled

================================================================================
                                 CTCPAL METHOD
================================================================================
                     Injection Volume: 1.00 ul
                         Syringe Size: 10ul
                           Cycle File: GC-Inj

                                CYCLE DETAILS
                               ---------------
                      Air Volume (µl): 0
          Pre Clean with Solvent 1 (): 2
          Pre Clean with Solvent 2 (): 0
             Pre Clean with Sample (): 1
                 Filling Speed (µl/s): 2
                   Filling Strokes (): 4
                            Inject to: GC Inj1
               Injection Speed (µl/s): 50
                Pre Inject Delay (ms): 500
               Post Inject Delay (ms): 500
         Post Clean with Solvent 1 (): 3
         Post Clean with Solvent 2 (): 0
Oven
Oven                                    On
Equilibration Time                       1 min
Oven Program
    60 degrees C for 5 min
    then 5 °C/min to 315 degrees C for 1 min

Post Run Temperature                    50 degrees C



Front Injector


Front Inlet SS
Heater                                  On    250 °C
Pressure                                On    31.833 psi
Total Flow                              On    14 mL/min
Septum Purge Flow                       On    3 mL/min
Mode                                   Split
Gas Saver                               On    20 mL/min After 2 min
Split Ratio                             10 :1
Split Flow                             10 mL/min
Injection Pulse Pressure                0 psi Until 0 min


Thermal Aux 2 {MSD Transfer Line}
Heater                                  On
Temperature Program
    290 degrees C for 0 min

Column #1
Agilent 19091S-001: 325 °C: 50 m x 200 µm x 0.5 µm
HP-PONA  Methyl Siloxane: 5209.36736
```

```
File       :D:\ikj\20210526_331_1TIL10.D
Operator   :
Acquired   : 26 May 2021  21:24     using AcqMethod ikj_svg_HPpona.M
Instrument :    GCMS2
Sample Name:
Misc Info  :
Vial Number: 3
```

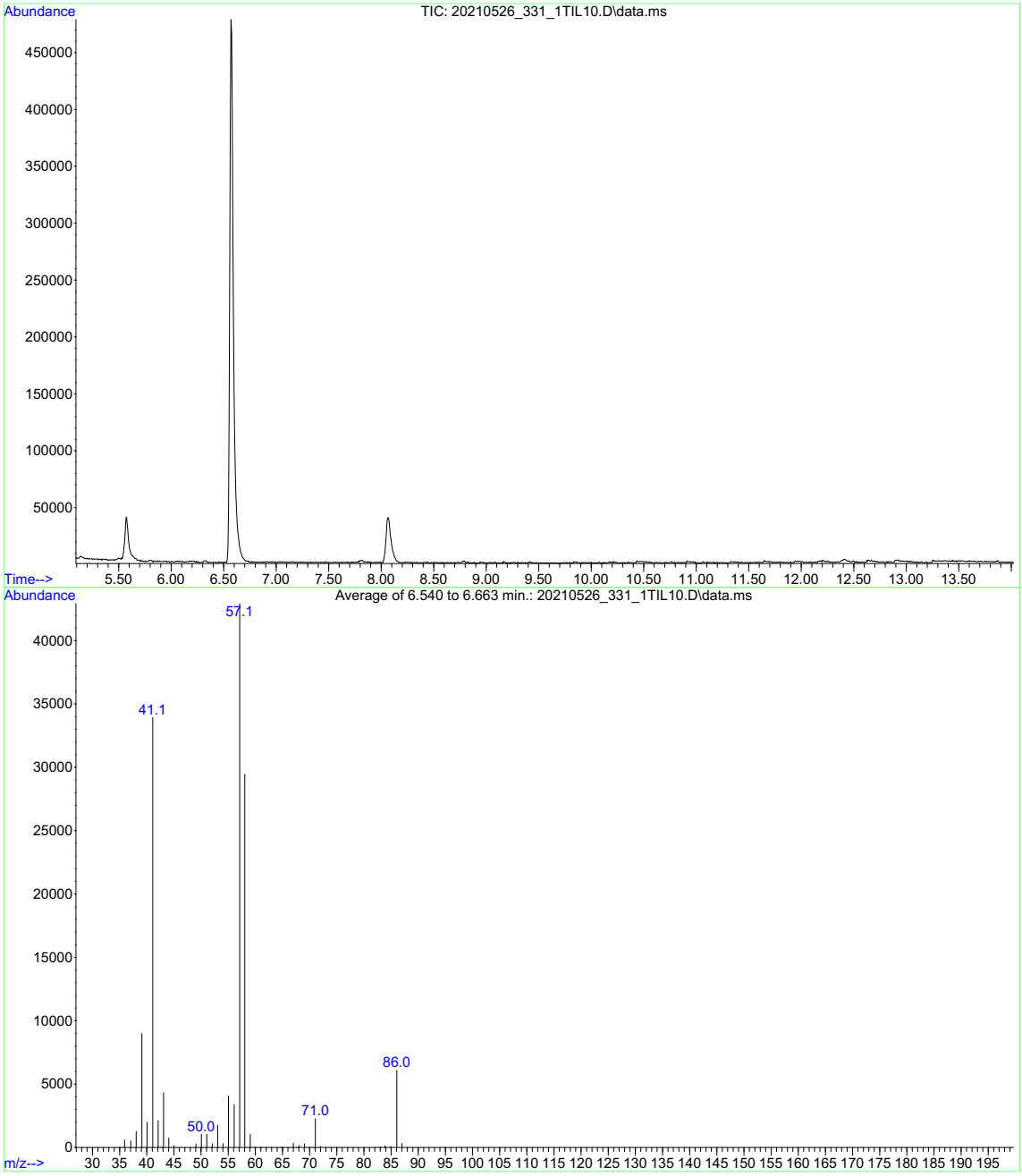

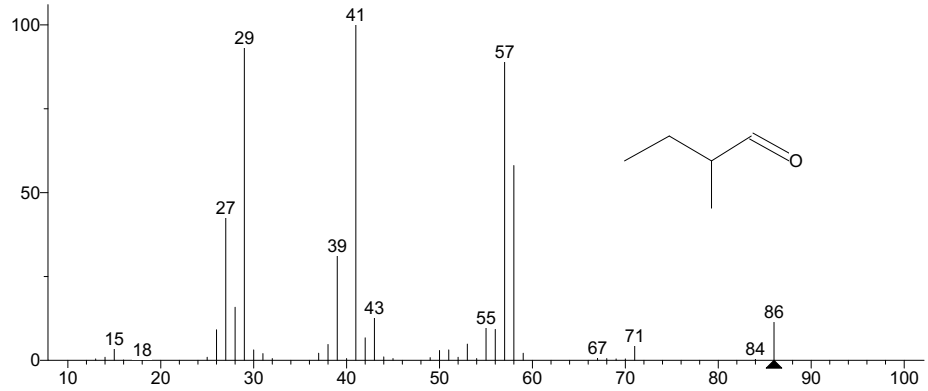

(mainlib) Butanal, 2-methyl-

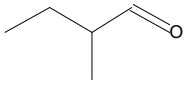

Name: Butanal, 2-methyl-
Formula: $C_5H_{10}O$
MW: 86 CAS#: 96-17-3 NIST#: 113208 ID#: 1828 DB: mainlib
Other DBs: Fine, TSCA, RTECS, NIH, EINECS, IRDB
Contributor: NIST Mass Spectrometry Data Center, 1990.
10 largest peaks:

41 999	29 930	57 888	58 580	27 425	39 312	28 158	43 127	86 113	55 97

40 m/z Values and Intensities:

13	4	14	9	15	34	16	1	18	1	25	9	26	91	27	425	28	158	29	930
30	31	31	20	32	5	37	21	38	47	39	312	40	5	41	999	42	67	43	127
44	10	45	5	49	8	50	29	51	31	52	9	53	48	54	5	55	97	56	92
57	888	58	580	59	21	67	6	68	5	69	4	70	4	71	44	84	5	86	113

Synonyms:
1.Butyraldehyde, 2-methyl-
2..alpha.-Methylbutanal
3..alpha.-Methylbutyraldehyde

Unknown: Average of 6.540 to 6.663 min.: 20210526_331_1TIL10.D\data.ms
Compound in Library Factor = 120

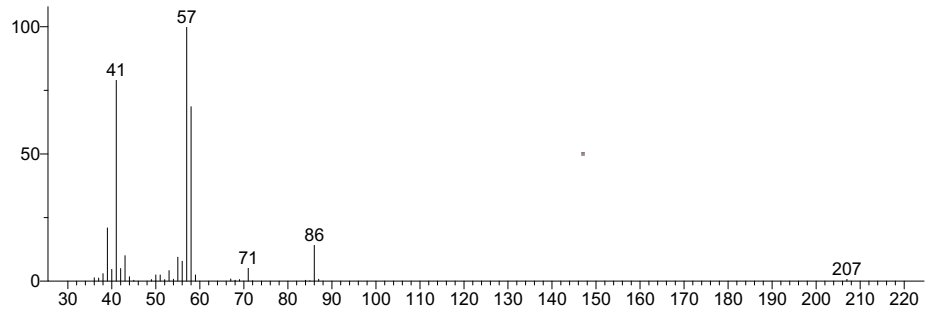

Hit 1 : Butanal, 2-methyl-
C5H10O; MF: 889; RMF: 897; Prob 74.9%; CAS: 96-17-3; Lib: mainlib; ID: 1828.

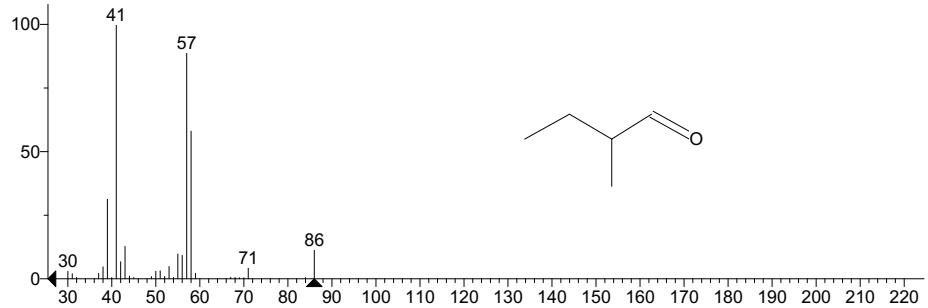

Hit 2 : Butanal, 2-methyl-
C5H10O; MF: 878; RMF: 883; Prob 74.9%; CAS: 96-17-3; Lib: replib; ID: 5082.

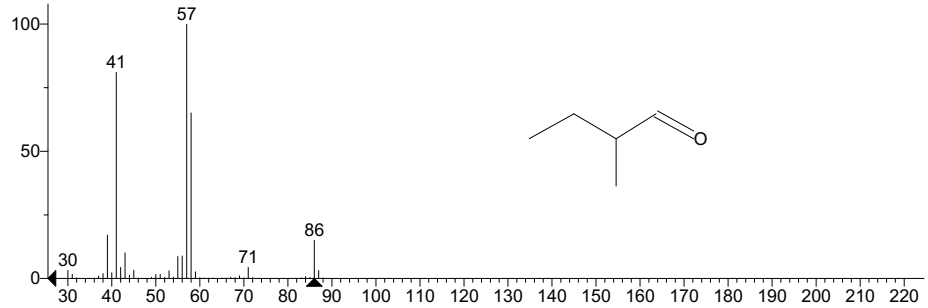

P 2-(trimethylsilyl)ethyl ((benzyloxy)carbonyl)-*L*-valinate (66)
P.1 ^{1}H-NMR for 66, 400 MHz, $CDCl_3$ (ppm)

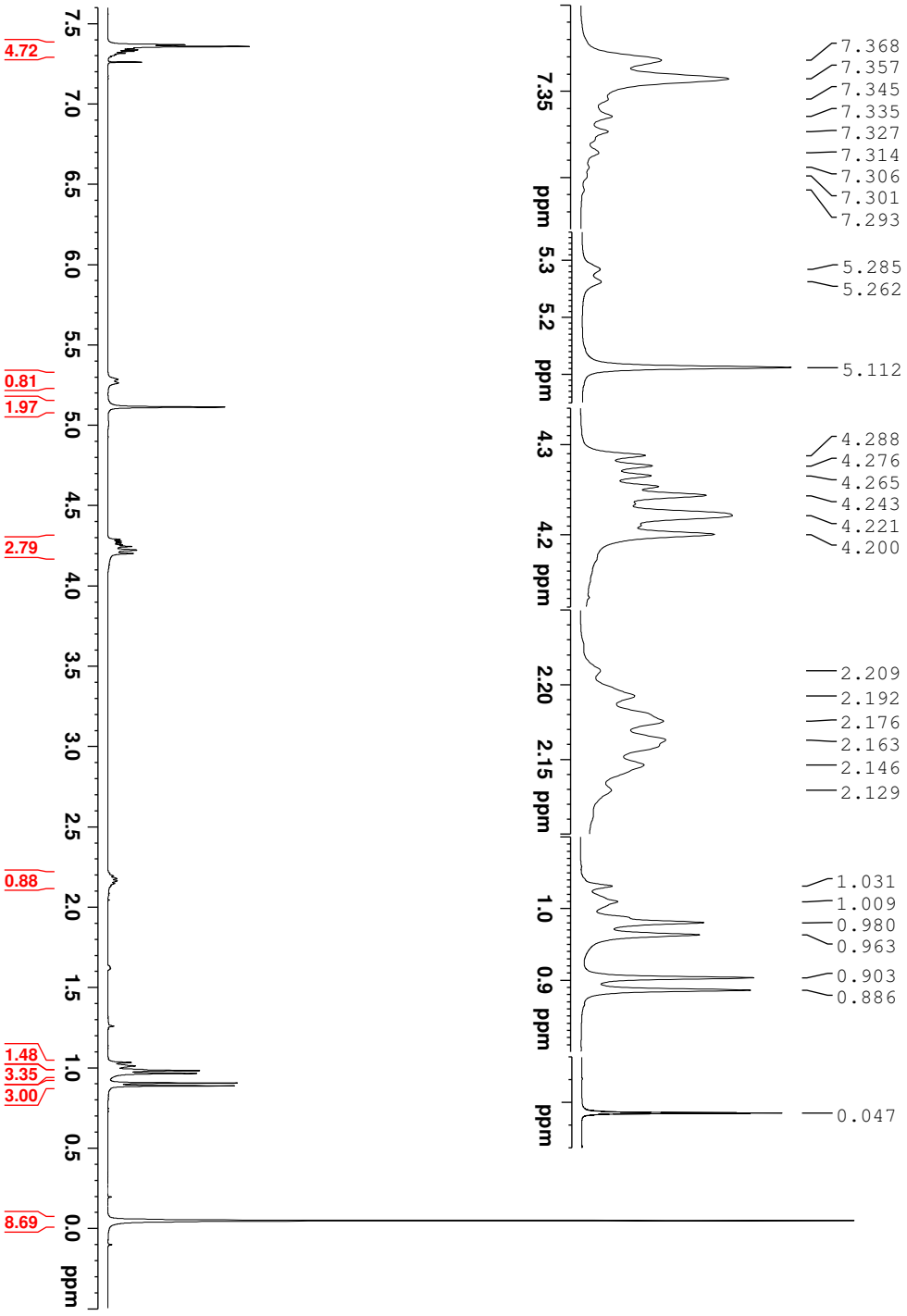

P.2 ^{1}H-NMR Spectrum of 66, 400 MHz, $CDCl_3$ (Hz)

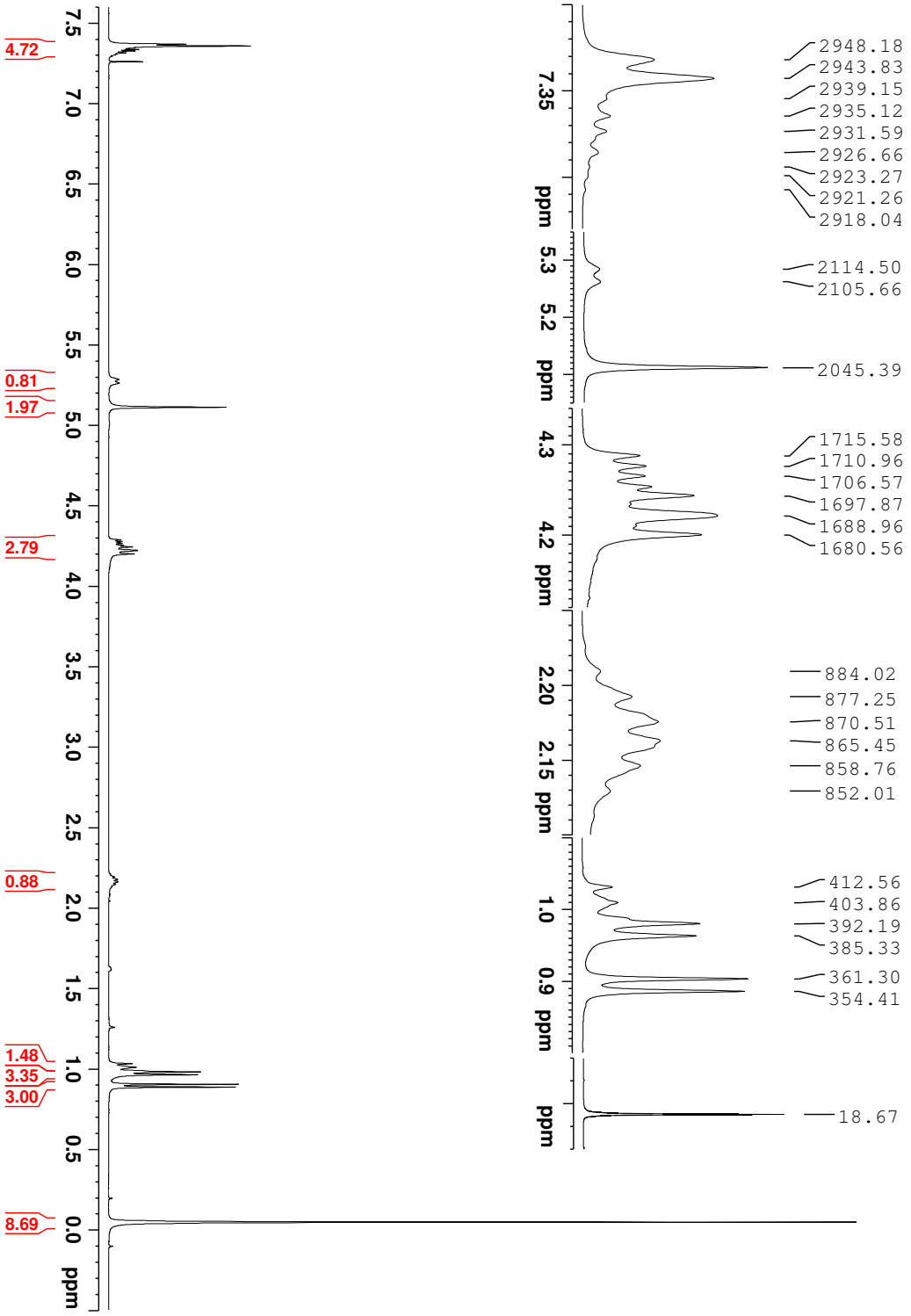

P.3 ^{13}C-NMR for 66, 400 MHz, $CDCl_3$ (ppm)

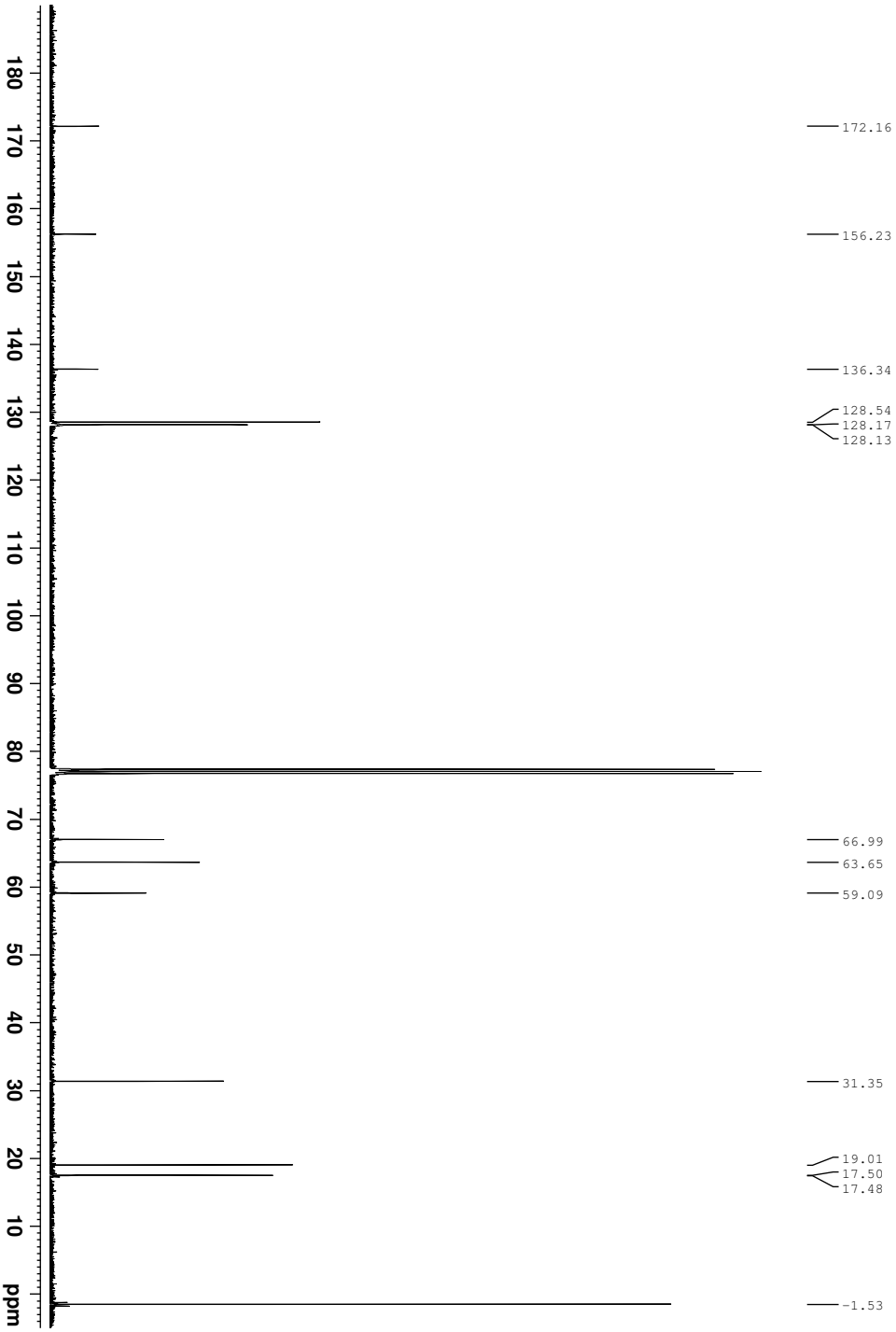

P.4 IR Spectrum of 66 (cm^{-1})

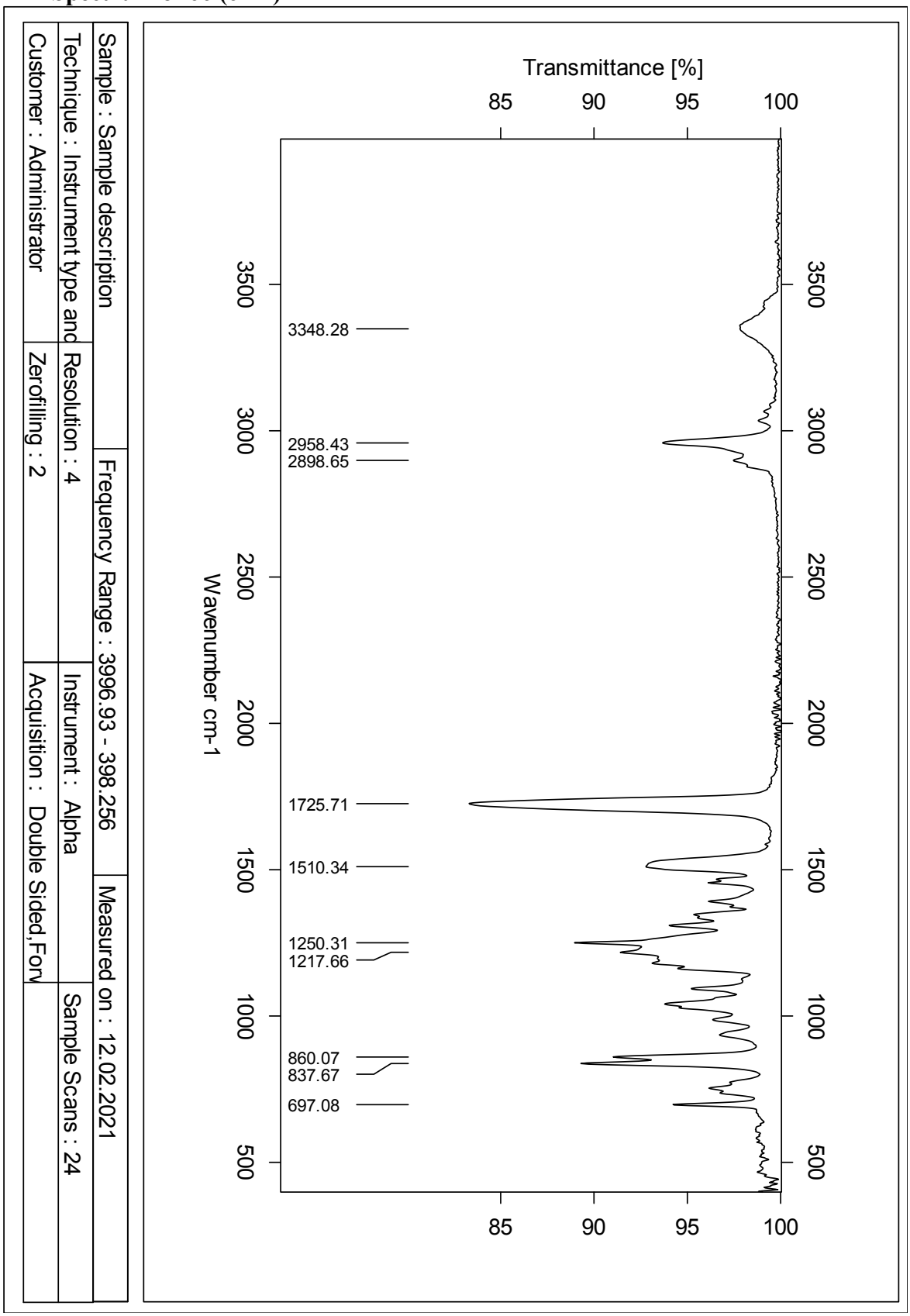

Elemental Composition Report

Single Mass Analysis

Tolerance = 3.0 PPM / DBE: min = -10.0, max = 50.0
Element prediction: Off
Number of isotope peaks used for i-FIT = 6

Monoisotopic Mass, Even Electron Ions
795 formula(e) evaluated with 2 results within limits (all results (up to 1000) for each mass)
Elements Used:
C: 0-100 H: 0-100 N: 0-3 O: 0-8 Na: 0-1 Si: 0-1

JA_20210218_58 82 (0.779) AM2 (Ar,35000.0,0.00,0.00); Cm (82:100)
1: TOF MS ES+

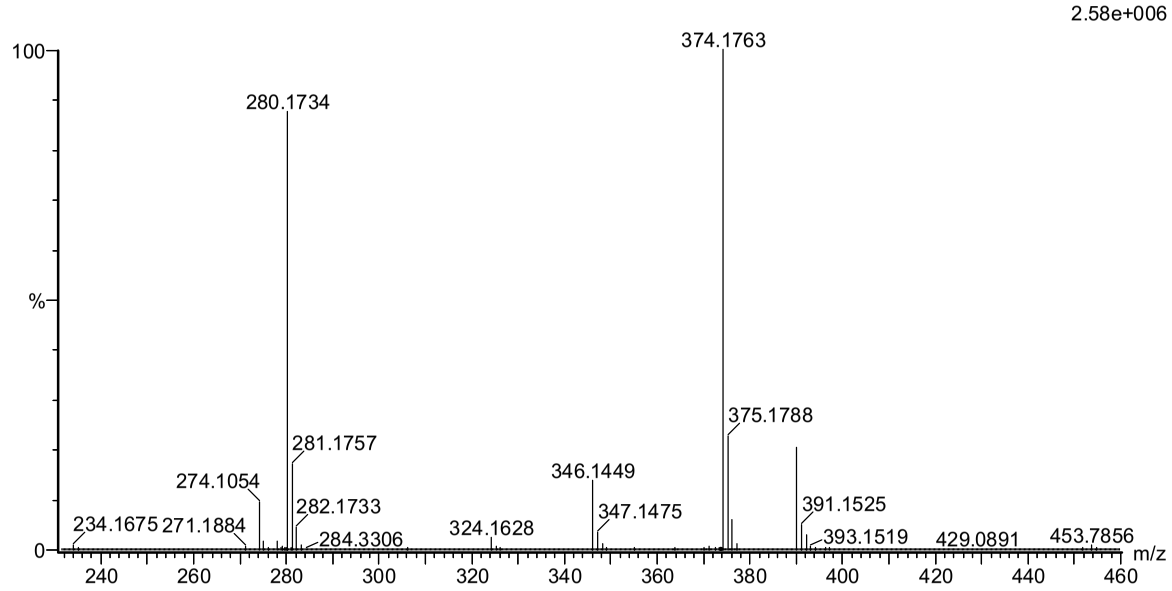

Minimum:				-10.0				
Maximum:		5.0	3.0	50.0				
Mass	Calc. Mass	mDa	PPM	DBE	i-FIT	Norm	Conf(%)	Formula
374.1763	374.1764	-0.1	-0.3	5.5	2282.3	0.000	100.00	C18 H29 N O4 Na Si
	374.1756	0.7	1.9	13.5	2294.7	12.346	0.00	C24 H24 N O3

Q 2-(trimethylsilyl)ethyl *L*-valinate (67)
Q.1 ^{1}H-NMR for 67, 400 MHz, $CDCl_3$ (ppm)

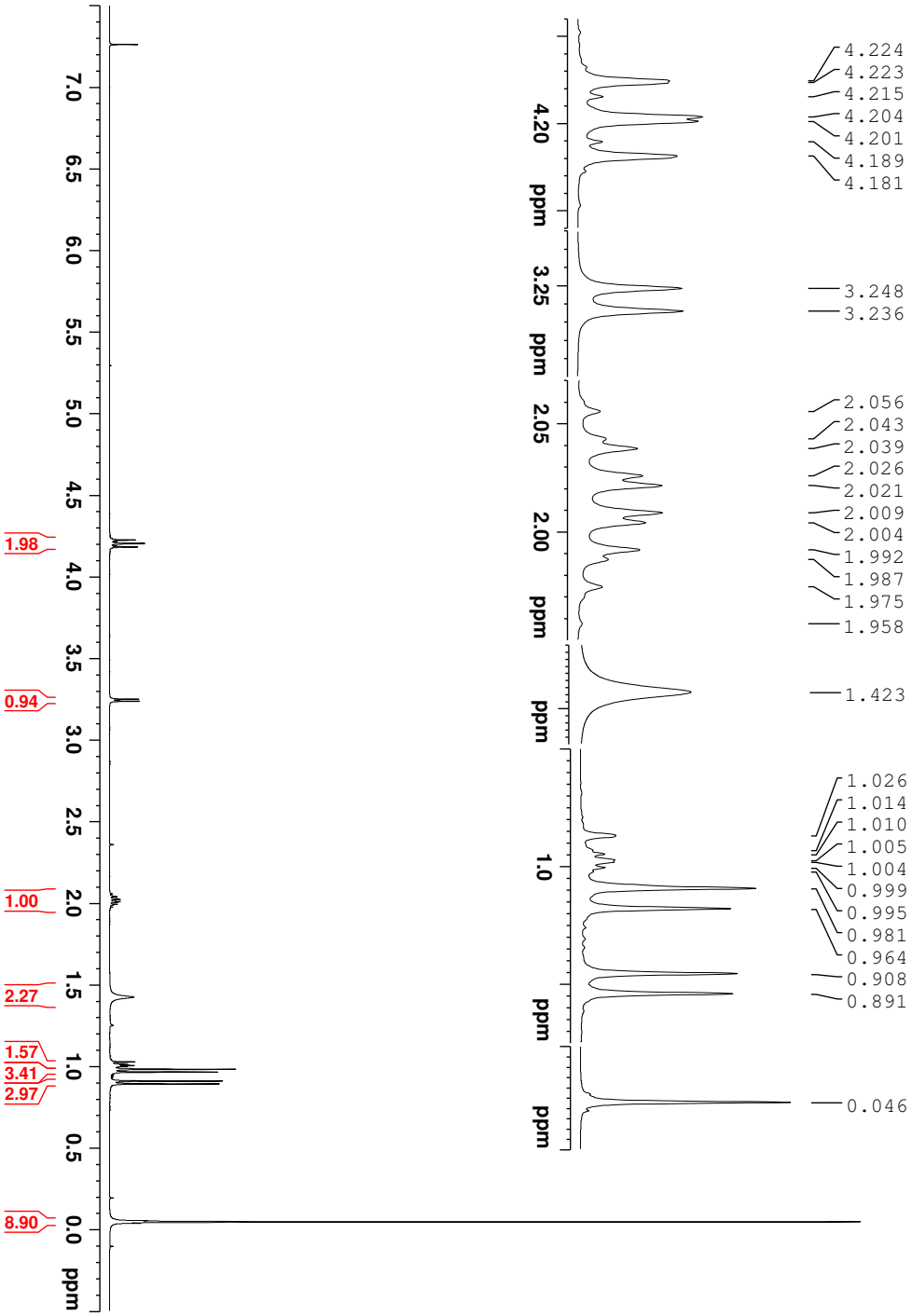

Q.2 ^{1}H-NMR Spectrum of 67, 400 MHz, $CDCl_3$ (Hz)

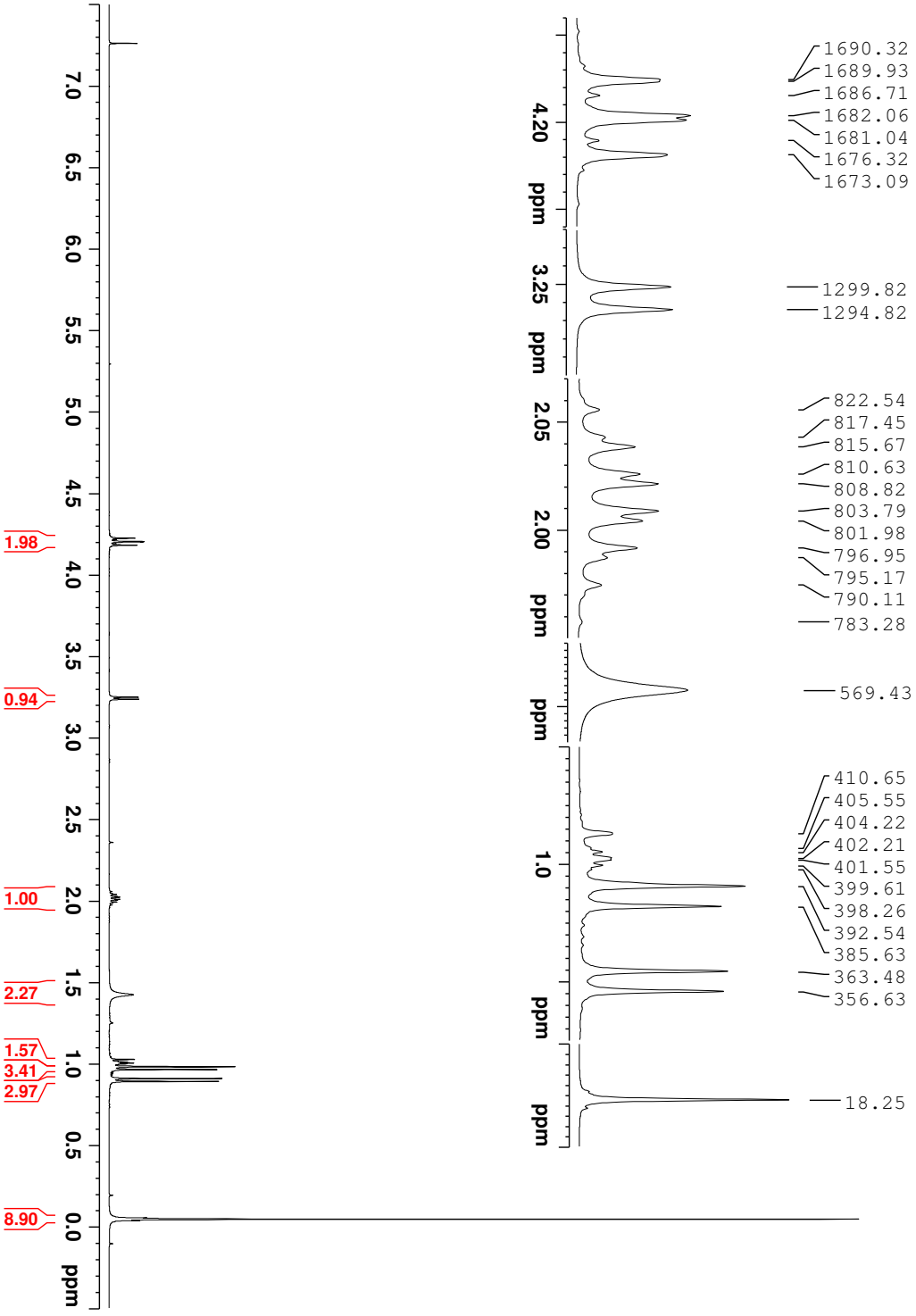

Q.3 ^{13}C-NMR Spectrum of 67, 400 MHz, $CDCl_3$ (ppm)

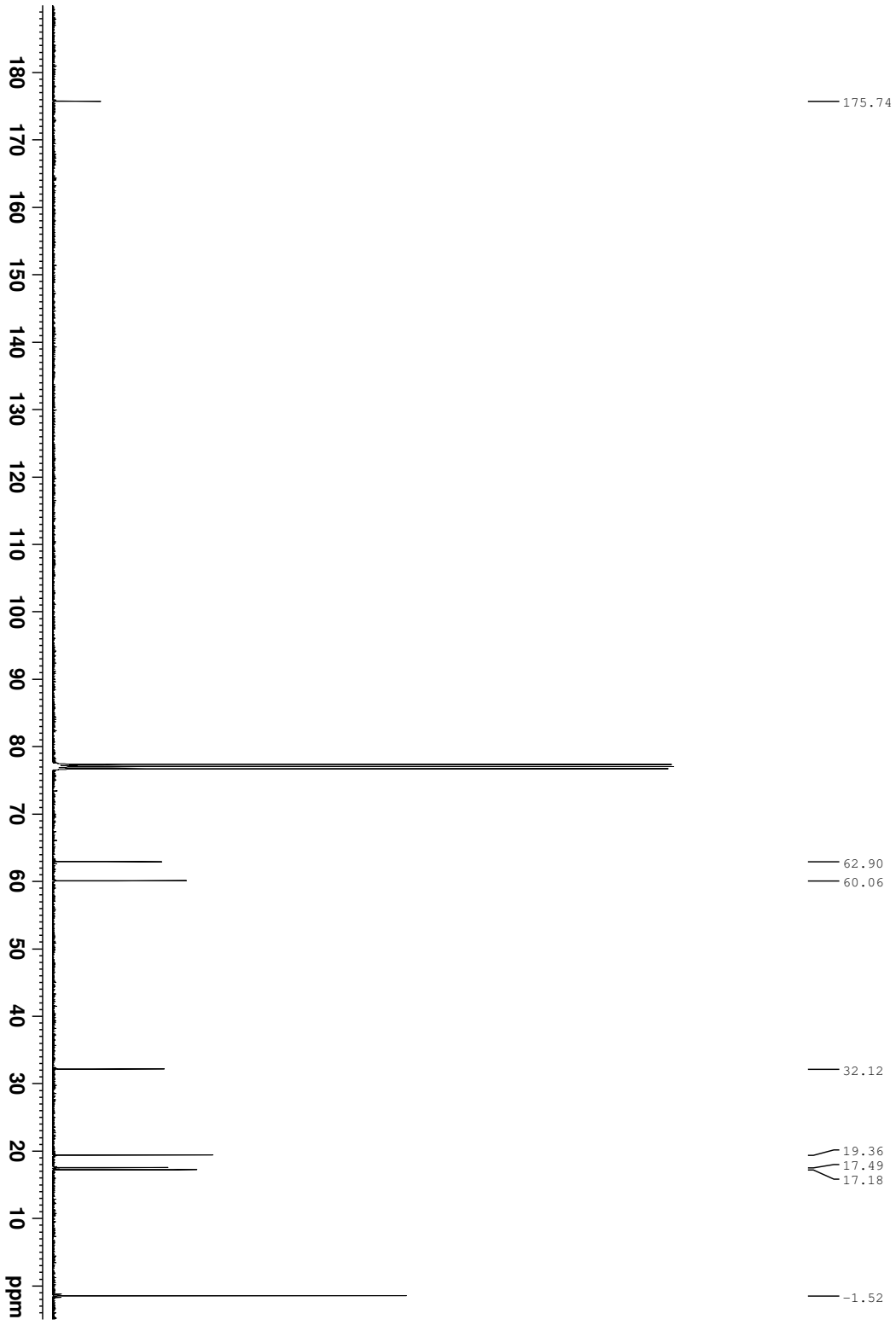

Q.4 IR Spectrum of 67 (cm^{-1})

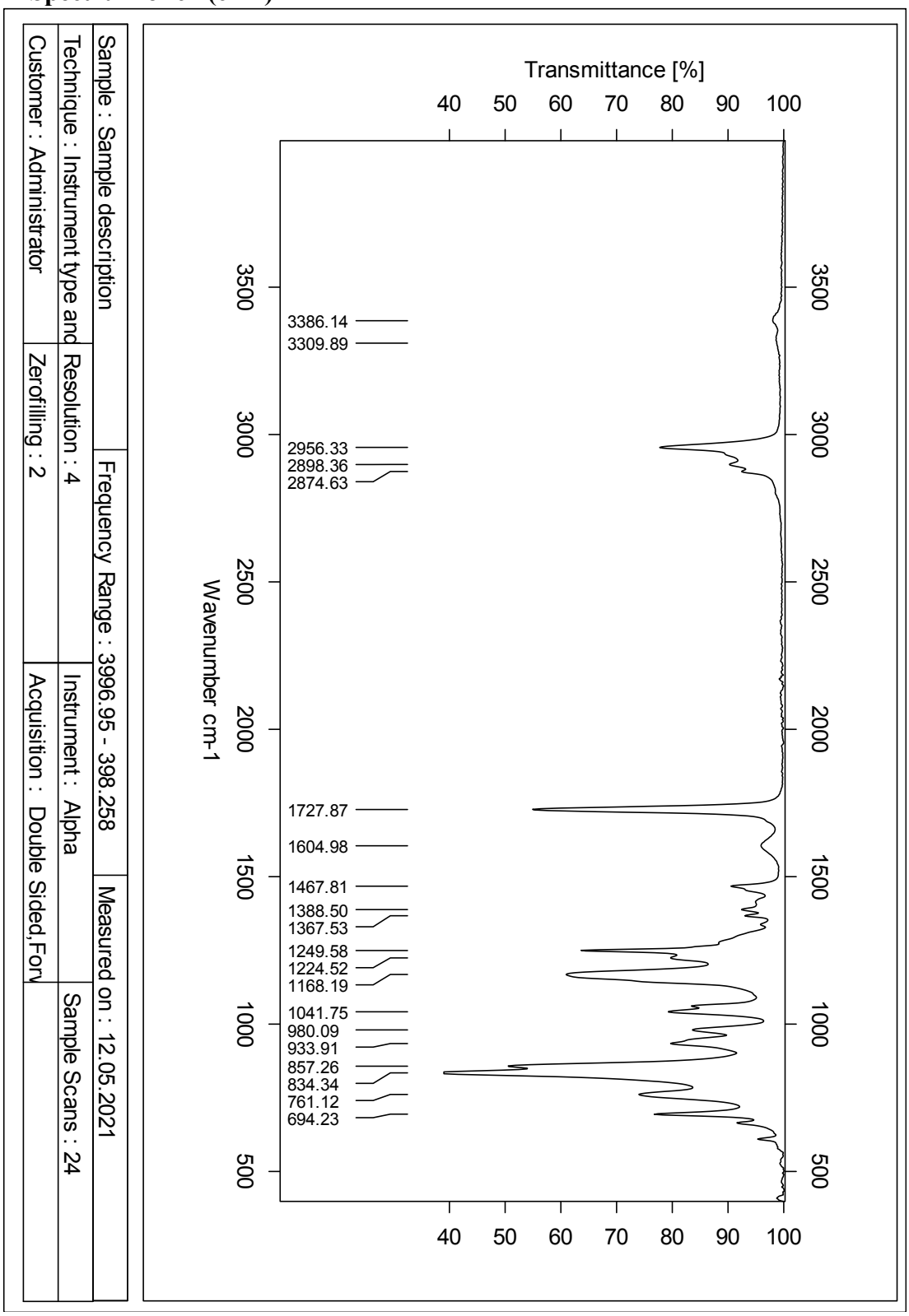

Elemental Composition Report

Single Mass Analysis

Tolerance = 2.0 PPM / DBE: min = -10.0, max = 50.0
Element prediction: Off
Number of isotope peaks used for i-FIT = 6

Monoisotopic Mass, Even Electron Ions
276 formula(e) evaluated with 1 results within limits (all results (up to 1000) for each mass)
Elements Used:
C: 0-100 H: 0-100 N: 0-5 O: 0-5 Si: 0-1

2021-115 17 (0.364) AM2 (Ar,35000.0,0.00,0.00); Cm (17:22)
1: TOF MS ASAP+

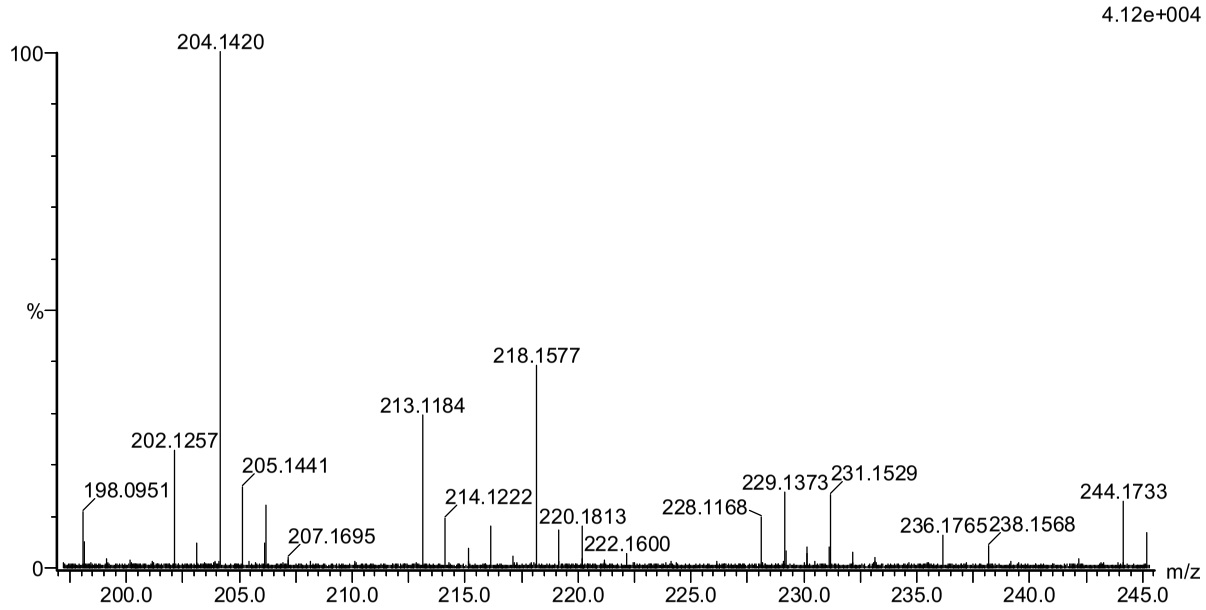

Minimum:				-10.0				
Maximum:		5.0	2.0	50.0				
Mass	Calc. Mass	mDa	PPM	DBE	i-FIT	Norm	Conf(%)	Formula
204.1420	204.1420	0.0	0.0	0.5	2878.6	n/a	n/a	C9 H22 N O2 Si

R Methyl 7-oxoheptanoate (69)
R.1 ^{1}H-NMR for 69, 400 MHz, $CDCl_3$ (ppm)

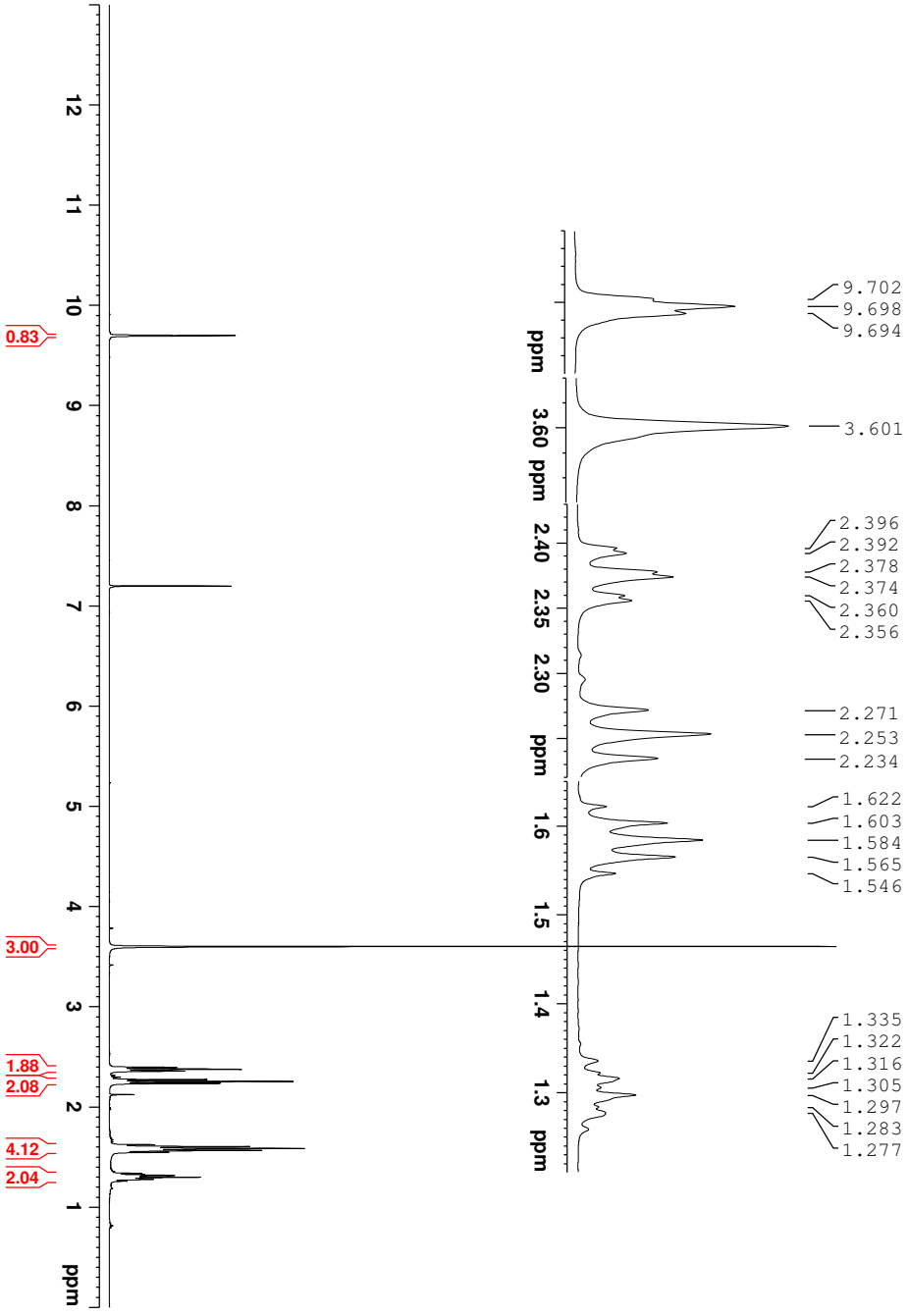

R.2 ^{1}H-NMR for 69, 400 MHz, $CDCl_3$ (Hz)

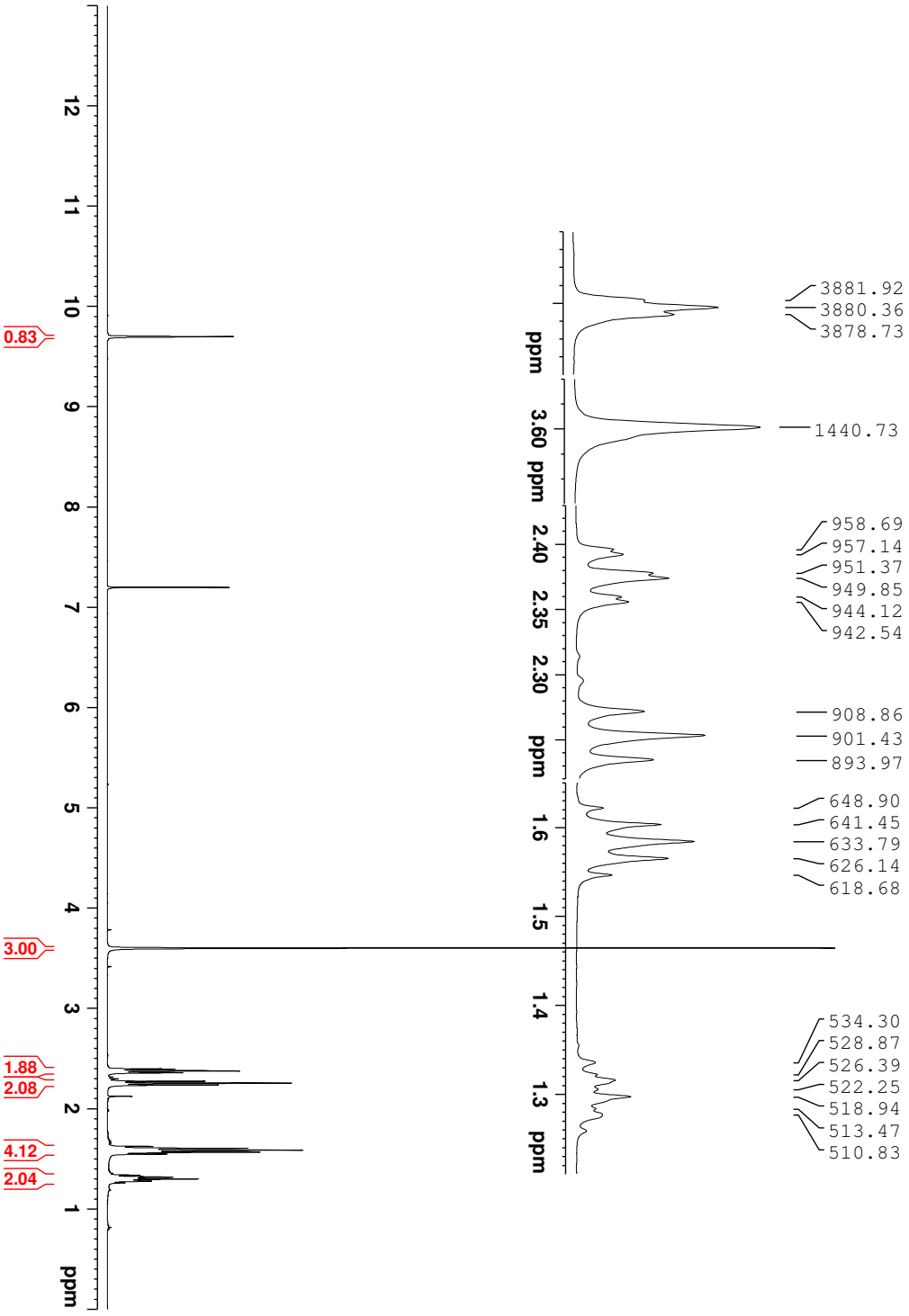

R.3 ^{13}C-NMR for 69, 400 MHz, $CDCl_3$ (ppm)

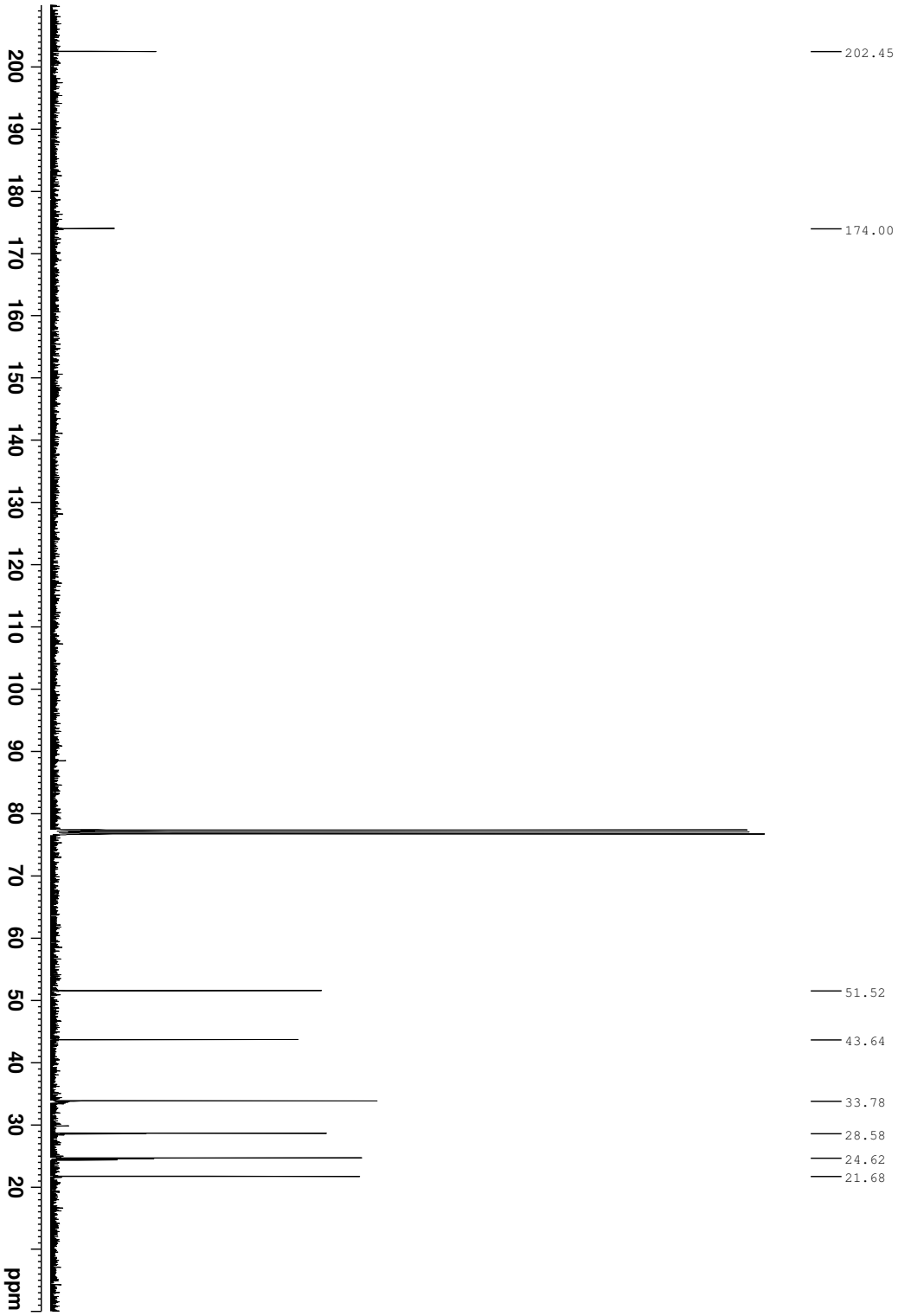

R.4 IR Spectrum of 69 (cm^{-1})

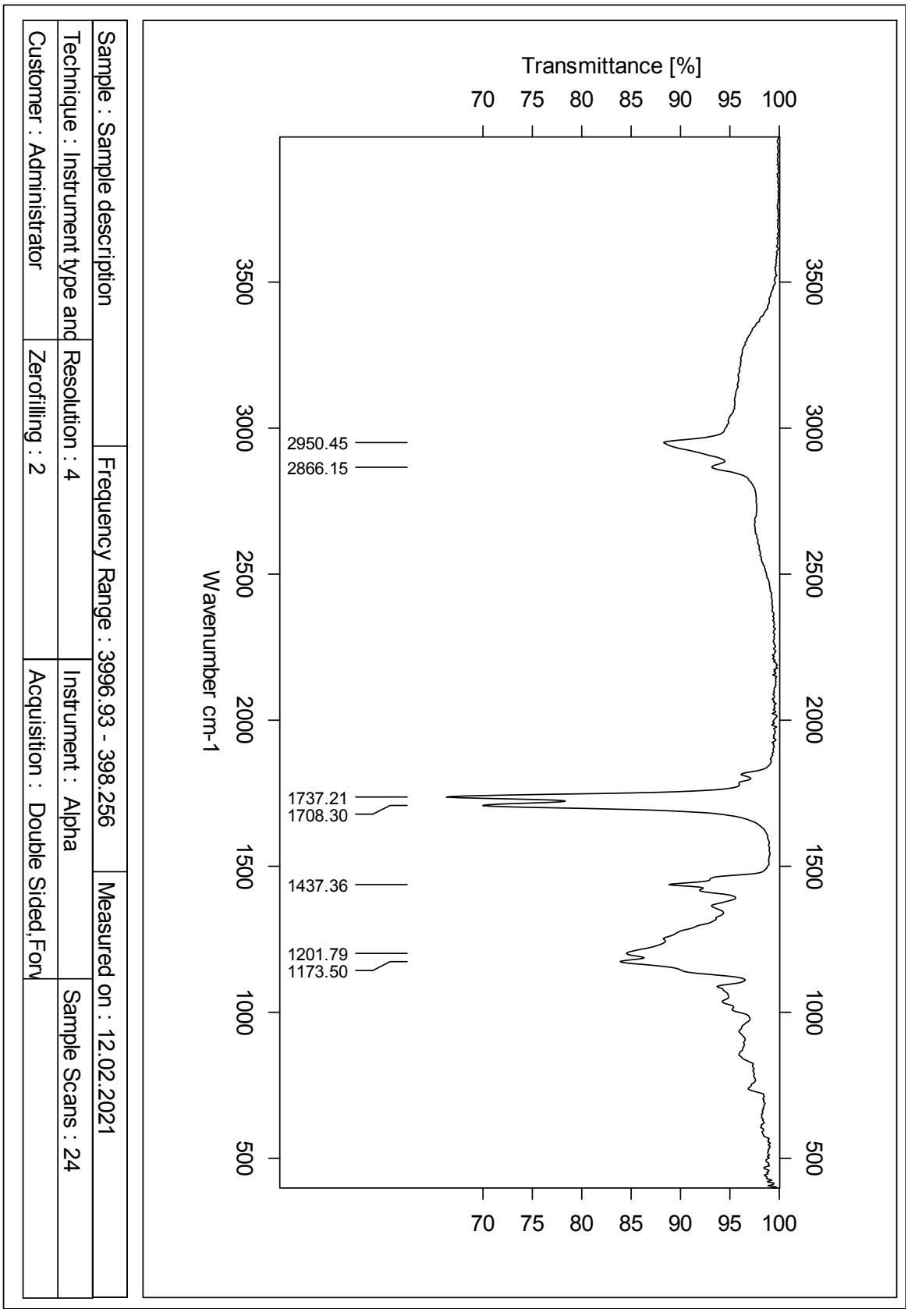

Single Mass Analysis

Tolerance = 2.0 PPM / DBE: min = -10.0, max = 50.0
Element prediction: Off
Number of isotope peaks used for i-FIT = 6

Monoisotopic Mass, Even Electron Ions
191 formula(e) evaluated with 1 results within limits (all results (up to 1000) for each mass)
Elements Used:
C: 0-100 H: 0-100 N: 0-2 O: 0-10 Na: 0-1
2021-96 59 (0.661) AM2 (Ar,35000.0,0.00,0.00); Cm (55:59)
1: TOF MS ES+

4.32e+005

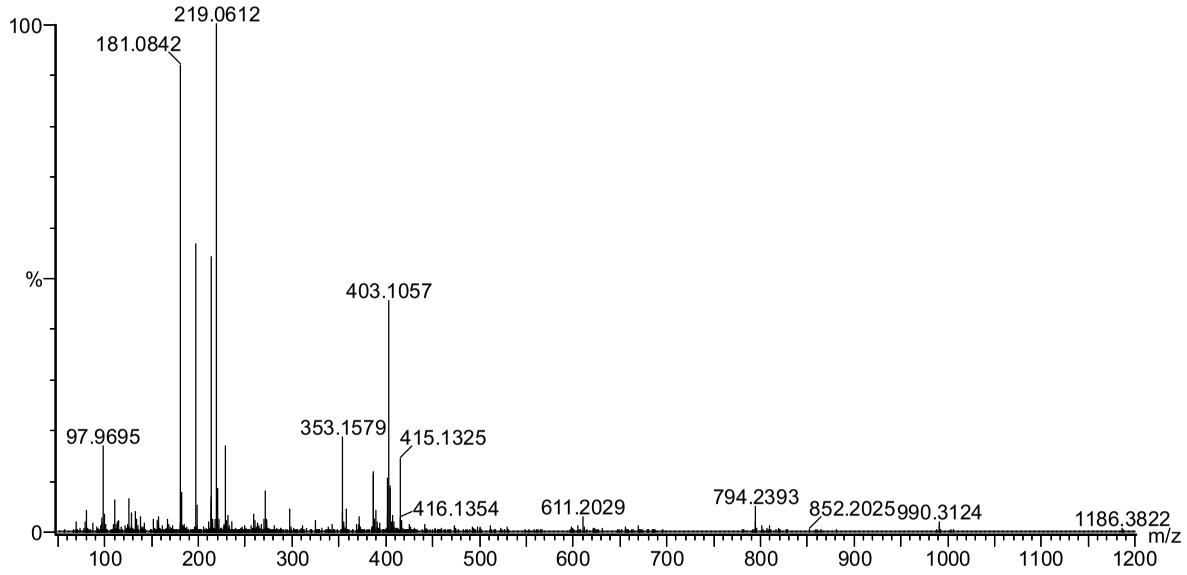

Minimum:				-10.0				
Maximum:		5.0	2.0	50.0				
Mass	Calc. Mass	mDa	PPM	DBE	i-FIT	Norm	Conf(%)	Formula
181.0842	181.0841	0.1	0.6	1.5	3215.1	n/a	n/a	C8 H14 O3 Na

S Methyl oct-7-ynoate (70)
S.1 ^{1}H-NMR for 70, 400 MHz, $CDCl_3$ (ppm)

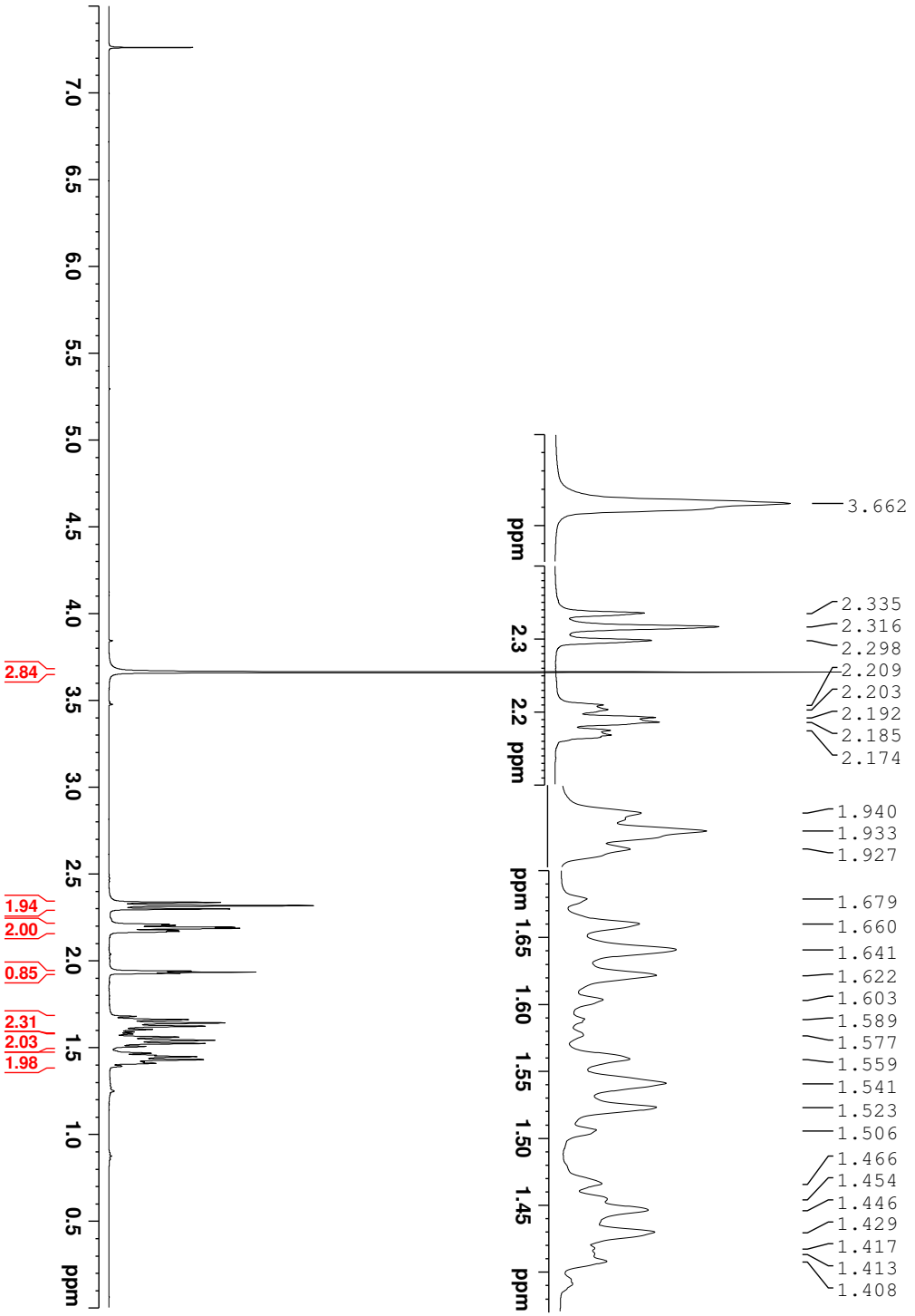

S.2 ^{1}H-NMR Spectrum of 70, 400 MHz, $CDCl_3$ (Hz)

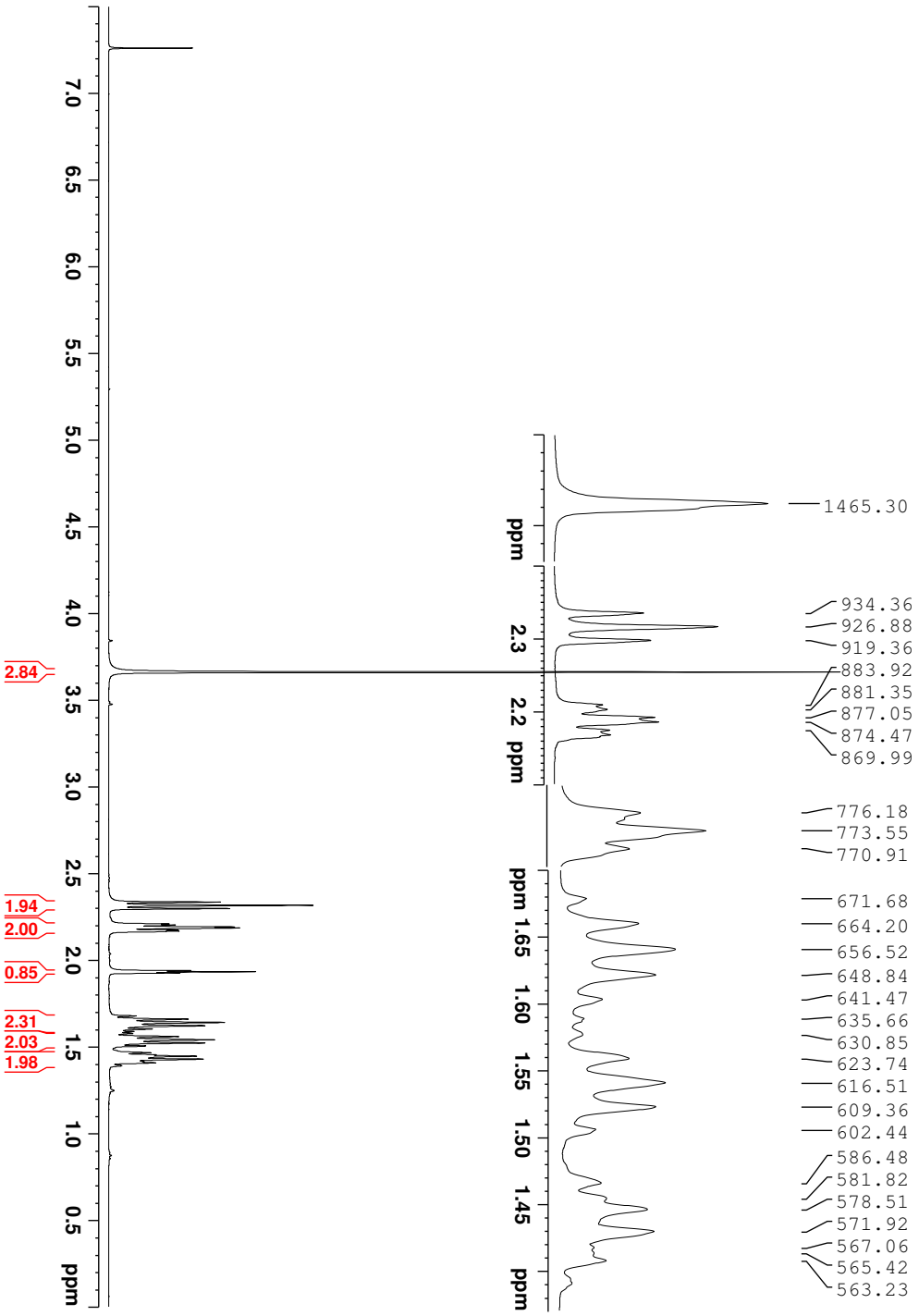

S.3 ^{13}C-NMR for 70, 400 MHz, $CDCl_3$ (ppm)

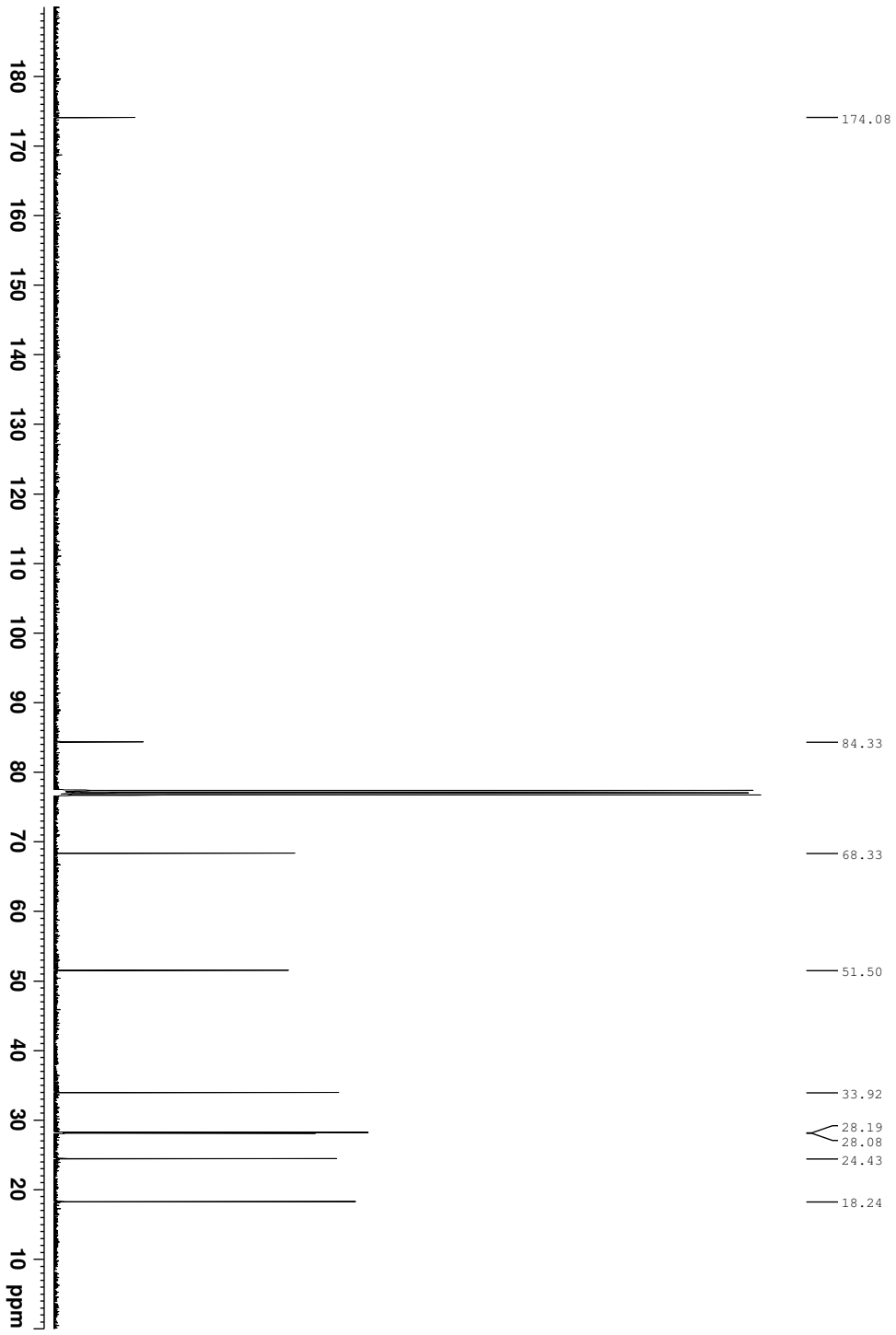

S.4 IR Spectrum of 70 (cm^{-1})

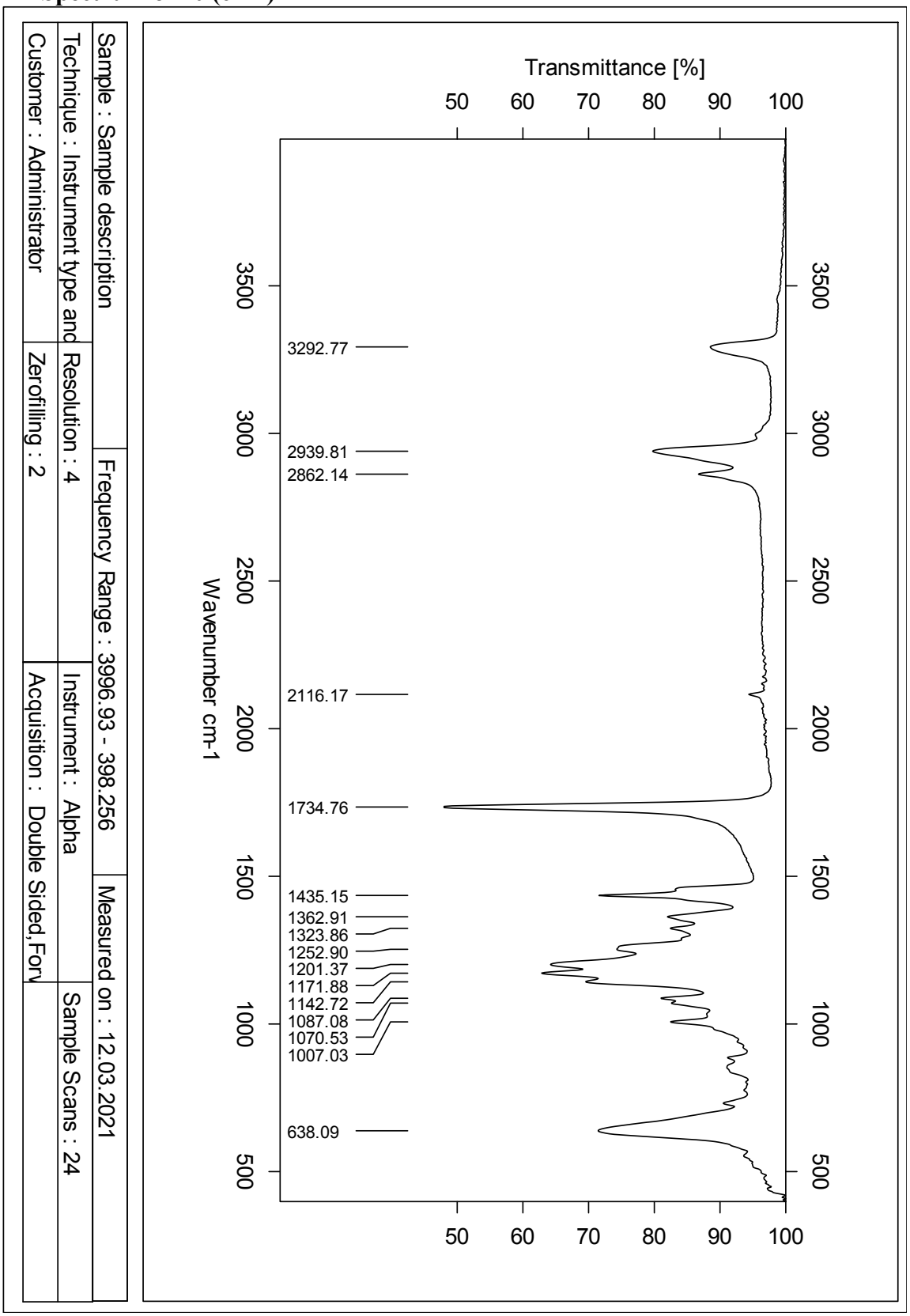

Sample : Sample description		Frequency Range : 3996.93 - 398.256	Measured on : 12.03.2021
Technique : Instrument type and	Resolution : 4	Instrument : Alpha	Sample Scans : 24
Customer : Administrator	Zerofilling : 2	Acquisition : Double Sided,Forv	

Elemental Composition Report

Single Mass Analysis

Tolerance = 2.0 PPM / DBE: min = -10.0, max = 50.0
Element prediction: Off
Number of isotope peaks used for i-FIT = 6

Monoisotopic Mass, Even Electron Ions
109 formula(e) evaluated with 1 results within limits (all results (up to 1000) for each mass)
Elements Used:
C: 0-100 H: 0-100 N: 0-1 O: 0-10 Na: 0-1
2021-148 15 (0.310) AM2 (Ar,35000.0,0.00,0.00); Cm (13:16)
1: TOF MS ASAP+

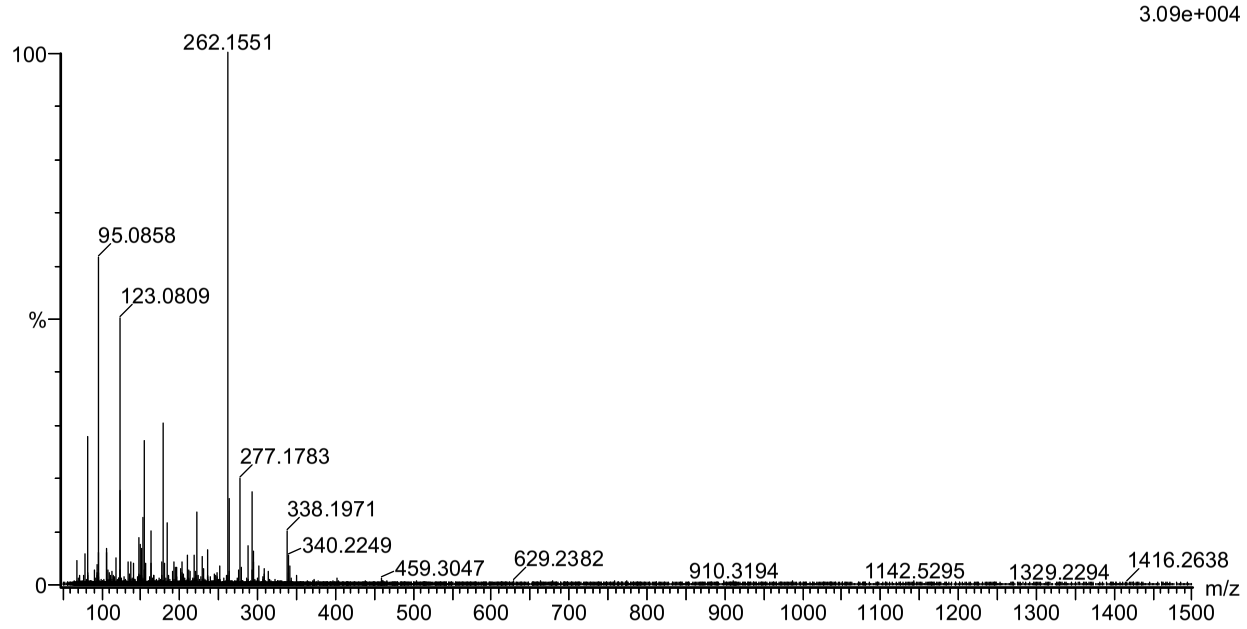

Minimum:				-10.0				
Maximum:		5.0	2.0	50.0				
Mass	Calc. Mass	mDa	PPM	DBE	i-FIT	Norm	Conf(%)	Formula
155.1070	155.1072	-0.2	-1.3	2.5	1189.6	n/a	n/a	C9 H15 O2

T Oct-7-ynoic acid (71)
T.1 ^{1}H-NMR for 71, 400 MHz, $CDCl_3$ (ppm)

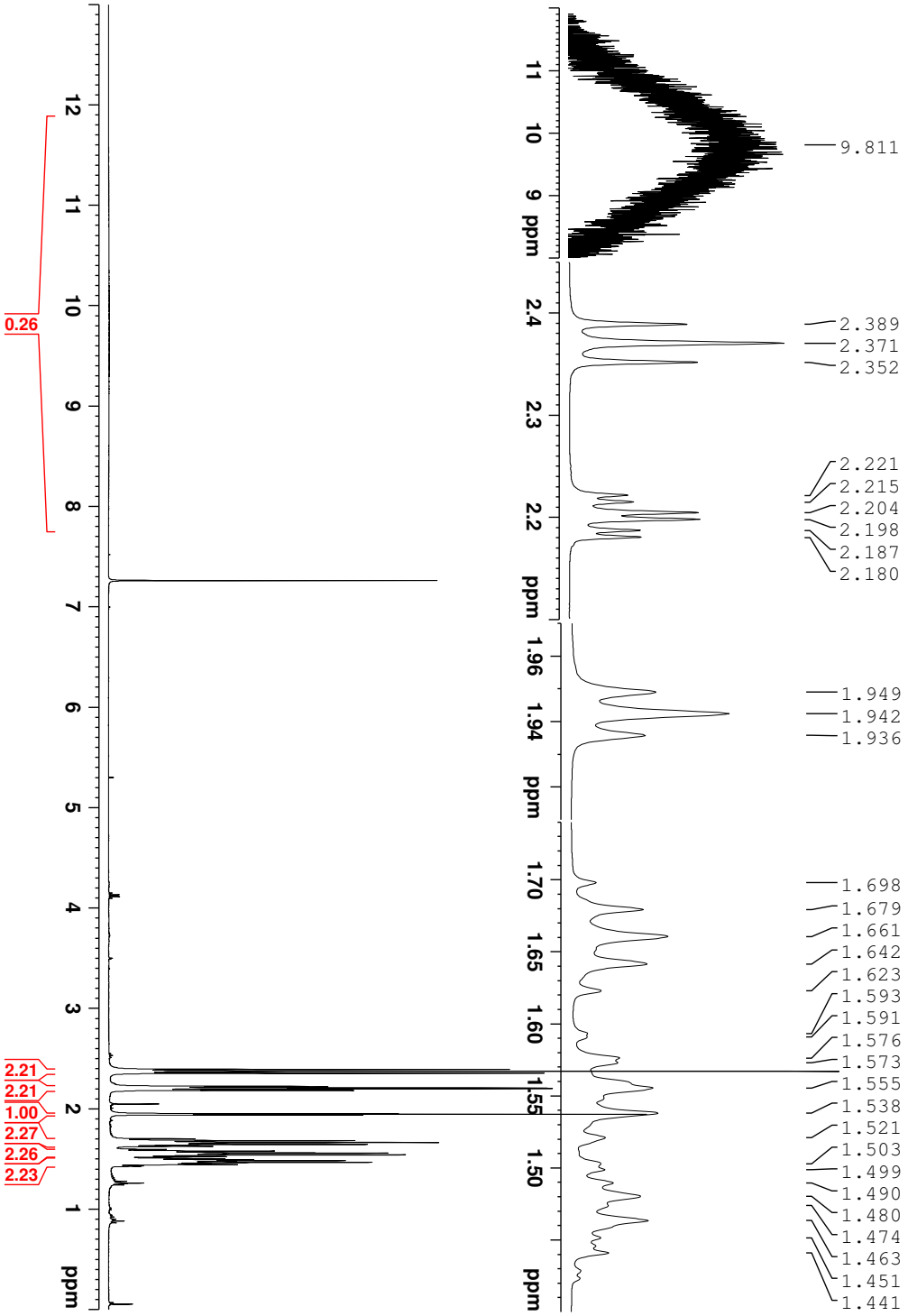

T.2 ^{1}H-NMR Spectrum of 71, 400 MHz, $CDCl_3$ (Hz)

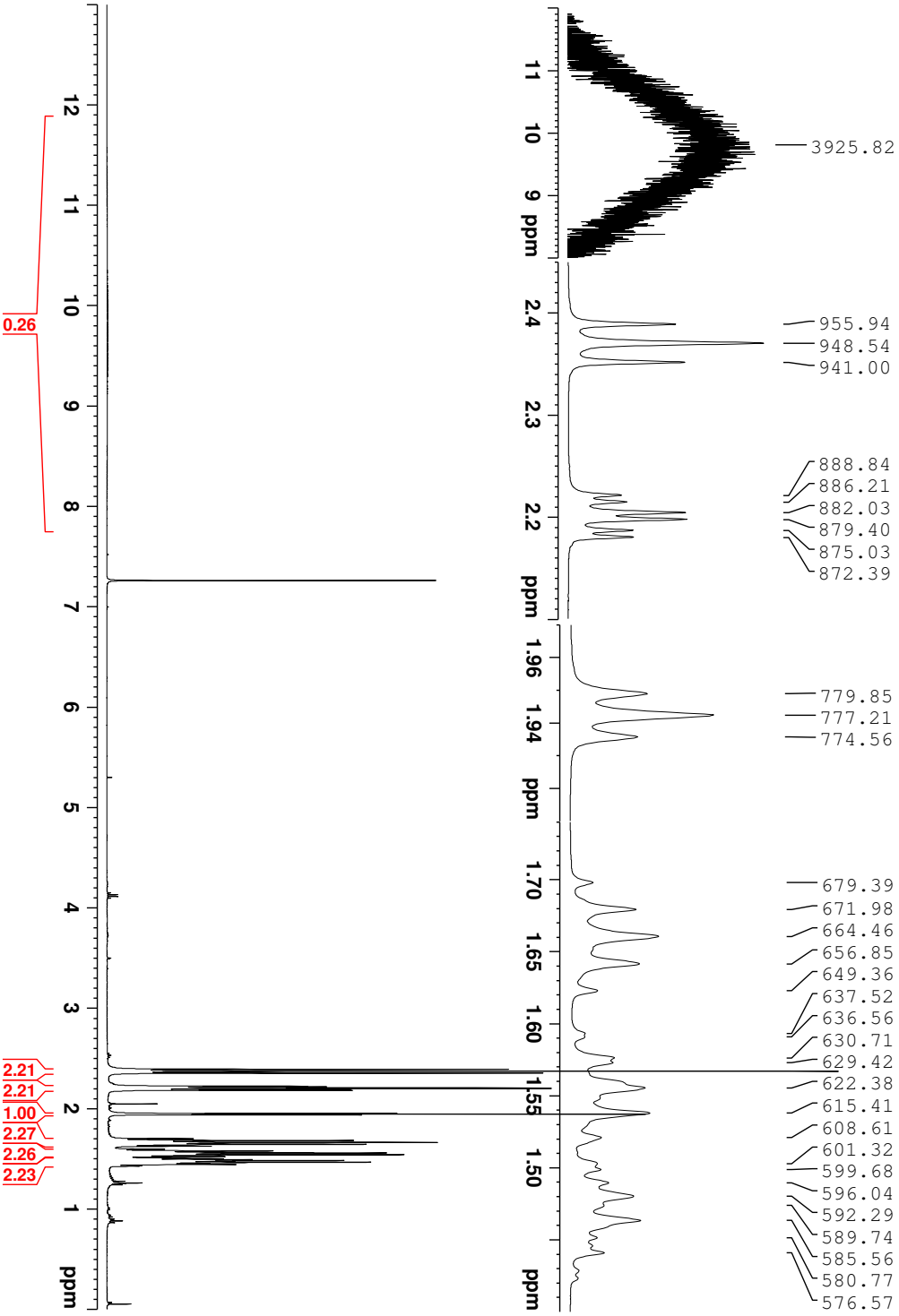

T.3 ^{13}C-NMR Spectrum of 71, 400 MHz, $CDCl_3$ (ppm)

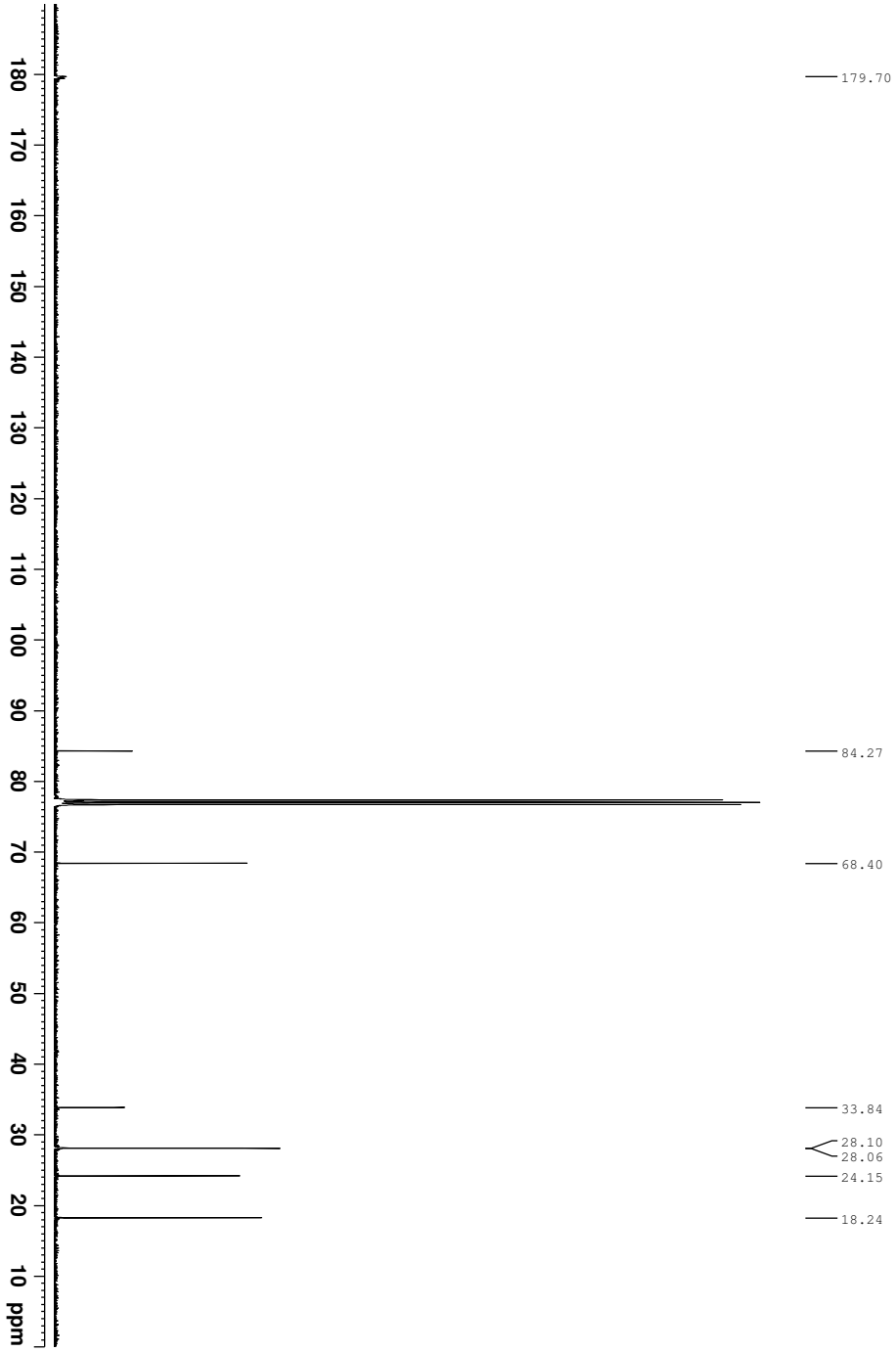

T.4 IR Spectrum of 71 (cm^{-1})

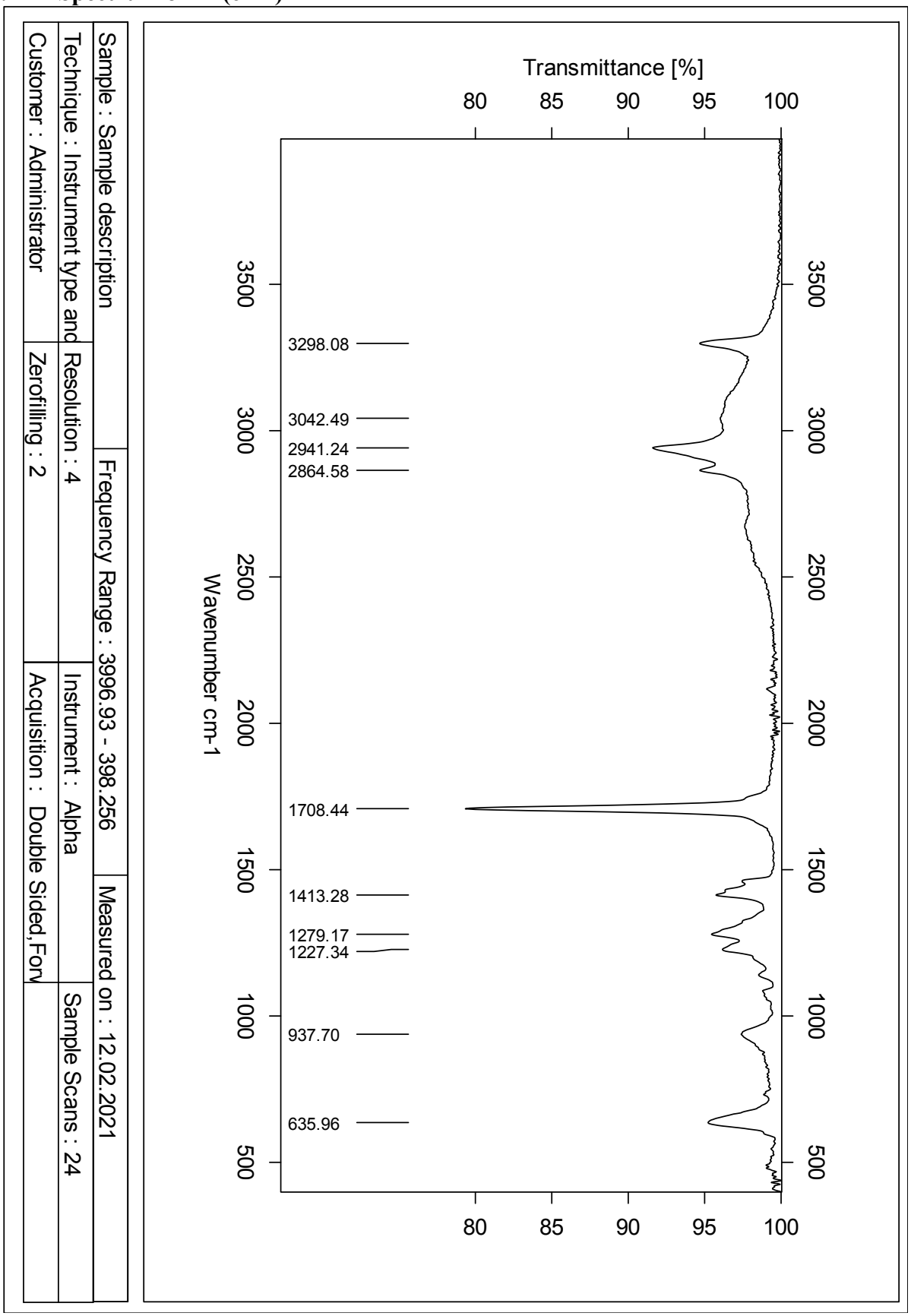

Elemental Composition Report

Single Mass Analysis

Tolerance = 15.0 PPM / DBE: min = -10.0, max = 50.0
Element prediction: Off
Number of isotope peaks used for i-FIT = 6

Monoisotopic Mass, Even Electron Ions
225 formula(e) evaluated with 1 results within limits (all results (up to 1000) for each mass)
Elements Used:
C: 0-100 H: 0-100 N: 0-12 O: 0-5 Na: 0-1
2021-177ESIWATER 52 (0.589) AM2 (Ar,35000.0,0.00,0.00)
1: TOF MS ES-

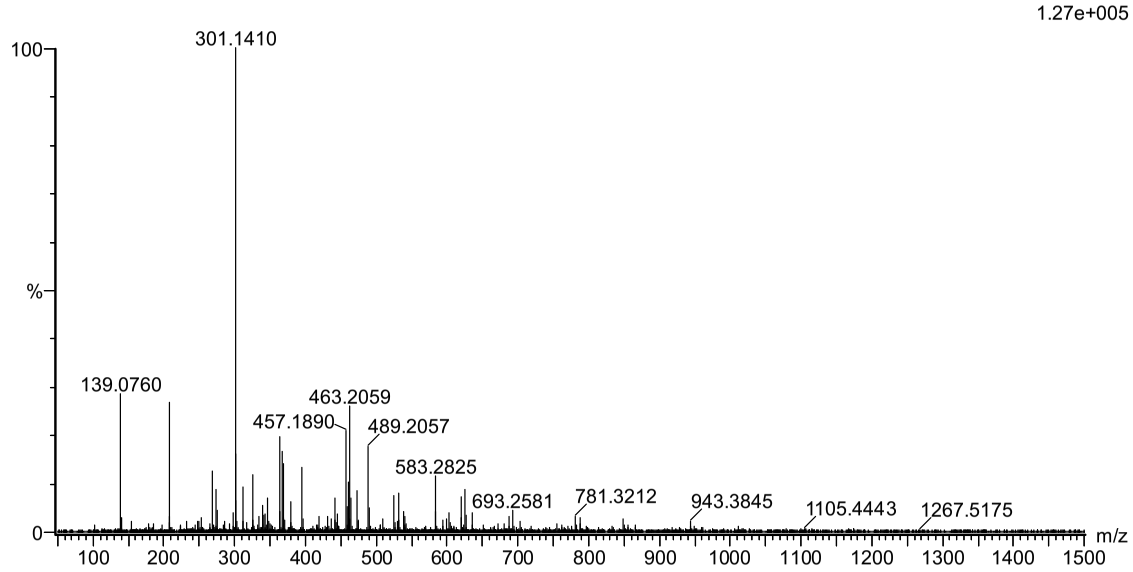

Minimum:				-10.0				
Maximum:		5.0	15.0	50.0				
Mass	Calc. Mass	mDa	PPM	DBE	i-FIT	Norm	Conf(%)	Formula
139.0760	139.0759	0.1	0.7	3.5	1824.7	n/a	n/a	C8 H11 O2

U 2-(trimethylsilyl)ethyl oct-7-ynoyl-*L*-valinate (72)

U.1 ^{1}H-NMR for 72, 400 MHz, $CDCl_3$ (ppm)

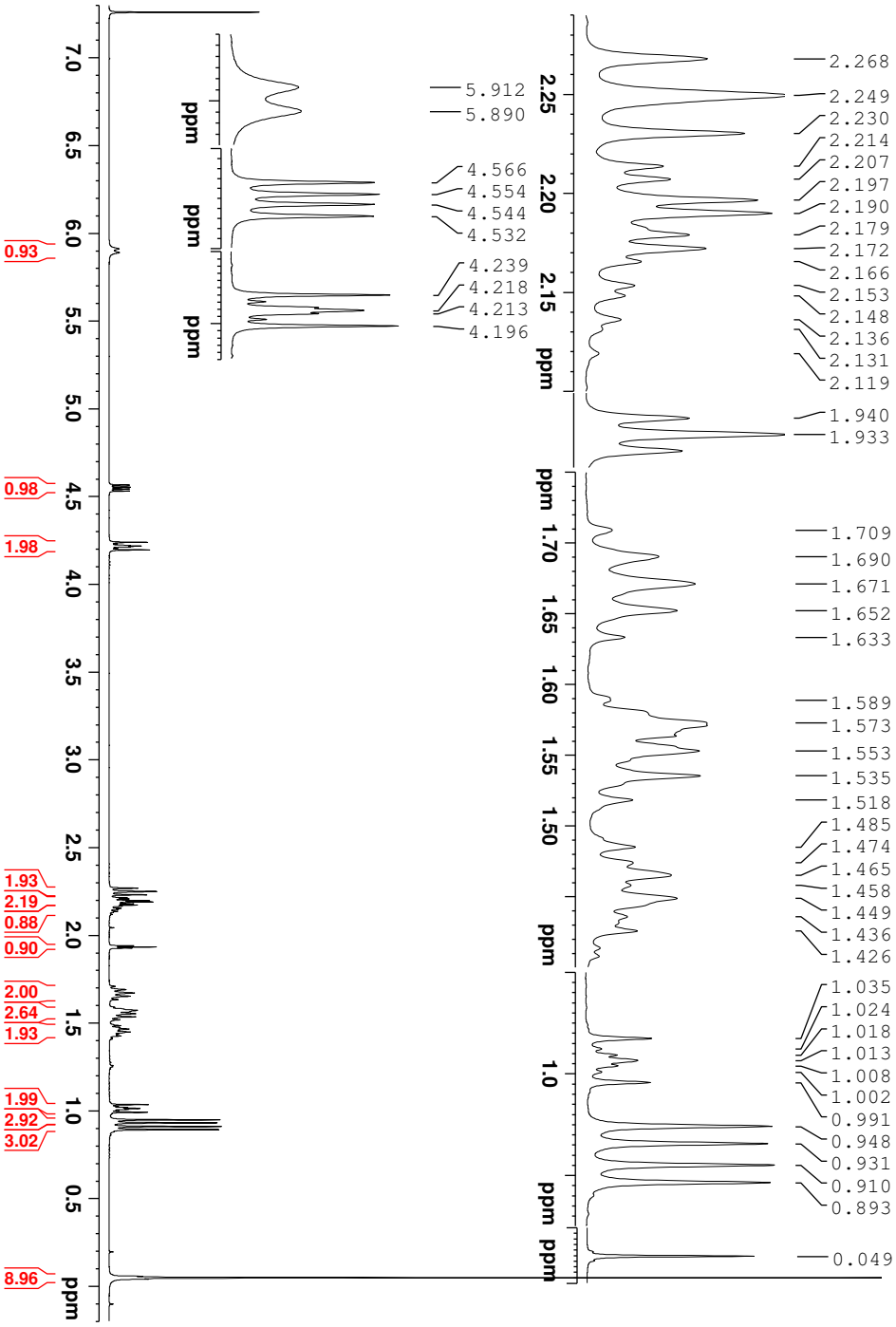

U.2 ^{1}H-NMR for 72, 400 MHz, $CDCl_3$ (Hz)

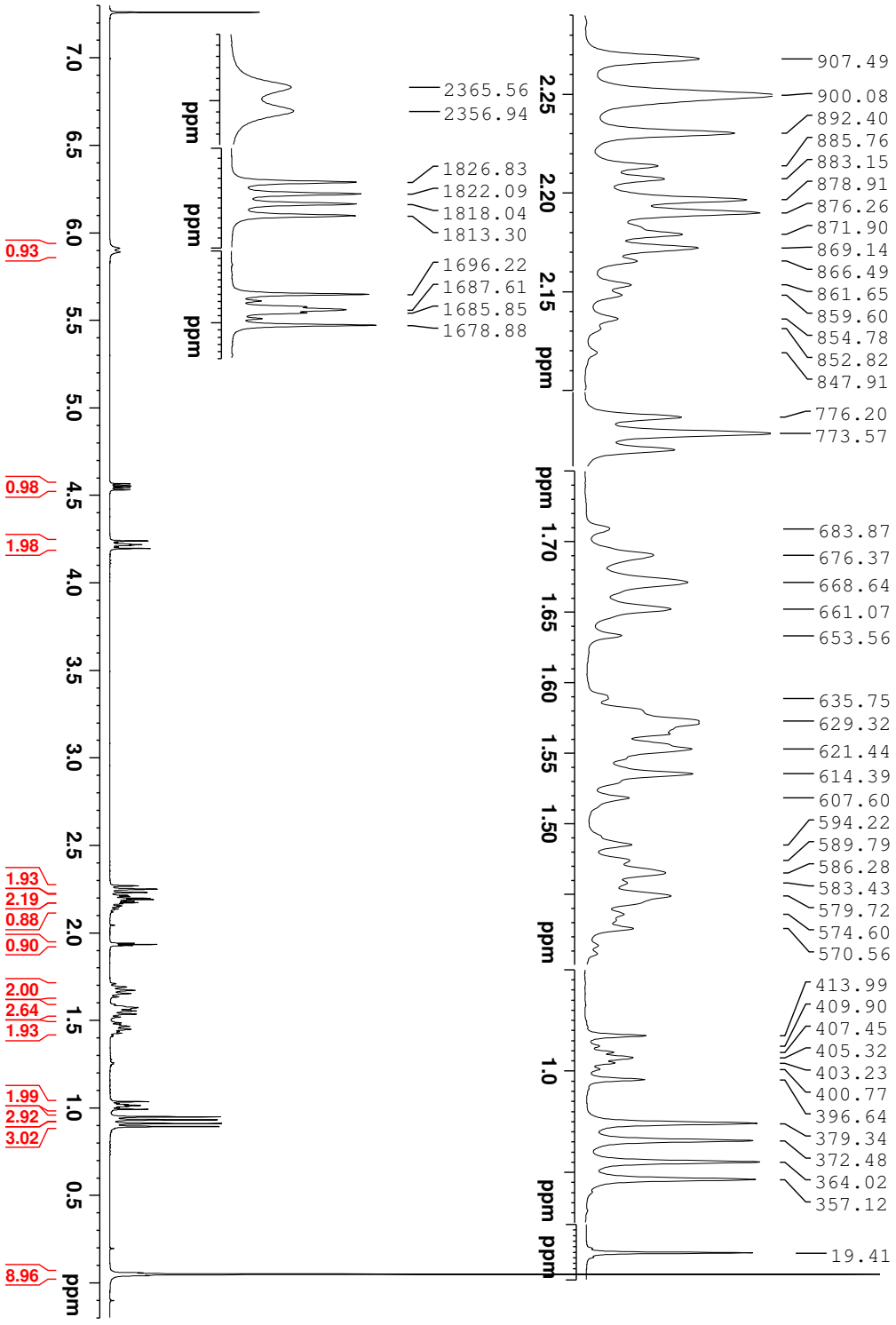

U.3 ^{13}C-NMR for 72, 400 MHz, $CDCl_3$ (ppm)

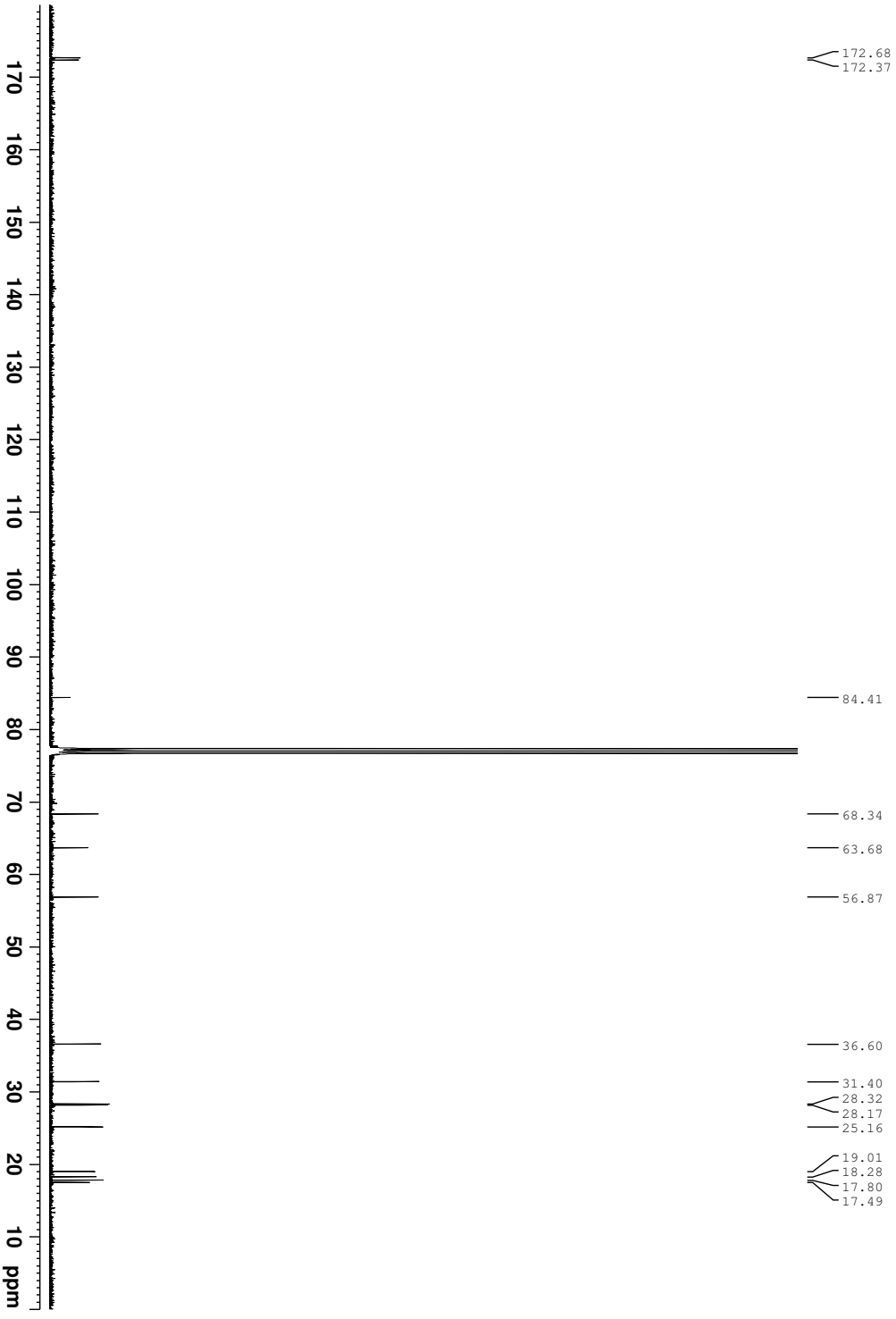

U.4 ^{1}H-^{1}H-COSY for 72, 400 MHz, $CDCl_3$ (ppm)

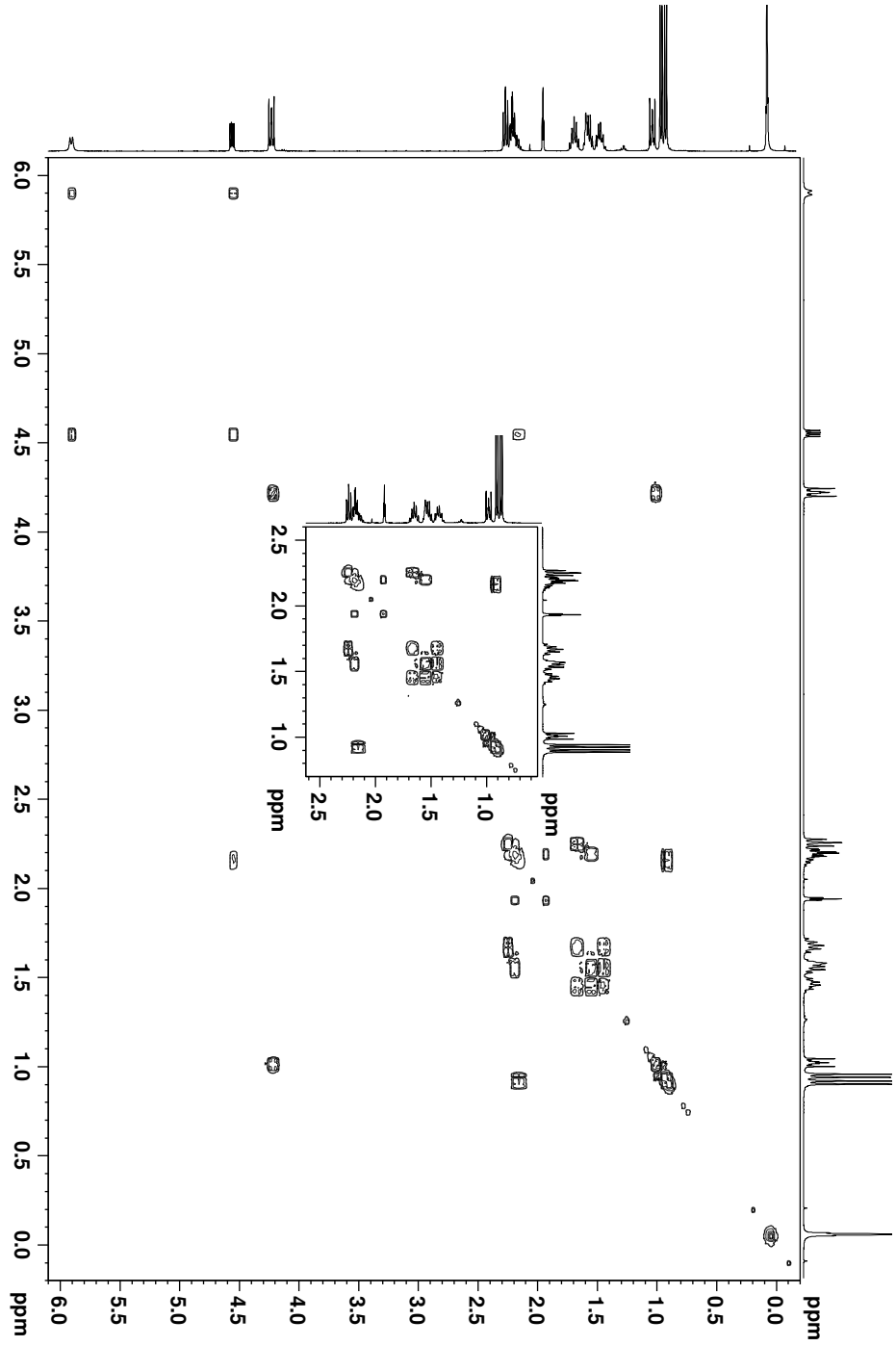

U.5 ^{1}H-^{13}C HSQC for 72, 400 MHz, $CDCl_3$

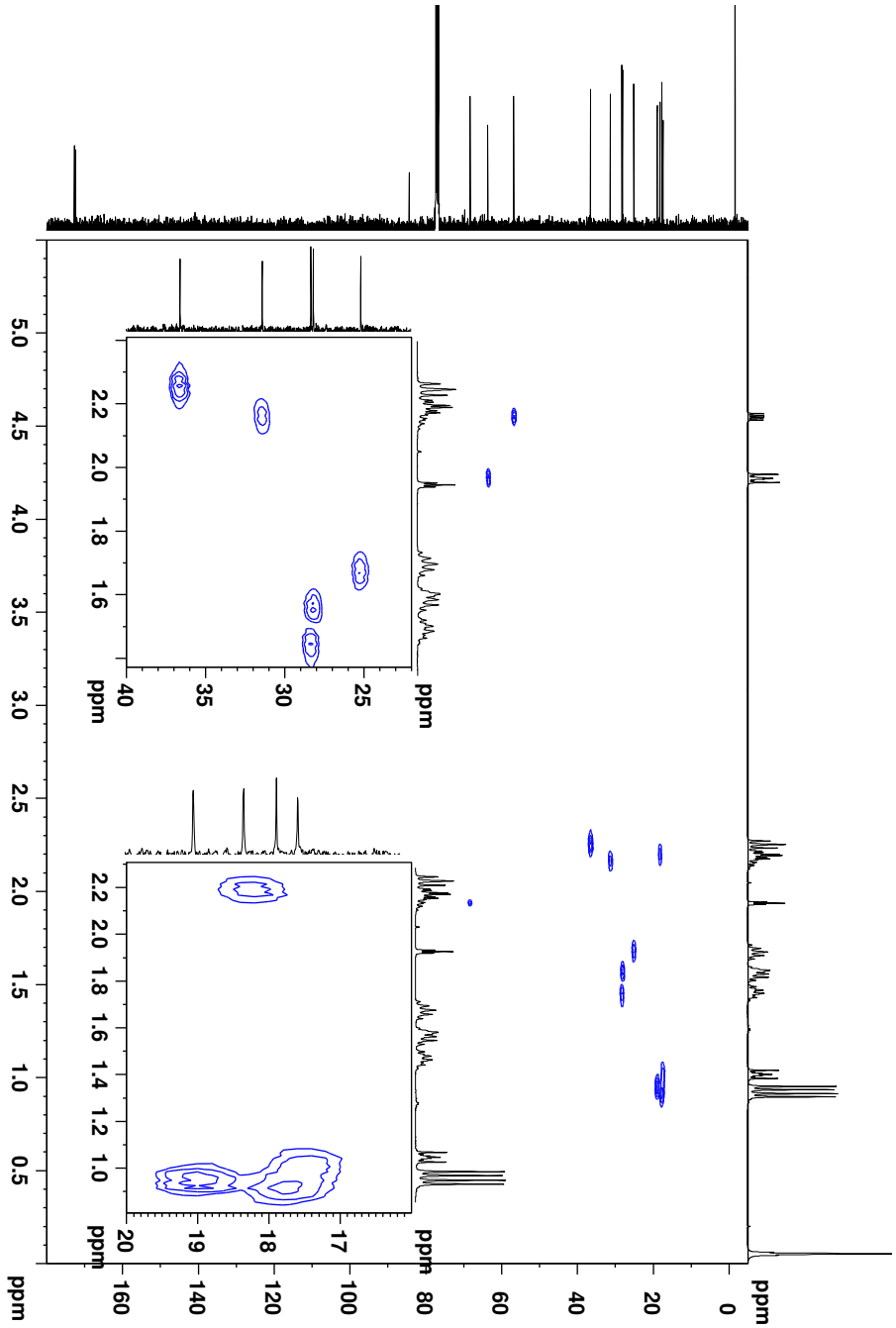

U.6 ^{1}H-^{13}C HMBC for 72, 400 MHz, $CDCl_3$ (ppm)

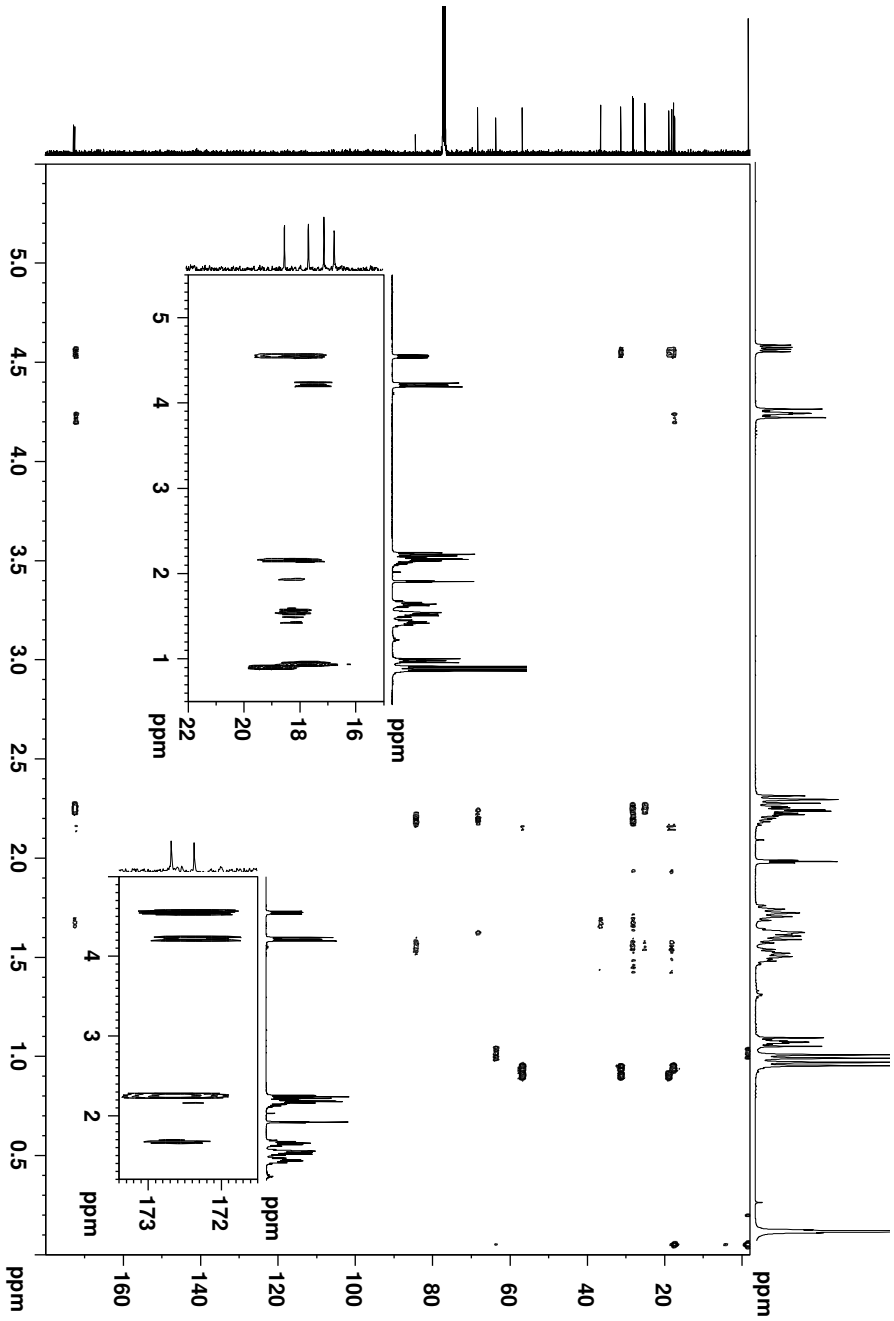

U.7 IR Spectrum of 72 (cm^{-1})

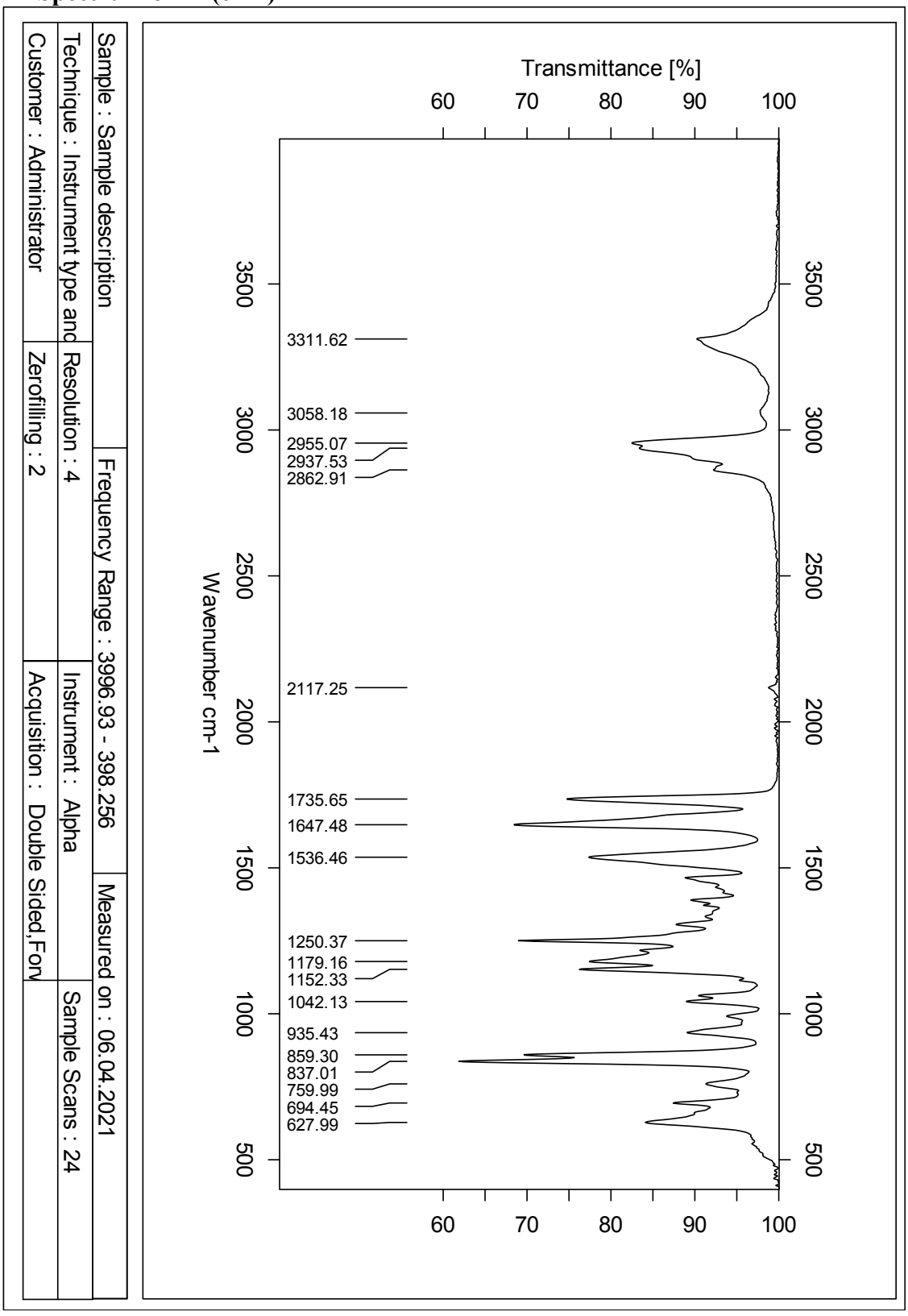

Elemental Composition Report

Single Mass Analysis

Tolerance = 2.0 PPM / DBE: min = -10.0, max = 50.0
Element prediction: Off
Number of isotope peaks used for i-FIT = 6

Monoisotopic Mass, Even Electron Ions
939 formula(e) evaluated with 1 results within limits (all results (up to 1000) for each mass)
Elements Used:
C: 0-100 H: 0-100 N: 0-6 O: 0-3 Si: 0-2 Na: 0-1

2021-193 77 (0.735) AM2 (Ar,35000.0,0.00,0.00); Cm (77:102)
1: TOF MS ES+

6.40e+006

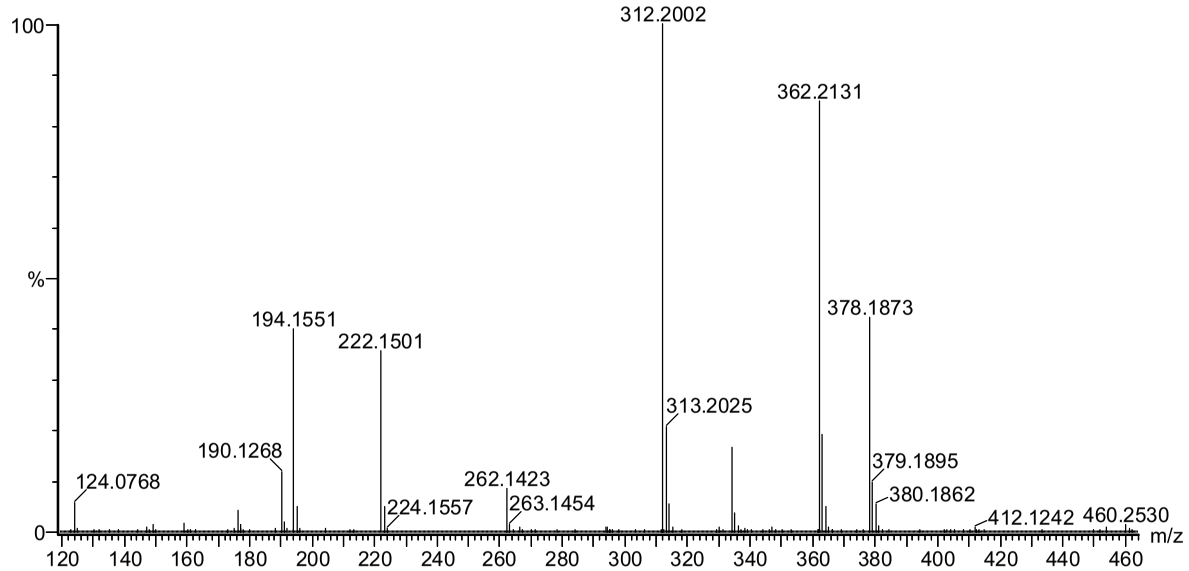

Minimum:				-10.0				
Maximum:		5.0	2.0	50.0				
Mass	Calc. Mass	mDa	PPM	DBE	i-FIT	Norm	Conf(%)	Formula
362.2131	362.2127	0.4	1.1	3.5	2630.2	n/a	n/a	C18 H33 N O3 Si Na

V (*R*)-2-(1-(benzyloxy)propan-2-yl)-2-ethyl-1,3-dithiane (75)
V.1 ^{1}H-NMR for 75, 600 MHz, $CDCl_3$ (ppm)

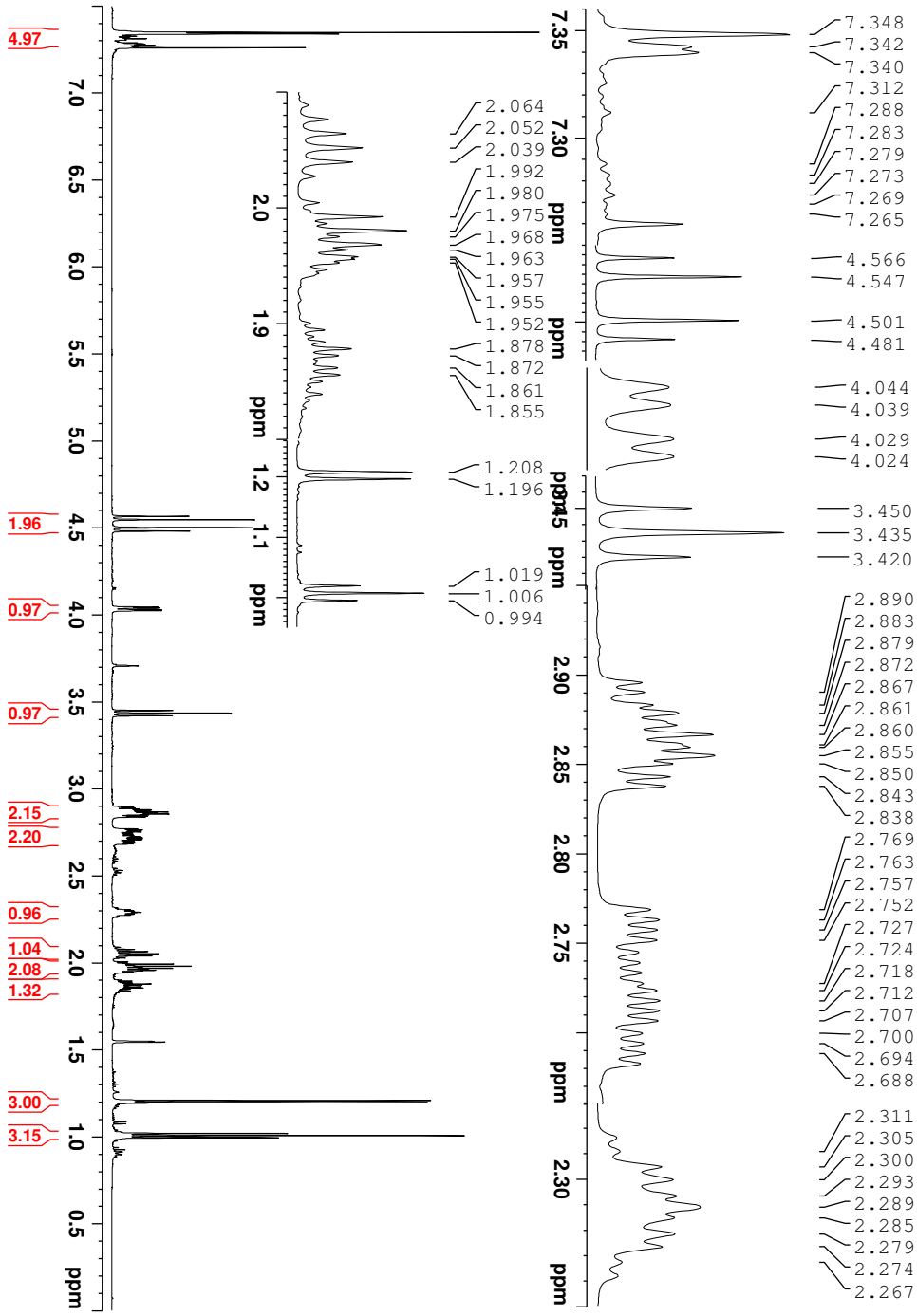

V.2 ^{1}H-NMR for 75, 600 MHz, $CDCl_3$ (Hz)

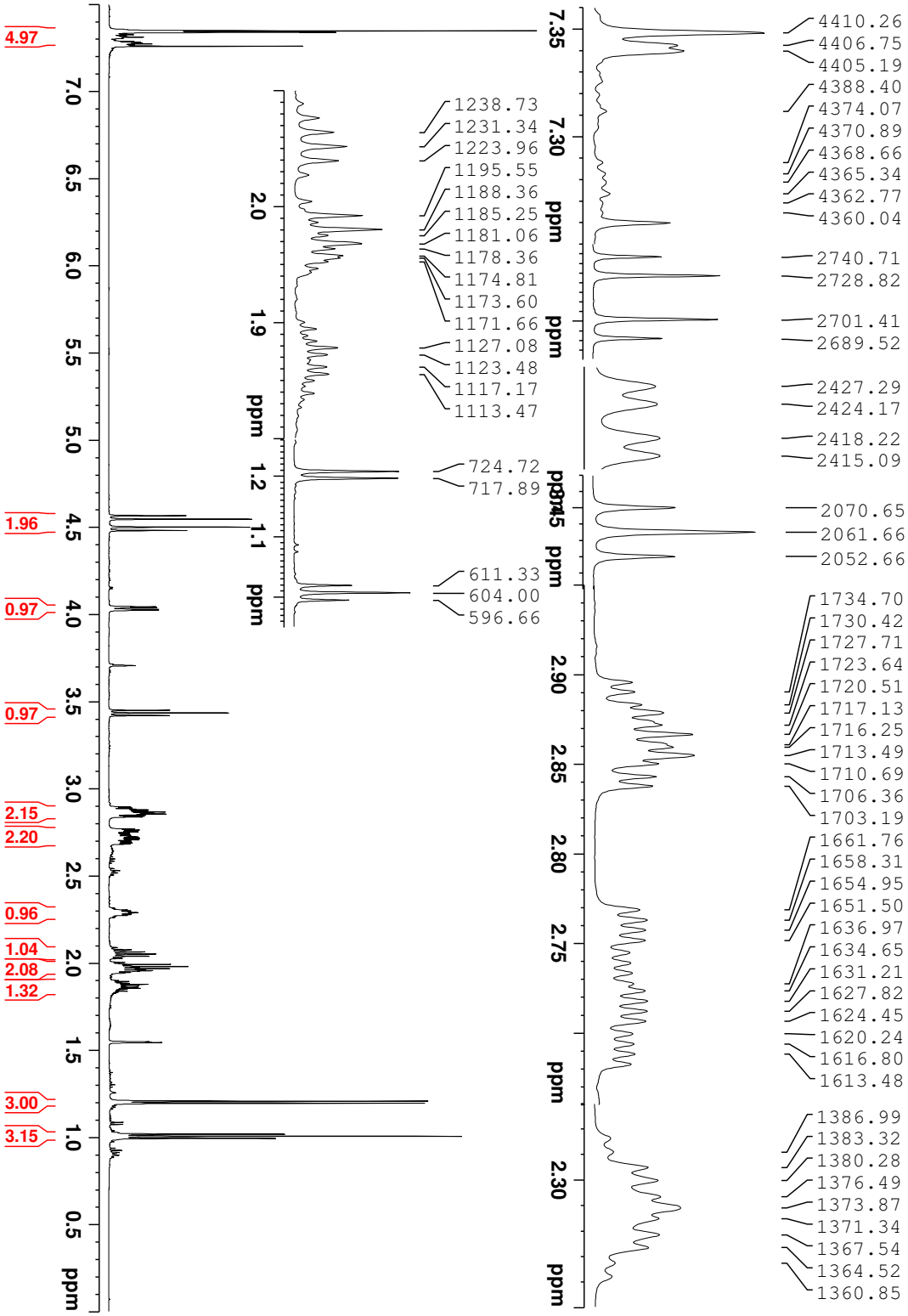

V.3 ^{13}C-NMR for 75, 600 MHz, $CDCl_3$ (ppm)

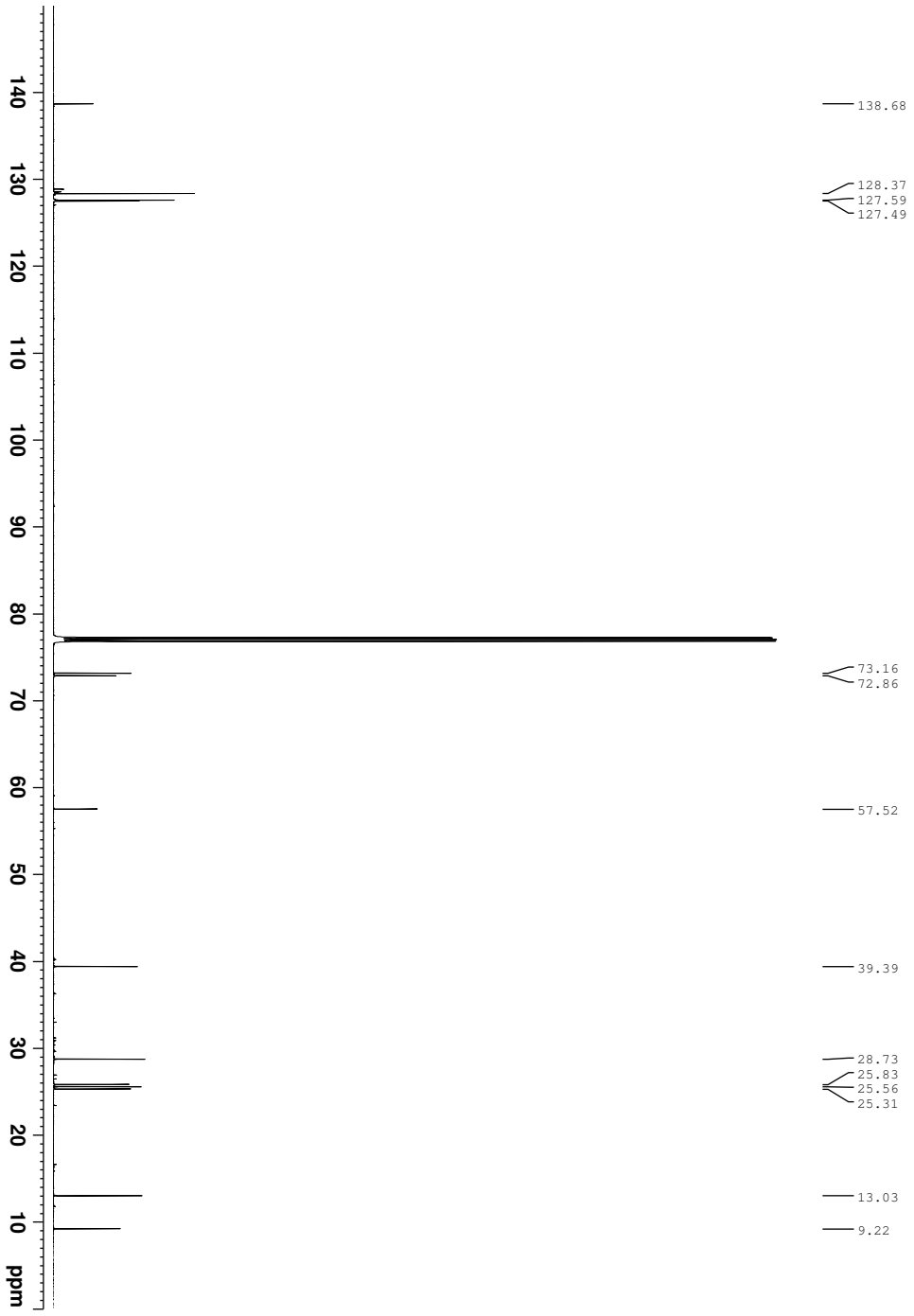

V.4 ^{1}H-^{1}H-COSY for 75, 600 MHz, $CDCl_3$

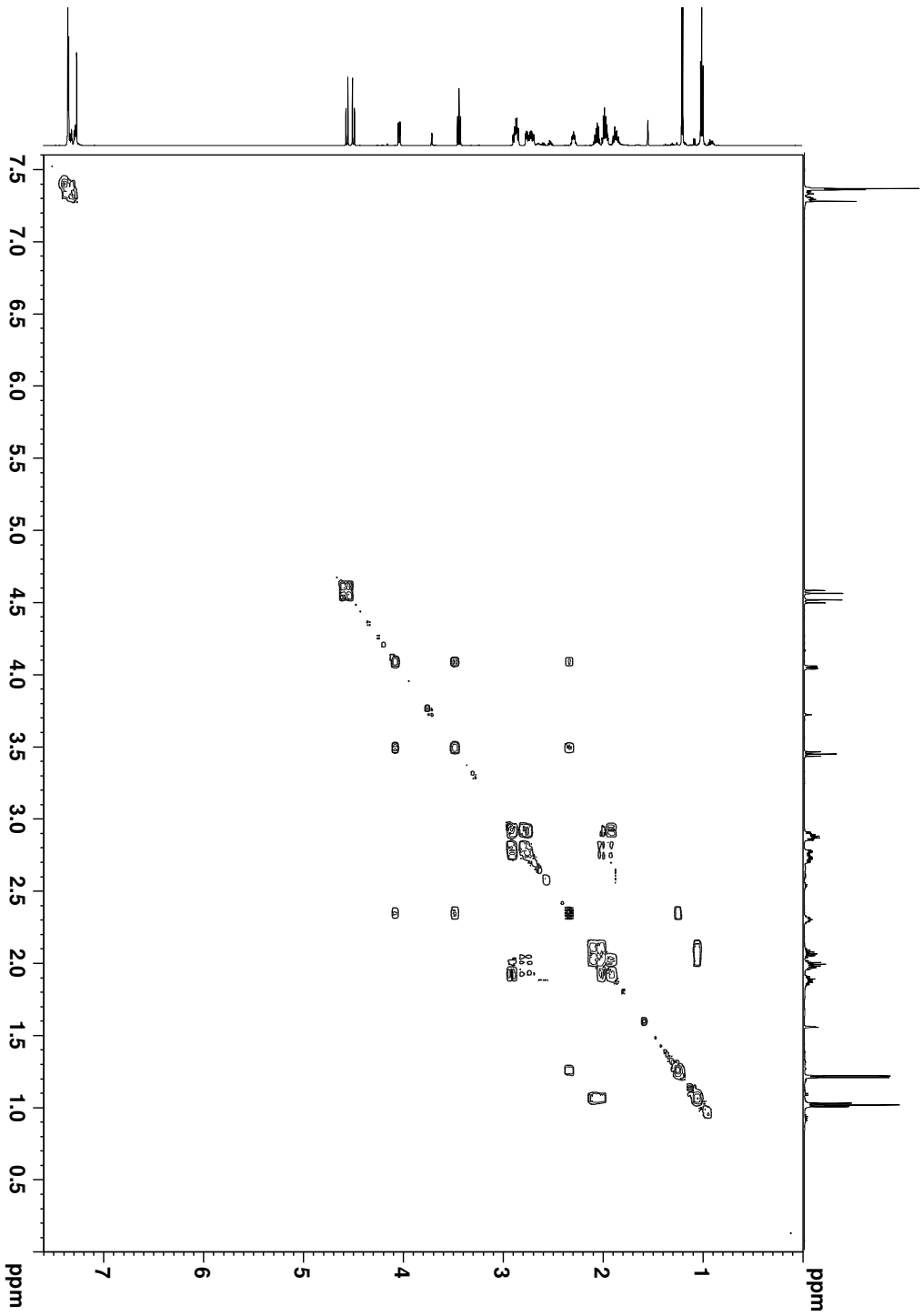

V.5 ^{1}H-^{13}C HSQC for 75, 600 MHz, $CDCl_3$

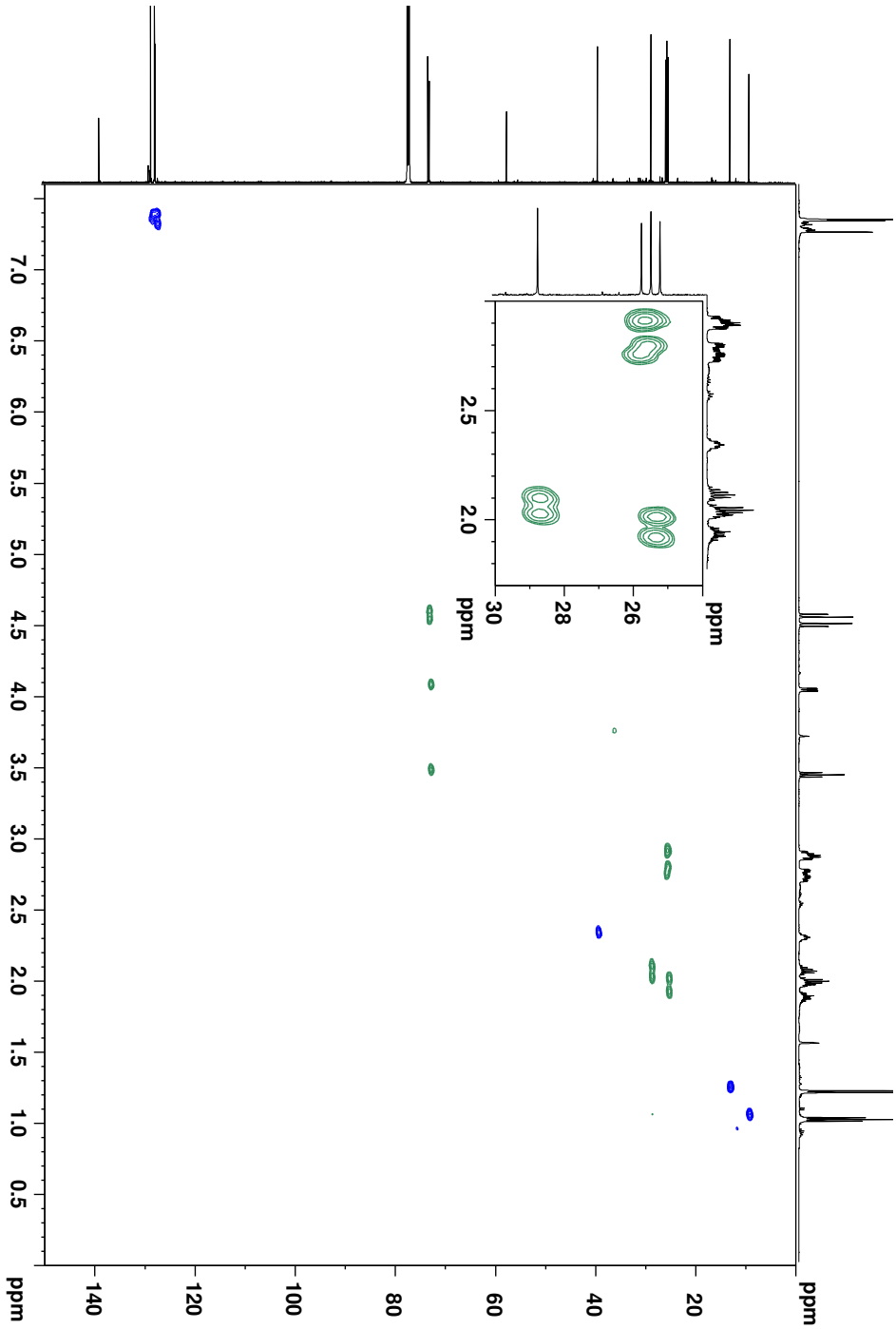

V.6 ^{1}H-^{13}C HMBC for 75, 600 MHz, $CDCl_3$

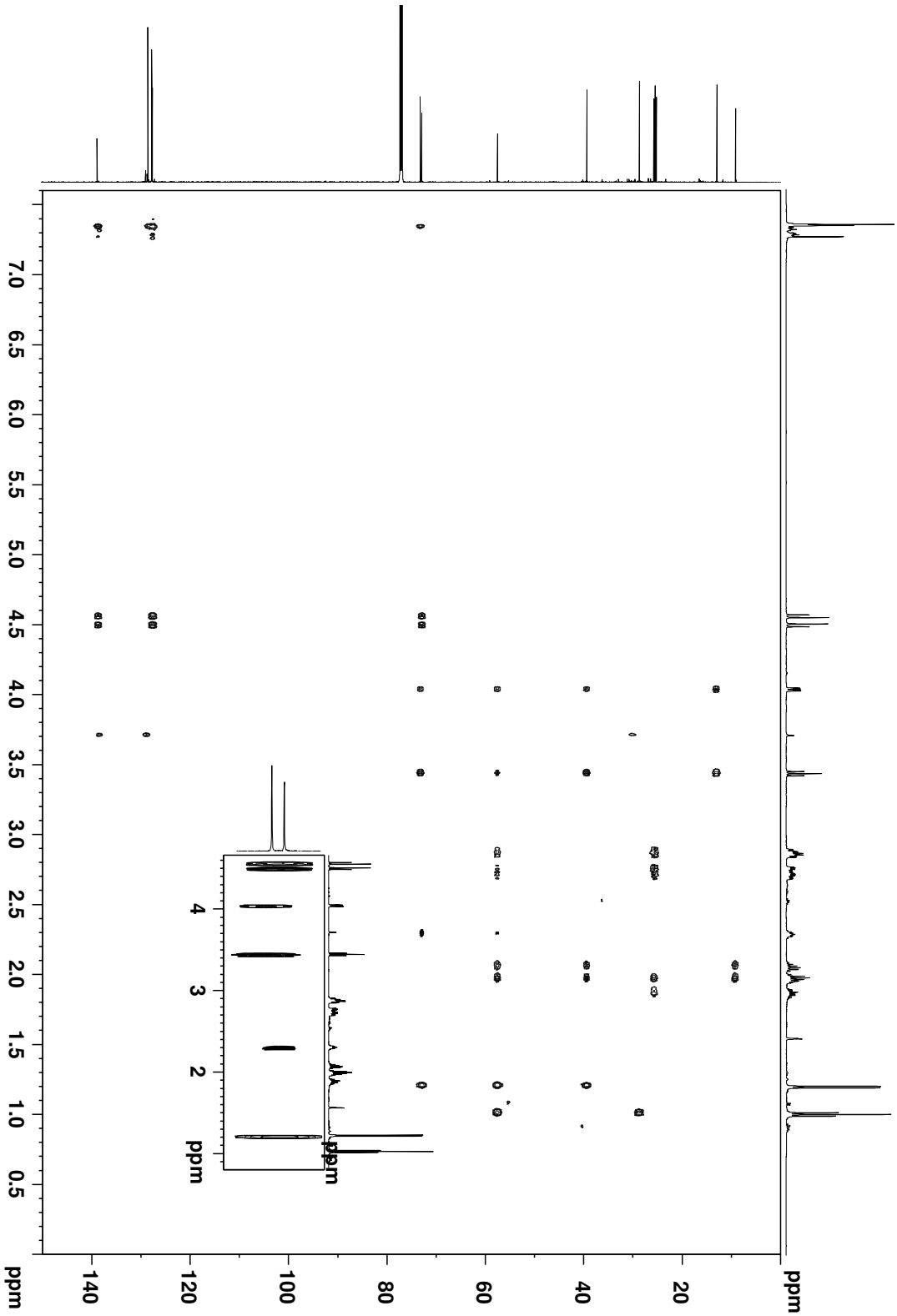

V.7 IR Spectrum of 75 (cm^{-1})

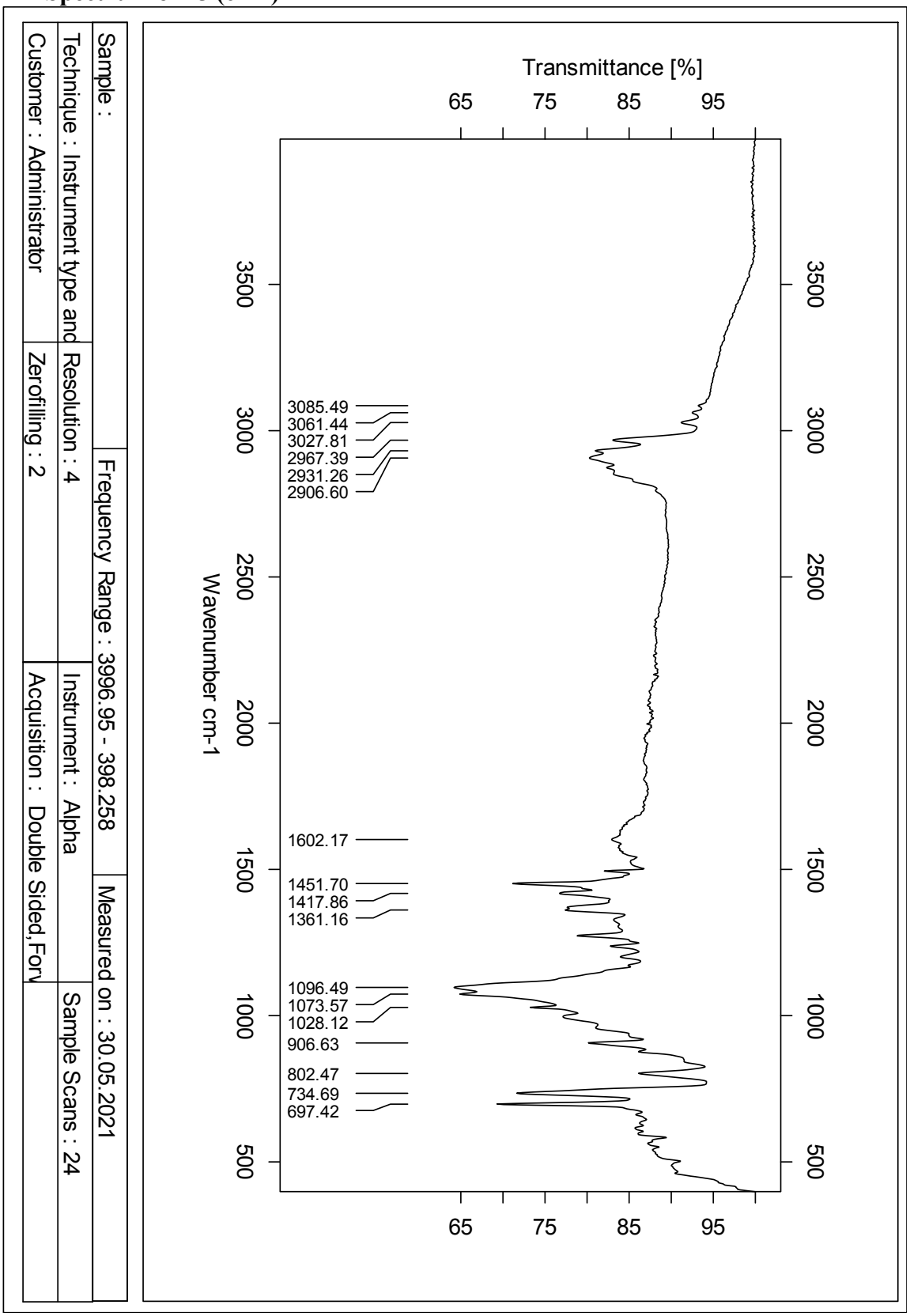

Single Mass Analysis

Tolerance = 2.0 PPM / DBE: min = -50.0, max = 100.0
Element prediction: Off
Number of isotope peaks used for i-FIT = 6

Monoisotopic Mass, Even Electron Ions
2543 formula(e) evaluated with 3 results within limits (all results (up to 1000) for each mass)
Elements Used:
C: 0-100 H: 0-100 N: 0-10 O: 0-10 S: 0-2
2020_435 64 (0.613) AM2 (Ar,35000.0,0.00,0.00); Cm (45:71)
1: TOF MS ES+

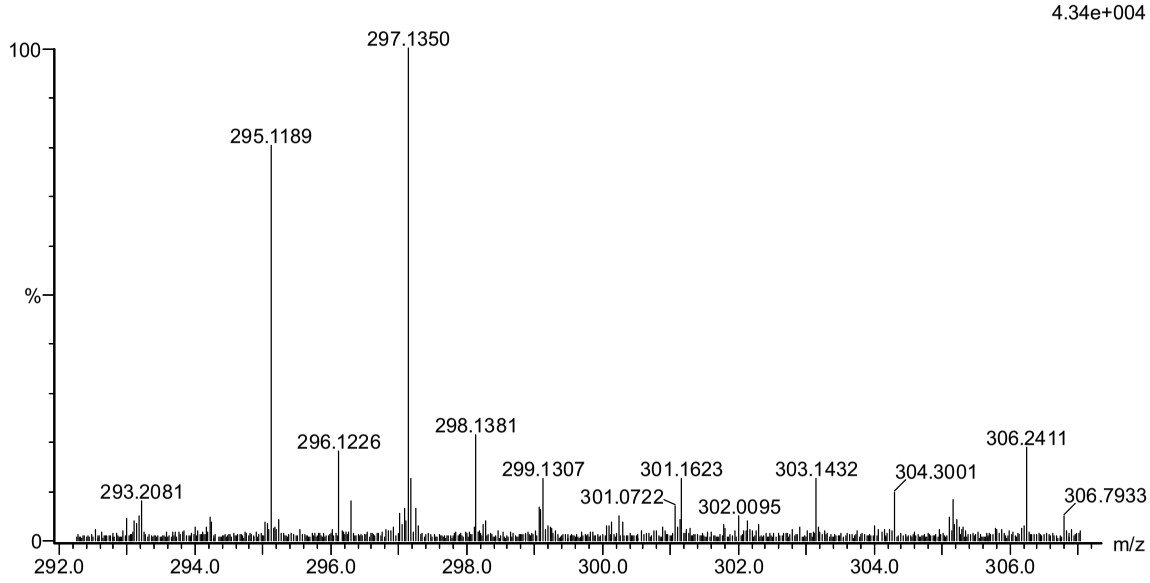

Minimum:				-50.0				
Maximum:		5.0	2.0	100.0				
Mass	Calc. Mass	mDa	PPM	DBE	i-FIT	Norm	Conf(%)	Formula
297.1350	297.1347	0.3	1.0	4.5	2772.5	2.041	12.99	C16 H25 O S2
	297.1345	0.5	1.7	1.5	2770.6	0.141	86.81	C8 H21 N6 O4 S
	297.1352	-0.2	-0.7	10.5	2776.6	6.204	0.20	C16 H17 N4 O2

W (2*R*,4*R*,5*R*,6*S*)-1-(benzyloxy)-2,4,6-trimethyloctane-3,5-diol 76
W.1 ^{1}H-NMR for 76, 600 MHz, $CDCl_3$ (ppm)

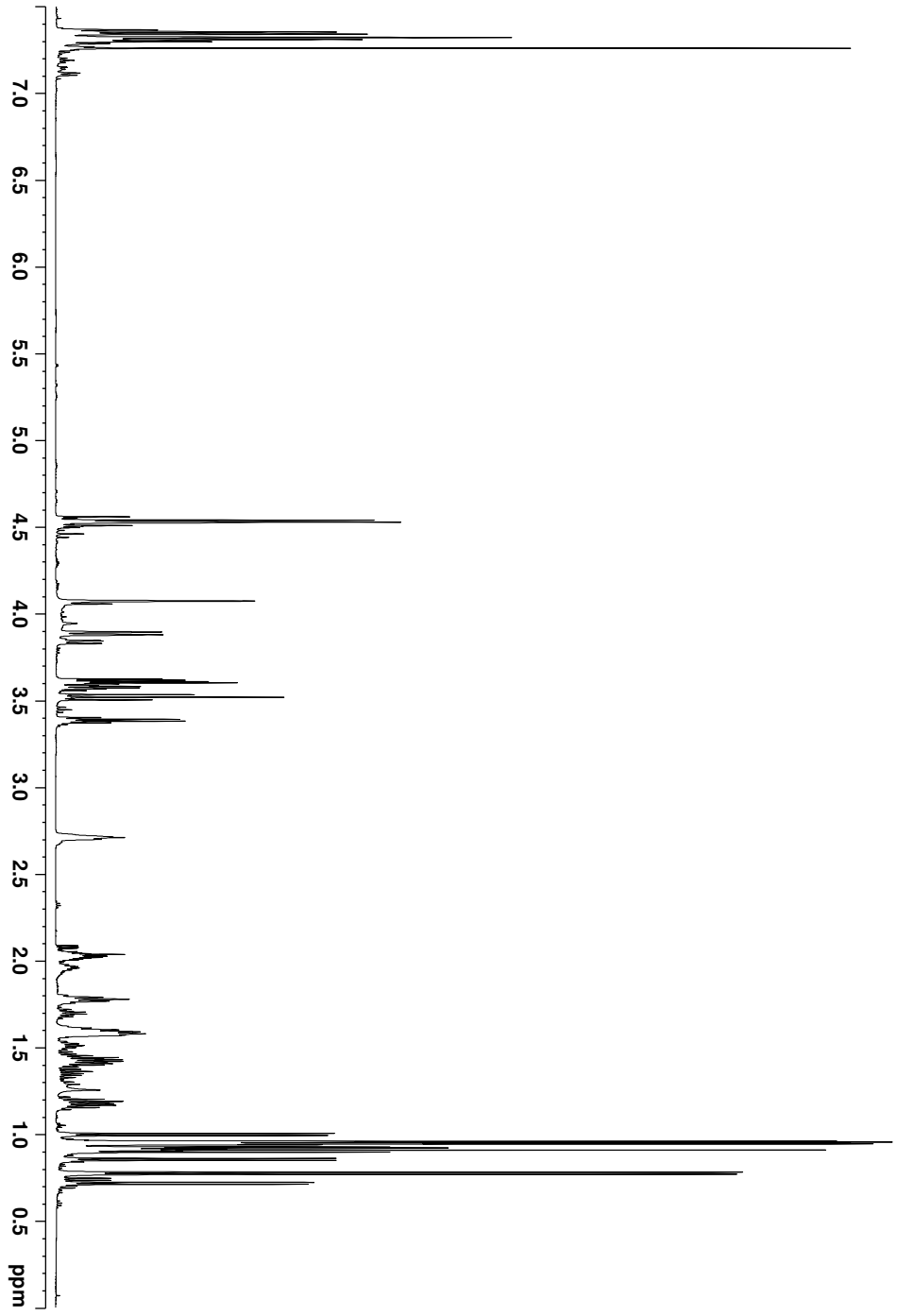

W.2 IR Spectrum of 76 (cm^{-1})

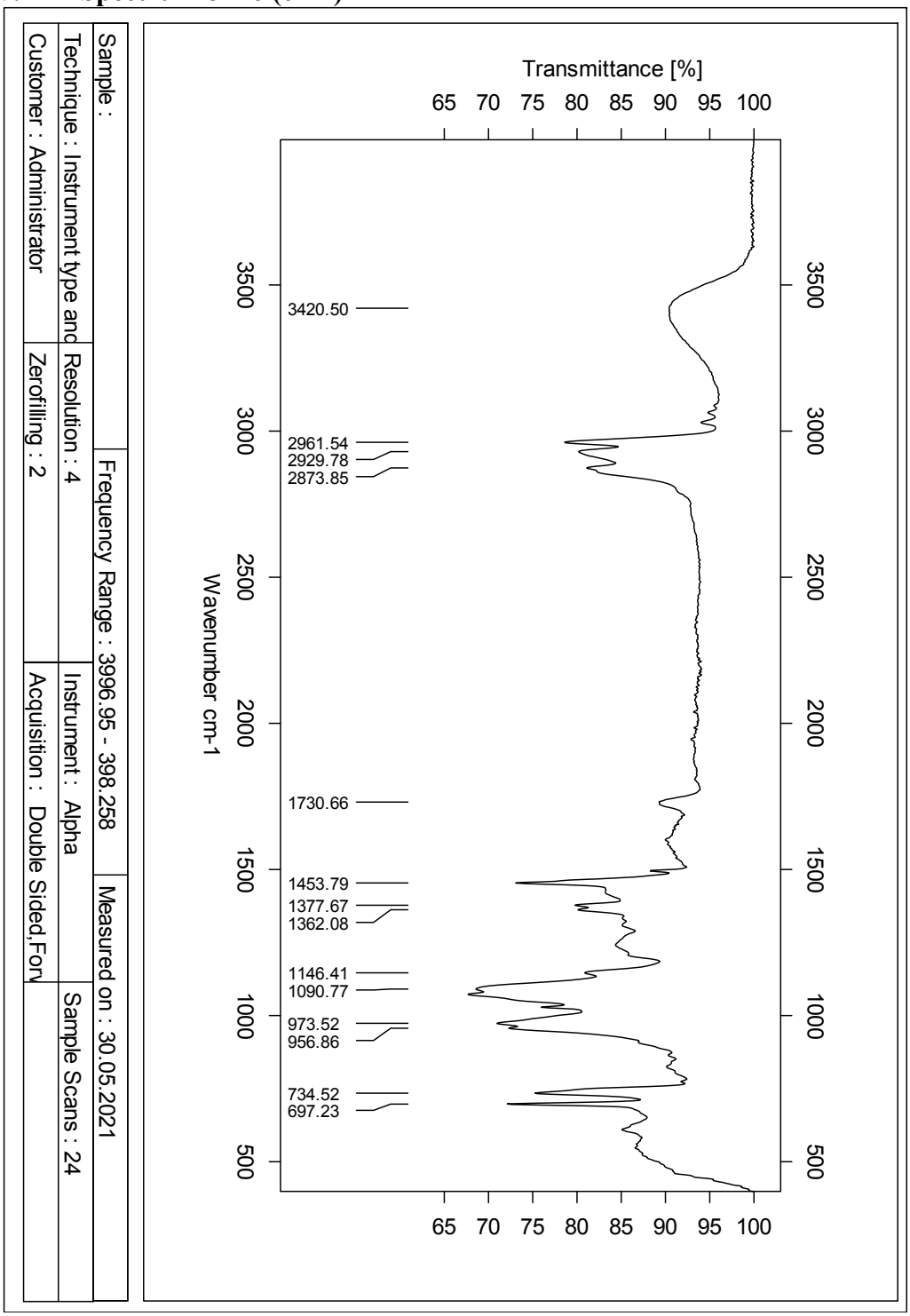

X Mixture of Methyl 7-oxoheptanoate (69) and 7-methoxy-7-oxoheptanoic acid (77) (sample stored for 3 months at −19 ℃)

X.1 ^{1}H-NMR for the mixture of 69 and 77, 400 MHz, $CDCl_3$ (ppm)

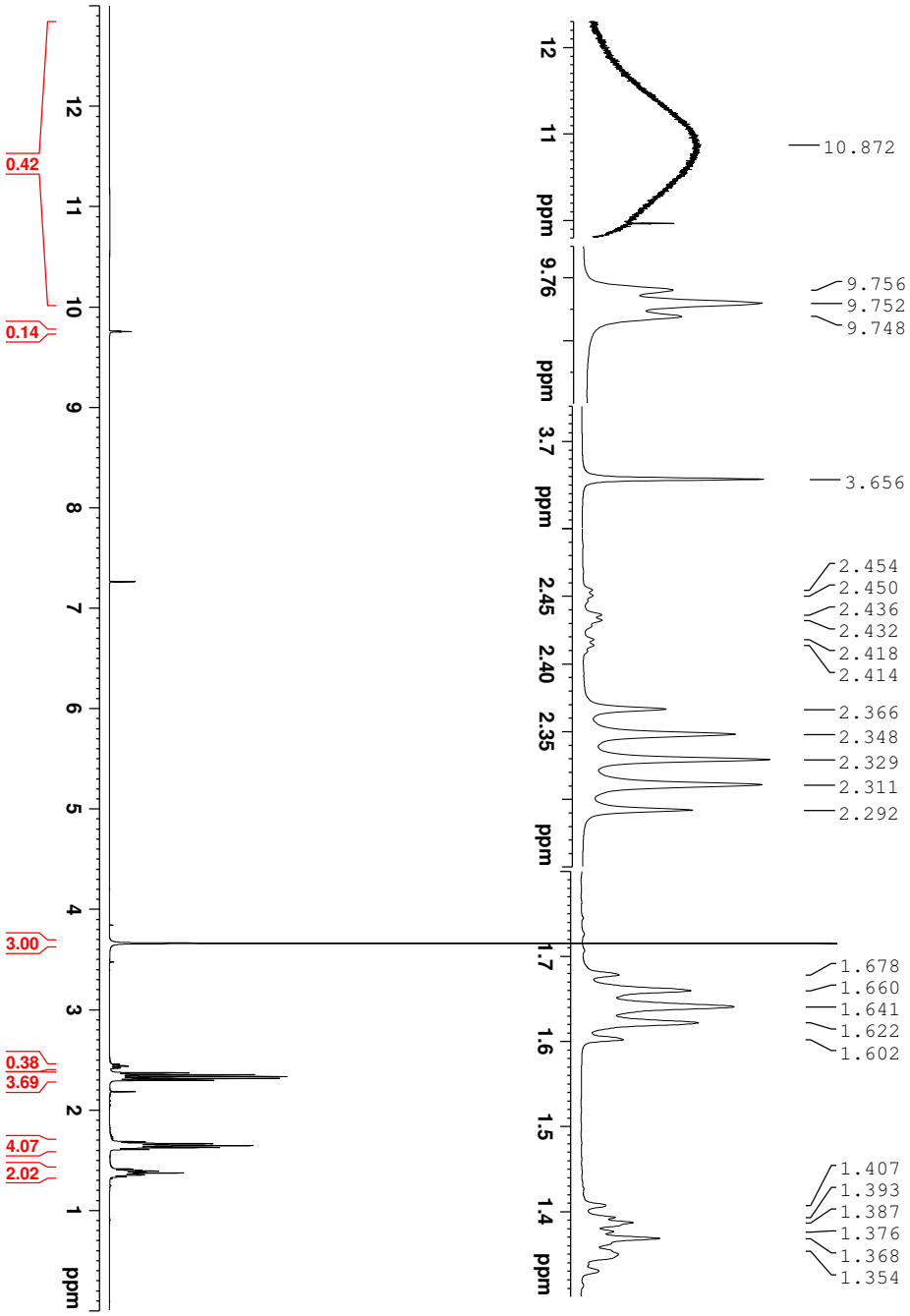

X.2 ^{13}C-NMR for mixture of 69 and 77, 400 MHz, $CDCl_3$ (ppm)

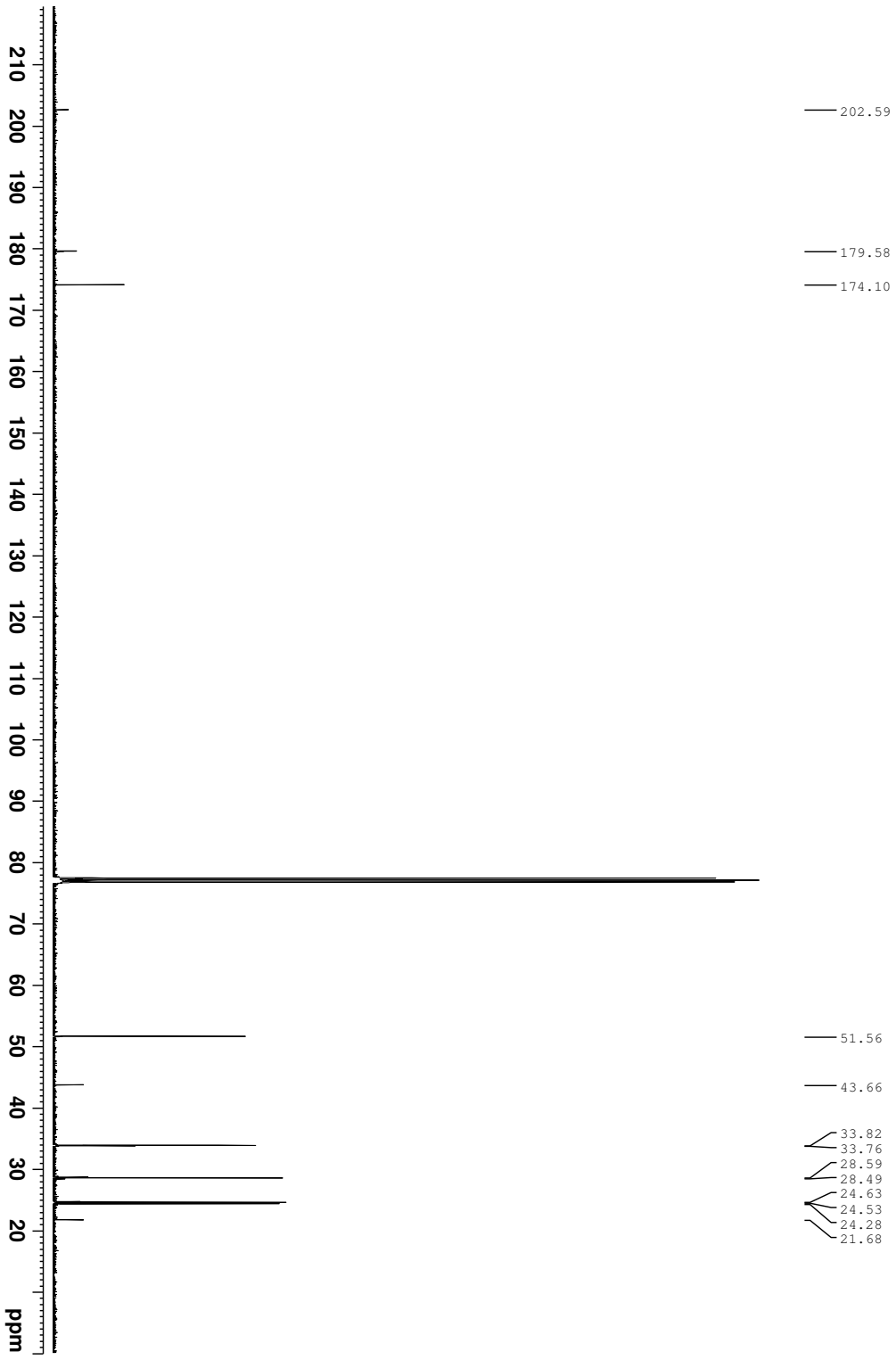

Y 7-methoxy-7-oxoheptanoic acid (77) (Sample stored for 3 months at rt)
Y.1 ^{1}H-NMR for 77, 400 MHz, $CDCl_3$ (ppm)

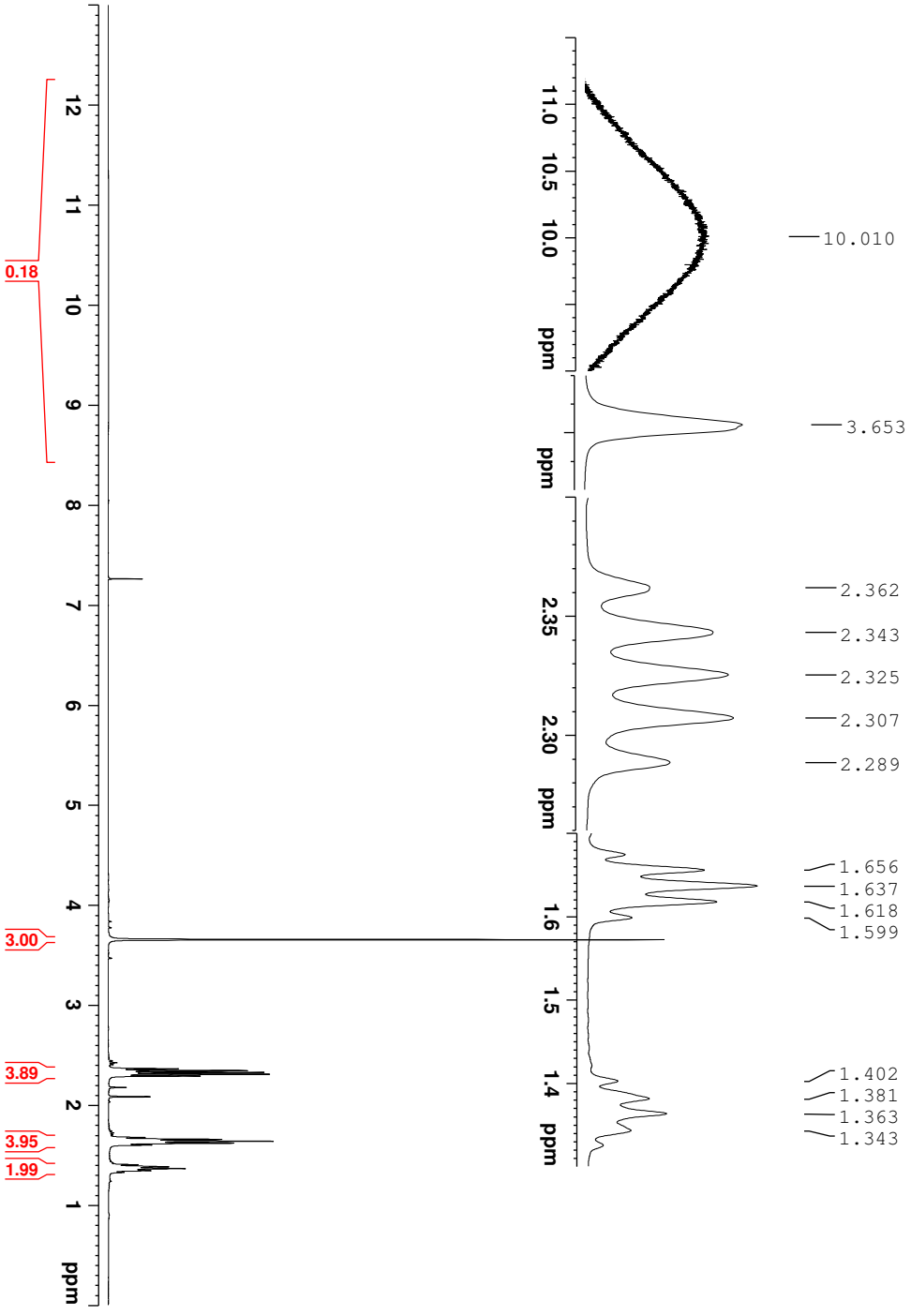

Y.3 ^{13}C-NMR Spectrum of 77, 400 MHz, $CDCl_3$ (ppm)

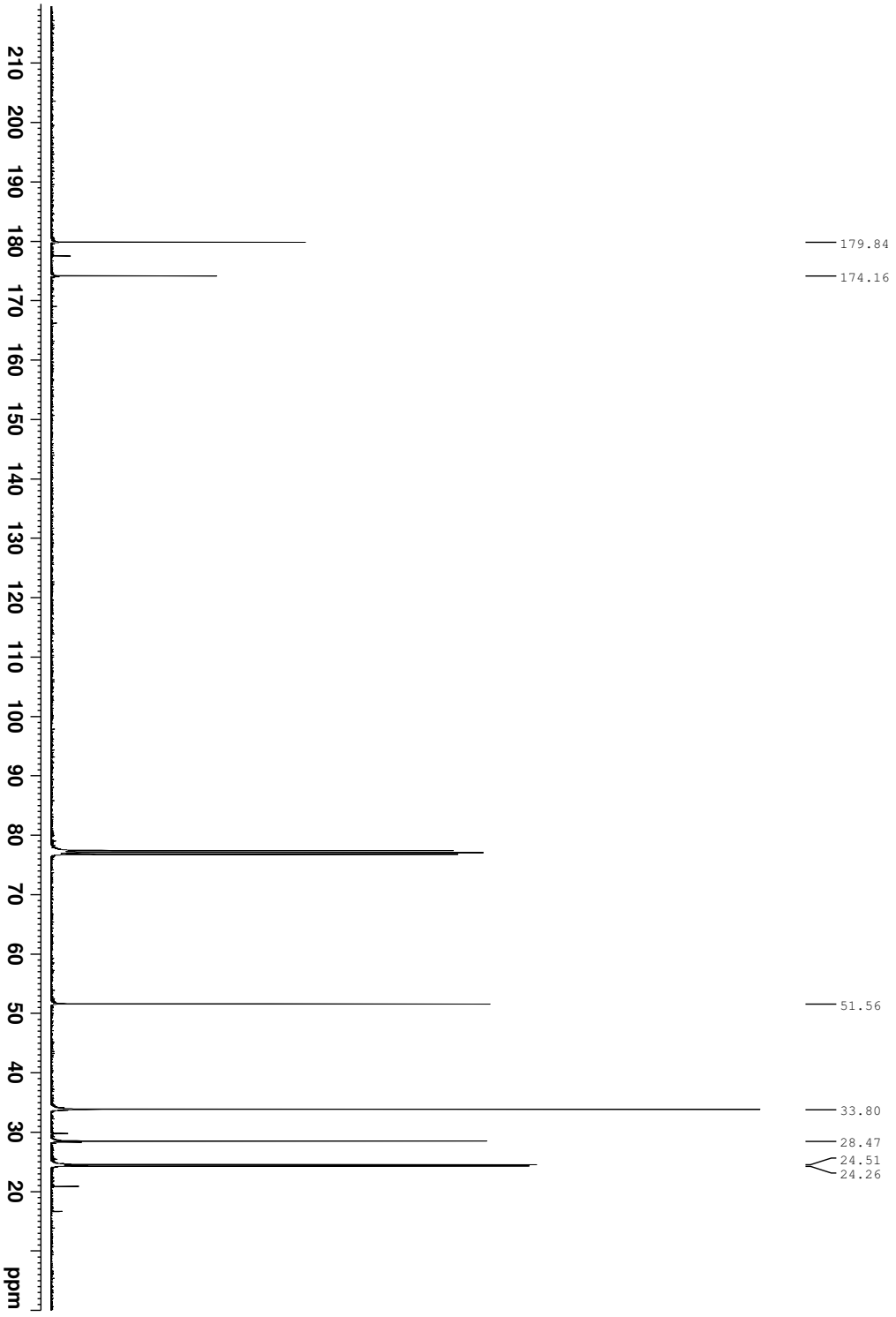

Y.4 ^{1}H-^{1}H-COSY for 77, 400 MHz, $CDCl_3$

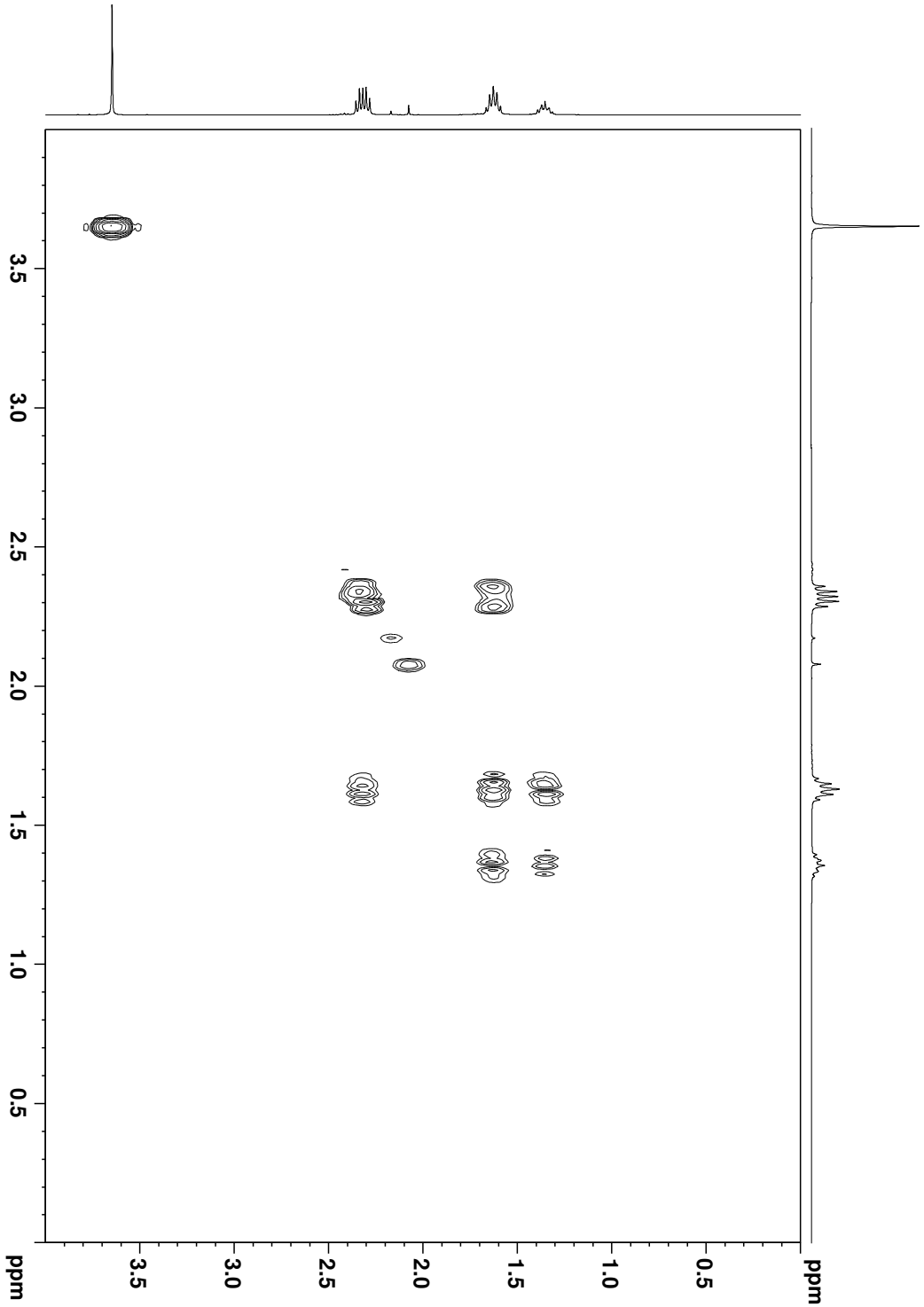

Y.5 ^{1}H-^{13}C HSQC for 77, 400 MHz, $CDCl_3$

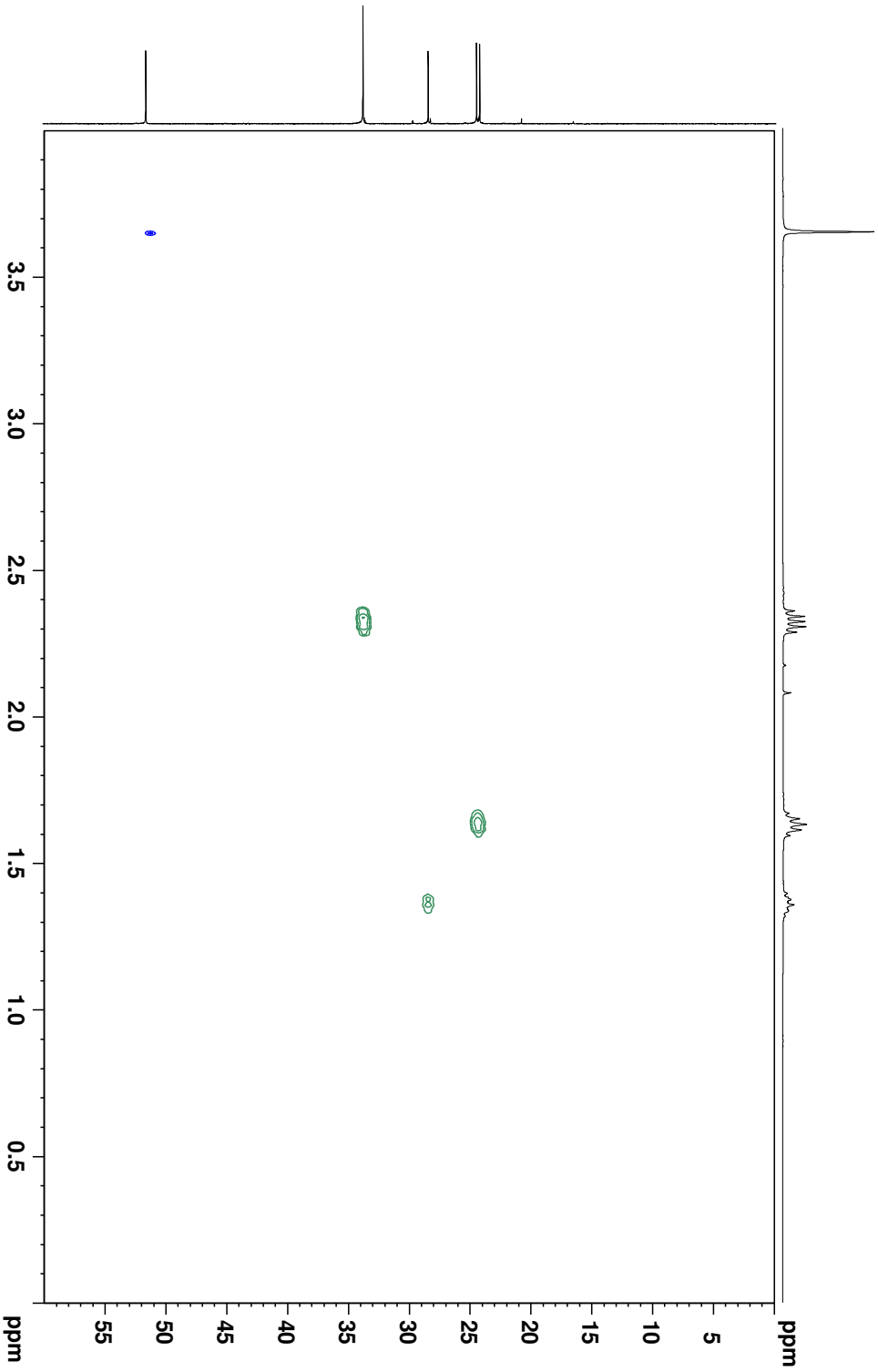

Y.6 ^{1}H-^{13}C HMBC for 77, 400 MHz, $CDCl_3$

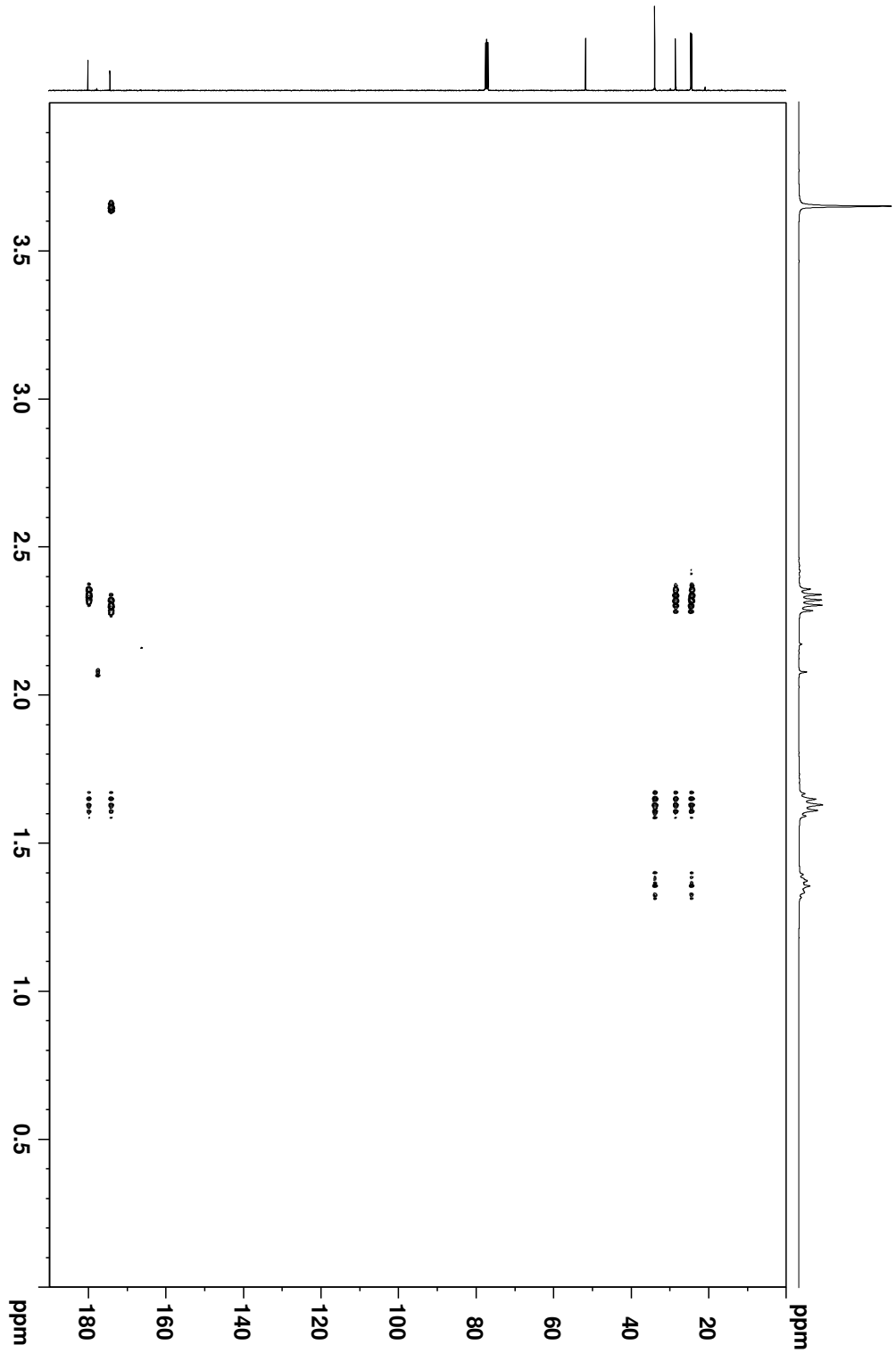

Y.7 IR Spectrum of 77 (cm^{-1})

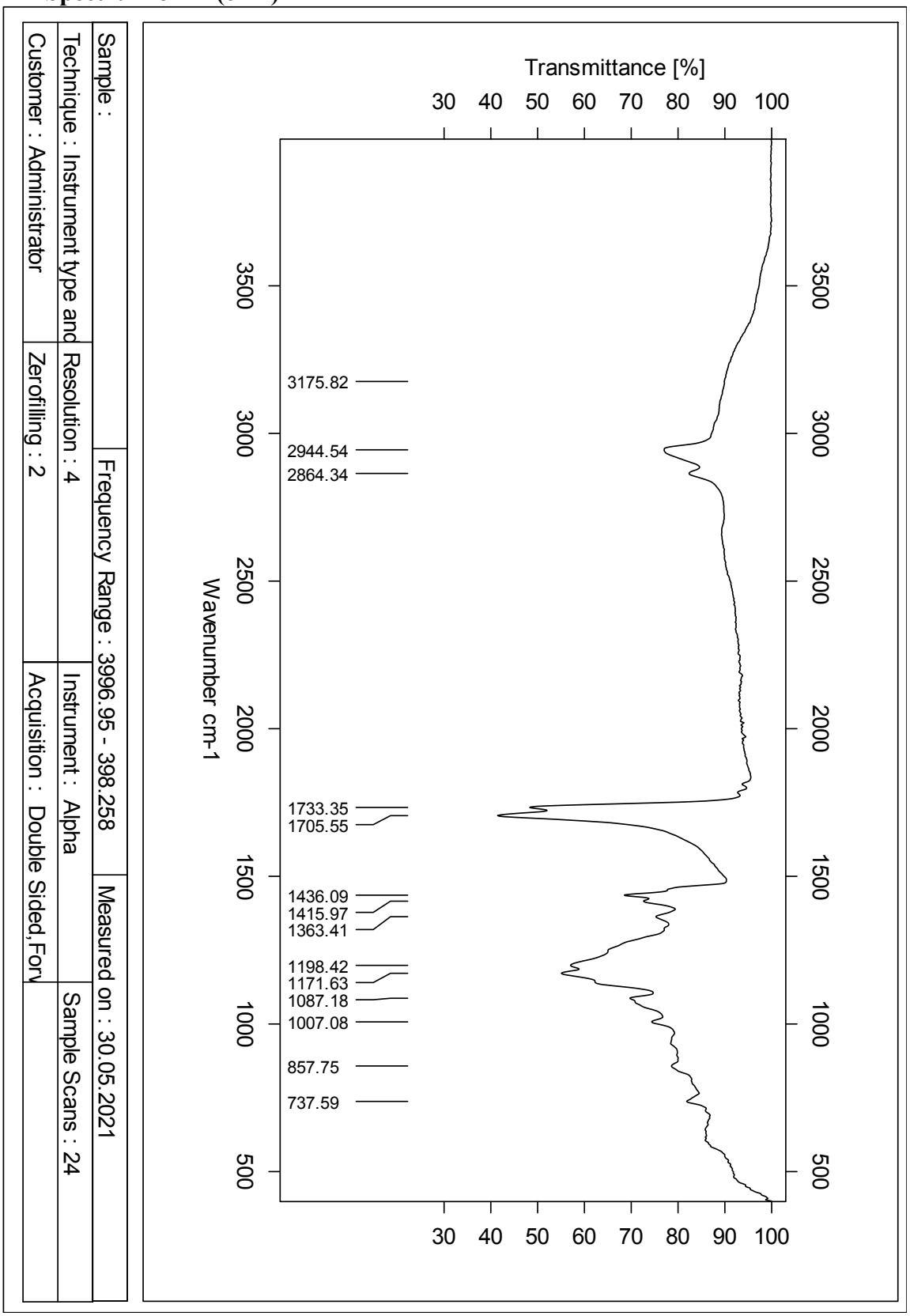

Single Mass Analysis

Tolerance = 3.0 PPM / DBE: min = -10.0, max = 50.0
Element prediction: Off
Number of isotope peaks used for i-FIT = 6

Monoisotopic Mass, Even Electron Ions
531 formula(e) evaluated with 1 results within limits (all results (up to 1000) for each mass)
Elements Used:
C: 0-100 H: 0-100 N: 0-5 O: 0-10 Na: 0-1 Br: 0-1

2021_39 46 (0.525) AM2 (Ar,35000.0,0.00,0.00); Cm (40:46)
1: TOF MS ES+

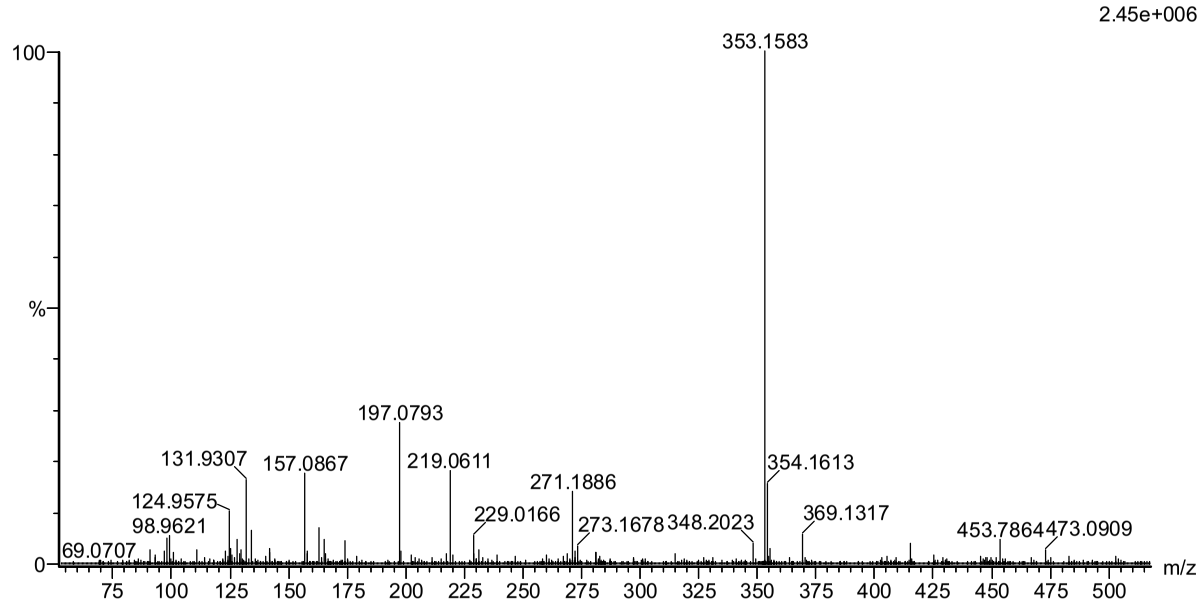

Minimum:				-10.0				
Maximum:		5.0	3.0	50.0				
Mass	Calc. Mass	mDa	PPM	DBE	i-FIT	Norm	Conf(%)	Formula
197.0793	197.0790	0.3	1.5	1.5	3979.3	n/a	n/a	C8 H14 O4 Na